MIT OpenCourseWare
http://ocw.mit.edu

Electromechanical Dynamics

For any use or distribution of this textbook, please cite as follows:

Woodson, Herbert H., and James R. Melcher. *Electromechanical Dynamics*.
3 vols. (Massachusetts Institute of Technology: MIT OpenCourseWare).
http://ocw.mit.edu (accessed MM DD, YYYY). License: Creative Commons
Attribution-NonCommercial-Share Alike

For more information about citing these materials or
our Terms of Use, visit: http://ocw.mit.edu/terms

ELECTROMECHANICAL DYNAMICS

Part III: Elastic and Fluid Media

ELECTROMECHANICAL

DYNAMICS

Part III: Elastic and Fluid Media

HERBERT H. WOODSON

Philip Sporn Professor of Energy Processing
Departments of Electrical and Mechanical Engineering

JAMES R. MELCHER

Associate Professor of Electrical Engineering
Department of Electrical Engineering

both of Massachusetts Institute of Technology

To our parents

PREFACE

Part III: Elastic and Fluid Media

In the early 1950's the option structure was abandoned and a common core curriculum was instituted for all electrical engineering students at M.I.T. The objective of the core curriculum was then, and is now, to provide a foundation in mathematics and science on which a student can build in his professional growth, regardless of the many opportunities in electrical engineering from which he may choose. In meeting this objective, core curriculum subjects cannot serve the needs of any professional area with respect to nomenclature, techniques, and problems unique to that area. Specialization comes in elective subjects, graduate study, and professional activities.

To be effective a core curriculum subject must be broad enough to be germane to the many directions an electrical engineer may go professionally, yet it must have adequate depth to be of lasting value. At the same time, the subject must be related to the real world by examples of application. This is true because students learn by seeing material in a familiar context, and engineering students are motivated largely by the relevance of the material to the realities of the world around them.

In the organization of the core curriculum in electrical engineering at M.I.T. electromechanics is one major component. As our core curriculum has evolved, there have been changes in emphasis and a broadening of the topic. The basic text in electromechanics until 1954, when a new departure was made, was *Electric Machinery* by Fitzgerald and Kingsley. This change produced *Electromechanical Energy Conversion* by White and Woodson, which was used until 1961. At that time we started the revision that resulted in the present book. During this period we went through many versions of notes while teaching the material three semesters a year.

Our objective has always been to teach a subject that combines classical mechanics with the fundamentals of electricity and magnetism. Thus the subject offers the opportunity to teach both mechanics and electromagnetic theory in a context vital to much of the electrical engineering community.

Our choice of material was to some extent determined by a desire to give the student a breadth of background sufficient for further study of almost any type of electromechanical interaction, whether in rotating machinery,

plasma dynamics, the electromechanics of biological systems, or magneto-elasticity. It was also chosen to achieve adequate depth while maintaining suitable unity, but, most important, examples were chosen that could be enlivened for the engineering student interested in the interplay of physical reality and the analytical model. There were many examples from which to choose, but only a few satisfied the requirement of being both mathematically lucid *and* physically demonstrable, so that the student could "push it or see it" and directly associate his observations with symbolic models. Among the areas of electrical engineering, electromechanics excels in offering the opportunity to establish that all-important "feel" for a physical phenomenon. Properly selected electromechanical examples can be the basis for discerning phenomena that are remote from human abilities to observe.

Before discussing how the material can be used to achieve these ends, a review of the contents is in order. The student who uses this book is assumed to have a background in electrostatics and magnetostatics. Consequently, Chapter 1 and Appendix B are essentially a review to define our starting point.

Chapter 2 is a generalization of the concepts of inductance and capacitance that are necessary to the treatment of electromechanical systems; it also provides a brief introduction to rigid-body mechanics. This treatment is included because many curricula no longer cover mechanics, other than particle mechanics in freshman physics. The basic ideas of Chapter 2 are repeated in Chapter 3 to establish some properties of electromechanical coupling in lumped-parameter systems and to obtain differential equations that describe the dynamics of lumped-parameter systems.

Next, the techniques of Chapters 2 and 3 are used to study rotating machines in Chapter 4. Physical models are defined, differential equations are written, machine types are classified, and steady-state characteristics are obtained and discussed. A separate chapter on rotating machines has been included not only because of the technological importance of machines but also because rotating machines are rich in examples of the kinds of phenomena that can be found in lumped-parameter electromechanical systems.

Chapter 5 is devoted to the study, with examples, of the dynamic behavior of lumped-parameter systems. Virtually all electromechanical systems are mathematically nonlinear; nonetheless, linear incremental models are useful for studying the stability of equilibria and the nature of the dynamical behavior in the vicinity of an equilibrium. The second half of this chapter develops the classic potential-well motions and loss-dominated dynamics in the context of electromechanics. These studies of nonlinear dynamics afford an opportunity to place linear models in perspective while forming further insights on the physical significance of, for example, flux conservation and state functions.

Chapter 6 represents our first departure from lumped-parameter systems into continuum systems with a discussion of how observers in relative motion will define and measure field quantities and the related effects of material motion on electromagnetic fields. It is our belief that dc rotating machines are most easily understood in this context. Certainly they are a good demonstration of field transformations at work.

As part of any continuum electromechanics problem, one must know how the electric and magnetic fields are influenced by excitations and motion. In quasi-static systems the distribution of charge and current are controlled by magnetic diffusion and charge relaxation, the subjects of Chapter 7. In Chapter 7 simple examples isolate significant cases of magnetic diffusion or charge relaxation, so that the physical processes involved can be better understood.

Chapters 6 and 7 describe the electrical side of a continuum electromechanical system with the material motion predetermined. The mechanical side of the subject is undertaken in Chapter 8 in a study of force densities of electric and magnetic origin. Because it is a useful concept in the analysis of many systems, we introduce the Maxwell stress tensor. The study of useful properties of tensors sets the stage for later use of mechanical stress tensors in elastic and fluid media.

At this point the additional ingredient necessary to the study of continuum electromechanics is the mechanical medium. In Chapter 9 we introduce simple elastic continua—longitudinal motion of a thin rod and transverse motion of wires and membranes. These models are used to study simple continuum mechanical motions (nondispersive waves) as excited electromechanically at boundaries.

Next, in Chapter 10 a string or membrane is coupled on a continuum basis to electric and magnetic fields and the variety of resulting dynamic behavior is studied. The unifying thread of this treatment is the dispersion equation that relates complex frequency ω with complex wavenumber k. Without material convection there can be simple nondispersive waves, cut off or evanescent waves, absolute instabilities, and diffusion waves. The effect of material convection on evanescent waves and oscillations and on wave amplification are topics that make a strong connection with electron beam and plasma dynamics. The method of characteristics is introduced as a convenient tool in the study of wave propagation.

In Chapter 11 the concepts and techniques of Chapters 9 and 10 are extended to three-dimensional systems. Strain displacement and stress-strain relations are introduced, with tensor concepts, and simple electromechanical examples of three-dimensional elasticity are given.

In Chapter 12 we turn to a different mechanical medium, a fluid. We first study electromechanical interactions with inviscid, incompressible

fluids to establish essential phenomena in the simplest context. It is here that
we introduce the basic notions of MHD energy conversion that can result
when a conducting fluid flows through a transverse magnetic field. We also
bring in electric-field interactions with fluids, in which ion drag phenomena
are used as an example. In addition to these basically conducting processes,
we treat the electromechanical consequences of polarization and magnetiza-
tion in fluids. We demonstrate how highly conducting fluids immersed in
magnetic fields can propagate Alfvén waves.

In Chapter 13 we introduce compressibility to the fluid model. This can
have a marked effect on electromechanical behavior, as demonstrated with
the MHD conduction machine. With compressibility, a fluid will propagate
longitudinal disturbances (acoustic waves). A transverse magnetic field and
high electrical conductivity modify these disturbances to magnetoacoustic
waves.

Finally, in Chapter 14 we add viscosity to the fluid model and study the
consequences in electromechanical interactions with steady flow. Hartmann
flow demonstrates the effect of viscosity on the dc magnetohydrodynamic
machine.

To be successful a text must have a theme; the material must be inter-
related. Our philosophy has been to get into the subject where the student
is most comfortable, with lumped-parameter (circuit) concepts. Thus many
of the subtle approximations associated with quasi-statics are made naturally,
and the student is faced with the implications of what he has assumed only
after having become thoroughly familiar with the physical significance and
usefulness of his approximations. By the time he reaches Chapter 4 he will
have drawn a circle around at least a class of problems in which electro-
magnetic fields interact usefully with media in motion.

In dealing with physical and mathematical subjects, as we are here, in
which the job is incomplete unless the student sees the physical laws put to
work in some kind of physical embodiment, it is necessary for the thread of
continuity to be woven into the material in diverse and subtle ways. A
number of attempts have been made, to which we can add our early versions
of notes, to write texts with one obvious, pedagogically logical basis for
evolving the material; for example, it can be recognized that classes of
physical phenomena could be grouped according to the differential equation
that describes the pertinent dynamics. Thus we could treat magnetic diffusion,
diffusion waves on elastic continua, and viscous diffusion waves in one
chapter, even though the physical embodiments are entirely different.
Alternatively, we could devise a subject limited to certain technological
applications or cover superficially a wide range of basically unrelated topics
such as "energy conversion" under one heading. This was the preva-
lent approach in engineering education a decade or so ago, even at the

undergraduate level. It seems clear to us that organizing material in a teachable and meaningful fashion is far more demanding than this. To confess our own mistakes, our material went originally from the general to the specific; it began with the relativistic form of Maxwell's equations, including the effects of motion, and ended with lumped-parameter devices as special cases. Even if this were a pedagogically tenable approach, which we found it was not, what a bad example to set for students who should be learning to distinguish between the essential and the superfluous! Ideas connected with the propagation of electromagnetic waves (relativistic ideas) must be included in the curriculum, but their connection with media in motion should be made after the student is aware of the first-order issues.

A meaningful presentation to *engineers* must interweave and interrelate mathematical concepts, physical characteristics, the modeling process, and the establishment of a physical "feel" for the world of reality. Our approach is to come to grips with each of these goals as quickly as possible (let the student "get wet" within the first two weeks) and then, while reinforcing what he has learned, continually add something new. Thus, if one looks, he will see the same ideas coming into the flow of material over and over again.

For the organization of this book one should look for many threads of different types. We can list here only a few, in the hope that the subtle reinforcing interplay of mathematical and physical threads will be made evident. Probably the essential theme is Maxwell's equations and the ideas of quasi-statics. The material introduced in Chapter 1 is completely abstract, but it is reinforced in the first few chapters with material that is close to home for the student. By the time he reaches Chapter 10 he will have learned that waves exist which intimately involve electric and magnetic fields that are altogether quasistatic. (This is something that comes as a surprise to many late in life.) Lumped-parameter ideas are based on the integral forms of Maxwell's equations, so that the dynamical effects found with lumped-parameter time constants L/R and RC in Chapter 5 are easily associated with the subjects of magnetic diffusion and charge relaxation. A close tie is made between the "speed voltage" of Chapter 5 and the effects of motion on magnetic fields, as described by field transformations in Chapters 6 to 14. Constant flux dynamics of a lumped coil in Chapter 5 are strongly associated with the dynamics of perfectly conducting continuous media; for example, Alfvén waves in Chapter 12.

Consider another thread of continuity. The book begins with the mathematics of circuit theory. The machines of Chapter 4 are essentially circuits in the sinusoidal steady state. In Chapter 5 we linearize to pursue lumped-parameter ideas of stability and other transient responses and then proceed to nonlinear dynamics, potential-well theory, and other approaches that should form a part of any engineer's mathematical background. By the time

the end of Chapter 10 is reached these ideas will have been carried into the continuum with the addition of tensor concepts, simple cases of the method of characteristics, and eigenvalue theory. The ω-k plot and its implication for all sorts of subjects in modern electrical engineering can be considered as a mathematical or a physical objective. The ideas of stability introduced with ordinary differential equations (exp st) in Chapter 5 evolve into the continuum stability studies of Chapter 10 [exp $j(\omega t - kx)$] and can be regarded as a mathematical or a physical thread in our treatment. We could list many other threads: witness the evolution of energy and thermodynamic notions from Chapters 3 to 5, 5 to 8, and 8 to 13.

We hope that this book is not just one more in the mathematics of electrical engineering or the technical aspects of rotating machines, transducers, delay lines, MHD converters, and so on, but rather that it is the mathematics, the physics, and, most of all, the engineering combined into one.

The material brought together here can be used in a variety of ways. It has been used by Professors C. N. Weygandt and F. D. Ketterer at the University of Pennsylvania for two subjects. The first restricts attention to Chapters 1 to 6 and Appendix B for a course in lumped-parameter electromechanics that both supplants the traditional one on rotating machines in the electrical engineering curriculum and gives the background required for further study in a second term (elective) covering Chapter 7 and beyond. Professors C. D. Hendricks and J. M. Crowley at the University of Illinois have used the material to follow a format that covers up through Chapter 10 in one term but omits much of the material in Chapter 7. Professor W. D. Getty at the University of Michigan has used the material to follow a one-term subject in lumped-parameter electromechanics taught from a different set of notes. Thus he has been able to use the early chapters as a review and to get well into the later chapters in a one-term subject.

At M.I.T. our curriculum seems always to be in a state of change. It is clear that much of the material, Chapters 1 to 10, will be part of our required (core) curriculum for the forseeable future, but the manner in which it is packaged is continually changing. During the fall term, 1967, we covered Chapters 1 to 10 in a one-semester subject taught to juniors and seniors. The material from Chapters 4 and 6 on rotating machines was used selectively, so that students had "a foot solidly in the door" on this important subject but also that the coverage could retain an orientation toward the needs of all the diverse areas found in electrical engineering today. We have found the material useful as the basis for early graduate work and as a starting point in several courses related to electromechanics.

Finally, to those who open this book and then close it with the benediction, "good material but unteachable," we apologize because to them we have not made our point. Perhaps not as presented here, but certainly as it is

represented here, this material is rich in teaching possibilities. The demands on the teacher to see the subject in its total context, especially the related problems that lie between the lines, are significant. We have taught this subject many times to undergraduates, yet each term has been more enjoyable than the last. There are so many ways in which drama can be added to the material, and we do not need to ask the students (bless them) when we have been successful in doing so.

In developing this material we have found lecture demonstrations and demonstration films to be most helpful, both for motivation and for developing understanding. We have learned that when we want a student to see a particular phenomenon it is far better for us to do the experiment and let the student focus his attention on what he should see rather than on the wrong connections and blown fuses that result when he tries to do the experiment himself. The most successful experiments are often the simplest—those that give the student an opportunity to handle the apparatus himself. Every student should "chop up some magnetic field lines" with a copper "axe" or he will never really appreciate the subject. We have also found that some of the more complex demonstrations that are difficult and expensive to store and resurrect each semester come through very well in films. In addition to our own short films, three films have been produced professionally in connection with this material for the National Committee on Electrical Engineering Films, under a grant from the National Science Foundation, by the Education Development Center, Newton, Mass.

Synchronous Machines: Electromechanical Dynamics by H. H. Woodson
Complex Waves I: Propagation, Evanescence and Instability by J. R. Melcher
Complex Waves II: Instability, Convection and Amplification by J. R. Melcher

An additional film is in the early stages of production. Other films that are useful have been produced by the Education Development Center for the National Committee on Fluid Mechanics Films and for the College Physics Film Program. Of particular interest, from the former series, is *Magnetohydrodynamics* by Arthur Shercliff.

A book like this can be produced only with plenty of assistance. We gratefully acknowledge the help we received from many directions and hope we have forgotten no one after seven years of work. First of all we want to acknowledge our students with whom we worked as the material developed. They are the one most essential ingredient in an effort of this sort. Next we want to thank Dr. S. I. Freedman, Professor H. H. Richardson, and Dr. C. V. Smith, Jr., for their assistance in framing worthwhile approaches to several of our key topics. In seven years we have had the help of many able

teachers in presenting this material to students. Their discussions and advice have been most useful. In this category we want particularly to mention Professors H. A. Haus, P. L. Penfield, D. C. White, G. L. Wilson, R. Gallager, and E. Pierson and Doctors J. Reynolds, W. H. Heiser, and A. Kusko. Professor Ketterer, who has taught this material at M.I.T. and the University of Pennsylvania, Professors C. D. Hendricks and J. M. Crowley, who have taught it at M.I.T. and the University of Illinois, and Professor W. D. Getty, who has taught it at M.I.T. and the University of Michigan, have been most generous with their comments. Messrs. Edmund Devitt, John Dressler, and Dr. Kent Edwards have checked the correctness of many of the mathematical treatments. Such a task as typing a manuscript repeatedly is enough to try the patience of anyone. Our young ladies of the keyboard, Miss M. A. Daly, Mrs. D. S. Figgins, Mrs. B. S. Morton, Mrs. E. M. Holmes, and Mrs. M. Mazroff, have been gentle and kind with us.

A lengthy undertaking of this sort can be successful only when it has the backing of a sympathetic administration. This work was started with the helpful support of Professor P. Elias, who was then head of the Department of Electrical Engineering at M.I.T. It was finished with the active encouragement of Professor L. D. Smullin, who is presently head of the Department.

Finally, and most sincerely, we want to acknowledge the perseverance of our families during this effort. Our wives, Blanche S. Woodson and Janet D. Melcher, have been particularly tolerant of the demands of this work.

This book appears in three separately bound, consecutively paged parts that can be used individually or in any combination. Flexibility is ensured by including with each part a complete Table of Contents and Index. In addition, for convenient reference, Parts II and III are supplemented by brief appendices which summarize the relevant material from the preceding chapters. Part III, Chapters 11 to 14, introduces three-dimensional elasticity and fluid dynamics while emphasizing important electromechanical phenomena involving these mechanical models.

H. H. Woodson
J. R. Melcher

Cambridge, Massachusetts
January 1968

CONTENTS

Part I: Discrete Systems

Part II: Fields, Forces, and Motion

Part III: Elastic and Fluid Media

Chapter 11

INTRODUCTION TO THE
ELECTROMECHANICS OF
ELASTIC MEDIA

11.0 INTRODUCTION

Most electromechanical effects and devices involving deformable solid media are best understood in terms of specific models. Elastic membranes and wires are examples of simple one-dimensional and two-dimensional models that can be developed without recourse to a more general theory of elasticity*. Any particular analysis can be developed in this way, and if our objective were to understand specific examples this would be our approach. A more general description of elastic media serves the purpose of giving a larger picture, with the specific examples placed in perspective. Our objective in this chapter is this larger picture. At the same time, examples which emphasize that special models still play an essential role are developed from the general theory.

The material of this chapter is, of course, relevant to the dynamics of a variety of electromechanical interactions with elastic solids. In particular, it relates to areas of electromechanics such as physical acoustics, the microwave electromechanics of crystals, and the development of electromechanical distributed circuits.

The one-dimensional example of a rod subject to longitudinal motions introduced in Section 9.1* illustrates the essential steps required to find the equations of motion for an elastic continuum. First, an equation expressing force equilibrium for a small volume of material is written in terms of the material displacement and the mechanical stresses. Then the stresses are related to the strain, hence to the displacement, by means of the stress-strain relations. The first step, which can be completed without regard to the

* See Chapter 9 or Table 9.2, Appendix G.

651

elastic properties of the material, is given in the next section. The second step, for isotropic media, is found in Section 11.2. In Section 11.5 we introduce enough of the properties of anisotropic materials to consider certain illustrative examples.

11.1 FORCE EQUILIBRIUM

Our first objective is to write an equation that expresses force equilibrium for an element of material. A small cube of the material, centered at (x_1, x_2, x_3), is shown in Fig. 11.1.1. To write Newton's law we must know the instantaneous acceleration of the material at this point. The particles of matter found at (x_1, x_2, x_3) have a displacement from their unstressed position given by

$$\boldsymbol{\delta}(x_1 - \delta_1, x_2 - \delta_2, x_3 - \delta_3, t). \tag{11.1.1}$$

This is true because $\boldsymbol{\delta}(a, b, c, t)$ is defined as the displacement of the particle with an unstressed position (a, b, c).* As pointed out in Section 9.1, displacements are small in many important situations. If we limit ourselves to small displacements, (11.1.1) can be expanded about the position (x_1, x_2, x_3) to give

$$\boldsymbol{\delta}(x_1 - \delta_1, x_2 - \delta_2, x_3 - \delta_3, t)$$
$$= \boldsymbol{\delta}(x_1, x_2, x_3, t) - \frac{\partial \boldsymbol{\delta}}{\partial x_1}\delta_1 - \frac{\partial \boldsymbol{\delta}}{\partial x_2}\delta_2 - \frac{\partial \boldsymbol{\delta}}{\partial x_3}\delta_3 + \cdots. \tag{11.1.2}$$
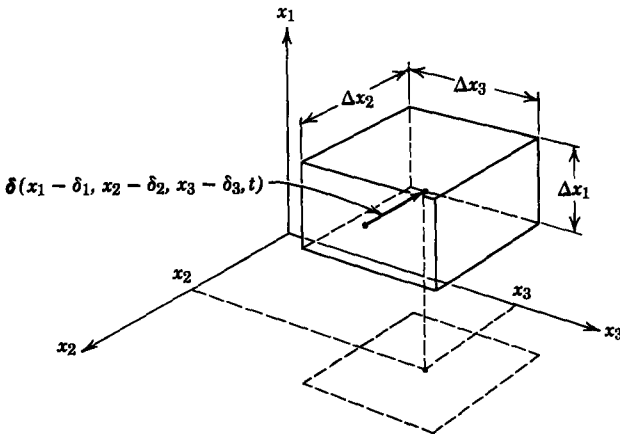
Fig. 11.1.1   Element of material with volume V centered at the position (x_1, x_2, x_3). The grain of material at the center of the cube has the unstressed position $(x_1 - \delta_1, x_2 - \delta_2, x_3 - \delta_3)$.

* A function such as $\boldsymbol{\delta}$, which follows the motion of a particular particle, is said to be written in Lagrangian coordinates. The coordinates indicate the particle under consideration.

If the displacement and its derivatives are small, we can approximate the displacement of the material at the center of the element (Fig. 11.1.1) by the first term on the right, which is the displacement evaluated at the center of the element. Newton's law for the small cube of Fig. 11.1.1 is then

$$\rho \frac{\partial^2 \boldsymbol{\delta}}{\partial t^2} = \mathbf{F}. \tag{11.1.3}$$

Because we ignore products of perturbation quantities, the mass density ρ is a constant in this expression. In an elastic solid there is always a force density $\mathbf{F}$ due to mechanical stresses imposed on the cube by the surrounding material. In the presence of electric or magnetic fields an additional contribution to $\mathbf{F}$ is made by forces of electrical origin. In the next section we develop the relation between elastic stresses and the displacement $\boldsymbol{\delta}$ (for homogeneous media) as a stress tensor, and in Chapter 8 it was found that forces due to free charges or free currents could be written as the divergence of a stress tensor*. Hence we can write (11.1.3) as

$$\rho \frac{\partial^2 \delta_m}{\partial t^2} = \frac{\partial T_{mn}}{\partial x_n}, \tag{11.1.4}$$

where it is understood that the stress tensor T_{mn} is due to mechanical (elastic) interactions and (if they are present in the problem) electrical interactions.

11.2 EQUATIONS OF MOTION FOR ISOTROPIC MEDIA

From (11.1.4) it is apparent that to formulate the equations of motion for an elastic medium it is necessary to make a connection between the applied stresses and the resulting deformations. It was shown in Section 9.1 that for a simple, one-dimensional problem this could be done by introducing the strain, which has a simple relationship both with the deformation of the material and the applied stresses. In the section that follows we consider how the strain gives a description of material deformation, hence the relation between the strain and the displacement of the material. Then in Section 11.2.2 a description is given of the relation between the stress and strain.

11.2.1 Strain-Displacement Relations

Two types of material deformation corresponding to the action of normal and shear stresses on the material, are possible. These are illustrated two-dimensionally in Fig. 11.2.1, in which the points A, B, and C represent tagged grains of material that, when strained, move from A to A', B to B', and C to C'. Note that in the unstrained condition the lines joining the tagged points are parallel to the coordinate axes. Because the effects considered are linear,

---

* See Sec. 8.2 or Appendix G.
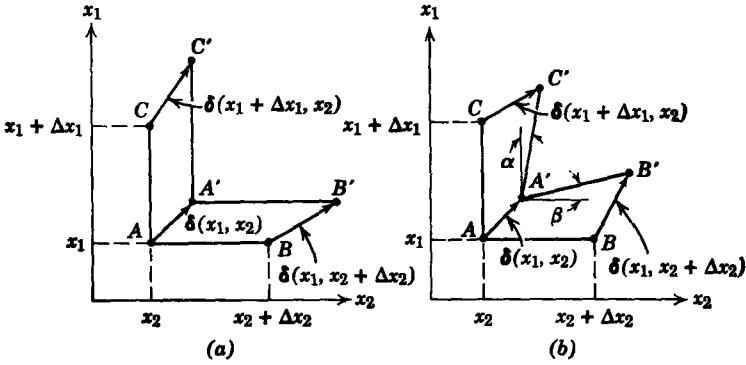
Fig. 11.2.1   (a) Strain produced by normal stresses; (b) strain produced by shear stresses.

the deformations can be considered separately and then superimposed. We shall shortly develop the strain from a formal point of view, and this will make the superposition principle more apparent. At first our development is more intuitive.

In Fig. 11.2.1a the deformation has lengthened the distances AB and AC to the distances $A'B'$ and $A'C'$, whereas in Fig. 11.2.1b these lengths have remained constant but the angles between the sides of the cube of material have changed. The first of the two types of deformation is a generalization of the kind of strain considered in Section 9.1 (the thin elastic rod); that is, we can *define* a normal strain in each of the axis directions as an elongation per unit length. In the x_1-direction this is

$$e_{11} = \lim_{\Delta x_1 \to 0} \frac{\delta_1(x_1 + \Delta x_1, x_2) - \delta_1(x_1, x_2)}{\Delta x_1} = \frac{\partial \delta_1}{\partial x_1}, \tag{11.2.1}$$

where $\delta(x_1, x_2, x_3, t)$ is the material displacement at the point x_1, x_2, x_3, as discussed in Section 11.1. Similarly,

$$e_{22} = \frac{\partial \delta_2}{\partial x_2}, \tag{11.2.2}$$

$$e_{33} = \frac{\partial \delta_3}{\partial x_3}. \tag{11.2.3}$$

In the second kind of deformation (Fig. 11.2.1b) the sides of the cube keep their original length but are deflected with respect to each other to an angle different from the original 90°. This strain is caused by the shear stresses (T_{12}, T_{31}, etc.) and can be visualized by placing the covers of a book under shear, as shown in Fig. 11.2.2. (The significance of the stress components is discussed in Section 8.2 and Appendix G.)

The shear-strains, like the normal strains, are *defined* functions. They are defined as one half the tangent of the change in angle between the originally perpendicular sides of the cube (Fig. 11.2.1b) in the limit in which the cube becomes very small. Hence in the diagram of Fig. 11.2.1b the strain resulting from a change in angle with respect to the x_1 and x_2 axes is designated e_{12}.

In terms of the angles defined in Fig. 11.2.1b the strain e_{12} is

$$e_{12} = \lim_{\substack{\Delta x_1 \to 0 \\ \Delta x_2 \to 0}} \tfrac{1}{2} \tan [\alpha + \beta] \qquad (11.2.4)$$

Note that a positive shear strain signifies that the angle between the originally perpendicular lines is less than 90°.

In Chapter 9, Example 9.1.1 was used to illustrate that the deformations commonly encountered in elastic solids are very small. For this reason the angles of deflection due to shear stresses are also commonly small and the tangent function in (11.2.4) can be approximated by the argument $(\alpha + \beta)$. For the same reason the angles α and β can in turn be approximated by their tangents to write

$$\alpha \approx \frac{[\delta_2(x_1 + \Delta x_1, x_2) - \delta_2(x_1, x_2)]}{\Delta x_1},$$

$$\beta \approx \frac{[\delta_1(x_1, x_2 + \Delta x_2) - \delta_1(x_1, x_2)]}{\Delta x_2}, \qquad (11.2.5)$$

(11.2.4) then becomes

$$e_{12} = \lim_{\substack{\Delta x_1 \to 0 \\ \Delta x_2 \to 0}} \frac{1}{2}\left\{\frac{[\delta_2(x_1 + \Delta x_1, x_2) - \delta_2(x_1, x_2)]}{\Delta x_1} + \frac{[\delta_1(x_1, x_2 + \Delta x_2) - \delta_1(x_1, x_2)]}{\Delta x_2}\right\},$$

$$(11.2.6)$$
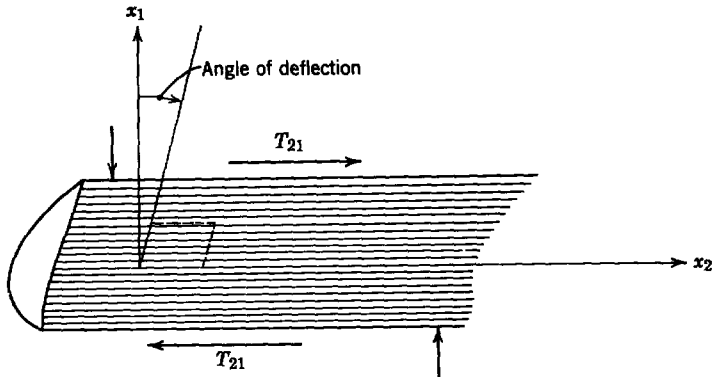
Fig. 11.2.2 Simple situation in which shear stresses result in a shear strain (the angle of deflection).

and in the limit we obtain a point relation between the component of strain e_{12} and the displacements:

$$e_{12} = \frac{1}{2}\left(\frac{\partial \delta_1}{\partial x_2} + \frac{\partial \delta_2}{\partial x_1}\right);$$ (11.2.7)

that is, e_{12} is evaluated at the unstressed position A. In the process of taking the limit in which $\Delta x_1 \to 0$ and $\Delta x_2 \to 0$ all of the approximations in going from (11.2.4) to (11.2.7) become exact except the one requiring small angular deflections, which remains the basic limitation of the theory.

A two-dimensional picture of shear strain has been used so far because it is easily visualized. A three-dimensional description of the strain follows by considering the deflections between the other two pairs of axes, with the results

$$e_{13} = \frac{1}{2}\left(\frac{\partial \delta_1}{\partial x_3} + \frac{\partial \delta_3}{\partial x_1}\right),$$ (11.2.8)

$$e_{23} = \frac{1}{2}\left(\frac{\partial \delta_2}{\partial x_3} + \frac{\partial \delta_3}{\partial x_2}\right).$$ (11.2.9)

The last three expressions make it evident that $e_{ij} = e_{ji}$, as would be expected from the definition of the shear strain. Altogether, we have defined nine components of the strain, which are presumably sufficient to describe the distortions of the material in the vicinity of a point x_1, x_2, x_3 related to the stress. We can summarize all the strain components with the expression

$$e_{ij} = \frac{1}{2}\left(\frac{\partial \delta_i}{\partial x_j} + \frac{\partial \delta_j}{\partial x_i}\right).$$ (11.2.10)

Note that e_{ij} is a Lagrangian variable in that it is evaluated at the unstressed position of a grain of material (A in Fig. 11.2.1). As discussed in Section 11.1, because the deflections are small it will not be necessary to distinguish between the strain evaluated at the unstressed position of the material and the strain evaluated at the stressed position of the material.

11.2.1a A Formal Derivation

Our remarks about the strain have so far been aimed at establishing the physical significance of each of the nine components. We have not shown in a formal way that the components e_{ij} are sufficient to describe the relative distortions of the material caused by the stresses (although e_{ij} does include all possible space derivatives of δ). To do so we must consider a general material deformation rather than the two particular forms shown in Fig. 11.2.1. The reasoning used now parallels that of the preceding discussion in that we again consider the relative positions of grains of matter.
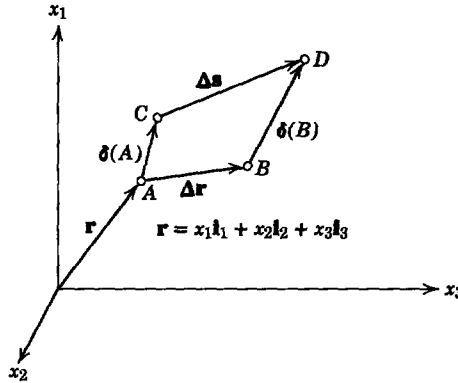
Fig. 11.2.3 Displacement of grains of matter in the unstressed positions A and B and final separation Δs.

Figure 11.2.3 shows two grains of material in the unstrained positions A and B. When the material is subjected to stress, these grains move to the new positions C and D. We are interested in that part of the material distortion that is produced by the stress. Hence we are not interested (when we define the strain) in a uniform translation of the material, or, as we shall see momentarily, we are not interested in uniform rotations of the material. The strain is defined to describe the stretching of the material between the points A and B; hence attention is given to the distance between the points originally at A and B, as they are distorted to points C and D. At first the relative displacement is Δr, whereas after the stress is applied the relative displacement is Δs, as shown in Fig. 11.2.3.

The coordinate of the material at A is r. By taking Δr ($\Delta r = \Delta x_1 i_1 + \Delta x_2 i_2 + \Delta x_3 i_3$) to be small it is possible to find the separation Δs between the points in the strained positions C and D. First, vector addition of the displacement components shown in Fig. 11.2.3 gives

$$\Delta s = \Delta r + \delta(B) - \delta(A), \qquad (11.2.11)$$

which becomes approximately (writing the ith component)*

$$\Delta s_i = \Delta x_i + \delta_i(x_1 + \Delta x_1,\, x_2 + \Delta x_2,\, x_3 + \Delta x_3,\, t) - \delta_i(x_1,\, x_2,\, x_3,\, t)$$

$$\cong \Delta x_i + \frac{\partial \delta_i}{\partial x_1} \Delta x_1 + \frac{\partial \delta_i}{\partial x_2} \Delta x_2 + \frac{\partial \delta_i}{\partial x_3} \Delta x_3$$

$$\equiv \Delta x_i + \frac{\partial \delta_i}{\delta x_k} \Delta x_k. \qquad (11.2.12)$$

* See Appendix G for index notation.

Now, if the quantity $\frac{1}{2}(\partial \delta_k / \partial x_i)\,\Delta x_k$ is both added to and subtracted from this equation, we obtain

$$\Delta s_i = \Delta x_i + \frac{1}{2}\left(\frac{\partial \delta_i}{\partial x_k} - \frac{\partial \delta_k}{\partial x_i}\right)\Delta x_k + \frac{1}{2}\left(\frac{\partial \delta_i}{\partial x_k} + \frac{\partial \delta_k}{\partial x_i}\right)\Delta x_k. \quad (11.2.13)$$

Here we have an expression for the ith component of the directed distance $\Delta \mathbf{s}$ between the points A and B after the material has been subjected to stress. This distance is written as a function of the initial distance $\Delta \mathbf{r}$ and the displacement $\boldsymbol{\delta}$ of the material in the vicinity of A. Note that in (11.2.13) the derivatives of $\boldsymbol{\delta}$ are evaluated at the unstressed position A.

In writing (11.2.13), we have divided the expression for the relative positions of A and B into a part that is due to a pure (rigid body) rotation of the material in the vicinity of A and a part resulting because of the material distortions produced by the applied stress. We have already agreed that a pure translation, and similarly a pure rotation, involve no strain deformation in the material. The bracketed part of the second term on the right in (11.2.13) is one component of the vector $\nabla \times \boldsymbol{\delta}$. Hence it describes a rotation of the material about the unstressed position A. This may be verified by defining a rotation vector $\boldsymbol{\Omega}$ in terms of the components of $\boldsymbol{\delta}$.

$$\boldsymbol{\Omega} = \frac{1}{2}\left(\frac{\partial \delta_3}{\partial x_2} - \frac{\partial \delta_2}{\partial x_3}\right)\mathbf{i}_1 + \frac{1}{2}\left(\frac{\partial \delta_1}{\partial x_3} - \frac{\partial \delta_3}{\partial x_1}\right)\mathbf{i}_2 + \frac{1}{2}\left(\frac{\partial \delta_2}{\partial x_1} - \frac{\partial \delta_1}{\partial x_2}\right)\mathbf{i}_3. \quad (11.2.14)$$

Then the second term in (11.2.13) can be written in terms of $\boldsymbol{\Omega}$ as

$$\frac{1}{2}\left(\frac{\partial \delta_i}{\partial x_k} - \frac{\partial \delta_k}{\partial x_i}\right)\Delta x_k = (\boldsymbol{\Omega} \times \Delta \mathbf{r})_i. \quad (11.2.15)$$

This is not obvious unless one substitutes (11.2.14) into (11.2.15).

Without specifying the direction of $\boldsymbol{\Omega}$, we can conclude from (11.2.15) that since $\boldsymbol{\Omega} \times \Delta \mathbf{r}$ is perpendicular to $\Delta \mathbf{r}$ the relative displacement represented by this term is also perpendicular to $\Delta \mathbf{r}$. In Fig. 11.2.4 the stressed and unstressed positions of the material are shown in the case in which the contribution of the last term in (11.2.13) is zero. The material initially at points A and B undergoes a uniform translation and then, because $\boldsymbol{\Omega}$ is perpendicular to $\Delta \mathbf{r}$, a rigid body rotation.

It is apparently the last term in (11.2.13) that represents a distortion of the material and therefore should be defined as the strain. This is, of course, consistent with our definition of the strain e_{ij} in the preceding section (11.2.10). In view of this definition, (11.2.13) provides an expression for the relative positions of two material particles with the initial relative positions $\Delta \mathbf{r}$.

$$\Delta s_i = \Delta x_i + (\boldsymbol{\Omega} \times \Delta \mathbf{r})_i + e_{ij}\,\Delta x_j. \quad (11.2.16)$$
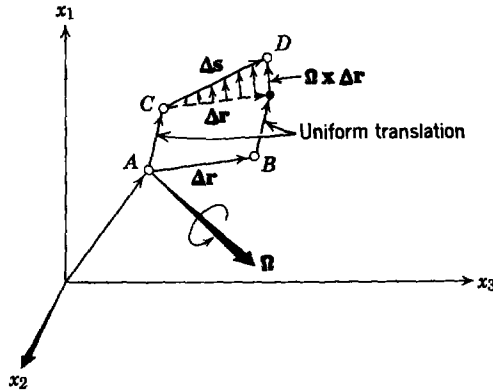
Fig. 11.2.4 Displacements of grains of matter in the undeformed positions A and B and deformed positions C and D. This material has suffered a uniform translation and a rigid body rotation.

The strain e_{ij} is evaluated at the unstressed position of the material. As mentioned in Section 11.2.1, however, we commit a negligible error by evaluating it at the stressed position of the material.

The strain has been defined in such a way that it has the transformation properties of a tensor. This purely mathematical fact is shown in the next section.

11.2.1b   *The Strain as a Tensor*

We can confirm that the components e_{ij} form a tensor by using the fact that the displacement $\boldsymbol{\delta}$ is a vector. Our discussion here parallels that given in Section 8.2.2 in which we used the transformation properties of the vector traction $\boldsymbol{\tau}$ to show that the stress was a tensor. In a similar way we begin here with the transformation of $\boldsymbol{\delta}$ to a primed coordinate system:

$$\delta_i' = a_{il}\delta_l. \tag{11.2.17}$$

A discussion of this vector transformation and the direction cosines a_{il} was given in Section 8.2.2 and is summarized in Appendix G.

It follows from (11.2.17) that since components of a_{il} are not functions of x_i

$$\frac{\partial \delta_i'}{\partial x_j'} = a_{il}\frac{\partial \delta_l}{\partial x_j'} = a_{il}\frac{\partial x_k}{\partial x_j'}\frac{\partial \delta_l}{\partial x_k}. \tag{11.2.18}$$

The position vector $\mathbf{r} = x_1\mathbf{i}_1 + x_2\mathbf{i}_2 + x_3\mathbf{i}_3$ is also transformed from a primed coordinate system by an equation in the form of [see (8.2.18) and (8.2.19)]

$$x_k = a_{jk}x_j'; \tag{11.2.19}$$

from this expression it follows that

$$\frac{\partial x_k}{\partial x'_j} = a_{jk} \qquad (11.2.20)$$

and (11.2.18) becomes

$$\frac{\partial \delta'_i}{\partial x'_j} = a_{il} a_{jk} \frac{\partial \delta_l}{\partial x_k}. \qquad (11.2.21)$$

The steps leading to this equation can be repeated with the indices i and j reversed.

The strain e'_{ij} in the primed coordinate system is by definition

$$e'_{ij} = \frac{1}{2}\left(\frac{\partial \delta'_i}{\partial x'_j} + \frac{\partial \delta'_j}{\partial x'_i}\right). \qquad (11.2.22)$$

The first derivative on the right in this expression is replaced by (11.2.21), whereas the second derivative is replaced by (11.2.21), with i and j reversed:

$$e'_{ij} = \frac{1}{2}\left(a_{il} a_{jk} \frac{\partial \delta_l}{\partial x_k} + a_{jl} a_{ik} \frac{\partial \delta_l}{\partial x_k}\right). \qquad (11.2.23)$$

We are required to sum over the indices l and k, and so these indices can be reversed in the second term on the right-hand side of this expression, which then becomes the desired transformation equation for e_{ij}:

$$e'_{ij} = a_{ik} a_{jl} e_{kl}. \qquad (11.2.24)$$

This expression for the transformation of the strain is the same as that found in Section 8.2.2 for the transformation of the stress T_{ij}; for example, the expressions for the components of stress in a cylindrical coordinate system, as derived in Example 8.2.5, could also be used here by replacing $T_{ij} \rightarrow e_{ij}$.

11.2.2 Stress–Strain Relations

Our objective in defining the strain was to provide a function of the material displacements δ that could be directly related to the stress. The relations between the components of strain and stress depend on material properties. A particular stress–strain relation was discussed in Section 9.1, in which the modulus of elasticity was introduced as an experimentally determined constant of proportionality between a one-dimensional normal stress and strain*. In this section we generalize this simple stress–strain relation to three-dimensional isotropic solids but again confine ourselves to those solids that can be modeled by an algebraically linear dependence of strain on the stress. This is not unduly restrictive because virtually all elastic media of interest to us are represented adequately by this model. In any case the stress–strain relations are ultimately empirical. Therefore it is reasonable to propose several simple experiments that lead to an understanding of them.

* See Table 9.2, Appendix G.
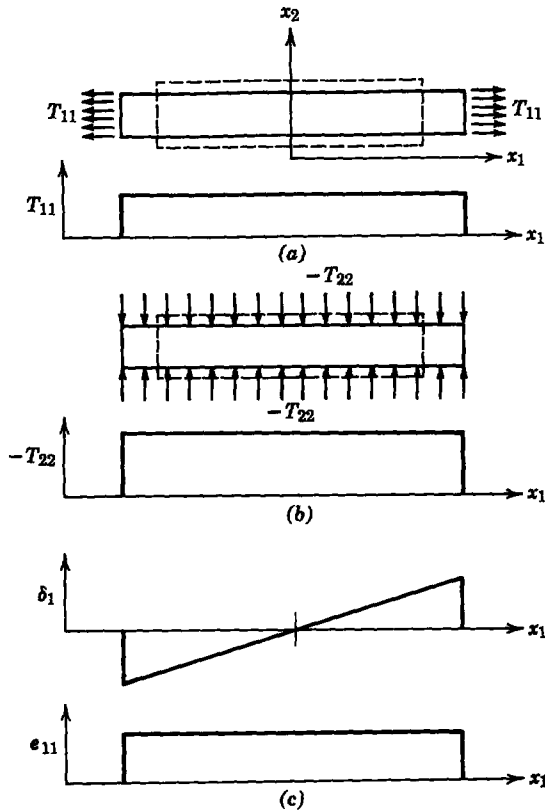
Fig. 11.2.5 (a) Deformations of a block due to a uniform normal stress T_{11}; (b) deformations identical to (a) produced by a uniform normal stress $-T_{22}$; (c) displacement and normal strain in the x_1-direction for both (a) and (b).

First, the effect of applying a normal stress to a block of material is considered. In Fig. 11.2.5 two ways of applying a normal stress are shown. Both can result in the same deformation of the material. A normal stress T_{11} is applied to the x_1-surfaces of the block in Fig. 11.2.5a; the result is elongation of the block in the x_1-direction. If no stresses are applied to the x_2 (or x_3)-surfaces, there is, in addition, a contraction of the material in the x_2 (and x_3)-directions. This "necking down" of the material is familiar to anyone who has observed what happens when a rubber band is stretched.

Figure 11.2.5b shows the same deformation of the bar as in Fig. 11.2.5a, except that the stress is now compressional and normal to the x_2-surfaces. Here the material is "squeezed out" in the x_1-directions by the stress T_{22}, which also reduces the thickness of the block. The x_1-displacement $\delta_1(x_1)$ of the block in each situation is shown in Fig. 11.2.5c. We see that e_{11} is

uniform over the length of the bar. In Fig. 11.2.5 the block is assumed to be constrained so that there are no displacements in the x_3-direction. Of course, in three-dimensional displacements a stress T_{11} could also produce displacements in the x_3-direction and a stress T_{33} could produce displacements in the x_1-direction.

To account for this experiment two constants E and ν are defined such that

$$e_{11} = \frac{1}{E}\,[T_{11} - \nu(T_{22} + T_{33})]. \tag{11.2.25}$$

This equation provides that a negative T_{22} can produce the same strain e_{11} as a positive T_{11}. The x_3-direction is equivalent to the x_2-direction in our experiment, hence T_{33} enters in (11.2.25) in the same way as T_{22}.

Because the material is isotropic, we can make the same arguments for the other components of the strain and write

$$e_{22} = \frac{1}{E}\,[T_{22} - \nu(T_{33} + T_{11})], \tag{11.2.26}$$

$$e_{33} = \frac{1}{E}\,[T_{33} - \nu(T_{11} + T_{22})]. \tag{11.2.27}$$

As pointed out in Chapter 9, E is called the modulus of elasticity, or Young's modulus, and (11.2.25) reduces to the stress-strain relation for a thin rod by setting $T_{22} = T_{33} = 0$. We comment further on the significance of this approximation in Section 11.4. The constant ν, which accounts for the necking down of the material in Fig. 11.2.5a, is called *Poisson's ratio*. Materials that are isotropic, hence could possibly be modeled by (11.2.25) to (11.2.27), are usually a conglomeration of minute crystals. Although each individual crystal is not isotropic, the conglomeration is isotropic on a macroscale. The physical properties of such materials are extremely difficult to predict. For this reason E and ν may be regarded as experimentally determined constants.
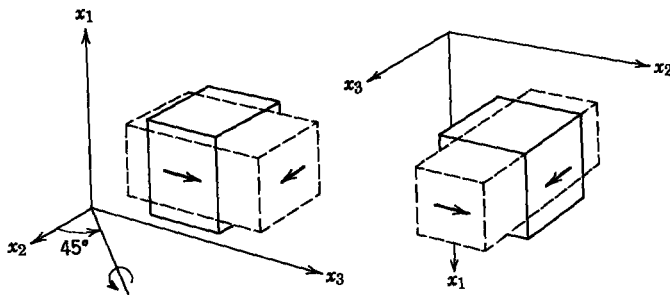
Fig. 11.2.6 Hypothetical situation in which a normal strain results from a shear stress.
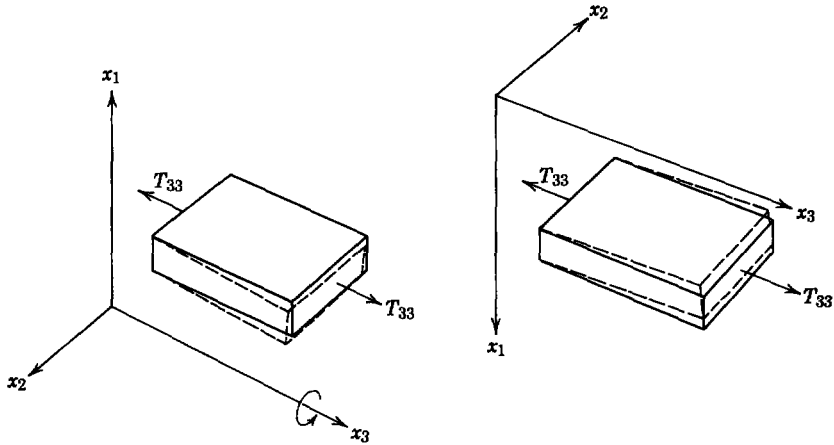
Fig. 11.2.7   Hypothetical situation in which a shear strain results from a normal stress.

In writing (11.2.25) to (11.2.27), we have not only assumed that the material is isotropic but that the normal strains do not depend on the shear stresses. A simple mental experiment shows that these assumptions are the same. Suppose a situation occurs in which normal strain results from a shear stress, as shown in Fig. 11.2.6. A rotation of the coordinates makes it evident that the same stress would give a very different strain, a result that contradicts our assumption of an isotropic material (a material with properties that do not depend on the orientation of the coordinates relative to the material).

This same kind of isotropy argument can be used to show that shear strains cannot depend on normal stresses. Now the conjecture is that we have shear strains that result from normal stresses, as shown in Fig. 11.2.7. Again, a rotation of the coordinate system as shown requires that the same normal stress produce the opposite shear strain.

Physical intuition tells us that each shear strain should be proportional to the corresponding shear stress. As an example, Fig. 11.2.8 shows a block of material subject to the shear stresses T_{13} and T_{31}. The change in angle

Fig. 11.2.8   The shear strain e_{13} results from the shear stresses T_{13} and T_{31}.

between the originally perpendicular sides of the block is in direct proportion to the applied stress. Hence

$$e_{ij} = \frac{T_{ij}}{2G}, \qquad i \neq j, \tag{11.2.28}$$

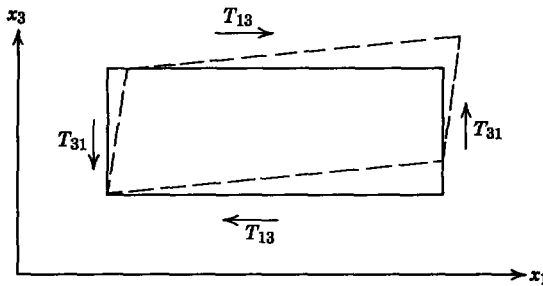where G is an experimentally determined constant called the *shear modulus*. In drawing Fig. 11.2.8 we have assumed that $T_{13} = T_{31}$, for otherwise there would be a net torque on the material. This assumption is implicit in (11.2.8), for we have already shown that $e_{ij} = e_{ji}$ (11.2.10).

Given the stress, we can use (11.2.25) to (11.2.28) to find any component of the strain. If, however, we made independent measurements of ν, E, and G, we would be expending more effort than necessary, since, in fact, these constants are related. An example illustrates this point.

Example 11.2.1. Figure 11.2.9 shows a cube of material that is subject to the shear stresses $T_{12} = T_{21} = T_0$ in the x_1, x_2, x_3-coordinate system. It is clear from this diagram that the components of the stress, viewed from the x_1', x_2', x_3'-coordinate system, are not in
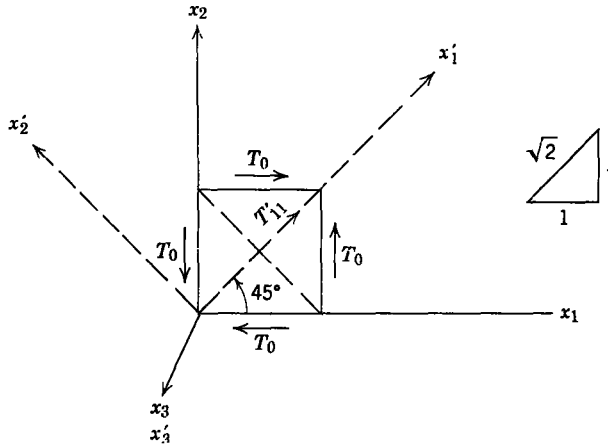
Fig. 11.2.9 A simple example of a pure shear in the x_j frame which transforms into a pure tension and compression in the x_i' frame.

shear but in tension and compression. It is because of this fact that E, ν, and G are not independent constants. A calculation of the strain e_{ij}', viewed in the x_i'-frame serves to illustrate this point.

The x_i'-coordinates of a point in space can be found from the x_j-coordinates by the transformation $x_i = a_{ij}x_j$ (Section 8.2.2 or Appendix G), in which

$$a_{ij} = \begin{bmatrix} \dfrac{1}{\sqrt{2}} & \dfrac{1}{\sqrt{2}} & 0 \\[2ex] -\dfrac{1}{\sqrt{2}} & \dfrac{1}{\sqrt{2}} & 0 \\[2ex] 0 & 0 & 1 \end{bmatrix}. \tag{a}$$

We are given that the material supports the stress

$$T_{ij} = \begin{bmatrix} 0 & T_0 & 0 \\ T_0 & 0 & 0 \\ 0 & 0 & 0 \end{bmatrix}, \tag{b}$$

hence from (11.2.28) that the material undergoes the strain

$$e_{ij} = \begin{bmatrix} 0 & \dfrac{T_0}{2G} & 0 \\ \dfrac{T_0}{2G} & 0 & 0 \\ 0 & 0 & 0 \end{bmatrix}. \tag{c}$$

The advantage of writing the stress and strain as tensors is that their components can be found in the x_i'-frame by means of the transformations $T_{ij}' = a_{ik}a_{jl}T_{kl}$ and $e_{ij}' = a_{ik}a_{jl}e_{kl}$. Hence from the last three equations it follows that

$$e_{ij}' = \begin{bmatrix} \dfrac{T_0}{2G} & 0 & 0 \\ 0 & -\dfrac{T_0}{2G} & 0 \\ 0 & 0 & 0 \end{bmatrix} \tag{d}$$

and

$$T_{ij}' = \begin{bmatrix} T_0 & 0 & 0 \\ 0 & -T_0 & 0 \\ 0 & 0 & 0 \end{bmatrix}, \tag{e}$$

or, as we suspected, the components of the stress and strain are purely diagonal. Because the material is isotropic, the stress-strain relations must hold, regardless of the coordinate system; that is, (11.2.25) to (11.2.28) must also hold for e_{ij}' and T_{ij}', and it follows from the above equations that

$$\frac{T_0}{2G} = \frac{1}{E}(T_0 + \nu T_0) \tag{f}$$

or

$$G = \frac{E}{2(1 + \nu)}. \tag{g}$$

This result is important, for it indicates that there are only two independent constants necessary to define the stress-strain relations for an isotropic material; for example, given the modulus of elasticity E and Poisson's ratio ν, the shear modulus G can be found from (g).

Characteristic values of ν and G are given in Table 11.2.1.

Table 11.2.1   Shear Modulus and Poisson's Ratio for Various Materials*

Material	G-units of 10^{10} N/m²	ν
Aluminum (pure and alloy)	2.55–3.65	0.32–0.34
Brass (60–70% Cu, 40–30% Zn)	3.6–4.1	0.33–0.36
Copper	4.0–4.6	0.33–0.36
Iron, cast (2.7–3.6% C)	3.6–5.6	0.21–0.30
Steel (carbon and low alloy)	7.6–8.2	0.26–0.29
Stainless steel (18% Cr, 8% Ni)	7.3	0.30
Titanium (pure and alloy)	4.1	0.34
Glass	2.6–3.2	0.21–0.27

* See Table 9.1 Appendix G for references and values of E, ρ, and $\sqrt{E/\rho}$.

11.2.3   Summary of Equations

We shall be occupied with electromechanical problems in which the stress T_{ij} and the displacement δ_i are the important variables. Therefore it is desirable to eliminate the strain as a variable from (11.2.25) through (11.2.28).

For the off-diagonal terms this leads directly to the stress as a function of the displacement, but for the diagonal terms three simultaneous conditions on the components T_{11}, T_{22}, and T_{33} result:

$$
\begin{aligned}
e_{11} &= \frac{1}{E}\,[T_{11} - \nu(T_{22} + T_{33})] = \frac{\partial \delta_1}{\partial x_1}, \\[2mm]
e_{22} &= \frac{1}{E}\,[T_{22} - \nu(T_{33} + T_{11})] = \frac{\partial \delta_2}{\partial x_2}, \\[2mm]
e_{33} &= \frac{1}{E}\,[T_{33} - \nu(T_{11} + T_{22})] = \frac{\partial \delta_3}{\partial x_3}.
\end{aligned}
\tag{11.2.29}
$$

These equations can be solved for T_{11}, T_{22}, and T_{33} in terms of the derivatives of δ to provide the diagonal terms in the expression (remember, we sum on a subscript that appears twice),

$$
T_{ij} =
\begin{bmatrix}
2G\dfrac{\partial \delta_1}{\partial x_1} + \lambda\dfrac{\partial \delta_k}{\partial x_k} & G\left(\dfrac{\partial \delta_1}{\partial x_2} + \dfrac{\partial \delta_2}{\partial x_1}\right) & G\left(\dfrac{\partial \delta_1}{\partial x_3} + \dfrac{\partial \delta_3}{\partial x_1}\right) \\[4mm]
G\left(\dfrac{\partial \delta_2}{\partial x_1} + \dfrac{\partial \delta_1}{\partial x_2}\right) & 2G\dfrac{\partial \delta_2}{\partial x_2} + \lambda\dfrac{\partial \delta_k}{\partial x_k} & G\left(\dfrac{\partial \delta_2}{\partial x_3} + \dfrac{\partial \delta_3}{\partial x_2}\right) \\[4mm]
G\left(\dfrac{\partial \delta_3}{\partial x_1} + \dfrac{\partial \delta_1}{\partial x_3}\right) & G\left(\dfrac{\partial \delta_3}{\partial x_2} + \dfrac{\partial \delta_2}{\partial x_3}\right) & 2G\dfrac{\partial \delta_3}{\partial x_3} + \lambda\dfrac{\partial \delta_k}{\partial x_k}
\end{bmatrix},
\tag{11.2.30}
$$

where (g) of Example 11.2.1 has been used to reduce the number of constants to two and λ is an elastic constant given by

$$\lambda = \frac{\nu E}{(1 + \nu)(1 - 2\nu)}. \tag{11.2.31}$$

The off-diagonal terms in 11.2.30 are given by (11.2.28). The parameter λ has been introduced purely for convenience and is sometimes called the Lamé constant.

The expression for the stress in terms of the displacements, given by (11.2.30), can be summarized in a compact form by using the Kronecker delta function introduced in Section 8.1.

$$T_{ij} = G\left(\frac{\partial \delta_i}{\partial x_j} + \frac{\partial \delta_j}{\partial x_i}\right) + \lambda \delta_{ij} \frac{\partial \delta_k}{\partial x_k}. \tag{11.2.32}$$

Remember that $\delta_{ij} = 0$ for $i \neq j$ [the off-diagonal terms in (11.2.30)], whereas $\delta_{ij} = 1$ if $i = j$ [the diagonal terms in (11.2.30)].

If there are no other forces acting on the elastic material besides the force arising from the elastic stresses given by (11.2.32), we shall have completed the task of finding the equations of motion for the material; that is, the stress given by (11.2.32) can be substituted into the force equation (11.1.4) to provide one vector equation for δ. In this equation the force density of elastic origin is $F_i = \partial T_{ij}/\partial x_j$. It is often more convenient to write the force density in vector notation. The following manipulations illustrate the use of tensor notation.

First, we simply write out the tensor divergence of (11.2.32):

$$F_i = \frac{\partial T_{ij}}{\partial x_j} = G\left(\frac{\partial^2 \delta_i}{\partial x_j \, \partial x_j} + \frac{\partial^2 \delta_j}{\partial x_i \, \partial x_j}\right) + \lambda \delta_{ij} \frac{\partial^2 \delta_k}{\partial x_j \, \partial x_k}. \tag{11.2.33}$$

The first term on the right will be recognized as $G\,\nabla^2\delta$, the second is the ith component of $G\,\nabla(\nabla \cdot \delta)$ and the last has value only when $i = j$ so that it is the ith component of $\lambda\,\nabla(\nabla \cdot \delta)$. Hence we can write (in vector notation)

$$\mathbf{F} = G\,\nabla^2\delta + (G + \lambda)\,\nabla(\nabla \cdot \delta). \tag{11.2.34}$$

It must be remembered that $\nabla^2\delta$ is a vector Laplacian defined by $\nabla^2\delta = \nabla(\nabla \cdot \delta) - \nabla \times (\nabla \times \delta)$, so that (11.2.34) can also be written

$$\mathbf{F} = (2G + \lambda)\,\nabla(\nabla \cdot \delta) - G\,\nabla \times (\nabla \times \delta). \tag{11.2.35}$$

This is a useful form of the force density because the material displacements leading to $\nabla \cdot \delta$ and $\nabla \times \delta$ are easily visualized. We defer this point until Section 11.4.

The elastic forces, represented by (11.2.35), are held in dynamical equilibrium by other forces that act on the material. As pointed out in Section 11.1,

Table 11.2.2   Equations Which Describe the Motions of Isotropic Perfectly Elastic Media

Force equation

$$\rho \frac{\partial^2 \delta_i}{\partial t^2} = \frac{\partial T_{ij}}{\partial x_j} + (F_{\text{ex}})_i \qquad \text{(tensor form)} \qquad (11.1.4)$$

$$\rho \frac{\partial^2 \delta}{\partial t^2} = (2G + \lambda) \nabla(\nabla \cdot \delta) - G\nabla \times (\nabla \times \delta) + \mathbf{F}_{\text{ex}} \qquad \text{(vector form)} \qquad (11.2.35)$$

Stress equation

$$T_{ij} = 2Ge_{ij} + \lambda \delta_{ij} e_{kk} \qquad \text{(Hooke's law)} \qquad (11.2.32)$$

$$T_{ij} = G\left(\frac{\partial \delta_i}{\partial x_j} + \frac{\partial \delta_j}{\partial x_i} \right) + \lambda \delta_{ij} \frac{\partial \delta_k}{\partial x_k} \qquad \text{(stress-displacement)} \qquad (11.2.32)$$

Strain equation

$$e_{ij} = \frac{1}{2} \left(\frac{\partial \delta_i}{\partial x_j} + \frac{\partial \delta_j}{\partial x_i} \right) \qquad \text{(strain-displacement)} \qquad (11.2.10)$$

$$e_{ij} = \frac{1}{2G} T_{ij} - \frac{\nu}{E} \delta_{ij} T_{kk} \qquad \text{(Hooke's law)} \qquad \begin{matrix}(11.2.28)\\(11.2.29)\end{matrix}$$

Relations among constants

$$\lambda = \frac{\nu E}{(1 + \nu)(1 - 2\nu)} \qquad (11.2.31)$$

$$G = \frac{E}{2(1+\nu)} \qquad \text{(g) of Example 11.2.1}$$

one of these forces (per unit volume) is an inertial force. In addition, there may be force densities produced by gravity or electromagnetic fields. The last two externally produced forces are called $\mathbf{F}_{\text{ex}}$ in the summary of equations given in Table 11.2.2. Other basic equations and relations of elasticity are shown in Table 11.2.2; equation numbers indicate their places in the text.

11.3   ELECTROMECHANICAL BOUNDARY CONDITIONS

Electromechanical coupling with elastic media often occurs through boundary conditions. One-dimensional illustrations of this type of problem were given in Sections 9.1.2. and 9.2.2, in which the boundary condition entered as the requirement of equilibrium for a mechanical terminal pair. In these examples the boundary condition related the stress and displacement at a given point in space. In this section we consider the more general three-dimensional situation.

Boundary conditions are required to describe solutions for the stress and displacement in a region in which material properties undergo abrupt changes. We have made general comments about boundary conditions in connection with the magnetic and electric field equations (Section 6.2)*. We have assumed that the field equations hold in the region of the discontinuity and performed integrations of these equations over the appropriate volumes or surfaces to provide the required "jump" conditions on the fields. Although the displacement vector and stress, like the electric and magnetic fields, are defined by differential equations that can be integrated through an abrupt change in material properties, the analogy is not complete. We were able to assume that Maxwell's equations applied throughout all the volume of interest. The equations of elasticity, however, apply only to a region occupied by an elastic solid and not, for example, to an adjoining region filled with fluid. Hence the boundary conditions resulting from an integration of (11.2.35) over a volume enclosing a section of the interface between two elastic materials are restricted to problems involving just elastic materials. Actually, the situation is not so complicated because a variety of physical problems is modeled by equations in the *form* of (11.1.4), if we are willing to recognize the stress T_{mn} as the total stress acting on the material. Because in writing this equation there are no implications regarding the relationship between T_{mn} and the material motions, we can use (11.1.4) to write a boundary condition of some generality.

In Section 11.1 it was pointed out that because the displacements δ are small no distinction need be made between the Lagrangian and Eulerian representations. We find it convenient here to view the equations of motion as though they were written in Lagrangian coordinates, that is, as though (x_1, x_2, x_3) denoted the unstrained position of the particle that is instantaneously displaced from (x_1, x_2, x_3) by the amount $\delta(x_1, x_2, x_3)$. We can define a surface in three dimensions by the equations

$$\begin{aligned} x_1 &= a(u, v), \\ x_2 &= b(u, v), \\ x_3 &= c(u, v), \end{aligned} \qquad (11.3.1)$$

where (u, v) are parameters, each pair of which defines a particular point on the boundary. When the boundary deforms, due to a material strain, particles on the boundary are then found at the position

$$\begin{aligned} x_1 &= a + \delta_1(a, b, c, t), \\ x_2 &= b + \delta_2(a, b, c, t), \\ x_3 &= c + \delta_3(a, b, c, t). \end{aligned} \qquad (11.3.2)$$

Hence the motion of a particular particle on the boundary in the unstrained position (a, b, c) is defined by (11.3.2). We now consider the situation in

* See Table 6.1, Appendix G.

which elastic media [regions (1) and (2) in Fig. 11.3.1] are joined along the boundary defined by (11.3.2). It is clear that if the boundary is to be well defined one of our boundary conditions is

$$\boldsymbol{\delta}^{(2)}(a, b, c, t) = \boldsymbol{\delta}^{(1)}(a, b, c, t).$$ (11.3.3)

This condition can also be considered a necessary consequence of our equations of motion, for if the displacement is not a continuous function the strain, hence the stress (which depends on rates of change of the displacement with respect to position), becomes singular at the boundary.

We are now in a position to integrate (11.1.4) over a small volume that includes the boundary.

$$\int_V \rho \frac{\partial^2 \delta_i}{\partial t^2} \, dV = \int_V \frac{\partial T_{ij}}{\partial x_j} \, dV.$$ (11.3.4)

The volume V is fixed with its center at the position (a, b, c), as shown in Fig. 11.3.1. The integration is carried out over the Lagrangian variables (x_1, x_2, x_3). Hence the time derivative and space integration on the left side of (11.3.4) can be reversed in order. The integral of the divergence of a stress tensor over a volume (see Section 8.1 or Appendix G) can be converted to a surface integral, and (11.3.4) becomes [variations in ρ with time are of the same order as $\boldsymbol{\delta}$, hence are second order in (11.3.4)]

$$\frac{\partial^2}{\partial t^2} \int_V \rho \delta_i \, dV = \oint_S T_{ij} n_j \, da.$$ (11.3.5)

We consider the situation in which the dimensions of the surfaces A (shown in Fig. 11.3.1) are small compared with the radius of curvature of the boundary but large compared with the thickness Δ of the volume element
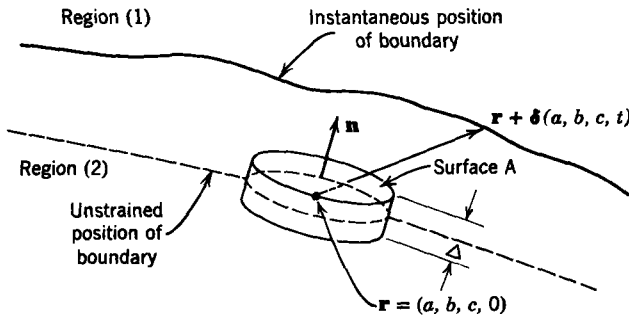

Fig. 11.3.1 Unstrained and strained (instantaneous) interface between regions (1) and (2). A small volume V, with normal **n**, encloses a section of the interface. Note that an integration over the volume centered at $(a, b, c, 0)$ is an integration over a volume that remains centered on the moving interface.

Then, if ρ and δ are finite, the volume integral of (11.3.5) vanishes as $\Delta \to 0$. Sometimes physical situations can be described by an elastic medium, bounded by a heavy layer of material. In these cases the effect of the layer of material is approximated by including a surface mass density ρ_s. Mathematically, the surface mass density is a singularity in the mass density ρ in the same way that the surface charge density is a singularity in the charge density (Section 6.2.2). Then the integral over the volume retains a finite value, and as $\Delta \to 0$ (11.3.5) can be approximated as

$$\rho_s \frac{\partial^2 \delta_i}{\partial t^2} = [T_{ij}^{(1)} - T_{ij}^{(2)}]n_j, \quad \text{on the boundary,} \tag{11.3.6}$$

where we have divided through by the area A and assumed that the stresses are always finite.

The boundary condition used in Section 9.1.2 was a special case of (11.3.6), in which the stresses T_{ij} were in part due to the elastic strains and in part to a force of electric origin. The condition of (11.3.5) is the continuum-mechanical extension of the requirement used in Chapter 2 that the sum of all forces applied to a mechanical node must be equal to the inertial force associated with that node. The right-hand side of (11.3.6) is the net traction (force per unit area), whereas the left side is an inertial force per unit area.

11.4   WAVES IN ISOTROPIC ELASTIC MEDIA

This section is devoted to establishing a picture of the kinds of dynamical behavior that can be expected in dealing with elastic materials. To this end, we extend the notions introduced in Chapter 9 and recognize that the vibrations of continuous media in three dimensions can also be understood in terms of waves and normal modes. We have already used simple elastic models in Chapters 9 and 10 to illustrate transverse and longitudinal motions in one and two dimensions (the thin rod and membrane). We now consider these motions in three dimensions.

11.4.1   Waves in Infinite Media

In the absence of externally applied forces $\mathbf{F}_{ex}$ the motions of an elastic material are described by (11.2.35), written as

$$\rho \frac{\partial^2 \delta}{\partial t^2} = (2G + \lambda) \nabla(\nabla \cdot \delta) - G \nabla \times (\nabla \times \delta) \tag{11.4.1}$$

This equation is in a particularly convenient form because it makes it possible to distinguish between two essentially different kinds of material displacement. If we take the divergence of (11.4.1), the time and space derivatives can

be permuted to obtain

$$\rho \frac{\partial^2 \psi}{\partial t^2} = (2G + \lambda)\, \nabla^2 \psi, \qquad\qquad (11.4.2)$$

where

$$\psi = \nabla \cdot \mathbf{\delta}$$

and where use has been made of the identity $\nabla \cdot (\nabla \times \mathbf{A}) \equiv 0$. In the same way the curl of (11.4.1) gives*

$$\rho \frac{\partial^2 \mathbf{C}}{\partial t^2} = G\, \nabla^2 \mathbf{C}, \qquad\qquad (11.4.3)$$

where $\mathbf{C} = \nabla \times \mathbf{\delta}$ and use has been made of the identity $\nabla \times (\nabla f) \equiv 0$. The scalar function ψ and vector function $\mathbf{C}$ represent kinds of displacement that are analogous to the field intensities $\mathbf{E}$ and $\mathbf{H}$ used to formulate Maxwell's equations. The function ψ can be thought of as a source of the displacement $\mathbf{\delta}$ in the same sense as the charge density ρ_f is a source of the electric displacement $\mathbf{D}$ [see (1.1.12)]†. Hence the displacements represented by ψ have the same character as the electric displacement that originates or terminates on the charge ρ_f. An intuitive example is shown in Fig. 11.4.1. In a region in which ψ is found to be positive the material displacements tend to diverge. Similarly, the material converges toward regions in which ψ is negative (just as electric lines of force end on negative charge).

Deformations that can be represented by the function ψ are referred to as dilatational, for they represent outward or inward displacements of the material that lead to a change in the volume occupied by the material.

In a similar way $\mathbf{C}$ can be thought of as a "current" that gives rise to a displacement $\mathbf{\delta}$ in the same way as an electrical current gives rise to a magnetic field $\mathbf{H}$ [see (Eq. 1.1.1)]†. The material displacements tend to follow circular paths about the vector $\mathbf{C}$, as shown in Fig. 11.4.2.
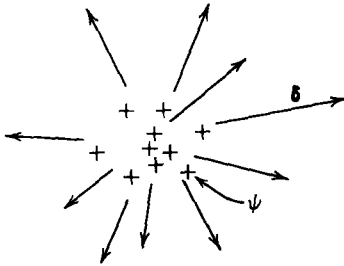

Fig. 11.4.1 Dilatational displacements $\mathbf{\delta}$ represented by the source function ψ.
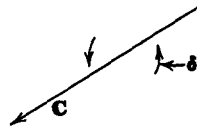

Fig. 11.4.2 Curl displacements represented by $\mathbf{C}$. The material tends to circulate about the vector field $\mathbf{C}$.

* $\nabla \times (\nabla \times \mathbf{C}) = \nabla(\nabla \cdot \mathbf{C}) - \nabla^2 \mathbf{C}$
† Table 1.2, Appendix G.

The components of C and the function ψ satisfy equations of the same form. Equations 11.4.2 and 11.4.3 are three-dimensional forms of the wave equation. The essential feature emphasized by these equations [illustrated one-dimensionally by (9.1.13) to (9.1.15)] is the propagating nature of the solutions. Dilatational motions apparently propagate more rapidly than the rotational motions. The wave dynamics are most easily seen by considering two one-dimensional special cases.

Example 11.4.1. Consider a one-dimensional dilatational motion that depends on $x_1 = x$. Then $\partial/\partial x_2 = \partial/\partial x_3 = 0$ and (11.4.2) becomes

$$\frac{\partial^2 \psi}{\partial t^2} = a_c^2 \frac{\partial^2 \psi}{\partial x^2}, \tag{a}$$

where

$$a_c = \left(\frac{2G + \lambda}{\rho}\right)^{1/2}.$$

A discussion of solutions to this wave equation was given in Section 9.1.1. To obtain a physical picture of the mechanics we consider a solution that is sinusoidal in space and time.

$$\psi = \psi_0 \sin\left[\omega\left(t - \frac{x}{a_c}\right)\right]. \tag{b}$$

This solution can be justified by direct substitution into (a) and can be thought of as a wave propagating with the phase velocity a_c in the x-direction.

Within an arbitrary constant that would be determined by the boundary conditions, the actual displacements follow from $\psi = \nabla \cdot \boldsymbol{\delta}$.

$$\delta = \frac{\psi_0 a_c}{\omega} \cos\left[\omega\left(t - \frac{x}{a_c}\right)\right]. \tag{c}$$

At a given instant these displacements appear as shown in Fig. 11.4.3. Note that the material is displaced out of the regions of positive ψ and into regions of negative ψ. We can imagine painting equidistant parallel lines in the unstressed material. Then a wave propagating perpendicular to these lines would distort their relative positions as shown in Fig. 11.4.3b. The material density is increased where the lines are closest together and where ψ is negative. Points of constant phase in the density distribution propagate to the right with the phase velocity a_c. Longitudinal waves of this kind are referred to as *compressional, acoustic,* or *dilatational.* Actually, they are a close relative of the compressional waves on a thin rod, encountered in Section 9.1.1. If the expressions for λ and G given in Tables 11.2.2 and 11.4.1 are used to write a_c as a function of E and ν (Poisson's ratio), we obtain

$$a_c = \left(\frac{E}{\rho}\right)^{1/2} N(\nu), \tag{d}$$

where

$$N(\nu) = \left[\frac{1 - \nu}{(1 + \nu)(1 - 2\nu)}\right]^{1/2}.$$

Measured values of ν are given in Table 11.2.1 and can be seen to fall between about 0.2 and 0.5. The function $N(\nu)$ in this range is shown in Fig. 11.4.4 and is greater than 1.
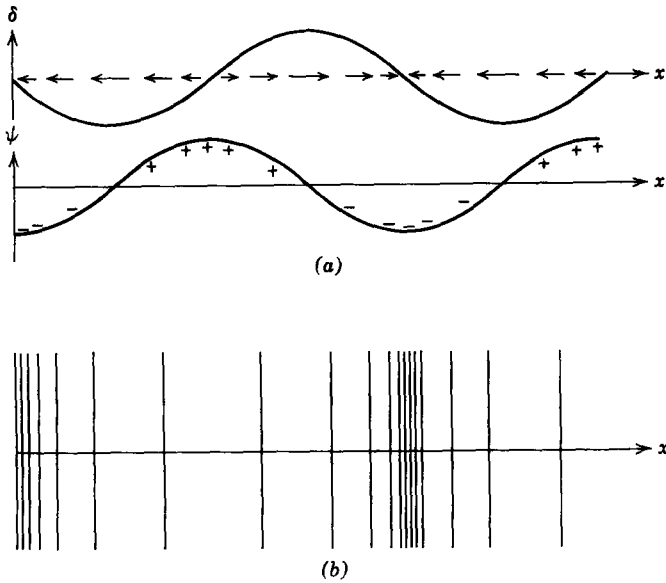
(a)

(b)

Fig. 11.4.3 Instantaneous view of the displacements δ and source function ψ for a one-dimensional dilatational wave: (a) relative distributions of δ and ψ; (b) exaggerated appearance of originally equidistant lines painted on the material. Lines compressed together indicate a compression of the material.
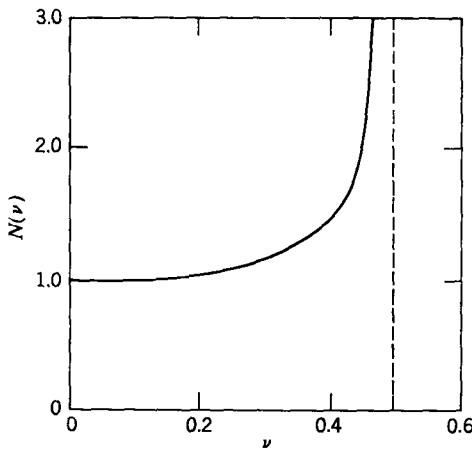

Fig. 11.4.4 The function $N(\nu)$, where ν is Poisson's ratio. Plane dilatational waves propagate with the velocity $a_c = (\sqrt{E/\rho})N$, whereas waves on a thin rod have the velocity $\sqrt{E/\rho}$. Hence N is the ratio of a_c to the acoustic velocity on a thin rod.

Remember that Poisson's ratio entered in the stress-strain relations because a longitudinal stress could lead to transverse displacements (Fig. 11.2.5). By assuming that the material motions were one-dimensional in nature, we have required that there be no transverse displacements. This means that there is a transverse stress (T_{22} or T_{33}) that can be computed from (11.2.26) and (11.2.27) with $e_{22} = e_{33} = 0$; for example,

$$T_{22} = \frac{\nu(1 + \nu)}{1 - \nu^2} T_{11}. \tag{e}$$

This stress tends to constrain the material from the sides and, through Poisson's ratio, to stiffen the material to longitudinal deformations. For this reason we have found a phase velocity a_c that always exceeds the velocity of waves on a thin rod $\sqrt{E/\rho}$. In the thin rod the transverse stresses are zero because of the free surfaces on the rod and longitudinal motions are not affected by Poisson's ratio. We see now that there are actually transverse material displacements on a thin rod. This point is discussed further in Section 11.4.2a, where we define the conditions under which a thin rod model can be used.

Dilatational waves involve normal stresses and normal strains. By contrast the rotational motions constitute a shearing of the medium. The next example illustrates these shear deformations in a one-dimensional case.

Example 11.4.2.   In one dimension ($x_1 = x$) the rotational equations (11.4.3) become

$$\frac{\partial^2 C_2}{\partial t^2} = a_s^2 \frac{\partial^2 C_2}{\partial x^2}, \tag{a}$$

$$\frac{\partial^2 C_3}{\partial t^2} = a_s^2 \frac{\partial^2 C_3}{\partial x^2}, \tag{b}$$

where $a_s = \sqrt{G/\rho}$ and because $\partial/\partial x_2 = \partial/\partial x_3 = 0$, $C_1 = 0$. By definition, the components C_2 and C_3 are related to the displacement by

$$C_2 = -\frac{\partial \delta_3}{\partial x}, \qquad C_3 = \frac{\partial \delta_2}{\partial x}. \tag{c}$$

Once again, the equations of motion (a) and (b) are wave equations. Now, however, the phase velocity a_s of the waves is less than the compressional wave velocity a_c in Example 11.4.1 and the corresponding material deformations are altogether different. The component C_2 represents displacements in the x_3-direction. Similarly, C_3 represents transverse motions of the elastic material in the x_2-direction. Because the stresses and strains are in shear rather than compression, transverse waves of this kind are referred to as *shear waves* or *waves of distortion*.

If we assume that the boundary conditions are such that only C_3 is excited, a traveling wave solution to (b) appears as shown in Fig. 11.4.5. In this figure the material displaces in the x_2-direction or in a direction that is perpendicular to both C_3 and the direction of propagation. Note that material tends to rotate about the vector C (Fig. 11.4.2) and that the local material density does not change as it did in the dilatational waves.

In this section we have seen that in an infinite medium we can separate rotational or shearing deformations from dilatational motions. Except in a few simple cases, elastic materials deform in such a way that both shearing
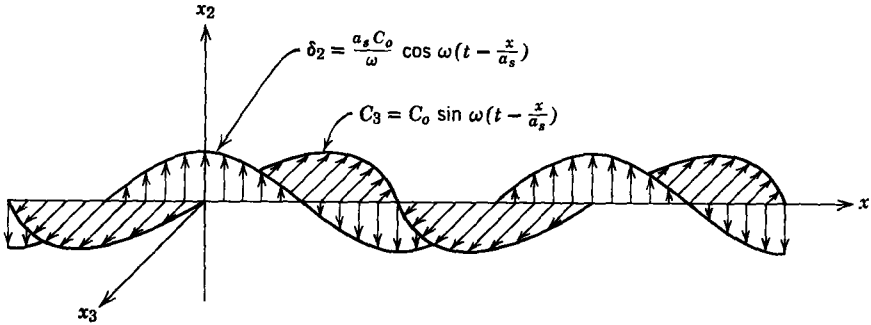
Fig. 11.4.5 Traveling shear wave, showing the spacial relation between material displacements δ_2 and the rotational vector component C_3. Note that material tends to "rotate" about the vector $C_3 i_3$, as shown in Fig. 11.4.2.

and dilatation are present. This is true because both types of motion must be present to satisfy boundary conditions.

A simple case in which the one-dimensional dilatational motions predicted by (11.4.2) are an exact solution even in the presence of boundaries is shown in Fig. 11.4.6. Here the transverse boundaries of a bar are constrained by rigid walls that prevent transverse motions but do not inhibit longitudinal motions. Given a driving condition at one end and a boundary condition at the other, the problem can be solved in a manner identical to that used for the thin rod in Section 9.1. If, however, the transverse walls constrain the bar in the x-direction or fail to constrain the transverse displacements, the motions are no longer purely dilatational. Shear strains are required to satisfy the boundary conditions.

The block of material shown in Fig. 11.4.7 is subject to boundary conditions that are satisfied by purely shearing motions. Here one edge is rigidly attached to a wall that prevents both perpendicular motion and slip. The opposite end is driven by a time-varying stress $T_{21} = T_o(t)$. The resulting motions are predicted by (11.4.3) if the boundaries transverse to the x-axis are driven by the same time-varying shear stress $T_{21}(x, t)$ (see Example 11.4.3 for a solution), but if these transverse boundaries are constrained by a rigid wall, or are free
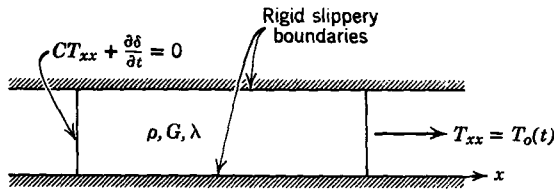

Fig. 11.4.6 An elastic bar with boundaries that permit purely dilatational motions in the x-direction.
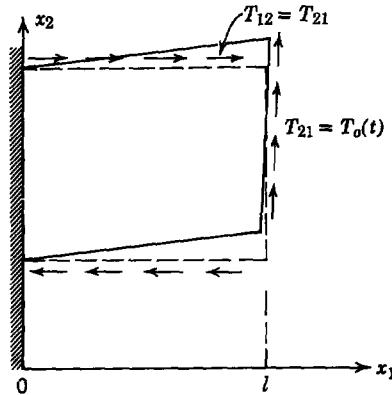
Fig. 11.4.7 An elastic bar with boundaries and driving stresses that permit purely shearing motions in the x_2-direction.

of stress, the motions must include a dilatational part; that is, any other boundary condition than that shown in Fig. 11.4.7 will couple the rotational and dilatational motions.

Because boundary conditions usually couple the compressional and shearing motions, any dynamical problem will involve a combination of the characteristic velocities a_s and a_c. These velocities are tabulated, along with characteristic values of λ, in Table 11.4.1.

Table 11.4.1   Phase Velocities for Shear and Compressional Waves in an Infinite Medium*

Material	λ (units of 10^{11} N/m^2)	a_s (units of 10^3 m/sec)	a_c (units of 10^3 m/sec)
Aluminum	0.626	3.0	6.35
Brass	1.04	2.2	4.7
Copper	1.17	2.3	4.8
Iron, cast	0.836	2.8	5.2
Steel	1.18	3.2	6.0
Stainless steel	1.19	3.0	5.8
Titanium	0.904	3.0	6.2
Glass	0.366	2.9	5.1

* When ranges of E, v, and G are given in Tables 9.1 (Appendix G) and 11.2.1, the largest values have been used.

Example 11.4.3.   In this example we seek to establish a further familiarity with shearing deformations. Figure 11.4.8 shows a slab of material rigidly attached to a wall at $x = 0$ and driven with a shear stress $T_{21} = \text{Re}\,[\hat{T}e^{j\omega t}]$ at $x = l$. The slab has infinite extent in the x_2- and x_3-directions; hence it is reasonable to assume that the motions are one-dimensional
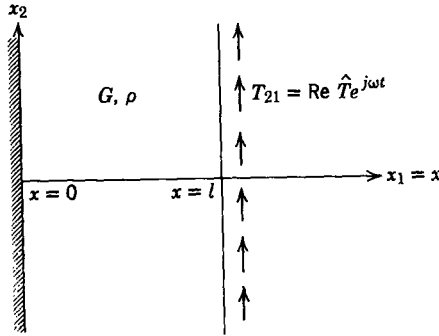
Fig. 11.4.8   An infinite slab of elastic material subjected to the uniformly distributed shear stress $T_{21} = \text{Re}\,(\hat{T}e^{j\omega t})$ at $x = l$ and fixed at $x = 0$.

$(\partial/\partial x_2 = \partial/\partial x_3 = 0)$. The following questions are to be answered: (1) What is the displacement of the material as a function of (x, t)? (2) If boundaries are introduced at $x_2 = 0$ and $x_2 = L$, what boundary conditions are required to make the one-dimensional assumption correct? (3) if the peak shear stress applied at $x = l$ is equal to 1 atm, what is the largest displacement of the material (as an example, consider a slab made of brass, $l = 1$ m, and the low frequency limit at which $\omega \to 0$). (4) At a frequency of 1 kc what is the least value of l required to produce a resonance?

1. The excitation tends to produce displacements δ_2, hence we guess that $C_2 = 0$. Our guess is justified if we can satisfy both differential equations and boundary conditions. Equations (b) and (c) of Example 11.4.2 then give

$$\frac{\partial^2 \delta}{\partial t^2} = a_s{}^2 \frac{\partial^2 \delta}{\partial x^2}, \tag{a}$$

where $\delta_2 = \delta$ and $x_1 = x$. Two boundary conditions are necessary to determine fully the sinusoidal steady-state solution to this equation. These conditions are evident from the statement of the problem

$$T_{21}(l, t) = \text{Re}\,(\hat{T}e^{j\omega t}) = G\frac{\partial \delta}{\partial x}(l, t) \tag{b}$$

and

$$\delta(0, t) = 0. \tag{c}$$

Now, if we assume solutions with the same frequency as the excitation

$$\delta = \text{Re}\,(\hat{\delta}e^{j\omega t}), \tag{d}$$

the unknown function $\hat{\delta}(x)$ can be found by substituting (d) into (a) and solving the resulting ordinary differential equation. Hence

$$\hat{\delta} = A \sin kx + B \cos kx, \tag{e}$$

where

$$k = \frac{\omega}{a_s}$$

and A and B are arbitrary constants determined by the boundary conditions. Condition (c) shows that $B = 0$, whereas condition (b) determines A as

$$A = \frac{\hat{T}}{kG \cos kl.}$$ (f)

It follows from (d) and (e) that the required solution for the displacement is

$$\delta = \text{Re} \left[\frac{\hat{T} \sin kx \, e^{j\omega t}}{kG \cos kl} \right].$$ (g)

2. In our solution all displacements are zero except $\delta_2 = \delta$, as given by (g). There are two components of stress (11.2.32). One was used to match the boundary condition at $x = l$:

$$T_{21} = G \frac{\partial \delta}{\partial x} = \text{Re} \left[\frac{\hat{T} \cos kx \, e^{j\omega t}}{\cos kl} \right].$$ (h)

The other is present because $T_{ij} = T_{ji}$ or, in particular,

$$T_{12} = T_{21}.$$ (i)

Hence, if the slab has boundaries at $x_2 = 0$ and $x_2 = L$, our solution will be correct only if there is a shearing stress on these boundaries given by (h) and (i). Note that this stress is a function of both x and t. In the limit at which $L \gg l$, we expect that the stress excitation on the transverse boundaries can be ignored and our one-dimensional solution will be approximately correct, regardless of the boundary conditions at $x_2 = 0$ and $x_2 = L$.

3. In the limit at which $\omega \to 0$ (quasi-static motions) $k \to 0$ and (g) shows that the peak δ occurs at $x = l$, where (since 1 atm $= 1.013 \times 10^5$ N/m^2 and G can be found from Table 11.2.1) (g) gives

$$|\delta|_{\text{peak}} = \frac{|\hat{T}|l}{G} = (1.01 \times 10^5)(1)/4.1 \times 10^{10}$$

$$= 2.5 \times 10^{-6} \text{ m} \quad \left(\text{about } \frac{1}{10,000} \text{ in.} \right)$$ (j)

We see that static deflections are likely to be very small.

4. The slab is in a resonant state when the denominator of (g) becomes zero or when

$$kl = \frac{n\pi}{2}, \qquad n = 1, 3, 5, \dots$$ (k)

Hence the smallest value of l that will produce a resonance at 1 kc (a_s in Table 11.4.1) is

$$l = \frac{\pi a_s}{2\omega} = \pi 2.2 \times \frac{10^3}{2(2\pi \times 10^3)} = 0.55 \text{ m}.$$ (l)

Under these conditions the 0.55-m thickness of the brass slab represents one quarter of a wavelength.

11.4.2 Principal Modes of Simple Structures

In most dynamical situations involving elastic media boundaries play an important role. Our development makes it natural to think of these boundaries
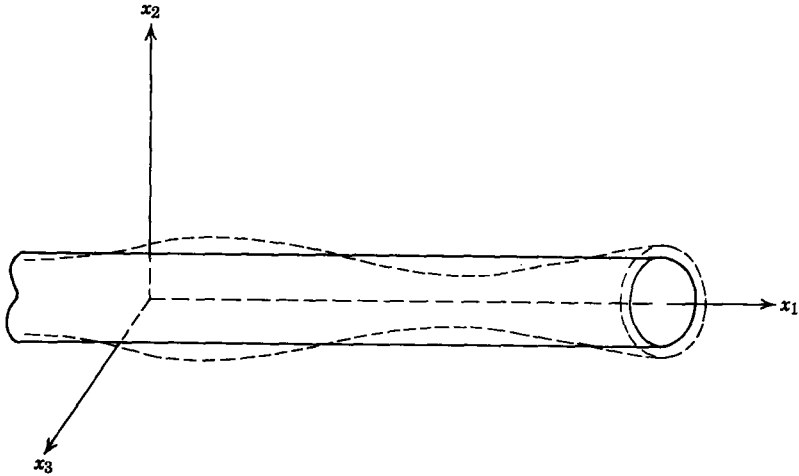
Fig. 11.4.9 A thin elastic rod with a longitudinal axis x_1 and transverse coordinates x_2 and x_3. An exaggerated transverse distortion of the material is shown as it accompanies longitudinal compression and extension of the rod.

as two types: longitudinal and transverse; that is, the elastic structure usually has one dimension that is greater than the others, such as the x-direction for the thin rod of Fig. 11.4.9, and it is natural to analyze the dynamics in terms of wave propagation in that direction. Conditions applied at discrete positions along the x_1-axis, referred to as longitudinal boundary conditions, were discussed in Section 9.1.1*b*. The extremities of the material in the x_2- and x_3-directions are referred to as transverse boundaries. It is the purpose of this section to introduce the effect that the transverse boundaries have on wave propagation in the longitudinal direction.*

   Even in the absence of electromechanical interactions, wave propagation in the presence of material boundaries is an involved subject. It serves our purposes here to consider two cases, both of which make the essential point in a simple way and have practical value. First, we reconsider in the light of three-dimensional elasticity the thin rod. Then in Section 11.4.2*b* the transverse motions of a thin beam are analyzed. In each of these cases it is assumed that the longitudinal wavelengths of interest are large compared with the transverse dimensions. In the general case in which no approximations are made concerning the wavelength, thin elastic structures support an infinite set of modes, each having a different dependence on the transverse coordinates. Most of these modes do not propagate at low frequencies. The waves on a thin rod and on a thin beam, as considered in Sections 11.4.2*a* and 11.4.2*b*,

---

* For those familiar with the theory of guided electromagnetic waves the waves of Section 11.4.1 are waves in "free space," whereas those discussed here are guided waves analogous to those found in a waveguide.

propagate even as the frequency approaches zero. Among all modes that are generally possible, they assume considerable practical importance and are called the *principal modes* of their respective structures. In Section 11.4.3 we illustrate the nature of the higher order modes by considering the dynamics of a plate subject to a shearing excitation. Here we find that at low frequencies the higher order modes appear as evanescent waves; hence we again encounter the topic of spatially growing (decaying) waves discussed in Section 10.1.2. A detailed presentation of wave propagation in elastic plates and cylinders is of interest* in the design of delay lines and electromechanical filters to be used at high frequencies (e.g., megahertz). At high frequencies the higher order modes are inadvertently excited because longitudinal wavelengths are on the order of the transverse dimensions.

11.4.2a   The Thin Rod

A thin elastic rod is shown in Fig. 11.4.9. In static equilibrium it has the geometry of a right circular cylinder, with its axis in the x_1-direction. An approximate description of the longitudinal motions was given in Section 9.1†. We are interested in having a second look at the dynamics to see what transverse motions of the material are implied by the three-dimensional equations of elasticity. We can argue that the equation of motion is the same as that found in Section 9.1 for longitudinal deformations by observing that the transverse surfaces of the rod are free of externally applied stresses. Hence, if the rod is very thin, the stresses T_{22}, T_{33} (essentially normal to the transverse surface) and T_{12} and T_{13} (essentially the shear stress on the surface) cannot be very different from zero inside the rod. This is the starting point in writing an approximate equation of motion.

Because we take $T_{12} = T_{13} = 0$, the force equation in the x_1-direction (11.1.4) becomes

$$\rho \frac{\partial^2 \delta_1}{\partial t^2} = \frac{\partial T_{11}}{\partial x_1} . \qquad (11.4.4)$$

In addition, because $T_{22} = T_{33} = 0$, (11.2.29) of Table 11.2.2 shows that

$$e_{11} = \frac{\partial \delta_1}{\partial x_1} = \left(\frac{1}{2G} - \frac{\nu}{E} \right) T_{11} \qquad , \qquad (11.4.5)$$

and because $G = E/2(1 + \nu)$ we obtain

$$T_{11} = E \frac{\partial \delta_1}{\partial x_1} . \qquad (11.4.6)$$

---

* See W. P. Mason, *Physical Acoustics*, Vol. I, Part A, Academic, New York, 1964, p. 111.
† Table 9.2, Appendix G.

This will be recognized as the relation used in Section 9.1. It follows from (11.4.4) and (11.4.6) that the longitudinal displacement is predicted by the equation

$$\rho \frac{\partial^2 \delta_1}{\partial t^2} = E \frac{\partial^2 \delta_1}{\partial x_1^2}. \tag{11.4.7}$$

Although they do not enter in the equation of motion, transverse displacements do accompany $\delta_1(x_1, t)$. They can be computed under the assumption that δ_1 is a known function. From (11.2.32) and the condition that the normal stress on the transverse boundaries be zero we have

$$T_{22} = 0 = (2G + \lambda) \frac{\partial \delta_2}{\partial x_2} + \lambda \left(\frac{\partial \delta_1}{\partial x_1} + \frac{\partial \delta_3}{\partial x_3} \right), \tag{11.4.8}$$

$$T_{33} = 0 = (2G + \lambda) \frac{\partial \delta_3}{\partial x_3} + \lambda \left(\frac{\partial \delta_1}{\partial x_1} + \frac{\partial \delta_2}{\partial x_2} \right). \tag{11.4.9}$$

Presumably, we have solved (11.4.7). Hence these last two equations can be simultaneously solved for $\partial \delta_2 / \partial x_2$ or $\partial \delta_3 / \partial x_3$; for example,

$$\frac{\partial \delta_2}{\partial x_2} = \frac{-\lambda}{2(G + \lambda)} \frac{\partial \delta_1}{\partial x_1} (x_1, t). \tag{11.4.10}$$

The right-hand side of this equation is dependent only on (x_1, t). Hence it can be integrated to obtain

$$\delta_2 = \frac{-\lambda}{2(G + \lambda)} \frac{\partial \delta_1}{\partial x_1} x_2 + f(x_1, x_3, t), \tag{11.4.11}$$

where f is an arbitrary function determined by the cross-sectional geometry; for example, if the rod is a right-circular cylinder, coaxial with the x_1-axis, symmetry requires that $\delta_2(x_1, 0, x_3) = 0$ or that $f = 0$. Similarly,

$$\delta_3 = \frac{-\lambda}{2(G + \lambda)} \frac{\partial \delta_1}{\partial x_1} x_3 + g(x_1, x_2, t), \tag{11.4.12}$$

where $g = 0$ for a right-circular cylinder. The last two equations show that the transverse displacements are largest for the material with the greatest distance from the x_1-axis. In regions in which the rate of change with respect to x_1 is large the transverse displacements are also large.

As an example, consider the traveling wave

$$\delta_1 = \delta_0 \sin (\omega t - kx_1), \tag{11.4.13}$$

where (11.4.7) shows that $\omega = k\sqrt{E/\rho}$. Then from (11.4.11)

$$\delta_2 = \frac{\delta_0 \lambda k x_2}{2(G + \lambda)} \cos (\omega t - kx_1). \tag{11.4.14}$$
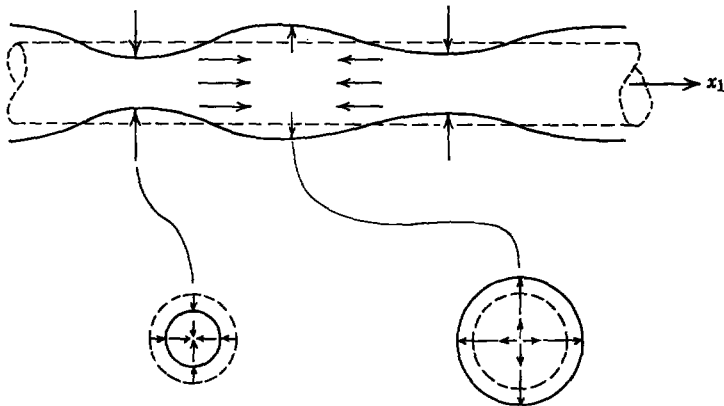
Fig. 11.4.10 An instantaneous view of displacements that accompany a compressional wave traveling in the x_1-direction on a thin rod. The transverse displacements are exaggerated in this figure.

The displacements represented by the last two equations can be pictured as shown in Fig. 11.4.10.

In retrospect, we see that δ_2 and δ_3 were ignored in the longitudinal force equation and were then found from the predicted displacements δ_1. This procedure is analogous to a quasi-static analysis (Sections B.2.2 and 9.1.3) in which variations with respect to time are at first ignored and then computed as second-order effects. In the rod, two-dimensional effects are second order and the analysis may be referred to as quasi-one-dimensional. Other quasi-one-dimensional models are introduced in the next section and in Chapter 13. Such models, which reduce the significant effects to a dependence on a single coordinate, are of considerable importance not only in continuum electromechanics but in many other areas as well. Very often they are referred to as "long-wave" limits, because the quasi-one-dimensional model is correct, provided wavelengths in the longitudinal direction are long enough. We can illustrate this point by recognizing that δ_2 is small compared with δ_1 if [from (11.4.13) and (11.4.14)]

$$\frac{\lambda k R}{2(G + \lambda)} \ll 1, \tag{11.4.15}$$

where we have used the rod radius R to evaluate δ_2. Remember that one wave-length is $2\pi/k$, and we see that (11.4.15) is fulfilled if wavelengths are large compared with the radius R.

11.4.2b The Thin Beam

The principal longitudinal or dilatational mode in the presence of boundaries is the subject of Section 11.4.2a. In this section we consider principal

shearing modes on a thin beam of elastic material. Vibrating reeds or bars (tuning forks), commonly used in electromechanical transducers, provide a familiar context for broadening our understanding of distributed dynamic systems.

By now it is a well-established notion that the dynamics of continuous media are closely related to the propagation of waves. The examples of Chapter 9, which describe thin rods and membranes, illustrate this point. Transverse motions of a beam are similar but involve several complications that prevent a misleading generalization from the simple systems considered so far. We find that beam deflections involve four boundary conditions, compared with the two conditions required for the rods and membranes. As a result, the eigenmodes are not simple sinusoids in space but rather have both propagating and evanescent components and the eigenfrequencies of the beam are not usually harmonics. We have encountered this effect of dispersion before (Chapter 10) but not in so familiar a context. If we clamp the end of a beam (steel ruler) at one end with the other end free, as shown in Fig. 11.4.11, the lowest eigenmode can be excited by releasing the beam from a deflected position. In a rod or membrane halving the length l will double the frequency (which can be measured with a strobotachometer). As we shall see in Example 11.4.4, the thin beam lacks this property.

Our object is to use the fact that the bar is thin (in the direction of the deflection) to write an equation of motion that contains only the longitudinal coordinate x_1 and the time t. As is usually the case in developing quasi-one-dimensional models, the starting point is motivated physically. A cross-sectional view of the bar, subject to a hypothetical deformation, is shown in Fig. 11.4.12. If there is no equilibrium (static) longitudinal tension on the bar (it is not being stretched in the x_1-direction as the membrane was*), the displacement of a line painted on the side of the bar will be as shown.
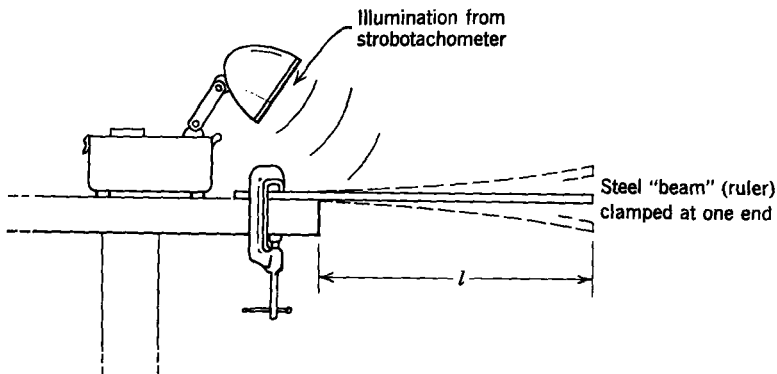
Fig. 11.4.11   The lowest eigenfrequency of a thin beam clamped at one end and free at the other can be measured by using a strobotachometer.

* See Table 9.2, Appendix G.

(a)

(b)

(c)
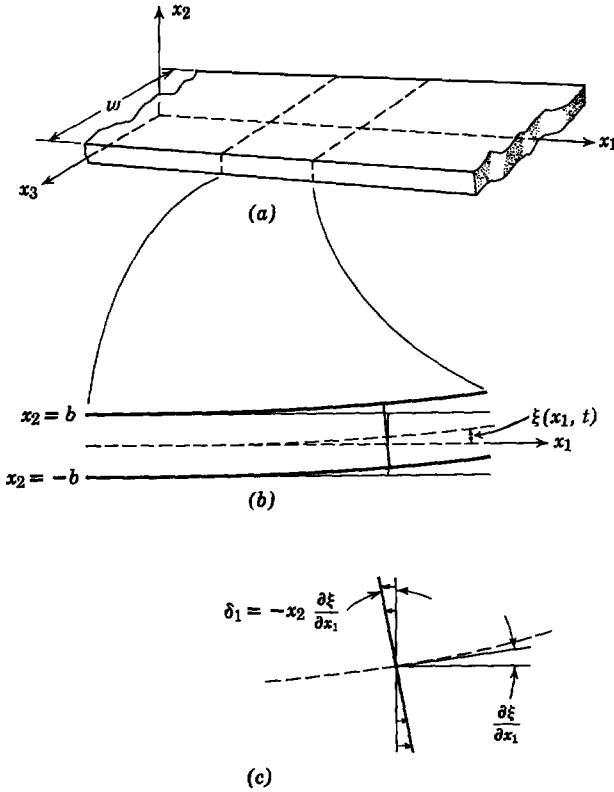
Fig. 11.4.12 Transverse vibrations of a thin bar: (a) in static equilbrium the axis of the bar is in the x_1-direction with material motions essentially in the x_2-direction; (b) a small section of the bar shows the deformation of a line perpendicular to the neutral plane; (c) a detailed view of a perpendicular line shows the relation to the transverse displacement ξ of the neutral plane.

Because the bar is not undergoing a net tension, there is an x_2–x_3 plane (called the neutral plane) in which the material has no x_1 displacement. Then for small deflections of the bar the angle of deflection of a cross-sectional line is given by $\partial\xi/\partial x_1$ (Fig. 11.4.12). The assumption is made that the bar is thin enough that the longitudinal material displacement δ_1 at any cross section can be approximated as having a linear dependence on the transverse dimension x_2. It follows that this linear dependence is about

$$\delta_1 = -x_2 \frac{\partial\xi}{\partial x_1}(x_1, t). \tag{11.4.16}$$

Then from (11.2.10) the normal strain is

$$e_{11} = \frac{\partial\delta_1}{\partial x_1} = -x_2 \frac{\partial^2\xi}{\partial x_1^2}(x_1, t). \tag{11.4.17}$$
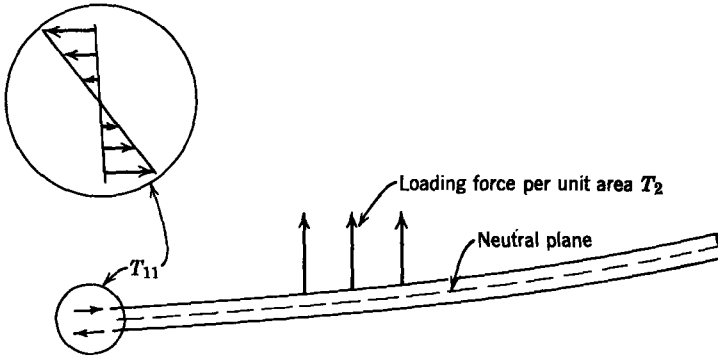
Fig. 11.4.13 Hypothetical beam deflection due to a surface force density T_2. Because the thickness is small compared with the length, the stresses T_{11} are much greater than either T_{22} or T_{33}.

A second approximation is now made. It is assumed that the strain e_{11} is largely created by T_{11} or that $T_{11} \gg T_{22}$ or T_{33}. A section of the bar is shown in Fig. 11.4.13. Because the bar is thin, the stress T_{22} is on the order of any loading force per unit area T_2. The stresses T_{11} must hold the vertical forces in force equilibrium, and because the beam is thin compared with its length it is apparent that we must have $T_{11} \gg T_{22}$. Because there are no loading forces in the x_3-direction, it is even more reasonable that the stresses T_{33} can be ignored, compared with T_{11}. It follows from (11.2.29) that

$$T_{11} = Ee_{11} = -x_2 E \frac{\partial^2 \xi}{\partial x_1^2}. \tag{11.4.18}$$

Altogether, we shall make four approximations based on the thinness of the beam and the transverse nature of the deflections under consideration. The third of these assumptions is now introduced—that the longitudinal inertial force makes no essential contribution to the dynamics. This is reasonable because the deflection considered is mainly in the x_2-direction. Then the x_1-component of the momentum equation for the elastic material [see (11.1.4)] becomes

$$\frac{\partial T_{11}}{\partial x_1} = -\frac{\partial T_{12}}{\partial x_2} = -Ex_2 \frac{\partial^3 \xi}{\partial x_1^3}. \tag{11.4.19}$$

This expression can be integrated to give

$$T_{12} = \frac{Ex_2^2}{2} \frac{\partial^3 \xi}{\partial x_1^3} + g(x_1, t). \tag{11.4.20}$$

The arbitrary function $g(x_1, t)$ is evaluated by requiring that the surfaces at $x_2 = \pm b$ support no shearing stress or that

$$T_{12} = \frac{(x_2^2 - b^2)}{2} E \frac{\partial^3 \xi}{\partial x_1^3}. \tag{11.4.21}$$

The x_2-component of (11.1.4), the force equation, is

$$\rho \frac{\partial^2 \delta_2}{\partial t^2} = \frac{\partial T_{21}}{\partial x_1} + \frac{\partial T_{22}}{\partial x_2}. \qquad (11.4.22)$$

The desired equation of motion can now be found by integrating this equation over an arbitrary cross section of the bar:

$$\rho \frac{\partial^2}{\partial t^2} \int_{-b}^{+b} \delta_2 \, dx_2 = \int_{-b}^{+b} \frac{\partial T_{21}}{\partial x_1} \, dx_2 + [T_{22}]_{x_2 = b} - [T_{22}]_{x_2 = -b}. \quad (11.4.23)$$

As a fourth (and last) approximation, the left-hand side of (11.4.23) is approximated by the product of the cross-sectional thickness $2b$ and the displacement of the bar center. Hence, making use of (11.4.21) and the fact that $T_{12} = T_{21}$,

$$2b\rho \frac{\partial^2 \xi}{\partial t^2} = \frac{\partial^4 \xi}{\partial x_1^4} E \int_{-b}^{+b} \left(\frac{x_2^2 - b^2}{2} \right) dx_2 + T_2, \qquad (11.4.24)$$

where T_2 is the sum of the forces per unit area acting on the x_2-surfaces of the bar and defined by

$$T_2 = [T_{22}]_{x_2 = b} - [T_{22}]_{x_2 = -b}. \qquad (11.4.25)$$

After the integration indicated by (11.4.24) the equation of motion for transverse displacements of the bar becomes

$$\frac{\partial^2 \xi}{\partial t^2} + \frac{Eb^2}{3\rho} \frac{\partial^4 \xi}{\partial x_1^4} = \frac{T_2}{2b\rho}. \qquad (11.4.26)$$

The independent variables in this expression are (x_1, t); hence we have formulated the dynamics in terms of a quasi-one-dimensional model. Beam deflections can be determined from this last equation, given four boundary conditions which arise because the ends of the beam are clamped in a certain fashion or because the ends are free of shear or normal stresses. To write boundary conditions on δ_1, T_{11}, and T_{12} in terms of ξ we can use (11.4.16), (11.4.18), and (11.4.21).

The dependence of the longitudinal and shear stresses on the transverse coordinate x_2 is shown in Fig. 11.4.14. Note that the x_2-dependences of T_{11}
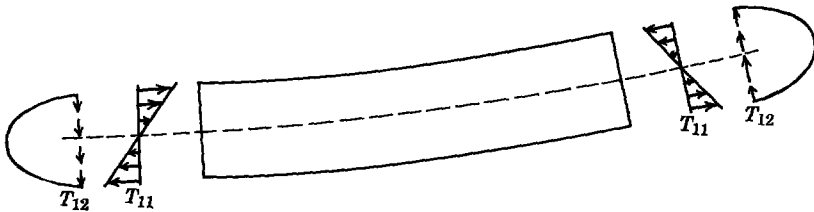
Fig. 11.4.14 Dependence of the normal and shear stresses on the transverse dimension of the beam.

and T_{12} are given by the lowest order polynomial expressions consistent with the requirements that there be no net longitudinal stress and that the shear stresses be zero at the surface of the beam.

Example 11.4.4. The situation shown in Fig. 11.4.15a provides an illustration of the role played by the boundary conditions. A thin beam is clamped at $x = 0$, so that both the transverse and longitudinal displacements of the material at this point are zero. The
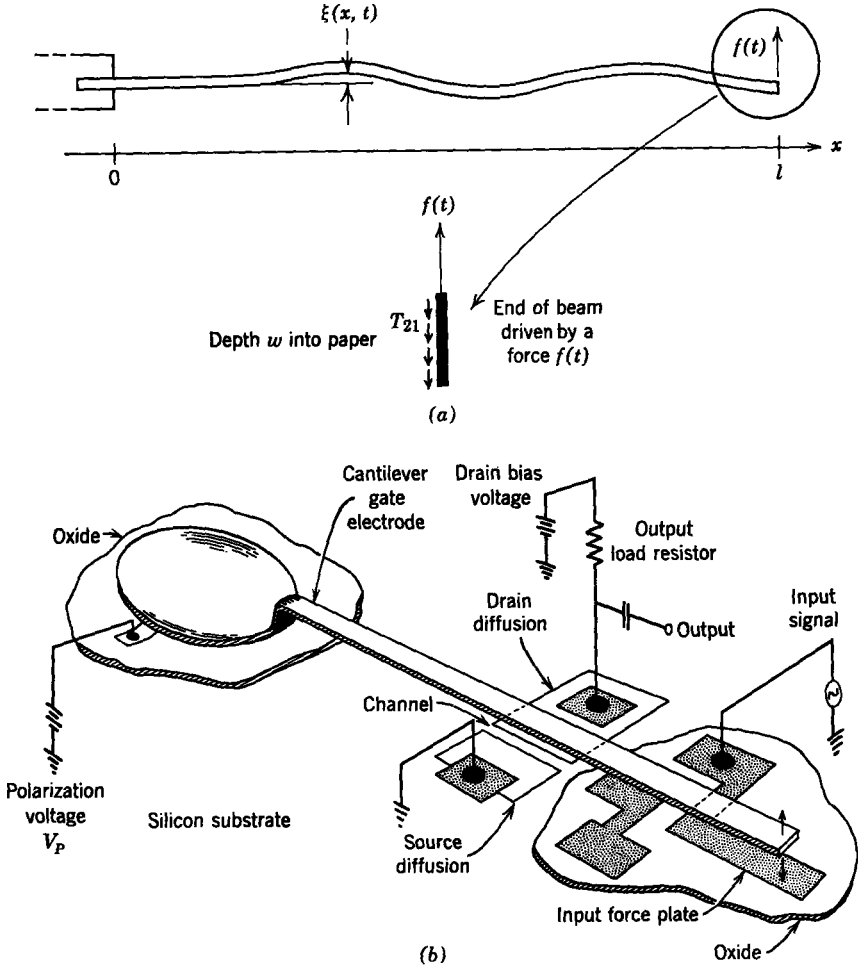
Fig. 11.4.15 (a) A thin elastic beam is driven to vibrate in a direction transverse to its smallest dimension by a force $f(t)$ applied at $x = l$. The end at $x = l$ is free of longitudinal stresses T_{11}, whereas the beam is clamped at $x = 0$. (b) One electromechanical application of the thin elastic beam is illustrated by the "Resonant Gate Transistor" (See W. E. Newell, "Ultrasonics in Integrated Electronics," *Proc. IEEE*, October 1965) A high Q integrated circuit incorporates an electrostatically driven beam. The elastic beam provides an inherently stable resonant element of extremely small proportions (see Fig. 11.4.15c).
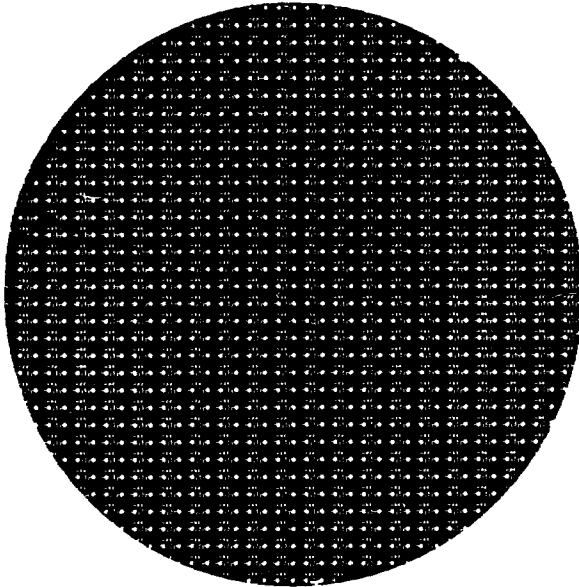
Fig. 11.4.15c Silicon wafer of 1-in. diameter containing nearly 500 . resonant gate transistors of the type shown in (b). (Courtesy of Westinghouse Electric Corp.)

opposite end at $x = l$ is free of longitudinal stresses and is set into vibration by a force $f(t)$, which is sinusoidal:

$$f(t) = \text{Re} \, [\hat{f} e^{j\omega t}]. \tag{a}$$

The sinusoidal steady-state deflections $\xi(x, t)$ are to be found. Of course, to find the driven response, we shall also find the natural frequencies of the beam. In an experiment such as that shown in Fig. 11.4.11 the bar vibrates at these eigenfrequencies. Hence the dependence of the lowest eigenfrequency on the length l will also be found.

The equation of motion is (11.4.26) with $T_2 = 0$. Because the drive assumes a sinusoidal form, we shall guess solutions:

$$\xi = \text{Re} \, [\hat{\xi}(x) e^{j\omega t}], \tag{b}$$

in which case (11.4.26) requires that

$$\frac{d^4 \hat{\xi}}{dx^4} - \alpha^4 \hat{\xi} = 0, \tag{c}$$

where

$$\alpha = \left[\omega^2 \left(\frac{3\rho}{Eb^2} \right) \right]^{1/4}.$$

The spatial dependence is found from (c) by again guessing exponential solutions $\hat{\xi} = e^{-jkx}$, in which substitution shows that $k^4 = \alpha^4$ or that there are four solutions for the spatial dependence:

$$k = \alpha, \; -\alpha, j\alpha, \quad \text{and} \quad -j\alpha. \tag{d}$$

Note that we have defined α as a positive real constant. We have assumed solutions of the form $e^{j(\omega t - kx)}$ and found [from (d)] a pair of waves propagating in each direction on the

beam and a pair of evanescent waves. The evanescent waves are required in addition to the ordinary waves to satisfy the four boundary conditions imposed on the beam. This is in contrast to the situation in Section 10.1.2, in which propagating waves became evanescent at a frequency below some cutoff frequency. Here, all four waves are present simultaneously.

As we have seen, a boundary value problem of this kind is more conveniently solved in terms of trigonometric and hyperbolic functions, rather than complex exponentials (traveling waves). Hence we use linear combinations of the four exponential solutions to write the solution in the form

$$\hat{\xi} = A \sin \alpha x + B \cos \alpha x + C \sinh \alpha x + D \cosh \alpha x, \tag{e}$$

where A, B, C, and D are to be evaluated by using the boundary conditions.

Because there is no longitudinal or transverse motion of the material at $x = 0$, two boundary conditions are

$$\hat{\xi}(0) = 0, \tag{f}$$

$$\frac{d\hat{\xi}}{dx}(0) = 0, \tag{g}$$

where (g) follows from the expression for δ_1 given by (11.4.16). Because $T_{11} = 0$ at $x = l$, (11.4.18) shows that

$$\frac{d^2\hat{\xi}}{dx^2}(l) = 0. \tag{h}$$

The fourth boundary condition arises from the transverse force equilibrium of the beam at $x = l$. The force $f(t)$ acts on a thin element of the beam at $x = l$, as shown in Fig. 11.4.15a. This force is held in equilibrium by the shear stress T_{21}. Hence, since the volume of material within the element is vanishingly small (there is no singularity of mass at the end of the beam), we can write (note that $T_{12} = T_{21}$)

$$f = w \int_{-b}^{b} T_{12} \, dx_2. \tag{i}$$

The boundary condition at $x = l$ in terms of $\hat{\xi}$ follows by using (11.4.21) to find

$$\hat{f} = \frac{wE}{2} \frac{d^3\hat{\xi}}{dx^3} \int_{-b}^{b} (x_2{}^2 - b^2) \, dx_2 \tag{j}$$

or

$$\hat{f} = -\frac{2w}{3} Eb^3 \frac{d^3\hat{\xi}}{dx^3}(l). \tag{k}$$

The first two boundary conditions show that

$$D = -B, \tag{l}$$

$$C = -A. \tag{m}$$

These two relations, together with the second two boundary conditions, give the equations

$$A[\sin \alpha l + \sinh \alpha l] + B[\cos \alpha l + \cosh \alpha l] = 0,$$

$$A[\cos \alpha l + \cosh \alpha l] - B[\sin \alpha l - \sinh \alpha l] = 2\hat{F}, \tag{n}$$

where

$$\hat{F} = \frac{3\hat{f}}{wE4b^3\alpha^3}.$$

Equations (n) provide simultaneous expressions for A and B which are solved to provide

$$A = \frac{\hat{F}(\cos \alpha l + \cosh \alpha l)}{1 + \cosh \alpha l \cos \alpha l},$$ (o)

$$B = \frac{-\hat{F}(\sin \alpha l + \sinh \alpha l)}{1 + \cosh \alpha l \cos \alpha l}.$$ (p)

To make this manipulation we have used the identities $\cos^2 x + \sin^2 x = 1$ and $\cosh^2 x - \sinh^2 x = 1$. The constants D and C follow from (l) and (m) to complete the solution for $\hat{\xi}$ given by (e).

$$\hat{\xi} = \hat{F} \left[\frac{(\cos \alpha l + \cosh \alpha l)(\sin \alpha x - \sinh \alpha x) - (\sin \alpha l + \sinh \alpha l)(\cos \alpha x - \cosh \alpha x)}{(1 + \cosh \alpha l \cos \alpha l)} \right].$$ (q)

The force f might be of electrical origin, in which case it might also depend on $\hat{\xi}$. For now we assume that the forcing function is independent of $\hat{\xi}$, that is, that $\hat{F}$ is a given complex constant. Then (b) provides $\xi(x, t)$.

When the denominator of (q) is zero, the response to the forcing function $\hat{F}$ is infinite. This resonance condition results when the frequency (remember that α is determined by the frequency) is such that

$$\cos \alpha l = -\frac{1}{\cosh \alpha l}.$$ (r)

The solutions to this equation are the points at which the curves shown in Fig. 11.4.16 intersect. Hence the first four modes have frequencies such that αl is as shown in Table 11.4.2. Given the value of αl, the resonance frequency follows from Eq. (c)* as

$$\omega = \frac{(\alpha l)^2}{l^2} \left(\frac{Eb^2}{3\rho} \right)^{1/2}.$$ (s)
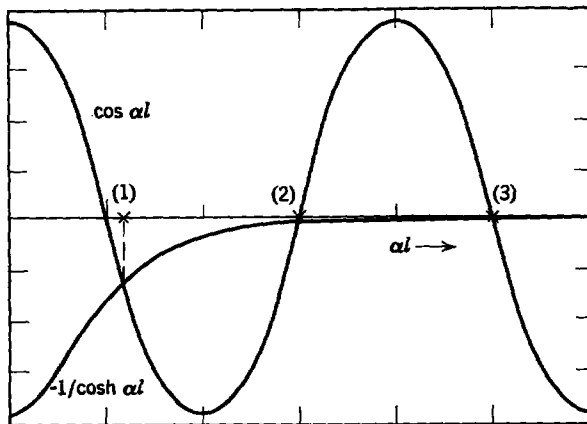
Fig. 11.4.16   Plot of the right- and left-hand sides of (r) (Example 11.4.4). The numbers indicate the solutions for the eigenvalues of the lowest three natural modes given in Table 11.4.2.

* An account of the theory of vibrating bars is given by Rayleigh in *The Theory of Sound*, 1st ed., 1877; Dover edition, 1945, p. 255, Vol. 1.

Table 11.4.2 Lowest Eigenmodes of the
Beam Shown in Fig. 11.4.15a

Mode	(αl)
1	1.875
2	4.694
3	7.855
4	10.996

Note that the resonance frequency of any given mode varies inversely as the square of the beam length l, a fact that is easily verified by the experiment in Fig. 11.4.11. The numerator of (q) is plotted in Fig. 11.4.17 to show the instantaneous spatial variation of the deflection at frequencies close to the eigenfrequencies. The role played by the evanescent wave portion of the solution is clear from these deflections. In the lowest mode the deflection appears to have an "exponential" character, which indicates that the evanescent solutions dominate.
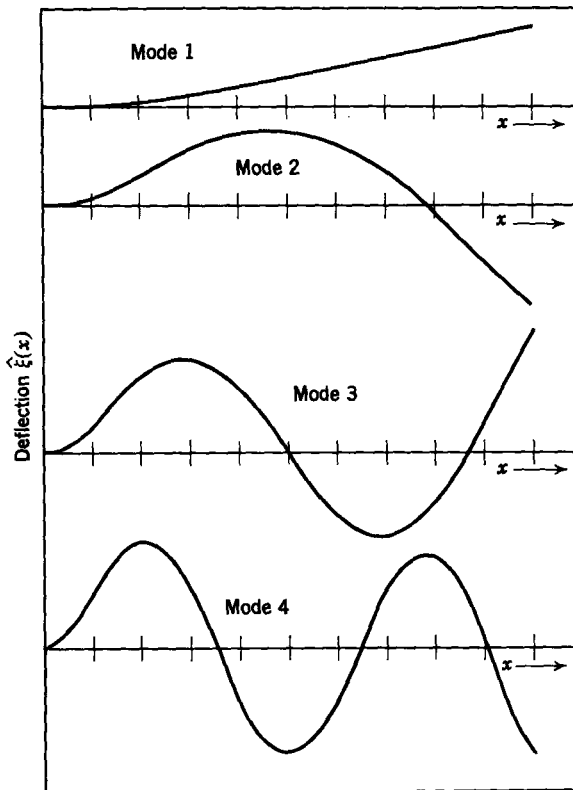
Fig. 11.4.17 Deflection of the beam as a function of the longitudinal position at an instant in time. The first four natural modes are shown, with αl as given in Table 11.4.2. The amplitude is exaggerated, with a different normalization for each mode.

By contrast the higher modes are dominated by the sinusoidal deflections of the ordinary wave solutions, with the evanescent solutions becoming apparent near the ends. This trend is also seen in Fig. 11.4.16, which shows that the higher modes (large αl) are given essentially by zeros of the function $\cos \alpha l$. These results are consistent with the notion that the evanescent waves are excited by the boundary conditions and affect only that region in the vicinity of the boundary.

The longitudinal and transverse modes considered in this section have been described in terms of quasi-one-dimensional models. As the frequency is increased, the longitudinal wavelengths take on the same magnitude as the transverse dimensions of the elastic structure. Under this condition the effect of higher order transverse modes cannot be ignored, as is illustrated in Section 11.4.3.

11.4.3   Elastic Vibrations of a Simple Guiding Structure

As mentioned in Section 11.4, the effect of boundaries is usually to couple shearing and dilatational motions of the material. As a result, the higher order modes, which become significant as the frequency is raised, are often mathematically complicated. We can, however, illustrate the basic physical effects by considering a particular class of modes composed of a purely shearing and rotational motion.*

Figure 11.4.18 shows a slab of elastic material with a thickness d. We
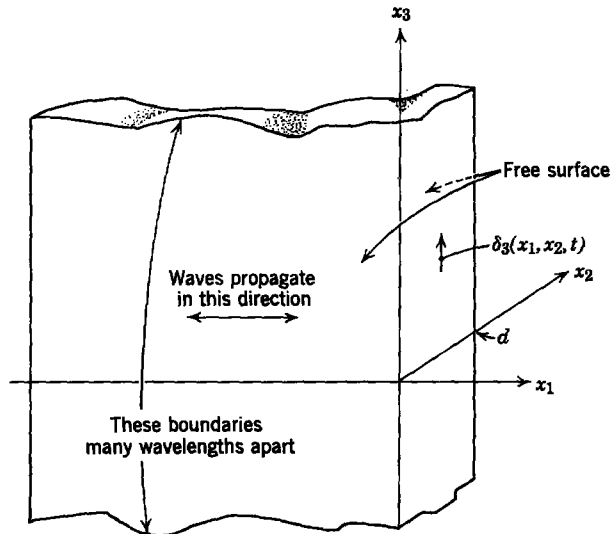
Fig. 11.4.18   Slab of elastic material with thickness d and extending to infinity in the x_3-direction. Shearing motions of the material in the x_3-direction are considered as they propagate in the x_1-direction.

* For a discussion of the general modes present in elastic plates and cylinders see W. P. Mason, *Physical Acoustics, loc. cit.*

consider motions of the material in the x_3-direction under the assumption that the slab has an infinite extent in the x_3-direction. Hence displacements $\delta_3 = \delta_3(x_1, x_2, t)$ are assumed at the outset, with $\delta_1 = \delta_2 = 0$ and $\partial/\partial x_3 = 0$. These assumptions are justified if we can find solutions that satisfy (11.4.1) and the boundary conditions. The surfaces of the slab at $x_2 = 0$ and $x_2 = d$ are free; hence we require that there be no shear stresses on these surfaces:

$$T_{32}(x_1, d, t) = 0, \tag{11.4.27}$$

$$T_{32}(x_1, 0, t) = 0. \tag{11.4.28}$$

With our assumptions, (11.4.1) reduces to

$$\rho \frac{\partial^2 \delta_3}{\partial t^2} = G\left(\frac{\partial^2 \delta_3}{\partial x_1^2} + \frac{\partial^2 \delta_3}{\partial x_2^2}\right). \tag{11.4.29}$$

The boundary conditions are written in terms of δ_3 by recognizing that (11.2.32)

$$T_{32} = G \frac{\partial \delta_3}{\partial x_2}. \tag{11.4.30}$$

Except for the boundary conditions, the mathematical problem is now identical to that described in Section 10.4.1, where the two-dimensional motions of a membrane were considered; that is, (11.4.29) has a variable separable solution

$$\delta_3 = \mathrm{Re}\,[X(x_1)\,Y(x_2)e^{j\omega t}], \tag{11.4.31}$$

and substitution shows that

$$\frac{d^2 X}{dx_1^2} + k^2 X = 0 \tag{11.4.32}$$

and

$$\frac{d^2 Y}{dx_2^2} + \alpha^2 Y = 0, \tag{11.4.33}$$

with k^2 and α^2 related by

$$k^2 + \alpha^2 = \frac{\omega^2 \rho}{G}. \tag{11.4.34}$$

The solution to (11.4.33), which satisfies the boundary conditions, is $\cos \alpha x_2$, with $\alpha = n\pi/d$, $n = 0, 1, 2, \ldots$. Solutions to (11.4.32) are $e^{\pm jkx_1}$. Hence it follows that the solution (11.4.31) can be written as

$$\delta_3 = \mathrm{Re}\,\cos \frac{n\pi x_2}{d}\,[\delta_+ e^{j(\omega t - kx_1)} + \delta_- e^{j(\omega t + kx_1)}], \tag{11.4.35}$$

where δ_+ and δ_- are complex constants determined by the longitudinal boundary conditions. For each value of n we have found solutions composed
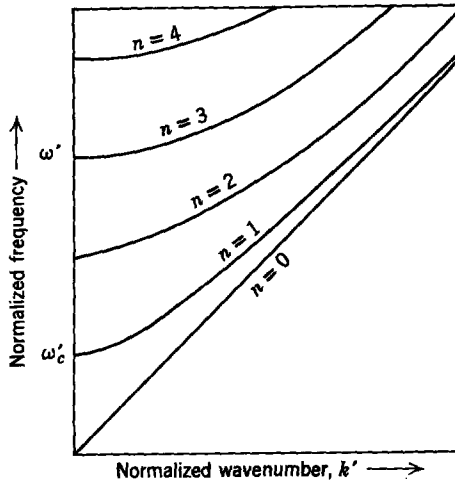
Fig. 11.4.19 Normalized frequency versus normalized wavenumber for shear modes in the elastic slab of Fig. 11.4.18: $\omega' = (\omega d/\pi)\sqrt{\rho/G}$ and $k' = kd/\pi$.

of waves that propagate along the x_1-axis. Given the frequency ω, the wave-number k follows from (11.4.34) as

$$k = \left[\frac{\omega^2 \rho}{G} - \left(\frac{n\pi}{d}\right)^2\right]^{\frac{1}{2}}, \qquad n = 0, 1, 2. \tag{11.4.36}$$

At a given frequency each of the modes has a different wavenumber and a different dependence on the transverse (x_2)-dimension. The relationship between frequency and wavenumber is shown graphically in Fig. 11.4.19. At frequencies less than $\omega' = \omega'_c$ all modes except one decay in the x_1-direction or are evanescent in character, as we found for the membrane in Section 10.4.1. By contrast with the membrane, however, a principal mode now propagates without dispersion, even as the frequency approaches zero.

The spatial dependence of the first two modes is illustrated in Fig. 11.4.20, in which we have assumed that the frequency is below cutoff. The evanescent modes arise because of the "stiffness" introduced by the walls. The principal mode is not affected by the transverse boundary conditions, hence does not possess a cutoff frequency.

From (11.4.36) only the principal mode propagates if

$$\omega\left(\frac{\rho}{G}\right)^{\frac{1}{2}} < \frac{\pi}{d}. \tag{11.4.37}$$

The wavelength of the principal mode is $2\pi/k = (2\pi/\omega\sqrt{\rho/G})$; hence condition (11.4.37) can also be stated as

$$\frac{2\pi}{k} > 2d. \tag{11.4.38}$$
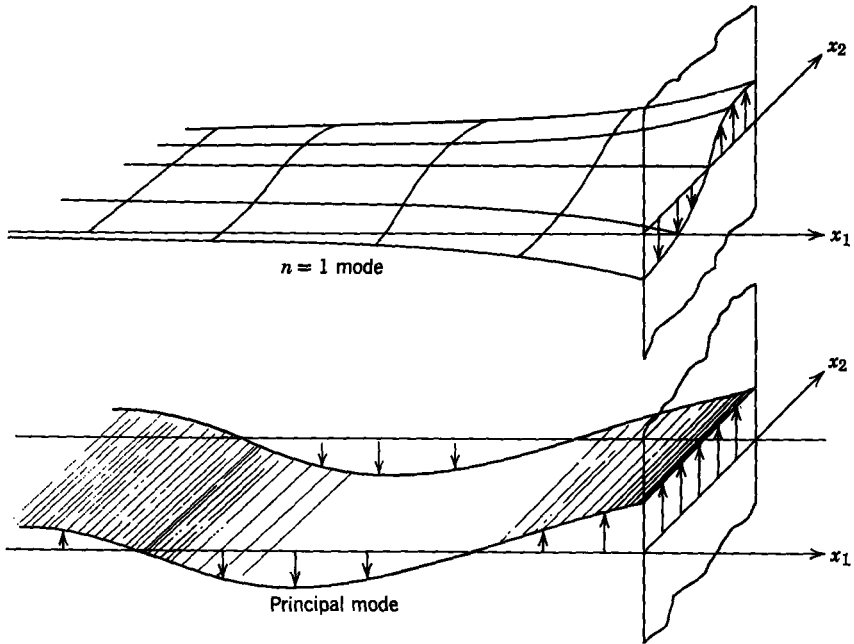
Fig. 11.4.20 Spatial distribution of the principal and $n = 1$ shear modes in an elastic slab. For the case shown the frequency is below the cutoff frequency of the $n = 1$ mode and the evanescent wave that decays in the $-x_1$-direction is shown.

This condition illustrates the general relationship between the principal modes discussed in Section 11.4.2 and higher order modes. As long as the wavelength is long compared with the thickness, only the principal modes propagate and need be considered far from the point of excitation. As we saw in Section 10.4.1 for the membrane and in Section 11.4.2b for the thin beam, the evanescent modes are present to satisfy boundary conditions.

Modes of the kind described here are often used in delay lines. The higher modes are dispersive, hence lead to a distortion of the transmitted signal. For this reason the cutoff frequency often represents an upper limit on the frequency spectrum that can be transmitted without distortion.

11.5 ELECTROMECHANICS AND ELASTIC MEDIA

Many electromechanical interactions with elastic media can be modeled in terms of terminal pairs. This was illustrated in Chapter 9, where, even though portions of the mechanical system required continuum descriptions, the effect of electrical forces could be accounted for by means of boundary conditions. In this chapter we have confined ourselves to the three-dimensional

dynamics of elastic solids in the absence of electromechanical bulk forces. We can now readily imagine using electromechanical transducers to excite or detect the waves discussed in Section 11.4.1. At least in simple situations a discussion in this regard would parallel that given in Section 9.1.2., in which mechanical waves propagated on a thin rod. In Example 11.4.4 vibrations of an elastic beam were reduced to a terminal-pair representation that provides a convenient model for coupling to a lumped-parameter device. In a similar manner we could use a transducer to excite or detect shear waves propagating through the slab of elastic material shown in Fig. 11.4.18. By contrast, in this section we highlight a few illustrative situations in which continuum coupling with elastic media is important, but even in these cases the terminal pair concept is useful.

11.5.1   Electromagnetic Stresses and Mechanical Design

The design of electromechanical systems is often intimately concerned with material stresses produced by electromagnetic forces. A case in point is the design of large rotating machines, such as in Chapter 4. Here the energy conversion process depends on a large magnetic torque being transmitted between the rotor and stator. Because action equals reaction, the rotor and stator materials are necessarily under significant stress due to the magnetic forces; for example, this is the primary reason that conductors are placed in slots. With the conductor imbedded in a highly permeable material, the bulk of the magnetic force is on the magnetic material rather than on the conductor. If this were not the case, it would be difficult to hold the conductors down in many machines. In fact, a significant number of machine failures have been traced to fatigue of conductors and their support structures stressed by magnetic forces.

In a less obvious class of situations in which electromagnetic stresses are a major design consideration the objective is not to convert energy electromechanically. Rather the forces of electrical origin are a necessary evil. Examples in which this is the case are transformers and magnets.

In an ordinary transformer, electromechanical effects come into play in at least three mechanisms, two of which involve magnetization forces on the laminated magnetic core of the transformer. These forces arise because of inhomogeneities of the core introduced with the laminations and because of changes in the volume of the magnetic material (magnetostriction). These forces were discussed in Section 8.5.2* and are responsible for much of the noise (hum or, in transformers used for speech amplification, "transformer talk") heard in the vicinity of an operating transformer.

A third mechanism for electromechanical effects is simply the $\mathbf{J} \times \mathbf{B}$ force density on the individual conductors in a transformer. This design consideration deserves critical attention because copper that is desirable from the point

* Summarized in Table 8.1, Appendix G.

of view of electrical conductivity tends to be lacking in mechanical strength. Transformers must be designed to withstand 25 or more times their rated currents in power applications to prevent mechanical damage under short circuit conditions. Figure 11.5.1*a* shows the primary and secondary windings of a distribution transformer which was intentionally subjected to currents in excess of its peak ratings. This is a step-down transformer with large
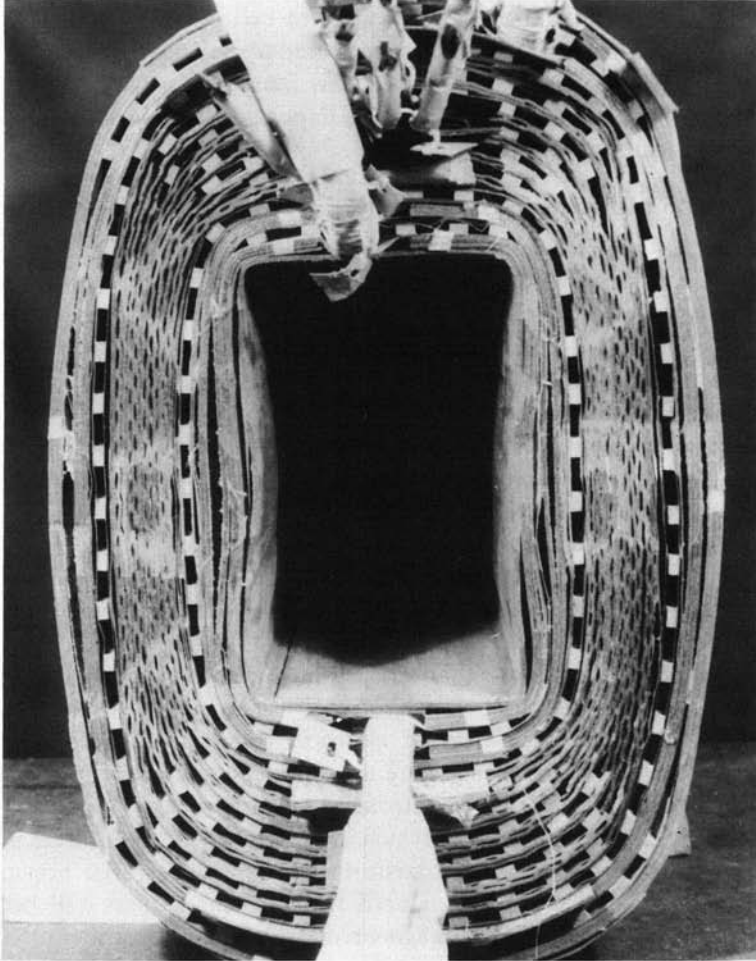
Fig. 11.5.1*a* End view of rectangular distribution transformer coils with core removed after being subjected to short-circuit currents in excess of design capability. Note how reaction forces on the inner secondary coil have buckled it inward on the long sides of the rectangle. Also note that forces on the outer secondary coil have rounded it outward on the long sides. Original shape of the coils on the long sides was flat. (Courtesy of the General Electric Co.)
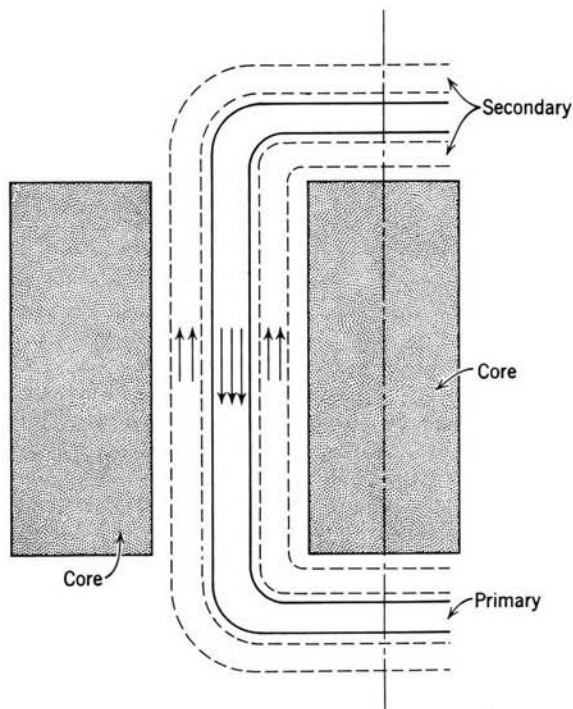
Fig. 11.5.1*b* Sketch of primary and secondary windings in relation to the magnetic transformer core. With the secondary short-circuited, the ampere turns in the secondary are essentially equal to those in the primary.

secondary conductors on the outside and inside and primary windings sandwiched between. The arrangement of the core and windings is sketched in Fig. 11.5.1*b*. The secondary windings are constructed of sheets of aluminum which were originally wound in an essentially rectangular shape. As shown in Fig. 11.5.1*a*, the excessive currents have distorted the secondary windings away from the primary windings. The copper secondary turns bulge inward on the inside and outward on the outside. Although, in this case, the result is not a gross mechanical failure of the structure, significant deformation of the insulation causes local damage that can lead to electrical breakdown. Also, the deformation increases the leakage reactance of the transformer. Increased leakage reactance increases regulation (voltage drops as load current increases) and this decreases the transformer efficiency, a crucial factor in distribution transformers.

So far in this chapter we have emphasized the elastic behavior of solid materials. Our main objective in this section is to draw attention to the fact that in many situations it is the *inelastic* behavior of a solid that is of interest.
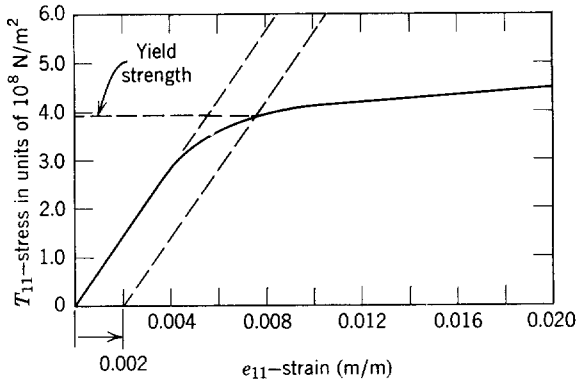
Fig. 11.5.2 Stress-strain for annealed aluminum* under tension showing definition of "yield strength" stress when limiting value of permanent strain is defined as $e_{11} = 0.002$.

If we wish to use solids to synthesize transducers, we must be careful to ensure that stresses are not so large that permanent or inelastic deformations will occur. Even more, in many situations like the one shown in Fig. 11.5.1 limiting stresses are an essential design consideration. We are then faced with the problem of defining meaningful limits on the stress that can be supported by the material. Because the inelastic behavior is an upper bound on the elastic deformation of the material, we can use the elastic theory developed in earlier sections as a starting point for computing limiting stresses.

A typical stress-strain relation for a polycrystalline metal is shown in Fig. 11.5.2. For small values of the stress and strain the relationship is essentially linear. As the stress is raised, however, a point is reached at which the resulting material strain increases more rapidly. Above this point, if the material is unloaded, it is likely that it will retain a permanent deformation. An index of the degree of this permanent set is the *yield strength* of the material, which is defined in Fig. 11.5.2. After the material has been loaded to the yield strength (the limiting stress) it is *assumed* that if it were unloaded it would return to the zero stress condition along a straight line parallel to the loading curve in the elastic range. To fix the yield strength of a material we must define the hypothetical permanent set (the strain) taken by the material when the stress is returned to zero. (In practice this might be 0.002 for metals in tension.*)

If the material has an elastic regime, it is possible to obtain an approximate prediction of material stresses that will lead to inelastic behavior by first predicting the stresses by means of the elastic model and then comparing the maximum stress to the yield strength. Generally such calculations are used to

---

* See S. H. Crandall and N. C. Dahl, *An Introduction to the Mechanics of Solids*, McGraw-Hill, New York, 1959, p. 173.

compute an upper bound on loading the material, with a margin of safety included in the design. The following example illustrates this procedure.

Example 11.5.1. In this example we illustrate how the simple model of an elastic beam can be used to provide insight into the limiting stresses that can be supported by current-carrying conductors in the situation illustrated in Fig. 11.5.1. We assume that the primary winding (sandwiched between the two secondary windings) will remain essentially rigid but that the secondary windings can be modeled by thin beams of the nature discussed in Section 11.4.2b. The problem then reduces to that illustrated in Fig. 11.5.3a, in which only the secondary conductors to the right of the primary are shown.

Under short circuit conditions the ampere turns in the secondary and primary are essentially equal. This means that the magnetic field between the conductors is essentially uniform and given by

$$H = \frac{I}{2w}, \tag{a}$$

for only half the secondary ampere turns are in the part of the windings shown in Fig. 11.5.3a.

For simplicity we assume that the section of secondary conductor can be considered as being clamped at $x_1 = 0$ and $x_1 = l$. Hence we have as boundary conditions

$$\xi(0) = 0; \qquad \xi(l) = 0, \tag{b}$$

$$\frac{d\xi}{dx_1}(0) = 0; \qquad \frac{d\xi}{dx_1}(l) = 0. \tag{c}$$
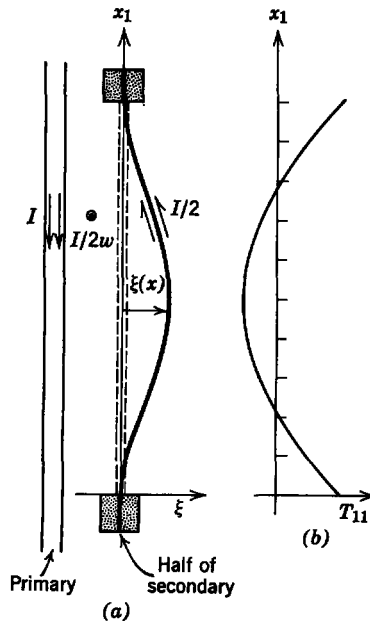
Fig. 11.5.3 (a) A simple model is used to predict elastic failure of the sheet secondary conductor. This example is a first approximation to the situation in Fig. 11.5.1; the primary is assumed to be rigid and the system has a width w into the paper. (b) Distribution of longitudinal stress T_{11} evaluated on the inside surface of the secondary.

Of course, in a transformer the currents, hence the magnetic forces, are not constant. In a distribution transformer the current alternates at 60 Hz, and the magnetic forces that depend on the square of the current are therefore composed of constant and second harmonic (120-Hz) parts. Now the conductors can respond, transducer fashion, to the alternating component of the $\mathbf{J} \times \mathbf{B}$ force.* Here, however, we are interested only in the deformations of the conductors that result over many cycles of the current. Hence we regard the magnetic force on the conductors as being constant and having its average value. Because this force varies as the square of the current, it amounts to using the rms value of the current in evaluating the magnetic force on the secondary conductors. In what follows it is assumed that I is the total rms ampere turns through the width w of the primary conductors.

Under steady conditions (11.4.26), which expresses the transverse force balance for the secondary conductors modeled as a single elastic beam, becomes

$$\frac{d^4\xi}{dx_1{}^4} = \frac{3}{2b^3E}\,T_2. \tag{d}$$

Here $2b$ is the thickness of the combined secondary conductors, E is the "equivalent" modulus of elasticity based on the combined conductors and insulation, and T_2 is the force per unit area acting in the transverse direction. Given T_2, it is a simple matter to compute the deflection ξ of the beam model.

It follows from the magnetic stress tensor† that the surface force T_2 is constant and that

$$T_2 = \tfrac{1}{2}\mu_0 \left(\frac{I}{2w}\right)^2, \tag{e}$$

which combines with (d) to provide a simple fourth-order ordinary equation that can be integrated directly:

$$\frac{d^4\xi}{dx_1{}^4} = a, \tag{f}$$

where

$$a = \frac{3\mu_0}{4b^3E}\left(\frac{I}{2w}\right)^2.$$

Four succeeding integrations lead to a solution that involves four constants $C_1 \cdots C_4$.

$$\xi = \frac{ax_1{}^4}{24} + \frac{C_1x_1{}^3}{6} + \frac{C_2x_1{}^2}{2} + C_3x_1 + C_4. \tag{g}$$

From boundary conditions (b) and (c) these constants are evaluated to obtain

$$\xi = \frac{al^4}{24}\left(\frac{x_1}{l}\right)^2\left(\frac{x_1}{l} - 1\right)^2 \tag{h}$$

for the deflection as a function of the longitudinal position x_1. This is the deflection plotted in Fig. 11.5.3a.

So far our calculations have been based on an elastic model for the beam. The objective is to determine the values of the current that lead to permanent deformations of the secondary winding. This is done by evaluating the maximum longitudinal stress T_{11} and comparing it to that required to give elastic failure of the material according to the preceding discussions of this section.

---

* In fact, under conditions of extreme loading the conductors of a large transformer can be seen to "breath" in and out at 120 Hz.
† See Table 8.1 of Appendix G.

Remember that the longitudinal stress varies linearly over the cross section of the beam (e.g., see Fig. 11.4.14). In the thin beam model this stress is related to the deflection by (11.4.18), which becomes

$$T_{11} = -x_2 E \frac{d^2 \xi}{dx_1^2} = \frac{-x_2 E a l^2}{2} \left[\left(\frac{x_1}{l} \right)^2 - \left(\frac{x_1}{l} \right) + \frac{1}{6} \right],$$ (i)

where x_2 is the transverse coordinate. The maximum stress is obtained at the beam surfaces, where $x_2 = \pm b$; for example, on the inside (left) surface of the beam

$$T_{11} = \left(\frac{l}{b} \right)^2 \frac{3}{8} \mu_0 \left(\frac{I}{2w} \right)^2 \left[\left(\frac{x_1}{l} \right)^2 - \left(\frac{x_1}{l} \right) + \frac{1}{6} \right].$$ (j)

The manner in which this function depends on the longitudinal position is shown in Fig. 11.5.3b. At the center of the beam ($x_1 = l/2$) the stress $T_{11}(x_2 = -b)$ is negative, indicating that the material is under compression. The maximum longitudinal stress is obtained at the ends, where the material on the left side of the beam is under tension. This maximum stress on the beam is

$$T_{11}(x_2 = -b, x_1 = 0) = \left(\frac{l}{b} \right)^2 \frac{1}{16} \mu_0 \left(\frac{I}{2w} \right)^2.$$ (k)

Now the beam is also subject to shear stresses T_{12}, which should also be considered in determining the maximum stress. The shear stress is related to the beam deflection by (11.4.21), which shows that if $b \ll l$ the shear stress will be small compared with the longitudinal stress. It is just this fact that the beam is thin that makes the mechanical stress T_{11} much greater than the magnetic pressure. The stress T_{11} acts over the cross section $2b$ of the beam through a lever arm that is less than b to hold in equilibrium the magnetic pressure $\frac{1}{2}\mu(I/2w)^2$ acting over the length l through a lever arm that is on the order of l (see Fig. 11.4.13). This is why (k) is proportional to the magnetic pressure amplified by $(l/b)^2$.

An order of magnitude calculation helps us to appreciate the significance of (k). In magnetic circuits, such as the transformer of Fig. 11.5.1, a magnetic flux density of 10 kG (1 Wb/m^2) is commonly induced. This corresponds to a magnetic pressure of

$$\frac{B^2}{2\mu_0} = \frac{1}{(2)(4\pi \cdot 10^{-7})} \approx 4 \cdot 10^5 \text{ N/m}^2.$$

If we use this number to replace the magnetic pressure $\frac{1}{2}(I/2w)^2 \mu_0$ in (k) and let $l/b = 20$, it follows that

$$T_{11}(x_2 = -b, x_1 = 0) = 2 \cdot 10^7 \text{ N/m}^2.$$

This is just above the 0.2% yield strength of annealed aluminum,[*] but considerably below the value in Fig. 11.5.2. The strength of aluminum can be increased considerably by cold working and alloying it with other substances. For example, considering the ability of the coil to withstand the mechanical forces imposed by short-circuit currents, a transformer designer is faced with the problem of balancing the mechanical strength of the core and coil against the cost and electrical characteristics. His problem is complicated because coil conductors that are most desirable in terms of their electrical characteristics are relatively low in mechanical strength.

A critical review of this model will show that we have ignored many facets of the problem that could be of major importance; for example, the secondary winding of the actual transformer is not a homogeneous solid but rather is composed of layers of conducting and

[*] A. E. Knowlton, *Standard Handbook for Electrical Engineers*, McGraw-Hill, New York, 1957, Section 4, p. 695.

insulating sheets. In practice we would probably measure an "equivalent" modulus of elasticity for this combination, although to be rigorous account should be taken of the anisotropic material in the basic model of the elastic beam.

Also, the inelastic behavior of materials is more complicated than might be deduced from our comments so far. The material is subject to repeated loading and unloading due to the second-harmonic force. This can result in a type of failure analogous to that found when a wire is bent back and forth repeatedly until it breaks. It depends on the number of cycles as well as the maximum stress and is therefore referred to as *fatigue* failure.

To complicate the picture still further, when materials are subjected to a constant stress over a long period of time, it is found that the strain has an initial value that can be predicted from the stress-strain relation but continues to increase with time. This *creep* phenomenon can eventually lead to the failure of the material. Copper is an example of a material that displays creep. Further discussion of the inelastic behavior of materials is beyond the scope of this book but should be recognized as required for the understanding of how materials are used in electromechanical systems.

11.5.2 Simple Continuum Transducers

This chapter is concluded with examples that show how quasi-one-dimensional models of elastic structures can be used in the design of electromechanical transducers.

11.5.2a Variable Capacitance Coupling

We begin with a situation that involves an electromechanical coupling similar to that studied back as far as Chapter 3—variable capacitance coupling. The object is to develop a simple and reliable low-frequency notch filter. It is required that the frequency of the notch be tuned by varying a voltage.

Example 11.5.2. An electromechanical filter, having as its basic element a simple cantilevered beam, is shown in Fig. 11.5.4. The beam, which is at the potential V_0, is free to vibrate between plane-parallel electrodes, and the input signal is imposed on the left electrode. Because v_i is much less than V_0, this produces a force on the beam proportional to the input signal. The beam deflections lead to a change in capacitance between the beam and the plate to the right. The resulting current through the resistance R is therefore proportional to the input signal with an amplitude determined by the response of the beam to the input.

It is assumed that the resistance R is small enough that the electrode to the right can be considered as grounded. Further, it is assumed that the capacitive reactance due to C is small compared with R, so that v_0 can be taken as the voltage drop across the resistance. The equation of motion for the beam is (11.4.26):

$$\frac{\partial^2 \xi}{\partial t^2} + \frac{Eb^2}{3\rho} \frac{\partial^4 \xi}{\partial x_1^4} = \frac{T_2}{2b\rho}. \tag{a}$$

We assume that $d \ll l$ so that the transverse force T_2 is simply the difference in Maxwell stress* acting on the opposite surfaces of the beam:

$$T_2 = T_{22}{}^a - T_{22}{}^b = \tfrac{1}{2}\epsilon_0 \left[\frac{(V_o + v_i)^2}{(d - \xi)^2} - \frac{V_o{}^2}{(d + \xi)^2} \right]. \tag{b}$$

* Table 8.1, Appendix G.
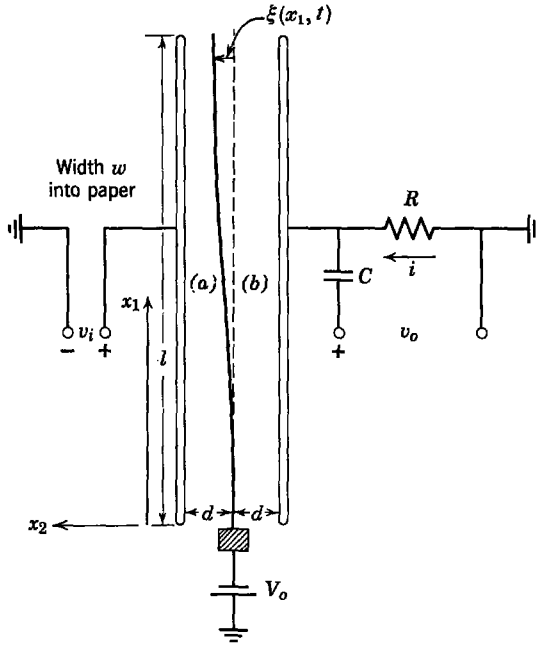
Fig. 11.5.4 A cantilevered beam has the potential V_o relative to plane-parallel driving and detecting electrodes. This device might be used as a low-frequency voltage tunable electromechanical filter.

For small deflections ξ and input voltage v_i this becomes

$$T_2 = 2\epsilon_0 \left(\frac{V_o}{d}\right)^2 \frac{\xi}{d} + \frac{\epsilon_0 V_o}{d^2} v_i. \tag{c}$$

The equation of motion (a) is then augmented by two additional forces, one having the nature of a spring with a negative spring constant and the other a driving force proportional to the driving voltage:

$$\frac{\partial^2 \xi}{\partial t^2} + \frac{Eb^2}{3\rho} \frac{\partial^4 \xi}{\partial x_1^4} = \frac{\epsilon_0 V_o^2}{b\rho d^3} \xi + \frac{\epsilon_0 V_o}{2b\rho d^2} v_i. \tag{d}$$

We confine attention to the sinusoidal steady-state response of the system and so assume that the drive and response have the form

$$v_i = \text{Re } \hat{v}_i e^{j\omega t},$$

$$\xi = \text{Re } \hat{\xi}(x_1) e^{j\omega t}. \tag{e}$$

Then (d) becomes

$$\frac{d^4 \hat{\xi}}{dx_1^4} - \alpha^4 \hat{\xi} = P\hat{v}_i, \tag{f}$$

where

$$\alpha^4 = \left[\frac{\epsilon_0 V_o^2}{d^3 b \rho} + \omega^2 \right] \frac{3\rho}{Eb^2}$$

$$P = \frac{3}{2} \frac{\epsilon_0 V_o}{d^2 b^3 E}.$$

This inhomogeneous ordinary equation has a homogeneous solution which is identical in form to that studied in Example 11.4.4 of Section 11.4.2b. In addition, there is now an inhomogeneous solution which, because the right-hand side of (f) is a constant, is simply a constant. The complete solution is

$$\hat{\xi} = A \sin \alpha x_1 + B \cos \alpha x_1 + C \sinh \alpha x_1 + D \cosh \alpha x_1 - \frac{P\hat{v}_i}{\alpha^4}. \tag{g}$$

The boundary conditions on the beam which determine the constants A, B, C, and D require that the clamped end of the beam be constrained so that no longitudinal or transverse displacement is there and that the free end of the beam at $x_1 = l$ is free of shear and longitudinal stress. In terms of the transverse displacement $\hat{\xi}$ of the beam, these conditions are

$$\hat{\xi}(0) = 0; \qquad \frac{d^2\hat{\xi}}{dx_1^2}(l) = 0,$$

$$\frac{d\hat{\xi}}{dx_1}(0) = 0; \qquad \frac{d^3\hat{\xi}}{dx_1^3}(l) = 0. \tag{h}$$

These conditions require that the following four simultaneous equations be satisfied:

$$A(0) \quad + \ B(1) \quad + C(0) \quad + \ D(1) \quad = P\hat{v}_i/\alpha^4,$$

$$A(1) \quad + \ B(0) \quad + C(1) \quad + \ D(0) \quad = 0,$$

$$A(-\sin \alpha l) + B(-\cos \alpha l) + C(\sinh \alpha l) + D(\cosh \alpha l) = 0,$$

$$A(-\cos \alpha l) + B(\sin \alpha l) \quad + C(\cosh \alpha l) + D(\sinh \alpha l) = 0. \tag{i}$$

The constants A, B, C, and D follow from these equations and the deflection of the beam is now known.

To compute the output voltage it is necessary first to recognize that the surface charge density on the right plate is

$$\sigma_f(x_1, t) = \frac{\epsilon_0 V_o}{d + \xi} \approx \frac{\epsilon_0 V_o}{d} - \frac{\epsilon_0 V_o \hat{\xi}}{d^2} \tag{j}$$

Then it follows that because the current through the resistance is the time rate of change of the total charge on the plate to the right

$$\hat{v}_o = -R\hat{i} = j\omega R \frac{w\epsilon_0 V_o}{d^2} \int_0^l \hat{\xi}\, dx_1. \tag{k}$$

It is a straightforward matter to carry out this integration, since $\hat{\xi}$ is given by (g). Note from (i) that each of the constants is proportional to $\hat{v}_i$ and inversely proportional to the determinant of the coefficients $\Delta(\omega)$. Hence (k) for the transfer response has the form

$$\hat{v}_o = \frac{H(\omega)}{\Delta(\omega)} \hat{v}_i, \tag{l}$$

and the poles of the transfer function are given by

$$\Delta(\omega) = 0. \tag{m}$$

These are the same poles found for the beam in Example 11.4.4; that is, the determinant of the coefficients is zero if (remember $\alpha = \alpha(\omega)$)

$$1 + \cosh \alpha l \cos \alpha l = 0. \tag{n}$$

The roots of this expression are given in Table 11.4.2.

If we call the roots of (n) $(\alpha l)_n$, it follows that the resonance frequencies are given by

$$\omega = \pm \left(\omega_n^2 - \frac{\epsilon_0 V_o^2}{d^3 b \rho} \right)^{\frac{1}{2}}, \tag{o}$$

where

$$\omega_n = \frac{(\alpha l)_n^2}{l^2} \left(\frac{E b^2}{3\rho} \right)^{\frac{1}{2}} \tag{p}$$

are the resonance frequencies of the beam without electromechanical coupling. At the frequencies given by (o) there is a resonance in the transfer function unless $H(\omega)$ happens to be zero. Note that these resonance frequencies can be tuned by varying the voltage V_o. As we might have expected at the outset, (o) shows that the beam has an unstable equilibrium at $\xi = 0$ when the lowest resonance frequency is reduced to zero and these lowest eigenfrequencies become imaginary. From (o) the condition for instability is

$$\frac{\epsilon_0 V_o^2}{d^3 b \rho} = \omega_1^2. \tag{q}$$

11.5.2b Magnetostrictive Coupling

The subject of magnetostriction in solids is sufficiently complex that a comprehensive treatment is inappropriate here. We can, however, gain a considerable qualitative insight into the subject by considering one-dimensional motions of a thin rod subject to magnetostrictive forces. In this context these forces can be viewed as described by the force density developed in Section 8.5.2.* There are two reasons why the force density developed in Chapter 8 is not entirely adequate. First of all, there is no guarantee that a solid remains isotropic after a magnetic field is applied, even though it may be isotropic in the absence of a magnetic field. Second, solids that exhibit significant magnetostrictive behavior tend to be magnetic; for example nickel and nickel iron alloys are commonly used in magnetostrictive transducers.† In these materials $\mathbf{B}$ is a linear function of $\mathbf{H}$ only over a limited range of $\mathbf{H}$. Hence the permeability μ relates $\mathbf{B}$ and $\mathbf{H}$ only so long as $\mathbf{B}$ is much less than its saturation value.

By limiting ourselves to one-dimensional motions and sufficiently small magnetic field intensities that $\mathbf{B} = \mu \mathbf{H}$ we can use the results of Chapter 8

---

* Table 8.1, Appendix G.

† A discussion of magnetostriction, including material characteristics and applications to the design of electronic devices is given in W. P. Mason, *Electromechanical Transducers and Wave Filters*, Van Nostrand, Princeton, New Jersey, 1958, 2nd. ed., p. 215.

to gain a meaningful understanding of the basic magnetostrictive interaction. Actually, most transducers are modeled as one-dimensional, and nonlinear effects are accounted for empirically by straightforward extensions of the linear model.

As discussed in Section 8.5, we can think of magnetostrictive interactions as resulting because dilatational motions of the material, which lead to local changes in the material density, also lead to a change in the local magnetic energy storage. This makes it possible to exert a magnetic force on a volume where material is initially homogeneous. An example in which this is a desirable attribute is given in Fig. 11.5.5a. There, a magnetic wire constitutes the propagating structure for an acoustic delay line. The device, which might be used as either an input or an output transducer, is easily moved along the wire to effect a change in the delay time. Now, if the wire were capable of only rigid body motion, there could be no longitudinal force produced by the input signal. The material must change its volume in order to effect any change in the magnetic energy stored in the system as a function of material displacements. This should be contrasted with the type of magnetization
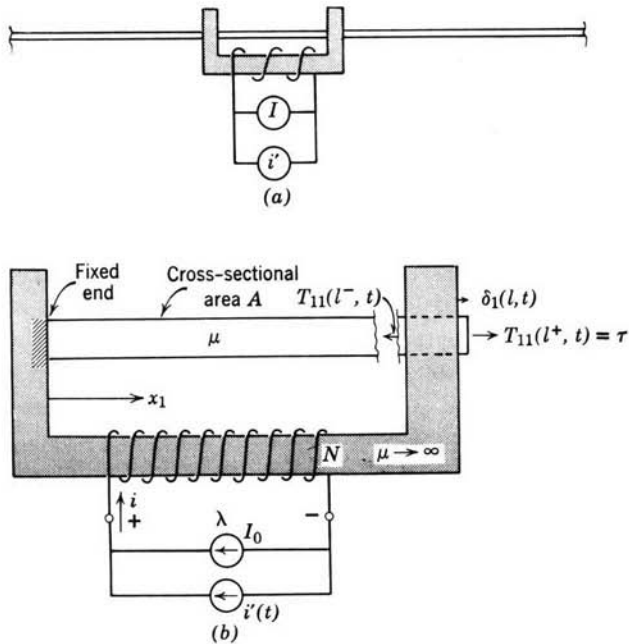
Fig. 11.5.5 Magnetostrictive transducer. Compressional motions are excited by the input current $i'(t)$: (a) transducer placed at a variable position along a magnetic wire which might be used as a delay line; (b) detail of a transducer in which the wire is fixed at one end of a magnetic circuit.

forces used in the delay line of Section 9.1.2, where the force resulted because of inhomogeneities (air gaps) in the material. The inconvenience of this mode of coupling is made apparent in Figure 9.1.14.

The following example illustrates the modeling of a magnetostrictive transducer.

Example 11.5.3. The transducer shown in Fig. 11.5.5b characterizes devices that have seen wide application. An input signal $i'(t)$ is transduced into a force τ that acts through a displacement $\delta_1(l, t)$, we wish to find the mechanical terminal relation between τ and $\delta_1(l, t)$. To simplify our discussion, it is assumed that the magnetostrictive material takes the form of a rod with cross-sectional area A and one end fixed at $x_1 = 0$.

According to (8.5.38), the rod is subject to the force density

$$\mathbf{F} = -\tfrac{1}{2}\mathbf{H} \cdot \mathbf{H} \, \nabla \mu + \nabla \left(\tfrac{1}{2}\mathbf{H} \cdot \mathbf{H} \, \frac{\partial \mu}{\partial \rho} \, \rho \right) \qquad (a)$$

In the rod it is reasonable to view μ and ρ as being uniquely related, $\mu = \mu(\rho)$. Note that if a material is inhomogeneous this is not a meaningful statement; for example, a material could have a uniform density but be composed by regions occupied by materials of different permeabilities μ. On the basis of the restriction that the force is valid only in the interior of the rod so that $\mu = \mu(\rho)$, we can write

$$\nabla \mu = \frac{\partial \mu}{\partial \rho} \, \nabla \rho. \qquad (b)$$

Then (a) reduces to

$$\mathbf{F} = \rho \, \nabla \left(\tfrac{1}{2} \frac{\partial \mu}{\partial \rho} \mathbf{H} \cdot \mathbf{H} \right). \qquad (c)$$

In what follows we make the assumption that insofar as the force is concerned variations in ρ can be ignored so that the mass density multiplying the gradient term in (c) is replaced by ρ_0. Note that this does not say that ρ is actually a constant, but simply that it can be approximated as constant in (c). Then the longitudinal equation of motion for the rod becomes

$$\rho_0 \frac{\partial^2 \delta_1}{\partial t^2} = \frac{\partial}{\partial x_1} \left(E \frac{\partial \delta_1}{\partial x_1} + \frac{\rho_0}{2} \frac{\partial \mu}{\partial \rho} \quad \cdot \mathbf{H} \right). \qquad (d)$$

It is a good approximation to ignore the effect of mechanical deformation on the field. This means that $\mathbf{H}$ is uniform over the length of the rod between $x_1 = 0$ and $x_1 = l$. Over this range, material displacements are then governed by the simple wave equation for the thin rod

$$\frac{\partial^2 \delta_1}{\partial t^2} = \left(\frac{E}{\rho_0} \right)^{1/2} \frac{\partial^2 \delta_1}{\partial x_1{}^2}. \qquad (e)$$

The influence of the magnetostrictive force is felt through the boundary condition at $x_1 = l$. Force equilibrium for a section of the rod in the neighborhood of $x_1 = l$ is shown in Fig. 11.5.6.

The quantity in brackets on the right-hand side of (d) is the longitudinal stress transmitted along the rod. Hence the left face of the section of material shown in Fig. 11.5.6 is subject to this stress acting over the cross section A of the rod. Within the length h of the material section the lines of magnetic field intensity are shunted into the magnetic circuit. The stress on the right surface is simply τA, where τ is the mechanical stress due to the system
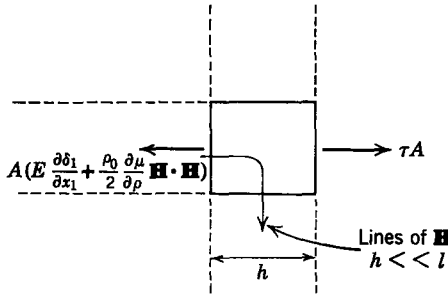
Fig. 11.5.6 A section of the rod shown in Fig. 11.5.5 in the neighborhood of $x_1 = l$. This section is assumed to have negligible length h compared with l.

being driven. We can argue that there are no shear stresses acting on the volume by recognizing from (c) that the magnetostriction force is capable only of producing normal stresses. Hence at $x = l$,

$$E \frac{\partial \delta_1}{\partial x_1}(l, t) + \rho_0 \frac{1}{2} \frac{\partial \mu}{\partial \rho} \mathbf{H}^2(l, t) = \tau. \qquad (f)$$

This becomes a useful boundary condition once $\mathbf{H}$ is evaluated in terms of the current i. For illustrative purposes we assume that the magnetic circuit is of much greater permeability than the magnetostrictive wire. Then

$$H = \frac{Ni}{l} = \frac{N}{l}(I_0 + i'). \qquad (g)$$

The force equilibrium represented by (f) has a constant part due to the bias current I_0 and a dynamic part due to small perturbations $i'(t)$ in the transducer current. We assume that the constant part is balanced out by a constant part of τ due to the system to the right. Then the linearized dynamic part of (f) is

$$\frac{\partial \delta'}{\partial x_1}(l, t) + \gamma i' = \frac{\tau'}{E}, \quad \text{where} \quad \gamma = \frac{\rho_0}{E} \frac{\partial \mu}{\partial \rho} \left(\frac{N}{l}\right)^2 I_0, \qquad (h)$$

and τ' and δ' are, respectively, the time-varying parts of the stress acting on the right surface of the transducer rod and displacement $\delta_1(x_1, t)$.

Our objective is to characterize the transducer by the relation between τ' and $\delta'(l, t)$, given the input signal $i'(t)$. This is easily accomplished for sinusoidal steady-state solutions in the form of

$$i' = \text{Re } \hat{i}e^{j\omega t},$$

$$\delta' = \text{Re } \hat{\delta}(x_1)e^{j\omega t}, \qquad (i)$$

$$\tau' = \text{Re } \hat{\tau}e^{j\omega t}$$

by recognizing that the solution to (e), which satisfies the condition that there be no displacement at $x_1 = 0$, is

$$\hat{\delta} = C \sin kx_1, \quad k = \omega \left(\frac{\rho_0}{E}\right)^{\frac{1}{2}}. \qquad (j)$$

The complex amplitudes of (i) must satisfy a further condition represented by (h),

$$Ck \cos kl + \gamma i = \frac{\hat{\tau}}{E}. \tag{k}$$

Finally, it follows from (j) that $C = \delta(l)/\sin kl$ and that this last expression becomes the required terminal relation between the mechanical variables $\delta'(l, t)$ and $\tau'(t)$ and the driving signal $i'(t)$.

$$\gamma i = \frac{\hat{\tau}}{E} - \delta(l)k \cot kl. \tag{l}$$

This terminal relation is all that is required to represent the magnetostrictive transducer as it affects the medium being driven; for example, if the transducer were used to drive a rod to the right (l) would constitute a boundary condition to be used at $x_1 = l$.

The constant γ can be positive or negative depending on the properties of the rod. As made familiar by preceding chapters, the transducer has a linear response only if it is biased by an external source such as I_0.

11.5.2c Piezoelectric Coupling

A salient feature of all the mechanisms for electromechanical coupling so far discussed has been that electromagnetic forces depend on the square of the applied currents, potentials, or other electrical excitations. This has meant that to obtain an electromagnetic force proportional to the applied signal a bias field is required. It has also been necessary to provide a bias field in situations in which a mechanical motion is to be transduced into an electrical signal. The magnetostrictive interaction discussed in Section 11.5.2b illustrates this point. The bias current I_0 is required to make the force a linear function of the input signal $i'(t)$. This bias current is also required if the transducer is to be used to detect the motion of the magnetized rod, as, for example, at the output end of a delay line.

Piezoelectric and piezomagnetic forms of electromechanical coupling are of interest because in effect they provide their own internal bias. The dielectric bar shown in Fig. 11.5.7 is an example of a piezoelectric transducer. That there are new ingredients to this physical situation is apparent from two simple experiments. First, suppose that a voltage is applied between the upper and lower electroded surfaces of the bar. The result is an expansion or contraction of the bar in the x-direction, depending on the sign of the applied voltage. The mechanical response reflects the sign of the applied signal. Second, suppose that the bar is stretched or compressed along the x-axis. A proportionate voltage will be developed across the terminals. These electrical-to-mechanical and mechanical-to-electrical effects are similar to those found in a transducer with an internal bias. In piezoelectric materials the effect of the bias is intrinsic to the material.

Materials that display peizoelectric properties can be either single crystals, for example, quartz, or polycrystalline ferroelectrics such as barium titanate ceramics. In the latter materials the "bias" referred to previously is provided
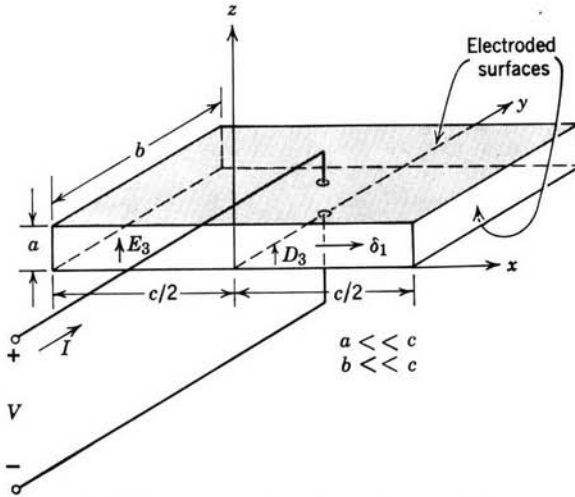
Fig. 11.5.7 Piezoelectric length expander bar.

by a permanent polarization. In single crystals the piezoelectric phenomenon is brought about by asymmetry in the crystal structure. In general, this subject therefore involves the elastic and electrical behavior of anisotropic solids. In the following introduction to this class of electromechanical interaction attention is confined to a particular one-dimensional type of interaction which allows us to develop some insight into the subject without becoming involved with general statements about the dynamics of anisotropic media.*

As might be imagined from the analogy between the piezoelectric transducer and the biased transducer, it is impossible to distinguish between electrical and mechanical forces in piezoelectric materials. If we refer to the total stress in the material as T_{11}, the electrical constitutive law relating D_3 and E_3 is

$$D_3 = \epsilon E_3 + \gamma T_{11}. \tag{11.5.1}$$

Here we have confined attention to quasi-one-dimensional motions of the bar along the x-axis and a crystal configuration such that the induced electric field is in the z-direction. Thus

$$\boldsymbol{\delta} = \delta_1(x, t)\mathbf{i}_1, \qquad \mathbf{E} = E_3(x, t)\mathbf{i}_3. \tag{11.5.2}$$

The mechanical constitutive law, which represents a generalization of the stress-strain relation, is

$$e_{11} = \gamma E_3 + S T_{11}. \tag{11.5.3}$$

* For a more general discussion, see W. P. Mason, *Physical Acoustics* Vol. 1, part A, Academic, New York, 1964 p. 170.

The parameter S will be recognized as the reciprocal of the modulus of elasticity. Note that the same constant γ appears in (11.5.1) and (11.5.3) to account for the electromechanical coupling. This is a consequence of a reciprocity condition, based on conservation of energy in much the same spirit discussed in Section 3.1.2c. To see this consider a section of the bar with length Δx which is subject to a slowly varying stress T_{11}, as shown in Fig. 11.5.8. T_{11} is the total stress (mechanical plus electrical), hence for slow variations it is constant over the length Δx of the section. The work done on the sample as it undergoes the incremental displacement $d\delta_1$ is

$$ab[T_{11}\,d\delta_1(x+\Delta x) - T_{11}\,d\delta_1(x)] \simeq abT_{11}\,\Delta x\,d\left(\frac{\partial\delta_1}{\partial x}\right) = abT_{11}\,\Delta x\,de_{11}.$$

$$(11.5.4)$$

Energy can also be added to the sample through the electrical terminals. The charge on the upper electrode is $q = -\Delta x b D_3$ and the voltage between the electrodes is $-aE_3$. A change in the charge dq on the upper plate corresponds to an addition of energy through the electrical terminals given by

$$v\,dq = ab\,\Delta x E_3\,dD_3.$$

$$(11.5.5)$$

It is now possible to write a conservation of energy equation by defining the energy density (mechanical and electrical) within the element as w:

$$ab\,\Delta x E_3\,dD_3 + ab\,\Delta x T_{11}\,de_{11} = ab\,\Delta x\,dw$$

$$(11.5.6)$$

or

$$E_3\,dD_3 + T_{11}\,de_{11} = dw.$$

$$(11.5.7)$$

Note that the thermodynamic subsystem described by this conservation of energy equation includes energy storage in the elastic deformation of the material. This is necessary because we cannot distinguish between mechanical and electrical stresses as we can in Chapter 3, where we consider forces f^e that are zero with the electrical terminals unexcited. It is appropriate to think of D_3 and e_{11} in (11.5.7) as thermodynamically independent variables. This representation is similar to that used in Chapter 3, in which D_3 would be the charge q and e_{11} would be the mechanical displacement. To make E_3 and T_{11} (which are analogous to the voltage and force) the independent variables we use Legendre's dual transformation (see Section 3.1.2b) to write (11.5.7) as

$$D_3\,dE_3 + e_{11}\,dT_{11} = dw',$$

$$(11.5.8)$$
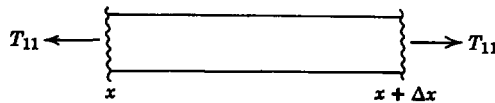
Fig. 11.5.8   Incremental length of bar shown in Fig. 11.5.7.

where the coenergy density w' is defined as

$$w' = E_3 D_3 + T_{11} e_{11} - w. \qquad (11.5.9)$$

Because $w' = w'(E_3, T_{11})$, we can also write

$$\frac{\partial w'}{\partial E_3} dE_3 + \frac{\partial w'}{\partial T_{11}} dT_{11} = dw'. \qquad (11.5.10)$$

Then comparison of (11.5.8) and (11.5.10) shows that

$$D_3 = \frac{\partial w'}{\partial E_3}, \qquad e_{11} = \frac{\partial w'}{\partial T_{11}}. \qquad (11.5.11)$$

It finally follows from this last pair of equations that

$$\frac{\partial D_3}{\partial T_{11}} = \frac{\partial e_{11}}{\partial E_3}, \qquad (11.5.12)$$

which is the desired reciprocity condition. The same coefficient γ appears in (11.5.1) and (11.5.3) because the electromechanical coupling is conservative. The following example indicates how these constitutive laws can be the basis for describing the electromechanical dynamics of the bar.

Example 11.5.4. We wish to determine the electrical input admittance to the device shown in Fig. 11.5.7. In this case the electric field intensity E_3 is related to the potential V by

$$E_3 = -\frac{V}{a}. \qquad (a)$$

Because E_3 is independent of x, the equation of motion in the bulk of the material does not involve electromechanical coupling; that is, the force equation in the x-direction is

$$\rho \frac{\partial^2 \delta_1}{\partial t^2} = \frac{\partial T_{11}}{\partial x}, \qquad (b)$$

and from (11.5.3), in which E_3 is independent of x, this becomes

$$\rho \frac{\partial^2 \delta_1}{\partial t^2} = \frac{1}{S} \frac{\partial^2 \delta_1}{\partial x^2}. \qquad (c)$$

The boundary conditions at the free ends of the bar, however, do reflect the effect of the electrical input. It follows from (11.5.3) that because $T_{11}(-c/2, t) = 0$ and $T_{11}(c/2, t) = 0$

$$\frac{\partial \delta_1}{\partial x}\left(\frac{-c}{2}, t\right) = \frac{-\gamma V}{a}, \qquad \frac{\partial \delta_1}{\partial x}\left(\frac{c}{2}, t\right) = \frac{-\gamma V}{a} \qquad (d)$$

The input admittance is defined as

$$Y = \frac{\hat{I}}{\hat{V}}, \qquad V = \mathrm{Re}\ \hat{V}e^{j\omega t},$$
$$I = \mathrm{Re}\ \hat{I}e^{j\omega t}, \tag{e}$$

where by conservation of charge on the upper plate

$$\hat{I} = -bj\omega \int_{-c/2}^{c/2} D_3\, dx. \tag{f}$$

In view of (11.5.1), (11.5.3), and (a), this expression can also be written as

$$\hat{I} = -j\omega b \int_{-c/2}^{c/2} \left[\frac{\gamma}{S}\frac{d\delta}{dx} - \frac{\epsilon V}{a}(1 - K^2) \right] dx, \qquad K^2 = \frac{\gamma^2}{\epsilon S}. \tag{g}$$

To proceed in the computation of the input current we require a knowledge of the distribution of the strain e_{11} over the length c of the transducer, which is obtained by solving the bulk equation (c) subject to boundary conditions (d). Solutions take the form $\delta = \mathrm{Re}\ \delta(x)\exp j\omega t$, where

$$\delta = A \sin kx + B \cos kx \left\{ \begin{aligned} &k = \frac{\omega}{\sqrt{\rho S}}, \\ &\delta_1 = \mathrm{Re}\ \delta(x)e^{j\omega t}. \end{aligned} \right. \tag{h}$$

The boundary conditions require that

$$A \cos\left(\frac{kc}{2}\right) + B \sin\left(\frac{kc}{2}\right) = -\frac{\gamma \hat{V}}{ak},$$
$$A \cos\left(\frac{kc}{2}\right) - B \sin\left(\frac{kc}{2}\right) = -\frac{\gamma \hat{V}}{ak}. \tag{i}$$

These conditions show that $B = 0$ unless $kc/2$ is a multiple of π. In what follows we assume that the driving frequency does not coincide with one of these natural frequencies of the even modes. Only the odd modes are excited by the electrical input. Then by adding the two equations of (i)

$$A = \frac{-\gamma \hat{V}}{ak \cos (kc/2)}. \tag{j}$$

It is now possible to use (h) and (j) to evaluate the current as given in (g). Division of this expression by the voltage $\hat{V}$ gives the required input admittance.

$$Y = j\omega \left(\frac{bc}{a}\right)\epsilon \left[(1 - K^2) + \frac{K^2 \tan (kc/2)}{(kc/2)} \right]. \tag{k}$$

In the absence of piezoelectric coupling the coupling coefficient K is zero and (k) reduces to the admittance of a parallel plate capacitor with a dielectric of permittivity ϵ. Even with the coupling the system appears as a simple capacitance at low frequencies. (Remember that k is proportional to the frequency so that, in the limit in which $\omega \to 0$, $kc \to 0$ and the last term in brackets reduces to K^2.)

As might be expected from the fact that the bar supports elastic waves, there are resonances in the response to a driving potential. The admittance is infinite at frequencies such that $\cos(kc/2) = 0$. For this reason the transducer is often used as a resonator with a single electrical terminal pair. Operation is then limited to frequencies in the neighborhood of one of the infinite admittance points. In this case the electromechanical system can be modeled by the electrical circuit shown in Fig. 11.5.9. which has the admittance
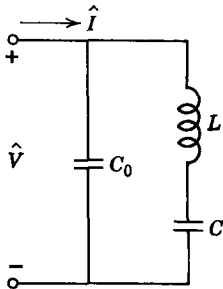
Fig. 11.5.9 Equivalent circuit for expander bar piezoelectric resonator.

$$Y = j\omega \left[C_0 + \frac{1/L}{(1/\sqrt{LC} + \omega)(1/\sqrt{LC} - \omega)} \right], \qquad (l)$$

which for ω approximately equal to $1/\sqrt{LC}$ can also be written as

$$Y = j\omega \left[C_0 + \frac{\sqrt{C/L}}{2} \left(\frac{1}{\sqrt{LC}} - \omega \right) \right]. \qquad (m)$$

In the neighborhood of the first resonance (k) can be written in this same form by expanding the second term in brackets about the first resonance frequency:

$$\omega = \omega_0 + \omega', \qquad \omega_0 = \frac{\pi}{c\sqrt{\rho S}}. \qquad (n)$$

Then

$$\frac{kc}{2} \approx \omega_0 \sqrt{\rho S} \frac{c}{2}, \qquad (o)$$

$$\cot\left(\frac{kc}{2}\right) \approx -\frac{c}{2}\sqrt{\rho S}\,\omega',$$

and (k) becomes

$$Y = j\omega \left(\frac{bc}{a}\right)_\epsilon \left[(1 - K^2) + \frac{4K^2}{c\pi\sqrt{\rho S}\,(\omega_0 - \omega)} \right]. \qquad (p)$$

Comparison of terms in (m) and (p) shows that the equivalent parameters in the electrical circuit of Fig. 11.5.9 are

$$C_0 = \frac{bc}{a}\,\epsilon(1 - K^2),$$

$$L = \frac{cS^2\rho a}{8\gamma^2 b},$$

$$C = \frac{8K^2\epsilon bc}{a\pi^2}.$$

Of course, even though we have represented the device by an electrical equivalent circuit, it is apparent from the expressions for L and C that the resonance is electromechanical in

nature. The transducer is one way of obtaining an extremely large equivalent L. In practice effects of damping would come into play. The effects of losses would introduce an equivalent resistance into the L-C branch of the equivalent circuit.

The simple piezoelectric resonator discussed in the preceding example can provoke only a small awareness of the wide variety of uses to which piezo-electric phenomena can be put. Much of the attractiveness of the devices based on this interaction is related to their small size and great reliability. Figure 11.5.10 shows a pair of devices that involve the same expander modes as discussed two-dimensionally in the example. Here a thin slab of lead titanate zirconate has several electroded regions, hence constitutes a multi-terminal pair system capable of performing logic and modulator functions. The relative size of the devices is apparent from the figure.

11.6 DISCUSSION

In this chapter we have extended the concepts of Chapters 9 and 10, which were developed by using one-dimensional elastic models, to obtain mathematical models for more complex situations.

This chapter completes our introduction to electromechanical interactions with elastic media. We now proceed to a consideration of electromechanical interactions with fluids.

Image removed due to copyright restrictions.

Fig. 11.5.10 A pair of piezoelectric devices with several electrical terminal pairs. Here the working material is a thin sheet of lead titanate zirconate which undergoes mechanical deformations essentially in the plane of the paper. Note the several electroded regions and the small size. (Courtesy of Sandia Corporation, Albuquerque, New Mexico.)

PROBLEMS

11.1. In Fig. 11P.1 a static elastic material is constrained along its vertical sides so that

$$\frac{\partial}{\partial x_2} = \frac{\partial}{\partial x_3} = 0.$$

In the absence of a gravitational field, the material has surfaces at $x_1 = 0$ and $x_1 = L$.

    (a) Compute the material displacement $\delta_1(x_1)$ caused by the gravitational field.

    (b) Find all components of the stress T_{ij}.
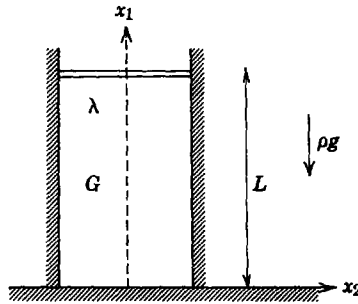
Fig. 11P.1

11.2. In Fig. 11P.2 a slab of elastic solid with constants ρ, G, λ and a thickness L is attached on one side to a rigid wall at $x_1 = 0$. A perfectly conducting thin plate of mass M is attached to the other side of the solid. A second perfectly conducting plate is fixed at $x_1 = -L - d$. Assume that $\partial/\partial x_2 = \partial/\partial x_3 = 0$ and $\delta_1(-L, t) \ll d$.

    (a) If the voltage between the two capacitor plates is $V(t) = V_0 + V_1 \cos \omega t$, find $\delta_1(-L, t)$ $V_1 \ll V_0$.

    (b) For what frequency range does the *mechanical* part of the system appear lumped?

    (c) Give the mechanical lumped parameters for the frequency range defined in (b).
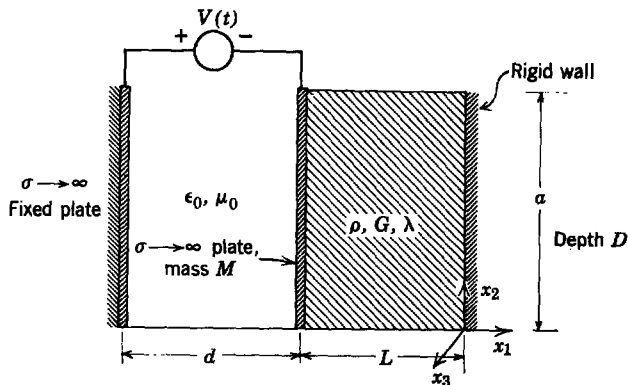
Fig. 11P.2
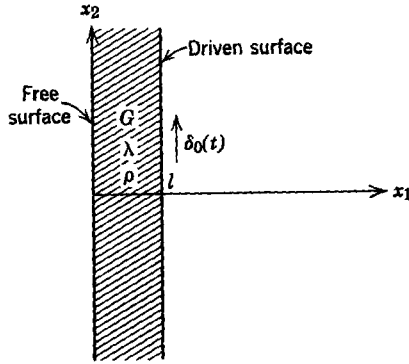
Fig. 11P.3

11.3. A slab of elastic material of length l in the x_1-direction and infinite in extent in the x_2- and x_3-directions has the elastic constants G and λ and mass density ρ. Its surface at $x_1 = l$ is driven in the x_2-direction uniformly by a displacement source $\delta_0(t)$. The surface at $x_1 = 0$ is free to move in the x_2-direction without restraint.

Assume that $\delta_0(t) = \text{Re} \,(\hat{\delta}_0 e^{j\omega t})$, where $\hat{\delta}_0$ and ω are given constants. Neglect the force of gravity and assume that

$$\frac{\partial}{\partial x_2} = \frac{\partial}{\partial x_3} = 0.$$

(a) Find the stress and displacement in the slab.
(b) In the limit of low frequency to what lumped mechanical element does the slab correspond?
(c) Find the lowest frequency for which the slab may be said to "resonate."

11.4. In a coordinate system (x_1, x_2, x_3) a surface with the normal vector n and supporting the stress T_{ij} is subject to the traction (see Section 8.2.2)* $\tau_i = T_{ij} n_j$. Assume that the stress components T_{ij} are known and that there is a surface with an orientation such that the traction is in the same direction as the normal vector; that is, $\tau_i = \alpha \delta_{ij} n_j$, where α is the stress acting normal to the surface.

(a) Write three equations in the three unknowns (n_1, n_2, n_3).
(b) Because these equations are homogeneous, their compatibility requires that the determinant of the coefficients vanish. Show that this gives an expression for α.
(c) Consider the case in which $T_{12} = T_{21} = T_0$ and all other components are zero. What are the possible values of the normal stress α? Compare your result with that found in Example 11.2.1.

11.5. In Example 11.2.1 it was shown that the three elastic constants (G, E, ν) must be related if a perfectly elastic material is isotropic [(g) of that example]. This was done by considering the transformation of a particular case of stress and strain from one coordinate system to a second with the same x_3-axis but a 45° rotation in the x_1-x_2 plane. Follow the arguments presented in Example 11.2.1 to show that the relation is implied for an arbitrary stress condition and an arbitrary rotation of coordinates. Remember that the a_{ij} that determine the rotation of coordinates are related by (8.2.23)* and that if $T'_{pq} = a_{pr} a_{qs} T_{rs}$ then $T_{rs} = a_{pr} a_{qs} T'_{pq}$.

* Appendix G.
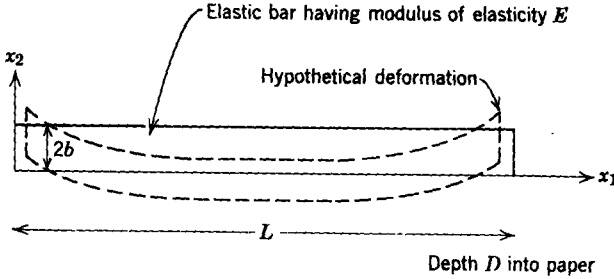
Fig. 11P.6

11.6. An elastic bar is often used in musical instruments as a source of audio-frequency tone. The bar is suspended by strings, attached to it at such points that the transverse (x_2) motion of the elastic material is not appreciably inhibited. (Examples are the vibraharp and marimba.) If the bar is struck by a mallet, it vibrates at one or more of its resonance frequencies. We consider here the problem of finding these frequencies, under the assumption that the bar is as shown in Fig. 11P.6. The bar is supported so that transverse motions are uninhibited, that is, both ends are free.

  (a) Find an equation of the form $\cos \beta \cosh \beta = 1$ $[\beta = \beta(\omega)]$ which stipulates the resonance frequencies.
  (b) Use a graphical solution of the equation found in (a) to determine the two lowest resonance frequencies in terms of E and the dimensions of the bar.
  (c) Sketch the transverse deflection as a function of x_1 for the lowest nontrivial mode.

11.7. A thin elastic beam of thickness $2b$, density ρ, and modulus of elasticity E is clamped on both ends to rigid walls. The total length of the beam is L, as shown in Fig. 11P.7.

  (a) If the beam is suddenly struck from above, what is the lowest (nonzero) frequency at which it will "ring"; that is, what is its lowest natural frequency?
  (b) Give a numerical answer for (a) in Hertz if the beam is steel with length $L = 50$ cm and thickness $2b = 0.10$ cm.
  (c) What is the numerical value, again in Hertz, of the next higher resonance frequency?
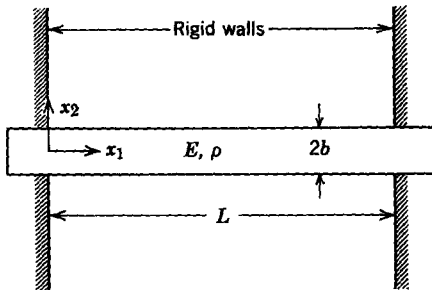
Fig. 11P.7
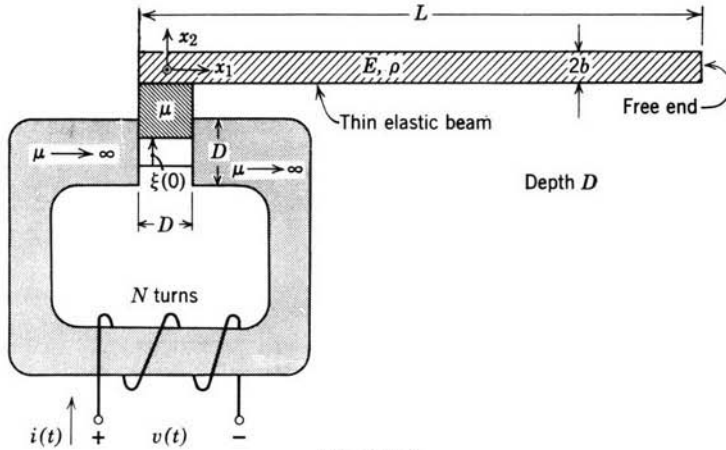
Fig. 11P.8

11.8. The electromechanical system shown in Fig. 11P.8 consists of a long thin elastic beam attached to the plunger of an electromagnet. The plunger has permeability μ and is free to slide between the faces of the electromagnet. Treat the plunger as a rigid body with mass M. Assume that $D \ll L$. The coil on the electromagnet is now excited with a current $i(t) = I_0 + i_1 \cos \omega t$, where $|i_1| \ll I_0$. You may assume that an externally applied force F_0 holds the plunger in equilibrium against the current I_0. Also in equilibrium, the displacement of the beam $\xi(0) = 0$.

(a) What is the value of F_0 required for equilibrium?
(b) Find an expression for the electrical impedance $Z(j\omega)$ seen at the terminals of the coil, where $Z(j\omega) = \hat{v}(j\omega)/i_1$, and $\hat{v}(j\omega)$ is the complex amplitude of the steady-state voltage developed at the terminals.
(c) What is the expression that determines the poles of the impedance $Z(j\omega)$?

11.9. A thin beam clamped to two rigid walls is shown in Fig. 11P.9. Suppose that the beam is perfectly conducting and that it is placed between two perfectly conducting rigid
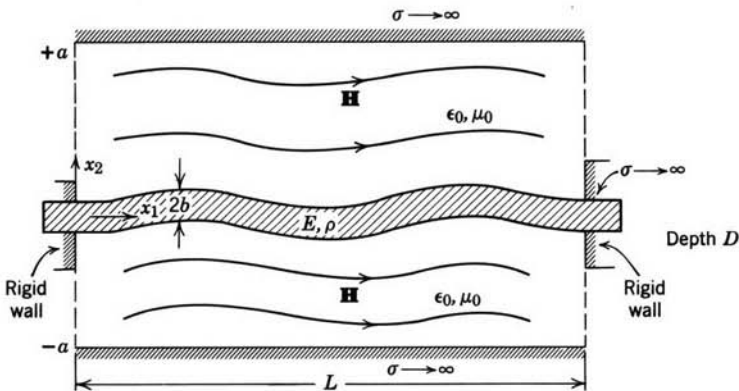
Fig. 11P.9

plates at $x_2 = \pm a$. Assume that there is a magnetic field trapped between the beam and the plates, so that *when the beam is flat* $H = H_0 i_1$ on both sides of the beam. (In the perfect conductor $H = 0$.) Make the approximations that wavelengths of a disturbance on the beam are *long* compared with a and that the magnetic field is always uniform in the x_2- and x_3-directions.

    (a) Write the equation of motion for the beam.
    (b) Compute the first resonance frequency of the beam.
    (c) Compare the result of (b) with Problem 11.7 and give a physical explanation for any differences which occur.
    (d) Can the system be unstable? Explain.

Depth D perpendicular to page
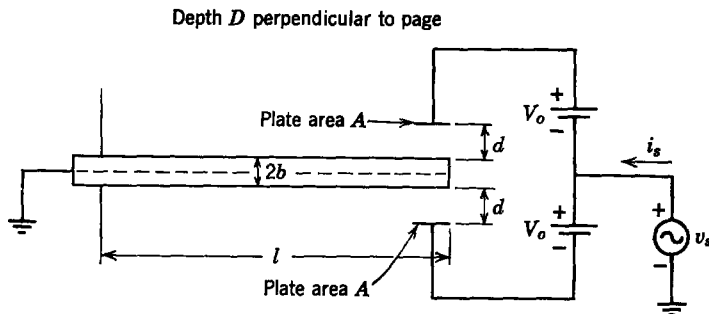
Fig. 11P.10

11.10. The system shown schematically in Fig. 11P.10 is similar to that discussed in Section 11.4.2b. The material of the beam is steel and the system constants and dimensions are

$$E = 2.2 \times 10^{11} \text{ N/m}^2 \qquad A = 10^{-4} \text{ m}^2$$
$$\rho = 7.9 \times 10^3 \text{ kg/m}^3 \qquad D = 10^{-2} \text{ m}$$
$$l = 10^{-1} \text{ m} \qquad b = 10^{-3} \text{ m}$$
$$V_0 = 1000 \text{ V} \qquad d = 10^{-3} \text{ m}$$

We are interested in investigating the impedance seen by the signal source v_s for values of exciting frequency near the first resonance of the elastic bar. This type of information would be essential if we planned to use this system to control the frequency of an oscillator. For sinusoidal excitation $v_s = \text{Re} [\hat{v}_s e^{j\omega t}]$ and small-signal, steady-state operation:

    (a) Find a *literal* expression for the input impedance $Z(j\omega) = \hat{v}_s/\hat{i}_s$, where $\hat{i}_s$ is the complex amplitude of the input current.
    (b) For the numerical values given find a *numerical value* for the lowest frequency ω_0 at which the impedance $Z(j\omega)$ has a zero.
    (c) Assume operation at frequencies near ω_0 by setting $\omega = \omega_0 + \Delta\omega$, where $|\Delta\omega| \ll \omega_0$ and $\Delta\omega$ can be either positive or negative. For this restriction the impedance Z appears as a series LC circuit. Find numerical values for the equivalent capacitance C and equivalent inductance L.

11.11. Consider the planar elastic waveguide of Fig. 11.4.18 but with the walls at $x_2 = 0$ and $x_2 = d$ fixed.

    (a) Find the dispersion equation for waves in the form of

$$\delta_3 = \text{Re } \hat{\delta}(x_2) \exp j(\omega t - kx_1).$$

(b) Sketch the results of part (a) as an ω-k plot and compare with Fig. 11.4.19. Is there a principal mode of propagation?

11.12. A cylindrical, circular elastic section of material with the shear modulus G, density ρ, and radius R is embedded in a perfectly rigid solid so that the material at $r = R$ is fixed. This structure is to be used as a waveguide for elastic shear waves. To find the dispersion equation for these waves, we confine interest to material displacements in the form of $\delta = \delta_\theta(r, z, t)\mathbf{i}_\theta$. Find the dispersion equation for all modes in this form. (A discussion of Bessel's functions is given on p. 207 of S. Ramo, J. Whinnery, and T. Van Duzer, *Fields and Waves in Communication Electronics*, Wiley, New York, 1965.)

Rigid wall at $r = R$
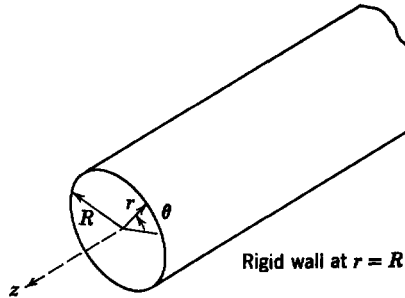
Fig. 11P.12

Chapter **12**

ELECTROMECHANICS
OF INCOMPRESSIBLE,
INVISCID FLUIDS

12.0 INTRODUCTION

We are all familiar with the distinctions between the three pure states of matter: solids, liquids, and gases. A solid body possesses a definite shape and size that is retained unless the body is acted on by outside forces. A given mass of liquid possesses a definite size (volume) but conforms in shape to its container. A particular mass of gas possesses neither definite size (volume) nor shape because it will deform to fill completely whatever vessel it occupies.

Liquids and gases are grouped together and called fluids when their dynamic behavior is to be studied. The essential difference between a solid and a fluid is that the force necessary to deform a solid is a function of the deformation (strain), whereas in a fluid the force necessary to produce a deformation is a function of the *rate* of deformation (strain rate) and a hydrostatic pressure. A fluid left to itself in a force-free environment will relax to a state that has no internal stresses except an isotropic (hydrostatic) pressure balanced by the surface forces exerted by the container or by surface tension.

Although because of some similarities liquids and gases are classified together as fluids, they also exhibit striking differences. Moderate changes in temperature and pressure cause very small fractional changes in the density of a liquid but the corresponding changes in a gas are quite large.

All real fluids exhibit internal friction that is described mathematically by the property called *viscosity*. The effects of viscosity can be large or small, depending on the physical situation being studied. It is standard practice for an electrical engineer to represent a real coil of wire mathematically by an

ideal, lossless circuit element called inductance. Similarly, the fluid dynamicist often uses an idealization of a fluid in which viscosity is neglected. Such an idealization is called an *inviscid* fluid.

In most electromechanical systems involving fluids the principal effects of viscosity result from the contact between the fluid and a solid boundary. As in most continuum problems, the effect of the boundary becomes less pronounced at greater distances from the boundary. Thus, when the behavior of a fluid is desired far from a boundary, an inviscid model is often adequate. How a distance that is adequate for the neglect of viscosity is determined is a rather complex subject and depends quite naturally on the system to be analyzed and the accuracy desired. Much experimental and theoretical data are available to answer this question.* We address ourselves to a few simple cases in which viscosity is important in Chapter 14.

Our purpose in this book is to present models and do analyses of systems in which electromechanical interactions are important. This means essentially that for coupling with a fluid the electromechanical forces must dominate the viscous forces. It is fortuitous that many situations exist in which this occurs, notably magnetohydrodynamic pumps and generators and plasma accelerators.† Consequently, our use of an inviscid fluid model is realistic with respect to the dominant electromagnetic forces and viscous effects can be added later as perturbations.

When a fluid flows past a solid boundary, the fluid friction makes the fluid particles that are in contact with the boundary remain at rest with respect to the boundary. This makes the flow of fluid parallel to the boundary vary with distance from the boundary and introduces a shear rate into the flow. At low velocities each fluid particle flows along a smooth path (a streamline), and the flow is said to be *laminar*. At high velocities the shearing effect of the boundary makes the flow unstable and each fluid particle has a significant random motion in addition to its average motion in the direction of flow. This flow regime is said to be *turbulent*. When a flow becomes turbulent, its internal friction (viscous) losses increase. In spite of this, we can often represent a fluid in turbulent flow in terms of a steady flow at the average velocity and obtain a good model for electromechanical interactions.

Compressibility is a property of a fluid that describes the fact that when the hydrostatic pressure on the fluid is increased the density increases. Every fluid exhibits this property to some extent. Liquids are only slightly compressible, whereas gases are highly compressible. Compressibility to fluids is

---

* H. Schlichting, *Boundary Layer Theory*, 4th ed., McGraw-Hill, New York, 1960, pp. 1–41.

† These situations are illustrated graphically in the film entitled "Magnetohydrodynamics" produced for the National Committee on Fluid Mechanics Films by Education Development Center, Newton, Mass.

what elastic modulus is to elastic solids. Thus we expect a compressible fluid
to transmit longitudinal (sound) waves just as an elastic solid does. When we
are interested in the flow of a liquid, the compressibility can often be neglected.
This is analogous to the treatment of the gross motion of an elastic solid as
the motion of a rigid body. Even though a gas is highly compressible, we
can sometimes treat gas flow by using an incompressible fluid model,
especially at very low flow velocities. In other cases the compressibility of a
gas will have a marked effect on the flow, and we must account for it in our
mathematical model.

Our interest here is in electromechanical interactions; in each case we
select the simplest mathematical model that illustrates the physical phenomena
of interest in a realistic way. Thus in many cases we use a simple fluid model
that adequately illustrates the electromechanical interactions but ignores some
fluid-mechanical phenomena. The inclusion of such phenomena is beyond
the scope of this book. For further information on these topics the reader can
consult a good treatise on fluid mechanics.* In this chapter we investigate
various phenomena that result from electromechanical interactions with
incompressible, inviscid fluids. In Chapter 13 we treat compressible inviscid
fluids and in Chapter 14 introduce viscosity.

12.1 INVISCID, INCOMPRESSIBLE FLUIDS

An incompressible inviscid fluid model lends itself to simple mathematical
analysis and to an understanding of many fluid-mechanical phenomena.
Moreover, it provides considerable insight into the fundamental interactions
of magnetohydrodynamics (MHD) and often gives an accurate description
of MHD interactions with liquid conductors such as liquid metals.

In what follows we first introduce the equations of motion for an in-
compressible inviscid fluid and then consider some simple, fluid-mechanical
examples. Finally, we investigate the important electromechanical interactions
appropriate for study with this model.

12.1.1 The Substantial Derivative

In the study of fluid mechanics we are concerned with describing the fluid
motion and relating it to the applied forces and boundary conditions. Most
often the desired information consists of determining a flow pattern in a
region of space at a given instant of time. Because of this desired result, fluid
dynamicists have focused their attention on fluid variables at a given position
in relation to a fixed reference frame. Since the fluid is moving past this point,
different material elements occupy the point at different instants in time. This

* See, for example, Schlichting, *op. cit.*

method of representing fluid properties (such as velocity) in terms of a fixed point in space is called an Eulerian or field description. An alternative method, called the Lagrangian description, gives the velocity and other properties of the individual particles.

The best-known example of the use of the Lagrangian description is in particle dynamics (or the rigid-body mechanics of Chapter 2) in which it is conventional to ascribe to each particle (or mechanical node) a velocity **v** which is a function of the initial position (a, b, c) of the particle and of time t. Thus $\mathbf{v}(a, b, c, t)$ describes the velocity of a particular particle. This same method is carried over into continuum mechanics by describing the velocity $\mathbf{v}(a, b, c, t)$ of the grain of matter at position a, b, c at $t = 0$. This Lagrangian description was used in Chapter 11, in which the displacement of a grain of elastic material was written as a function of the unstrained (initial) position.

For electrical engineering students the best-known example of the use of an Eulerian description is in electromagnetic field theory. We usually describe the electromagnetic field and source quantities as functions of space and time. Thus for a cartesian coordinate system (x_1, x_2, x_3) we give the electric field intensity as $\mathbf{E}(x_1, x_2, x_3, t)$. This prescribes the field intensity at the point (x_1, x_2, x_3) at any instant of time t. Using the Eulerian description, we can describe a velocity field $\mathbf{v}(x_1, x_2, x_3, t)$ that ascribes a velocity to a position in space rather than to a particular grain of matter. At the point (x_1', x_2', x_3') the velocity $\mathbf{v}(x_1', x_2', x_3', t')$ specifies the velocity of that grain of matter that occupies the point (x_1', x_2', x_3') at the instant of time t'. If at a later time t'' this grain of matter is at point (x_1'', x_2'', x_3''), its velocity will be $\mathbf{v}(x_1'', x_2'', x_3'', t'')$. The Eulerian system is normally used in the study of fluid mechanics and is also used here.*

Later in this chapter we shall need the time derivative of an Eulerian function as experienced by a particular grain of matter. The acceleration of a grain of matter is such a derivative and we shall need it to write Newton's second law.

Consider a system of moving matter with an Eulerian or field description of the velocity, $\mathbf{v}(x_1, x_2, x_3, t)$ and of the quantity $f(x_1, x_2, x_3, t)$. It is necessary to find the time rate of change of f experienced by a grain of matter. Consider the grain of matter that occupies position (x_1, x_2, x_3) at time t and has velocity $\mathbf{v}(x_1, x_2, x_3, t)$ with components v_1, v_2, and v_3. At time $(t + \Delta t)$ the grain will occupy a new position, given to first order in (Δt) by $(x_1 + v_1 \Delta t, x_2 + v_2 \Delta t, x_3 + v_3 \Delta t)$. Thus in the interval (Δt) the grain has experienced a change in f of

$$\Delta f = f(x_1 + v_1 \Delta t, x_2 + v_2 \Delta t, x_3 + v_3 \Delta t, t + \Delta t) - f(x_1, x_2, x_3, t) \quad (12.1.1)$$

* For a more thorough discussion of these alternative representations, see, for example, H. Lamb, *Hydrodynamics*, 6th ed., Dover, New York, 1945, Chapter I, Articles, 4 to 9, 13, and 14.

The first term in this expression is expanded in a Taylor series about the point (x_1, x_2, x_3, t) and second- and higher order terms in Δt are discarded to obtain

$$\Delta f = \frac{\partial f}{\partial t} \Delta t + \frac{\partial f}{\partial x_1} v_1 \Delta t + \frac{\partial f}{\partial x_2} v_2 \Delta t + \frac{\partial f}{\partial x_3} v_3 \Delta t. \qquad (12.1.2)$$

The desired time rate of change is defined as

$$\frac{Df}{Dt} = \lim_{\Delta t \to 0} \frac{\Delta f}{\Delta t}. \qquad (12.1.3)$$

Substitution of (12.1.2) into (12.1.3) yields

$$\frac{Df}{Dt} = \frac{\partial f}{\partial t} + v_1 \frac{\partial f}{\partial x_1} + v_2 \frac{\partial f}{\partial x_2} + v_3 \frac{\partial f}{\partial x_3}, \qquad (12.1.4)$$

which is written in the compact form

$$\frac{Df}{Dt} = \frac{\partial f}{\partial t} + (\mathbf{v} \cdot \nabla) f. \qquad (12.1.5)$$

The function f may be considered to be one component of a cartesian vector $\mathbf{f}$. Equation 12.1.5 holds for each component of the vector; consequently, the time rate of change of a vector field quantity $\mathbf{f}(x_1, x_2, x_3, t)$ experienced by a grain of matter is given by

$$\frac{D\mathbf{f}}{Dt} = \frac{\partial \mathbf{f}}{\partial t} + (\mathbf{v} \cdot \nabla)\mathbf{f}. \qquad (12.1.6)$$

This derivative is variously called the Stokes, total, particle, material, substantial, or convective derivative.

The interpretation of the physical meaning of (12.1.5) or (12.1.6) is quite simple. It merely states that an observer moving with the velocity $\mathbf{v}$, relative to the coordinate system (x_1, x_2, x_3) in which the quantity $f(x_1, x_2, x_3, t)$ is defined, will detect a time rate of change of f made up of two parts: $(\partial f/\partial t)$ is the rate of change of f at a fixed point and $(\mathbf{v} \cdot \nabla)f$ is the change in f that results from the motion of the observer through a fixed (in time) distribution of f. In fact, $(\mathbf{v} \cdot \nabla)f$ is simply the space derivative of f taken in the direction of $\mathbf{v}$ and weighted by the magnitude of $\mathbf{v}$.

An example of the application of (12.1.6), which will occur in Section 12.1.3 is the acceleration of a grain of matter moving in a velocity field $\mathbf{v}(x_1, x_2, x_3, t)$. According to (12.1.6),

$$\frac{D\mathbf{v}}{Dt} = \frac{\partial \mathbf{v}}{\partial t} + (\mathbf{v} \cdot \nabla)\mathbf{v}. \qquad (12.1.7)$$

Example 12.1.1. As an example of the calculation of an acceleration, consider the velocity

$$\mathbf{v} = \frac{V_o}{a}\,(\mathbf{i}_1 x_2 - \mathbf{i}_2 x_1), \tag{a}$$

where V_o and a are positive constants. This will be recognized as the velocity of a fluid undergoing a rigid-body rotation about the x_3-axis. In fact, the angular velocity of the fluid is V_o/a, where $r = \sqrt{x_1^2 + x_2^2}$ is the radial distance from the x_3-axis. Note that $\partial \mathbf{v}/\partial t = 0$. Yet we know that the fluid is accelerating (centrifugal acceleration), and it is this acceleration that is given by the second term in (12.1.7), which becomes

$$\frac{D\mathbf{v}}{Dt} = (\mathbf{v} \cdot \nabla)\mathbf{v} = \left(v_1 \frac{\partial v_1}{\partial x_1} + v_2 \frac{\partial v_1}{\partial x_2}\right)\mathbf{i}_1 + \left(v_1 \frac{\partial v_2}{\partial x_1} + v_2 \frac{\partial v_2}{\partial x_2}\right)\mathbf{i}_2, \tag{b}$$

because v_3 and $\partial/\partial x_3$ are zero. Substitution of (a) into (b) gives

$$\frac{D\mathbf{v}}{Dt} = \left(\frac{V_o}{a}\right)^2 [-x_1(1)]\mathbf{i}_1 + [x_2(-1)]\mathbf{i}_2 \tag{c}$$

as the acceleration of the fluid. This acceleration is directed radially inward toward the x_3-axis and has the expected magnitude $(V_o/a)^2 r$ (the centrifugal acceleration).

We now obtain differential equations of motion that are appropriate for studying the dynamical behavior of incompressible inviscid fluids. We obtain the desired equations from two postulates:

1. Conservation of mass.
2. Conservation of momentum (Newton's second law).

The validity of these postulates has been verified by a variety of experiments.

12.1.2   Conservation of Mass

The conservation of mass states that mass can be neither created nor destroyed and thus must be conserved. To apply this postulate to a particular system consider the system of Fig. 12.1.1 in which an arbitrary volume V enclosed by the surface S is defined in a region containing material with a mass
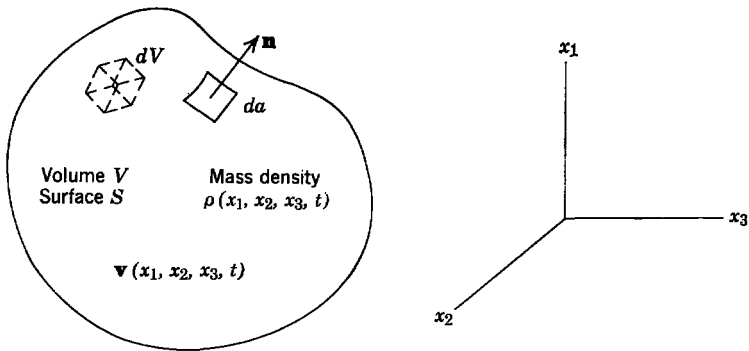
Fig. 12.1.1   Definition of system for writing conservation of mass.

density $\rho(x_1, x_2, x_3, t)$ (kg/m^3) and a velocity $\mathbf{v}(x_1, x_2, x_3, t)$ (m/sec). A differential volume element is dV, a differential surface element is da, and the normal vector $\mathbf{n}$ is normal to the surface and directed outward from the volume.

Because mass must be conserved, we can write the expression for the system in Fig. 12.1.1:

$$\oint_S (\rho \mathbf{v} \cdot \mathbf{n}) \, da = - \frac{d}{dt} \int_V \rho \, dV. \qquad (12.1.8)$$

The left side of this expression evaluates the net rate of mass flow (kg/sec) out of the volume V across the surface S. The right side indicates the rate at which the total mass within the volume decreases. Note the similarity between (12.1.8) and the conservation of charge described by (1.1.26)* in Chapter 1.

Example 12.1.2. The system in Fig. 12.1.2 consists of a pipe of inlet area A_i and outlet area A_o. A fluid of constant density ρ flows through the pipe. The velocity is assumed to be uniform across the pipe's cross section. The instantaneous fluid velocity at the inlet is

$$\mathbf{v}_i = \mathbf{i}_1 v_i$$

and is known. We wish to find the velocity $\mathbf{v}_o$ at the outlet.

We use the closed surface S indicated by dashed lines in Fig. 12.1.2 with the conservation of mass (12.1.8) to find $\mathbf{v}_o$. Because the density ρ is constant,

$$\oint_S (\mathbf{v} \cdot \mathbf{n}) \, da = 0.$$

The only contributions to this integral come from the portions of the surface that coincide with the inlet and outlet. The result is

$$\oint_S (\mathbf{v} \cdot \mathbf{n}) \, da = [\mathbf{v}_i \cdot (-\mathbf{i}_1)]A_i + (\mathbf{v}_o \cdot \mathbf{i}_1)A_o = 0$$

from which

$$\mathbf{v}_o = \mathbf{i}_1 v_o = \mathbf{i}_1 \frac{A_i}{A_o} v_i \, .$$

This expresses the intuitively apparent fact that in the steady state as much fluid leaves the closed surface S as enters it.
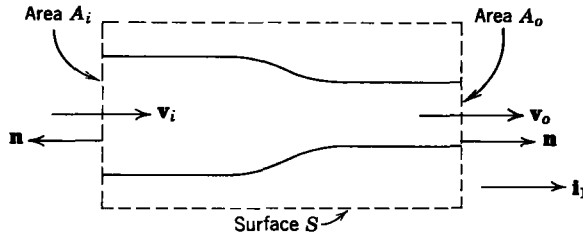
Fig. 12.1.2 Example for application of conservation of mass.

* Table 1.2, Appendix G.

We now write (12.1.8) in differential form by using the divergence theorem*

$$\oint_S (\mathbf{A} \cdot \mathbf{n}) \, da = \int_V (\nabla \cdot \mathbf{A}) \, dV$$

to change the surface integral in (12.1.8) to a volume integral

$$\int_V (\nabla \cdot \rho\mathbf{v}) \, dV = -\int_V \frac{\partial \rho}{\partial t} \, dV. \qquad (12.1.9)$$

The time derivative has been taken inside the integral sign because we assume that the volume V is stationary. This expression holds for any arbitrary volume V; therefore it must hold for a differential volume. Thus

$$\nabla \cdot \rho\mathbf{v} = -\frac{\partial \rho}{\partial t}, \qquad (12.1.10)$$

which is the partial differential equation that describes the conseivation of mass.

The left side of (12.1.10) can be expanded and the terms rearranged to obtain

$$\rho(\nabla \cdot \mathbf{v}) = -\frac{D\rho}{Dt}, \qquad (12.1.11)$$

where the derivative on the right is the substantial derivative defined by (12.1.5). Equation 12.1.11 relates the rate of density decrease in a grain of matter to the divergence of the velocity and is in a form particularly useful when studying incompressible fluids because then the time rate of change of the density as viewed by a particle of fluid is zero, that is, $D\rho/Dt = 0$. Equation 12.1.11 indicates that in this case the velocity field has no divergence $(\nabla \cdot \mathbf{v} = 0)$.

12.1.3   Conservation of Momentum (Newton's Second Law)

The second postulate of fluid mechanics is that Newton's second law of motion (conservation of momentum) must hold for each grain of matter. To express this postulate mathematically we assume that in the coordinate system (x_1, x_2, x_3) there exists a fluid of density $\rho(x_1, x_2, x_3, t)$ moving in a velocity field $\mathbf{v}(x_1, x_2, x_3, t)$. The mass of a grain of matter occupying the differential volume element $dx_1 \, dx_2 \, dx_3$ is $\rho \, dx_1 \, dx_2 \, dx_3$. We multiply this mass by the instantaneous acceleration found in (12.1.7) and equate the result to

* F. B. Hildebrand, *Advanced Calculus for Engineers*, Prentice-Hall, New York, 1948, pp. 312–315.

the total force **f** applied to the grain of matter*

$$\rho(dx_1\,dx_2\,dx_3)\left[\frac{\partial \mathbf{v}}{\partial t} + (\mathbf{v} \cdot \nabla)\mathbf{v}\right] = \mathbf{f}. \qquad (12.1.12)$$

We now divide both sides of this expression by the volume element and define the force density **F** as

$$\mathbf{F} = \frac{\mathbf{f}}{dx_1\,dx_2\,dx_3} \qquad (12.1.13)$$

to obtain the result

$$\rho\,\frac{D\mathbf{v}}{Dt} = \rho\,\frac{\partial \mathbf{v}}{\partial t} + \rho(\mathbf{v} \cdot \nabla)\mathbf{v} = \mathbf{F}. \qquad (12.1.14)$$

This is the differential form of the conservation of momentum equation that we use most often in our treatment of continuum electromechanics.

The force density **F** in (12.1.14) can be written as

$$\mathbf{F} = \mathbf{F}^e + \rho\mathbf{g} + \mathbf{F}^m, \qquad (12.1.15)$$

where $\mathbf{F}^e$ represents the electromagnetic forces that were expressed in various forms in Sections 8.1 and 8.3 of Chapter 8†, $\rho\mathbf{g}$ represents the force density resulting from gravity, and $\mathbf{F}^m$ represents mechanical forces applied to the grain of matter by adjacent material. This latter force density $\mathbf{F}^m$ depends on the physical properties of the fluid and will thus be described in Section 12.1.4 (on constituent relations).

Equation 12.1.14 can be expressed in a particularly simple and often useful form when we recognize that the force density on the right can be expressed as the space derivative of a stress tensor. We have already shown in Sections 8.1 and 8.3 of Chapter 8 that this is true. The ith component of the electromagnetic force density $\mathbf{F}^e$ is

$$F_i{}^e = \frac{\partial T_{ij}{}^e}{\partial x_j}, \qquad (12.1.16)$$

where $T_{ij}{}^e$ is the Maxwell stress tensor given for magnetic-field systems by (8.1.11)† and for electric field systems by (8.3.10)†. Because the gravitational field is conservative, we can write the gravitational force as the negative

---

* Newton's second law, written as $\mathbf{f} = M\mathbf{a}$, applies only for a mass M of fixed identity. Because $D\mathbf{v}/Dt$ is a derivative following a grain of matter, it is the acceleration of a set of mass particles ($\rho\,dx_1\,dx_2\,dx_3$) of fixed identity. Thus (12.1.12) is a valid description of Newton's second law written as $\mathbf{f} = M\mathbf{a}$ and is valid even when ρ is changing with space and time.
† See Table 8.1, Appendix G.

gradient of a scalar potential. We define the gravitational potential as U and write

$$\rho \mathbf{g} = -\nabla U, \tag{12.1.17}$$

or, in index notation, the ith component is

$$\rho g_i = -\frac{\partial U}{\partial x_i} = -\frac{\partial}{\partial x_j}(\delta_{ij}U). \tag{12.1.18}$$

We obtain the force density $\mathbf{F}^m$ of mechanical origin as the derivative of a stress tensor in Section 12.1.4 and therefore assume that the ith component of the mechanical force density $\mathbf{F}^m$ is

$$F_i{}^m = \frac{\partial T_{ij}{}^m}{\partial x_j}, \tag{12.1.19}$$

where $T_{ij}{}^m$ is the mechanical stress tensor to be calculated later.

Now the total stress tensor T_{ij} for the system is

$$T_{ij} = T_{ij}{}^e - \delta_{ij}U + T_{ij}{}^m, \tag{12.1.20}$$

and we can express the ith component of (12.1.14) simply as

$$\rho \frac{Dv_i}{Dt} = \frac{\partial T_{ij}}{\partial x_j}. \tag{12.1.21}$$

This form is particularly useful in applying boundary conditions.

Equation 12.1.14 is often useful when it is expressed in integral form. To achieve this end we multiply the conservation of mass (12.1.11) by the velocity **v** and add it to (12.1.14) to obtain

$$\rho \frac{D\mathbf{v}}{Dt} + \mathbf{v}\frac{D\rho}{Dt} + \rho \mathbf{v}(\nabla \cdot \mathbf{v}) = \mathbf{F}. \tag{12.1.22}$$

Because zero has been added to the left side of (12.1.14), (12.1.22) still expresses Newton's second law. Combination of the first two terms of (12.1.22) into the derivative of the product $(\rho \mathbf{v})$ and use of the definition of (12.1.6) leads to

$$\frac{\partial(\rho \mathbf{v})}{\partial t} + (\mathbf{v} \cdot \nabla)\rho \mathbf{v} + \rho \mathbf{v}(\nabla \cdot \mathbf{v}) = \mathbf{F}. \tag{12.1.23}$$

The ith component of this expression is

$$\frac{\partial(\rho v_i)}{\partial t} + (\mathbf{v} \cdot \nabla)\rho v_i + \rho v_i(\nabla \cdot \mathbf{v}) = F_i. \tag{12.1.24}$$

Combination of the second two terms on the left side of this expression yields

$$\frac{\partial(\rho v_i)}{\partial t} + (\mathbf{\nabla} \cdot \rho v_i \mathbf{v}) = F_i. \tag{12.1.25}$$

We now integrate (12.1.25) throughout a volume V to obtain

$$\int_V \frac{\partial(\rho v_i)}{\partial t}\, dV + \int_V (\mathbf{\nabla} \cdot \rho v_i \mathbf{v})\, dV = \int_V F_i\, dV. \tag{12.1.26}$$

The divergence theorem is used to change the second term on the left to an integral over the surface S that encloses the volume V and has the outward directed normal $\mathbf{n}$; thus

$$\int_V \frac{\partial(\rho v_i)}{\partial t}\, dV + \oint_S \rho v_i (\mathbf{v} \cdot \mathbf{n})\, da = \int_V F_i\, dV. \tag{12.1.27}$$

Using the definition of the total force density in terms of a stress tensor* in (12.1.21), we can also write (12.1.27) as

$$\int_V \frac{\partial(\rho v_i)}{\partial t}\, dV + \oint_S \rho v_i (v_j n_j)\, da = \oint_S T_{ij} n_j\, da. \tag{12.1.28}$$

Equation 12.1.27 can be written for each of the three components and then combined to obtain the vector form

$$\int_V \frac{\partial(\rho \mathbf{v})}{\partial t}\, dV + \oint_S \rho \mathbf{v}(\mathbf{v} \cdot \mathbf{n})\, da = \int_V \mathbf{F}\, dV. \tag{12.1.29}$$

This is the integral form of the equation that expresses conservation of momentum (Newton's second law).

The momentum density of the fluid is $\rho \mathbf{v}$; consequently, the first term on the left of (12.1.29) represents the time rate of increase of momentum density of the fluid that is instantaneously in the volume V. The second term gives the net rate at which momentum density is convected by the flow out of the volume V across the surface S. Thus the left side of (12.1.29) represents the *net* rate of increase of momentum in the volume V. The right side of (12.1.29) gives the net force applied to all the matter instantaneously in the volume V.

12.1.4   Constituent Relations

To complete the mathematical description of a fluid we must describe mathematically how the physical properties of the fluid affect the mechanical behavior. The physical properties of a fluid are described by constituent relations (equations of state), and the form of the equations depends on the fluid model to be used.

---

* See (8.1.13) and (8.1.17) of Appendix G.

A homogeneous, incompressible fluid, which is the model we are considering at present, has constant mass density, independent of other material properties (density and temperature) and of time. Thus one constituent relation is

$$\rho = \text{constant.} \tag{12.1.30}$$

This constituent relation is normally expressed in a different form by substituting (12.1.30) into (12.1.11) to obtain the equation

$$\nabla \cdot \mathbf{v} = 0, \tag{12.1.31}$$

which is the mathematical description normally used to express the property of incompressibility. Note, however [from (12.1.11)], that ρ does not have to be constant for (12.1.31) to hold. The fluid could be inhomogeneous and still be incompressible.

The next step in the description of physical properties is to determine how the mechanical force density $\mathbf{F}^m$ of (12.1.15) arises in a fluid.

First, consider a fluid at rest. By definition, a fluid at rest can sustain no shear stresses. Moreover, a fluid at rest can sustain only compressive stresses and a homogeneous, isotropic fluid will sustain the same compressive stress across a plane of arbitrary orientation. This isotropic compressive stress is defined as a positive hydrostatic pressure p.

We can define a mechanical stress tensor for the fluid at rest in the nomenclature of Sections 8.2 and 8.2.1*. Thus, because there are no shear stresses,

$$T_{ij}{}^m = 0, \quad \text{for} \quad i \neq j. \tag{12.1.32}$$

The normal stresses are all given by

$$T_{11}{}^m = T_{22}{}^m = T_{33}{}^m = -p. \tag{12.1.33}$$

The information contained in (12.1.32) and (12.1.33) can be written in compact form by using the Kronecker delta defined in (8.1.7) of Chap. 8*; therefore

$$T_{ij}{}^m = -\delta_{ij}p. \tag{12.1.34}$$

We can verify that the stress tensor in (12.1.34) describes an isotropic, normal compressive stress by calculating the traction* τ^m applied to a surface of arbitrary orientation. To do this assume a surface with normal vector

$$\mathbf{n} = n_1\mathbf{i}_1 + n_2\mathbf{i}_2 + n_3\mathbf{i}_3. \tag{12.1.35}$$

Now use (8.2.2) of Chapter 8 with (12.1.34) and (12.1.35) to calculate the ith component of τ^m,

$$\tau_i{}^m = T_{ij}{}^m n_j = -p\,\delta_{ij}n_j = -pn_i \tag{12.1.36}$$

The vector traction then is

$$\tau^m = -p(n_1\mathbf{i}_1 + n_2\mathbf{i}_2 + n_3\mathbf{i}_3) = -p\mathbf{n}. \tag{12.1.37}$$

* Appendix G.
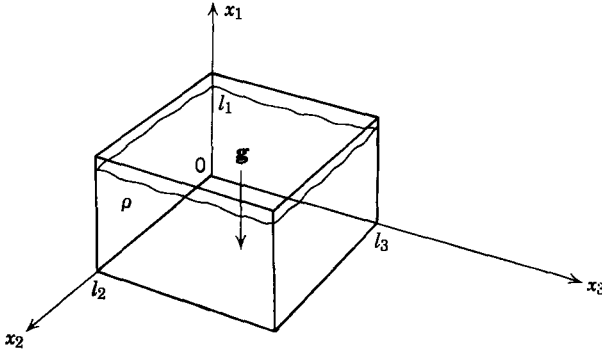
Fig. 12.1.3   Example for the application of stress tensor to a fluid at rest.

This traction is normal to the surface and in the direction opposite to the normal vector **n**. Thus the stress tensor of (12.1.34) describes an isotropic compressive stress.

The pressure p may be a function of position; consequently, a volume force density can result from a space variation of pressure. To find this force density we use (8.2.7)* to evaluate the ith component

$$F_i{}^m = \frac{\partial T_{ij}{}^m}{\partial x_j} = -\delta_{ij} \frac{\partial p}{\partial x_j} = -\frac{\partial p}{\partial x_i}. \tag{12.1.38}$$

When the three components are combined, the vector force density becomes

$$\mathbf{F}^m = -\left(\frac{\partial p}{\partial x_1} \mathbf{i}_1 + \frac{\partial p}{\partial x_2} \mathbf{i}_2 + \frac{\partial p}{\partial x_3} \mathbf{i}_3 \right) \tag{12.1.39}$$

$$\mathbf{F}^m = -\nabla p.$$

Example 12.1.3.   As an example of the application of this mechanical force density, consider the system shown in Fig. 12.1.3 which consists of a container of lateral dimensions l_2 and l_3 and filled to a height l_1 with a fluid of constant mass density ρ. The acceleration of gravity **g** acts in the negative x_1-direction. The fluid is open to atmospheric pressure p_o at the top. We wish to find the hydrostatic pressure at any point in the fluid.

The fluid is at rest, so the acceleration is zero. Moreover, the only forces applied to the material are the force of gravity and the mechanical force from adjacent material. Thus the conservation of momentum (12.1.14) and (12.1.15) yields for this system

$$0 = -\mathbf{i}_1 \rho g - \nabla p.$$

In component form this equation becomes

$$0 = -\rho g - \frac{\partial p}{\partial x_1},$$

$$0 = -\frac{\partial p}{\partial x_2},$$

$$0 = -\frac{\partial p}{\partial x_3}.$$

* See Appendix G.

We integrate these three equations to find that p is independent of x_2 and x_3 and is given in general by

$$p = -\rho g x_1 + C.$$

The integration constant C is determined by the condition that in the absence of surface forces the pressure must be continuous at $x_1 = l_1$. Thus

$$p = p_o + \rho g (l_1 - x_1).$$

Equations 12.1.34 and 12.1.39 describe mechanical properties of a fluid at rest. In a real fluid, motion will result in internal friction forces that add to the pressure force. In an *inviscid* fluid, however, motion results in no additional mechanical forces other than the forces of inertia already included in the momentum equation (12.1.14). Consequently, in the inviscid model the only mechanical force density [$\mathbf{F}^m$ in (12.1.15)] results from a space variation of pressure expressed by (12.1.39).

For an incompressible inviscid fluid the physical properties are completely specified by (12.1.31) and (12.1.39). Therefore, when boundary conditions and applied force densities (electrical and gravity) are specified, these constituent relations and (12.1.14) can be used to determine the motion of the fluid. We treat first some of the purely fluid-mechanical problems to identify the kinds of flow phenomena to be expected from this fluid model and then add electromechanical coupling terms.

12.2 MAGNETIC FIELD COUPLING WITH INCOMPRESSIBLE FLUIDS

An important class of electromechanical interactions is describable by irrotational flow; that is,

$$\nabla \times \mathbf{v} = 0. \tag{12.2.1}$$

When such an approximation is appropriate, the equations of motion can be solved quite easily because a vector whose curl is zero can be expressed as the gradient of a potential. Thus we define the class of problems for which (12.2.1) holds as *potential flow* problems and we define a *velocity potential* ϕ such that

$$\mathbf{v} = -\nabla\phi. \tag{12.2.2}$$

For incompressible flow $\nabla \cdot \mathbf{v} = 0$ from (12.1.31) and the potential ϕ must satisfy Laplace's equation

$$\nabla^2\phi = 0. \tag{12.2.3}$$

A solution of a potential flow problem then reduces to a solution of Laplace's equation that fits the boundary conditions imposed on the fluid.

We can now establish some important properties of potential flow. The momentum equation (12.1.14) takes the form

$$\rho \frac{\partial \mathbf{v}}{\partial t} + \rho(\mathbf{v} \cdot \nabla)\mathbf{v} = -\nabla p - \nabla U + \mathbf{F}^e, \tag{12.2.4}$$

where we have used the definition of the substantial derivative in (12.1.6) and the definition of the gravitational potential U in (12.1.17). The use of the vector identity

$$(\mathbf{v} \cdot \nabla)\mathbf{v} = \tfrac{1}{2}\nabla(v^2) - \mathbf{v} \times (\nabla \times \mathbf{v}),$$

where $v^2 = \mathbf{v} \cdot \mathbf{v}$, and (12.2.1) yields (12.2.4) in the alternative form

$$\rho \frac{\partial \mathbf{v}}{\partial t} + \tfrac{1}{2}\rho\,\nabla(v^2) = -\nabla p - \nabla U + \mathbf{F}^e. \tag{12.2.5}$$

We now use the facts that ρ is constant, that the space (∇) and time ($\partial/\partial t$) operators are independent, and that the velocity is expressed by (12.2.2) to write (12.2.5) in the form

$$\nabla\left(\rho \frac{\partial \phi}{\partial t} + \tfrac{1}{2}\rho v^2 + p + U\right) = \mathbf{F}^e. \tag{12.2.6}$$

By taking the curl of both sides of (12.2.6) we find that potential flow is possible only when

$$\nabla \times \mathbf{F}^e = 0. \tag{12.2.7}$$

If this condition is not satisfied, the assumption that $\nabla \times \mathbf{v} = 0$ is not valid.

Thus we restrict the treatment of the present section to electromechanical interactions in which the force density of electrical origin has no curl (12.2.7). In view of (12.2.7), we express the force density $\mathbf{F}^e$ as

$$\mathbf{F}^e = -\nabla\psi, \tag{12.2.8}$$

where ψ is an electromagnetic force potential, and write (12.2.6) as

$$\nabla\left(\rho \frac{\partial \phi}{\partial t} + \tfrac{1}{2}\rho v^2 + p + U + \psi\right) = 0. \tag{12.2.9}$$

The most general solution for this differential equation is

$$\rho \frac{\partial \phi}{\partial t} + \tfrac{1}{2}\rho v^2 + p + U + \psi = H(t); \tag{12.2.10}$$

that is, this expression can be a function of time but not a function of space.

When the flow is steady, $\partial \phi/\partial t = 0$ and none of the other quantities on the left of (12.2.10) is a function of time. Then (12.2.10) reduces to

$$\tfrac{1}{2}\rho v^2 + p + U + \psi = \text{constant}. \tag{12.2.11}$$

This result, known as *Bernoulli's equation*, expresses a constant of the motion and is useful in the solution of certain types of problem.

Example 12.2.1. As an example of the application of Bernoulli's equation, consider the system in Fig. 12.2.1. This system consists of a tank that is open to atmospheric pressure p_0 and filled to a height h_1 with an inviscid, incompressible fluid. The fluid discharges through a small pipe at a height h_2 with velocity v_2. The area of the tank is large compared with the area of the discharge pipe; thus we assume that the tank empties so slowly that we can neglect the vertical velocity of the fluid and consider this as a steady flow problem.
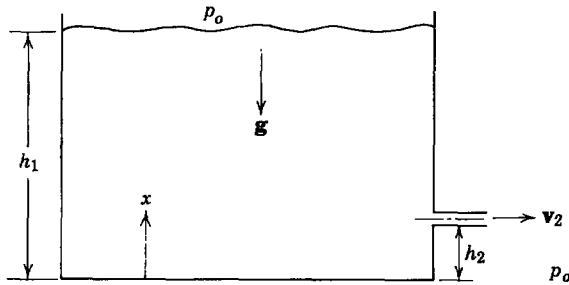
Fig. 12.2.1   Example of application of Bernoulli's equation.

There are no externally applied forces other than pressure and gravity, which has a downward acceleration g. We wish to find the discharge speed v_2.

The gravitational potential U is

$$U = \rho g x,$$

where we assume that x is measured from the bottom of the tank. (We could choose any other convenient reference point.)

Application of Bernoulli's equation (12.2.11) with $\psi = 0$ (there are no electromagnetic forces) at the top of the fluid and at the outlet of the discharge pipe yields

$$p_0 + \rho g h_1 = p_0 + \rho g h_2 + \tfrac{1}{2}\rho v_2^2,$$

from which

$$v_2 = \sqrt{2g(h_1 - h_2)}.$$

We now apply the equations of motion for potential flow to examples involving electromechanical coupling.

12.2.1   Coupling with Flow in a Constant-Area Channel

We first consider the flow of an incompressible inviscid fluid in a horizontal channel with the dimensions and coordinate system defined in Fig. 12.2.2. At the channel inlet ($x_1 = 0$) the fluid velocity is constrained to be
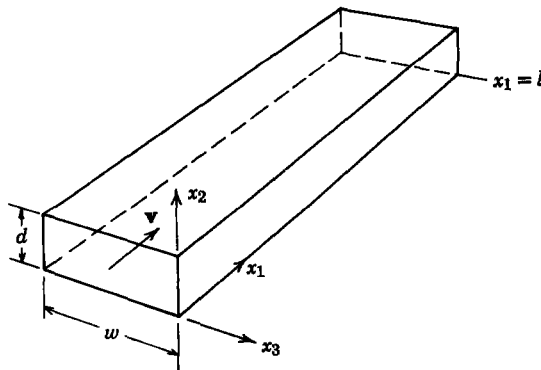
Fig. 12.2.2   A channel of constant cross-sectional area.

uniform and in the x_1-direction

$$\mathbf{v}(0, x_2, x_3, t) = \mathbf{i}_1 v_o(t). \tag{12.2.12}$$

At a fixed channel wall, the normal component of velocity must be zero and the tangential component is unconstrained (for an inviscid fluid); consequently, the velocity of flow throughout the channel is

$$\mathbf{v}(x_1, x_2, x_3, t) = \mathbf{i}_1 v_o(t) \tag{12.2.13}$$

and the velocity potential is

$$\phi(x_1, x_2, x_3, t) = -x_1 v_o(t). \tag{12.2.14}$$

Note that this potential satisfies Laplace's equation (12.2.3) and the boundary conditions.

Equation 12.2.13 is the velocity distribution in the constant-area channel with the boundary condition specified (12.2.12) regardless of the space distributions or time variations of applied force densities but with the restriction that these force densities be irrotational (12.2.7).

12.2.1a Steady-State Operation

In this section we analyze a simple coupled system that is the basic configuration for illustrating the most important phenomena in magnetohydrodynamic (MHD) conduction machines. In spite of the myriad factors (viscosity, compressibility, turbulence, etc.) that affect the properties of real devices, the model presented is used universally for making initial estimates of electromechanical coupling in MHD conduction machines of all types.

The basic configuration is illustrated in Fig. 12.2.3 and consists of a rectangular channel of length l, width w, and depth d, through which an electrically
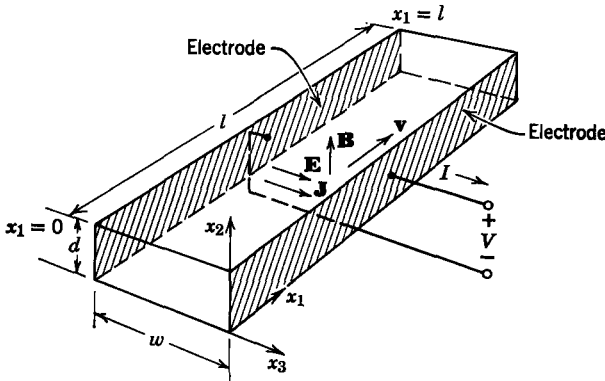
Fig. 12.2.3 Conduction-type, MHD machine.

conducting nonmagnetizable fluid flows with velocity $\mathbf{v}$ in the x_1-direction. The two channel walls perpendicular to the x_2-direction are insulators and the two walls perpendicular to the x_3-direction are highly conducting electrodes from which terminals are connected to an external circuit. The flux density $\mathbf{B}$ is in the x_2-direction and is produced by external coils or magnets not shown. The electrical conductivity σ of the fluid is high enough that the system can be modeled as a quasi-static magnetic field system.

We are considering an inviscid fluid model and we assume that the inlet ($x_1 = 0$) velocity is uniform as expressed by (12.2.12); thus the velocity is uniform throughout the channel as expressed by (12.2.13). We neglect fringing magnetic fields and the magnetic field due to current in the fluid* and assume that $\mathbf{B}$ is uniform:

$$\mathbf{B} = \mathbf{i}_2 B, \tag{12.2.15}$$

where B is constant. Because we are dealing with a steady-flow problem with time-invariant boundary conditions, $\partial/\partial t = 0$ and Faraday's law yields

$$\nabla \times \mathbf{E} = 0. \tag{12.2.16}$$

Once again we neglect fringing fields at the ends of the channel† and obtain the resulting solution

$$\mathbf{E} = -\mathbf{i}_3 \frac{V}{w}, \tag{12.2.17}$$

where V is the potential difference between the electrodes with the polarity defined in Fig. 12.2.3.

We now use Ohm's law for a moving conductor of conductivity σ (6.3.5),

$$\mathbf{J} = \sigma(\mathbf{E} + \mathbf{v} \times \mathbf{B}) \tag{12.2.18}$$

to write the current density for the system of Fig. 12.2.3 as

$$\mathbf{J} = \mathbf{i}_3 \sigma \left(-\frac{V}{w} + v_o B \right). \tag{12.2.19}$$

Note that this current density is uniform and therefore satisfies the conservation of charge condition $\nabla \cdot \mathbf{J} = 0$. Because the current density is uniform, it can

* The neglect of the self-field due to current in the fluid is justified for MHD generators when the magnetic Reynolds number based on channel length is much less than unity (see Section 7.1.2a).

† This assumption is quite good provided the l/w ratio of the channel is large (five or more). This result has been obtained in a detailed analysis of end effects by using a conformal mapping technique. The results of this analysis are presented in "Electrical and End Losses in a Magnetohydrodynamic Channel Due to End Current Loops," G. W. Sutton, H. Hurwitz, Jr., and H. Poritsky, Jr., *Trans. AIEE* (Comm. Elect.), **81**, 687–696 (January 1962).

be related to the terminal current by the area of an electrode; thus

$$\mathbf{J} = \mathbf{i}_3 \frac{I}{ld}. \qquad (12.2.20)$$

To obtain the electrical terminal characteristics of this machine, we combine (12.2.19) and (12.2.20) to obtain

$$IR_i = -V + v_o Bw, \qquad (12.2.21)$$

where we have defined the internal resistance R_i as

$$R_i = \frac{w}{\sigma ld}. \qquad (12.2.22)$$

Equation 12.2.21 can be represented by the equivalent circuit of Fig. 12.2.4. The open-circuit voltage ($v_o Bw$) is generated by the motion of the conducting fluid through the magnetic field and has the same physical nature as speed voltage generated in conventional dc machines using solid conductors (see Section 6.4). This speed voltage can supply current to a load through the internal resistance R_i which is simply the resistance that would be measured between electrodes with the fluid at rest. From an electrical point of view the electromechanical interaction occurs in the equivalent battery ($v_o Bw$) in Fig. 12.2.4.
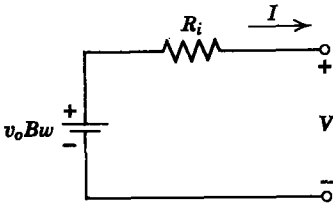
Fig. 12.2.4 Electrical equivalent circuit of conduction-type MHD machine.

To describe the properties of the MHD machine of Fig. 12.2.3, viewed from the electrical terminals, we have obtained a relation between terminal voltage and terminal current (12.2.21). From a mechanical point of view a similar relation is that between the pressure difference over the length of the channel and the velocity through the channel. This mechanical terminal relation is obtained from the x_1-component of the momentum equation (12.2.4):

$$0 = -\frac{\partial p}{\partial x_1} - \frac{IB}{ld}. \qquad (12.2.23)$$

Integration of this equation over the length of the channel yields

$$\Delta p = -\frac{IB}{d}, \qquad (12.2.24)$$

where the pressure rise Δp is defined by

$$\Delta p = p(l) - p(0). \qquad (12.2.25)$$
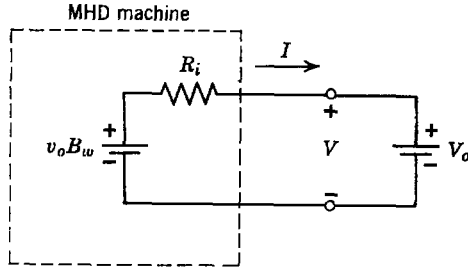
Fig. 12.2.5 MHD conduction machine with a constant-voltage constraint on the electrical terminals.

Equation 12.2.24 indicates that for this system the pressure rise along the channel is a function of the terminal current only and independent of the fluid velocity. This is reasonable because the pressure gradient is balanced by the $\mathbf{J} \times \mathbf{B}$ force density, regardless of the velocity. For an arbitrary electrical source or load the pressure rise will vary with velocity because the current depends on velocity through (12.2.21).

To study the energy conversion properties of the machine in Fig. 12.2.3 we constrain the electrical terminals with a constant-voltage source V_o as indicated in Fig. 12.2.5 and study the behavior of the device as a function of the fluid velocity v_o. For this purpose we use (12.2.21) to find the current I as

$$I = \frac{v_o Bw - V_o}{R_i} \tag{12.2.26}$$

Substitution of this result into (12.2.24) yields for the pressure rise

$$\Delta p = -\frac{B}{dR_i}(v_o Bw - V_o). \tag{12.2.27}$$

The current and pressure rise are shown plotted as functions of velocity v_o in Fig. 12.2.6.

To determine the nature of the device we define the electric power output P_e which, when positive, indicates a flow of electric energy from the MHD machine into the source V_o:

$$P_e = IV_o. \tag{12.2.28}$$

We also define the mechanical power out P_m, which represents power flow from the MHD machine into the velocity source v_o:

$$P_m = \Delta pwdv_o. \tag{12.2.29}$$

For the range of velocities

$$v_o > \frac{V_0}{Bw}$$

we have

$$P_e > 0, \qquad P_m < 0$$

and the device is a generator; that is, mechanical power input is in part converted to electric power. For the velocity range

$$0 < v_o < \frac{V_o}{Bw}$$

we have

$$P_e < 0, \qquad P_m > 0$$

and the device is a pump. Electric power input is converted in part to mechanical power. For the velocity range

$$v_o < 0,$$

$$P_e < 0, \qquad P_m < 0;$$

that is, both mechanical and electrical power are into the MHD machine. All of this input power is dissipated in the internal resistance of the machine. In this region the machine acts as an electromechanical brake because electric
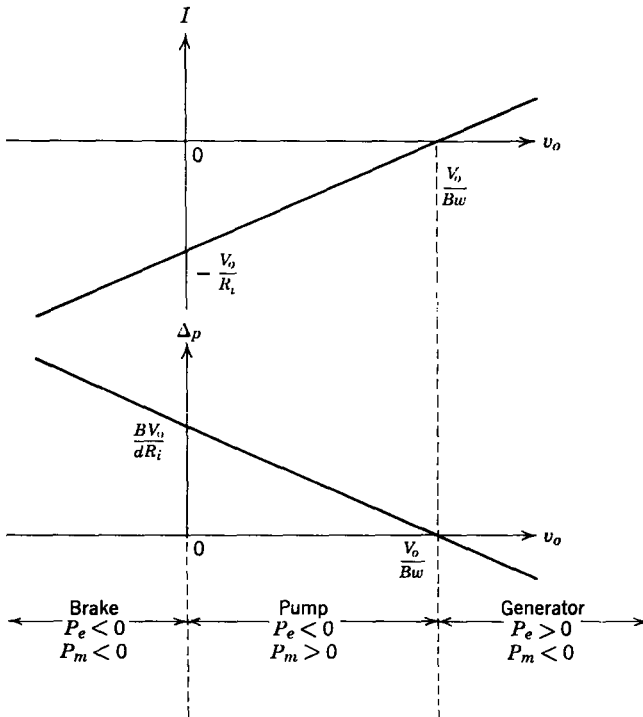
Fig. 12.2.6 Terminal characteristics of an MHD conduction-type machine with constant terminal voltage.

power is put in, and the only electromechanical result is to retard the fluid flow.

The properties of the MHD machine, as indicated by the curves of Fig. 12.2.6, can be interpreted in terms of the equivalent circuit of Fig. 12.2.5. We substitute (12.2.24) into (12.2.29) to find that the mechanical output power is expressible as

$$P_m = -I(v_o Bw). \tag{12.2.30}$$

Reference to Fig. 12.2.5 shows that this is the power input to the battery that represents the speed voltage. Thus, when the battery $(v_o Bw)$ absorbs power, energy is being supplied to the velocity source by the MHD machine. When the battery $(v_o Bw)$ supplies power, energy is being supplied to the external voltage source by the MHD machine. When the battery $(v_o Bw)$ supplies power, energy is being extracted from the velocity source. Thus, when the two batteries of Fig. 12.2.5 have opposing polarities, energy can flow from one battery to the other and the machine can operate as a pump or a generator, the operation being determined by the relative values of the two battery voltages. When the polarities of both batteries are in the same direction $(v_o < 0$ in Fig. 12.2.5), the two batteries supply energy to the resistance R_i, and the MHD machine acts as a sink for both electrical and mechanical energy. This is operation as a brake.

This analysis has been done for a particular set of terminal constraints. Essentially the same techniques can be used for other constraints. It is worthwhile to point out that (12.2.24) indicates that if the machine is constrained mechanically by a constant pressure source the electrical output will be at constant current.

The analysis just completed provides the basic model used in any examination of the electromechanical coupling process in conduction-type MHD devices, regardless of whether they are pumps or generators and whether the working fluid is a liquid or gas. The model and its consequences should be compared with those of commutator machines (Section 6.4.1) and of homopolar machines (Section 6.4.2). The similarities are evident and the opportunity of using the results of the analysis of one device for interpreting the behavior of another will broaden our understanding of electromechanical interactions of this kind.

An alternative method of achieving electromechanical coupling between an electrical system and a conducting fluid is to use a system that is analogous to the squirrel-cage induction machine analyzed in Section 4.1.6b. We shall not analyze this type of system here, but the analysis is a straightforward extension of concepts and techniques already presented. The system consists basically of a channel of flowing conducting fluid that is subjected to a transverse magnetic field in the form of a wave traveling in the direction of

flow. This wave is most often established by a distributed polyphase winding (Sections 4.1.4 and 4.1.7). When the wave of magnetic field travels faster than the fluid, the fluid is accelerated by the field and pumping action results. When the fluid travels faster than the magnetic field wave, the fluid is decelerated and electric power is generated. In the analysis of an induction machine magnetic diffusion and skin effect are important (Section 7.1.4).

Both conduction- and induction-type MHD machines are used for pumping liquid metals[*]; they are proposed for power generation with liquid metals[†] and used to accelerate ionized gases for space propulsion systems[‡]; both are proposed for power generation with ionized gases,[§] although the conduction-type machine appears more attractive by far for this purpose.

12.2.1b   Dynamic Operation

We now consider the kinds of phenomena that can result from electromechanical coupling with an incompressible fluid of time-varying velocity. We start by considering the fluid dynamic behavior of a simple example, which will then be the basis for a study of electromechanical transient effects.

The configuration to be studied is shown in Fig. 12.2.7. The system consists of a rigid tube of rectangular cross section bent into the form of a U. The depth d of the tube is small compared with the radius of the bends. The tube is filled with an incompressible inviscid fluid to a length l measured along the center of the tube. The two surfaces are open to atmospheric pressure p_o and gravity acts downward as shown.

It is clear that for static equilibrium the two surfaces of the fluid are at the same height. The displacement of the two surfaces from the equilibrium positions are designated x_a and x_b.

To study the dynamic behavior of this system we displace the fluid from equilibrium, release it from rest, and study the ensuing fluid motions.

The equations for solving this problem express conservation of mass and force equilibrium. Conservation of mass (12.1.31) used with the irrotational flow condition (12.2.1) and the fact that the channel has constant cross-sectional area leads to the conclusion that the flow velocity is uniform across the channel. (Here we ignore effects due to the channel curvature.)

* L. R. Blake, "Conduction and Induction Pumps for Liquid Metals," *Proc. Inst. of Elec Engrs. (London)*, **104A**, 49 (1957).

† D. G. Elliott, "Direct-Current Liquid Metal MHD Power Generation," *AIAA J.*, 627–634 (1966). M. Petrick and K. V. Lee, "Performance Characteristics of a Liquid Metal MHD Generator," *Intl. Symp. MHD Elec. Power Gen.*, Vol 2, pp. 953–965, Paris, July 1964.

‡ E. L. Resler and W. R. Sears, "The Prospects for Magnetohydrodynamics," *J. Aerospace Sci.*, **25**, No. 4, 235–245 (April 1958).

§ H. H. Woodson, "Magnetohydrodynamic AC Power Generation," *AIEE Pacific Energy Conversion Conf. Proc.*, pp. 30-1–30-2, San Francisco, 1964.
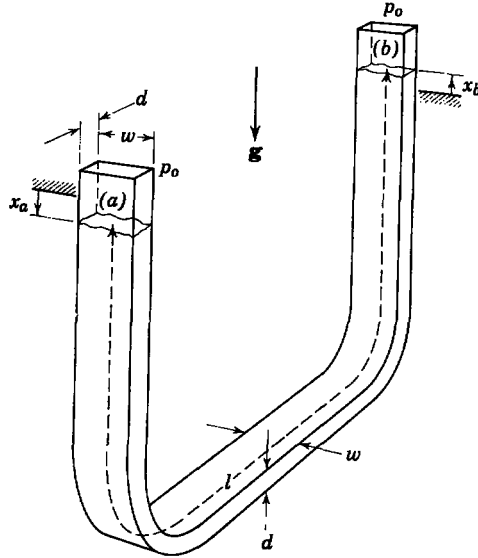
Fig. 12.2.7 Configuration for transient flow problem.

Furthermore, the displacements of the two surfaces are equal

$$x_a = x_b. \tag{12.2.31}$$

The form of the momentum equation that is most useful for this example is (12.2.5) with $\mathbf{F}^e = 0$.

$$\rho \frac{\partial \mathbf{v}}{\partial t} = -\nabla \left(p + \rho \frac{v^2}{2} + U \right), \tag{12.2.32}$$

where U is the gravitational potential. We now do a line integration of (12.2.32) from the surface at (a) to the surface at (b) along the center of the tube to obtain

$$\int_a^b \rho \frac{\partial \mathbf{v}}{\partial t} \cdot d\mathbf{l} = \int_a^b -\nabla \left(p + \rho \frac{v^2}{2} + U \right) \cdot d\mathbf{l} \tag{12.2.33a}$$

$$\rho l \frac{\partial v}{\partial t} = -2\rho g x_a. \tag{12.2.33b}$$

This result could have been obtained by using (12.2.10), a fact that is not surprising because the steps leading from (12.2.32) to (12.2.33) parallel those used in Section 12.2.

The velocity v is given by

$$v = \frac{dx_a}{dt};$$

thus we rewrite (12.2.33) as

$$l \frac{d^2 x_a}{dt^2} + 2g x_a = 0, \qquad (12.2.34)$$

which is a convenient expression for the surface displacement x_a. It shows that the dynamics are those of an undamped second-order system.

We now displace the fluid surface at (a) to the position

$$x_a(0) = X_o \qquad (12.2.35)$$

and release it from rest

$$\frac{d x_a}{dt}(0) = 0. \qquad (12.2.36)$$

The solution of (12.2.34) with the initial conditions of (12.2.35) and (12.2.36) is

$$x_a(t) = u_{-1}(t) X_o \cos \omega t, \qquad (12.2.37)$$

where $u_{-1}(t)$ is the unit step and the frequency ω is given by

$$\omega = \left(\frac{2g}{l} \right)^{\frac{1}{2}}. \qquad (12.2.38)$$

Note that this lossless, fluid-mechanical system has the basic property of a simple pendulum in that the natural frequency depends only on the acceleration of gravity and the length of fluid in the flow direction and is independent of the mass density of the fluid.

We now couple electromechanically to the system of Fig. 12.2.7 with an MHD machine of the kind analyzed in Section 12.2.1a placed in the U tube as shown in Fig. 12.2.8. The total length of fluid between the surfaces at (a) and (b) is still l and the length of the MHD machine in the flow direction is l_1. The flux density B is uniform over the length of the MHD machine and is again produced by a system not shown. As in Section 12.2.1a, we neglect the magnetic field due to current in the fluid as well as the end and edge effects. The terminals of the MHD machine are loaded with a resistance R.

In this analysis we are interested in the fluid dynamical transient that will usually be much slower than purely electrical transients whose time constant depends on the inductance of the electrode circuit. Thus we neglect the inductance of the electrode circuit and the electric terminal relation is obtained from (12.2.21) by setting

$$V = IR. \qquad (12.2.39)$$

The resulting relation between current and velocity is

$$I = \frac{vBw}{R_i + R}, \qquad (12.2.40)$$
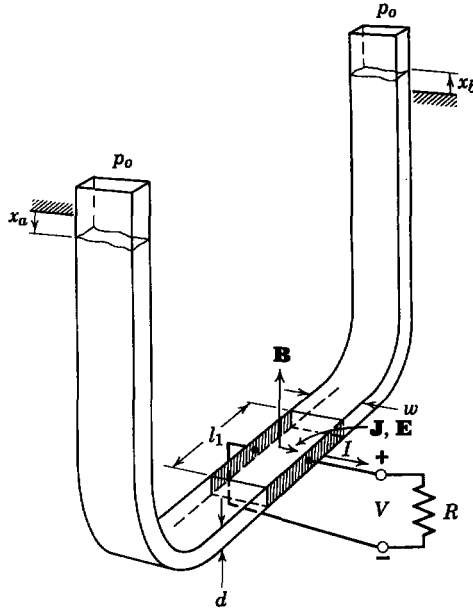
Fig. 12.2.8   Transient-flow problem with electromechanical coupling.

where the internal resistance is

$$R_i = \frac{w}{\sigma l_1 d}$$

and σ is the electrical conductivity of the fluid.

The addition of the electrical force term to the momentum equation (12.2.32) yields

$$\rho \frac{\partial \mathbf{v}}{\partial t} = -\nabla \left(p + \rho \frac{v^2}{2} + U \right) + \mathbf{J} \times \mathbf{B}. \tag{12.2.41}$$

Integration of this expression between the two fluid surfaces in the manner of (12.2.33) yields

$$\rho l \frac{\partial v}{\partial t} = -2\rho g x_a - \frac{IB}{d}. \tag{12.2.42}$$

Note that the last term on the right is simply the pressure rise through the MHD machine due to the electromagnetic force density (12.2.24).

Substitution of (12.2.40) and $v = dx_a/dt$ into (12.2.42) yields the differential equation in x_a

$$\rho l \frac{d^2 x_a}{dt^2} + \frac{B^2 w}{d(R_i + R)} \frac{dx_a}{dt} + 2\rho g x_a = 0. \tag{12.2.43}$$

Comparison of (12.2.43) with (12.2.34) shows that the electromechanical coupling with a resistive load has added a damping term to the differential equation. This is easily understandable in terms of the analysis of the MHD machine in Section 12.2.1a. The fluid motion produces a voltage proportional to speed, a resistive load on this voltage produces a current proportional to speed, and the current in the fluid interacts with the applied flux density to produce a retarding force proportional to speed. Thus the electrical force appears as a damping term in the differential equation.

To consider the kind of behavior that can result in a real system of this kind we assume that the fluid is mercury, which has the following constants

$$\rho = 13,600 \text{ kg/m}^3, \qquad \sigma = 10^6 \text{ mhos/m}.$$

The system dimensions are chosen to be

$$l = 1 \text{ m}, \qquad l_1 = 0.1 \text{ m},$$
$$w = 0.02 \text{ m}, \qquad d = 0.01 \text{ m}.$$

We set the load resistance R equal to the internal resistance R_i

$$R = R_i = 2 \times 10^{-5} \text{ }\Omega.$$

For these given constants the differential equation (12.2.43) reduces to

$$\frac{d^2 x_a}{dt^2} + 3.68B^2 \frac{dx_a}{dt} + 19.6x_a = 0. \tag{12.2.44}$$

When the fluid is released from rest with the initial conditions of (12.2.35) and (12.2.36), the resulting transients in fluid position and electrode current are shown in Fig. 12.2.9. It is clear that with attainable flux densities the electromechanical coupling force can provide significant damping for the system.*

Some properties of the curves of Fig. 12.2.9 are worth noting. First, for very small time ($t < 0.1$ sec) the response in fluid position is essentially unaffected by the force of electric origin. This occurs because the initial velocity is zero and it takes velocity to generate voltage and drive current. Thus the initial increase in velocity is independent of the value of flux density and the initial current buildup is proportional to flux density.

The resistive load on the electrodes of the MHD machine in Fig. 12.2.8 can be replaced by an electrical source and the fluid displacement can be driven electrically. In such a case, when the fluid motion is of interest, (12.2.21) and (12.2.42) are adequate for the study.

---

* An experiment to demonstrate this effect is complicated by the fact that the contact resistance between the liquid metal and the electrodes is likely to be appreciable.

.
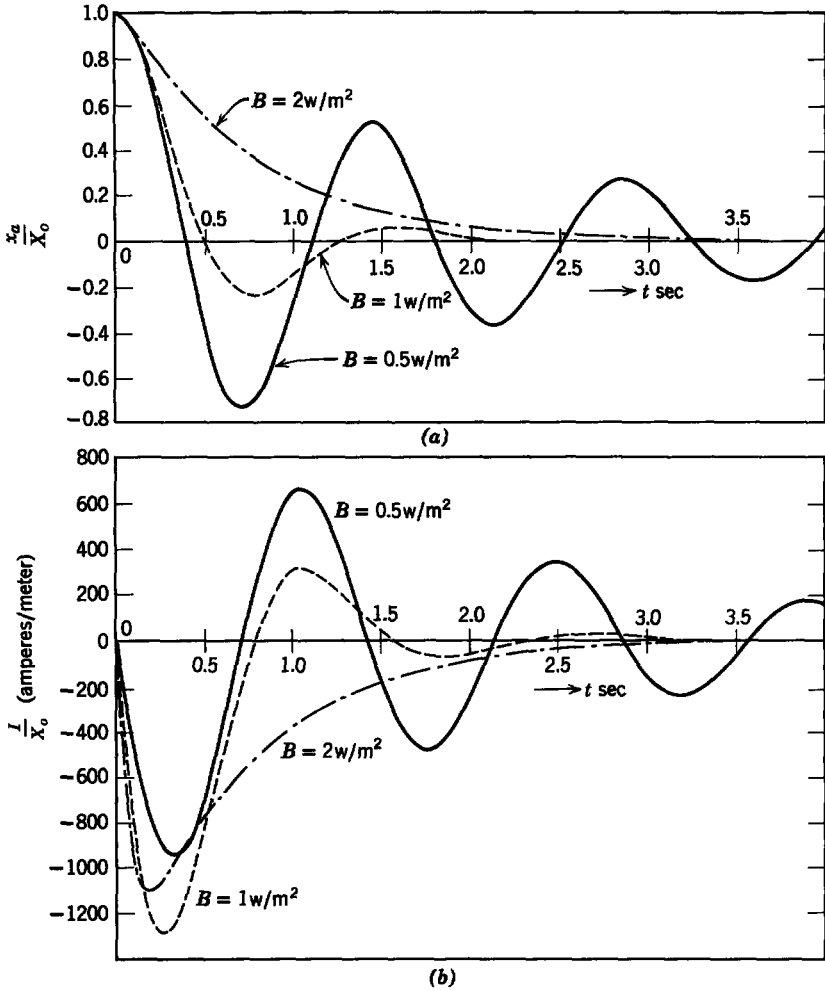
Fig. 12.2.9 Transient response of MHD-damped system: (*a*) fluid position; (*b*) electrode current.

12.2.2 Coupling with Flow in a Variable-Area Channel

To establish some insight into the properties of potential flow in two dimensions, consider the flow around a corner in the configuration of Fig. 12.2.10. The fluid container has constant depth in the x_3-direction and the fluid is incompressible and inviscid. There are no electrical forces, and we neglect gravity effects (assume gravity to act in the x_3-direction).

For potential flow the velocity is given by (12.2.2) as $\mathbf{v} = -\nabla\phi$ and the velocity potential ϕ satisfies Laplace's equation ($\nabla^2\phi = 0$). The boundary

condition is that the normal component of velocity must be zero along the
rigid surfaces. The solution of Laplace's equation which satisfies these
boundary conditions is

$$\phi = \frac{v_o}{\sqrt{2a}}(x_2{}^2 - x_1^2), \qquad (12.2.45)$$

where $2v_o$ is the speed of the fluid at $x_1 = x_2 = a$. The velocity is thus given by

$$\mathbf{v} = \mathbf{i}_1\sqrt{2}\,v_o\,\frac{x_1}{a} - \mathbf{i}_2\sqrt{2}\,v_o\,\frac{x_2}{a}. \qquad (12.2.46)$$

Equipotential lines and streamlines are shown in Fig. 12.2.10. This solution
is valid, even if v_o is time-varying.

We now restrict our attention to a steady-flow problem (v_o = constant)
and find that Bernoulli's equation (12.2.11) yields

$$\tfrac{1}{2}\rho v^2 + p = \text{constant}. \qquad (12.2.47)$$

We note from (12.2.46) that at $x_1 = x_2 = 0$ the velocity $\mathbf{v} = 0$. Because the
velocity is zero, this is called a *stagnation point*. If we designate the pressure
at the stagnation point as p_o, (12.2.47) becomes

$$\tfrac{1}{2}\rho v^2 + p = p_o. \qquad (12.2.48)$$

Thus with a knowledge of the stagnation point pressure and the velocity
distribution we can find the pressure at any other point in the fluid. The use of
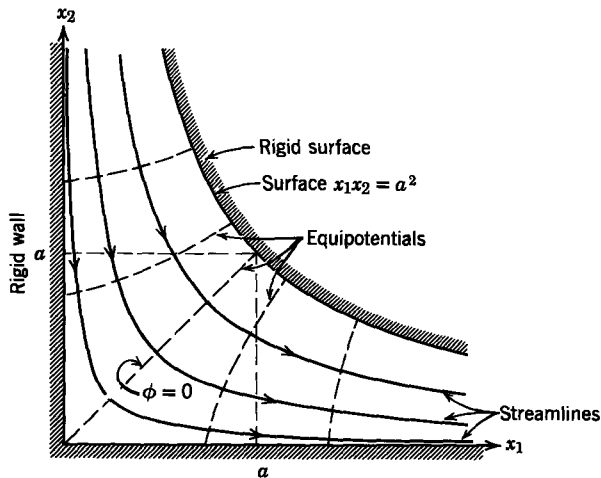
Fig. 12.2.10   Example of potential flow.
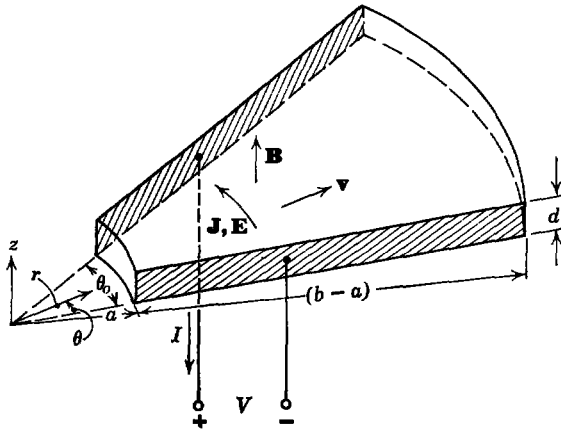
Fig. 12.2.11   MHD conduction machine with variable area.

(12.2.46) in (12.2.48) yields for the pressure at point (x_1, x_2)

$$p = p_o - \frac{\rho v_o^2}{a^2}(x_1^2 + x_2^2). \tag{12.2.49}$$

From this result we conclude that in a flowing incompressible fluid the highest pressure occurs at the stagnation point. Moreover, for a given flow the higher the local fluid speed, the lower the local pressure.*

This example indicates that the pressure can be changed by changing the velocity and vice versa. Variations of velocity are obtained by varying the cross-sectional area of the fluid flow. We now do an example of an MHD interaction with a two-dimensional fluid flow in which the geometry of the channel can be adjusted to vary the relation between input pressure and velocity and output pressure and velocity. Such freedom is desirable in many MHD applications. Here it allows us to extend the basic ideas introduced in Section 12.2.1a to a case in which the fluid is accelerating but the flow is steady $(\partial/\partial t = 0)$.

The system to be considered is the conduction machine shown schematically in Fig. 12.2.11. The channel forms a segment of a cylinder. The inlet is at radius $r = a$ and the outlet is at radius $r = b$. The insulating walls perpendicular to the z-direction are separated by a distance d. The electrodes are in radial planes separated by the angle θ_o. We use a cylindrical coordinate system r, θ, z, defined in Fig. 12.2.11. There is an applied flux density **B** in

---

* Even though (12.2.49) indicates that the pressure p can go negative, in fact it cannot. As long as we use an incompressible model, the pressure appears in only one place in the equations of motion, and they remain unaltered if an arbitrary constant is added to (or subtracted from) p. Other effects, such as compressibility, depend on an equation of state that is sensitive to the absolute magnitude of the pressure. If these effects are included, a negative pressure is not physically possible.

the z-direction. The electrodes are connected to electrical terminals at which the voltage V and current I are defined.

The velocity at the inlet $(r = a)$ and the velocity at the outlet $(r = b)$ are assumed to be radial and constant in magnitude. We assume solutions with cylindrical symmetry. These solutions are quite accurate, provided the angle θ_o is reasonably small. Again the magnetic field generated by current in the fluid is neglected (low magnetic Reynolds number).

As already assumed, the fluid is incompressible and inviscid with electrical conductivity σ and permeability μ_0. The velocity is radial

$$\mathbf{v} = \mathbf{i}_r v_r \tag{12.2.50}$$

and the electric field intensity and current density are azimuthal

$$\mathbf{E} = \mathbf{i}_\theta E_\theta, \tag{12.2.51}$$

$$\mathbf{J} = \mathbf{i}_\theta J_\theta. \tag{12.2.52}$$

We have already specified that the total flux density is

$$\mathbf{B} = \mathbf{i}_z B_z, \tag{12.2.53}$$

where B_z is a constant.

We first assume that at the inlet $(r = a)$ the radial component of velocity is

$$v_r = v_a. \tag{12.2.54}$$

Next, conservation of mass for incompressible flow requires that

$$\oint_S \mathbf{v} \cdot \mathbf{n} \, da = 0. \tag{12.2.55}$$

The value of v_r at any radius r follows as

$$v_r = \frac{a}{r} v_a. \tag{12.2.56}$$

Steady-state operation yields $\nabla \times \mathbf{E} = 0$ and the z-component of $\nabla \times \mathbf{E} = 0$ [assuming that $\mathbf{E}$ takes the form of (12.2.51)] is

$$\frac{1}{r} \frac{\partial(rE_\theta)}{\partial r} = 0. \tag{12.2.57}$$

This yields the result that

$$E_\theta = \frac{A}{r}, \tag{12.2.58}$$

where A is a constant to be determined from the boundary conditions. To evaluate the constant A, the definition of the terminal voltage

$$-\int_0^{\theta_o} E_\theta r \, d\theta = V \tag{12.2.59}$$

is used to obtain

$$E_\theta = -\frac{V}{r\theta_o}. \qquad (12.2.60)$$

Substitution of (12.2.53), (12.2.56), and (12.2.60) into the θ-component of Ohm's law for a moving, conducting medium (12.2.18) yields

$$J_\theta = \sigma\left(-\frac{V}{r\theta_o} + \frac{a}{r} v_a B_z\right). \qquad (12.2.61)$$

Note that this expression satisfies $\nabla \cdot \mathbf{J} = 0$.

A relation between current density and terminal current can be obtained from the expression

$$I = \int_a^b J_\theta d\, dr. \qquad (12.2.62)$$

Performance of this integration yields

$$IR_i = -V + a\theta_o v_a B_z, \qquad (12.2.63)$$

where we have defined the internal resistance R_i as

$$R_i = \frac{\theta_o}{\sigma d \ln(b/a)} \qquad (12.2.64)$$

Note the similarity between (12.2.63) and (12.2.21) for the simpler geometry in Fig. 12.2.3.

The radial component of the momentum equation (12.2.4) for steady-state conditions is

$$\rho v_r \frac{\partial v_r}{\partial r} = -\frac{\partial p}{\partial r} + J_\theta B_z. \qquad (12.2.65)$$

Multiplication of the expression by dr, integration from $r = a$ to $r = b$, and use of (12.2.56) and (12.2.62) yields

$$\tfrac{1}{2}\rho v_a^2\left[\left(\frac{a}{b}\right)^2 - 1\right] = -\Delta p - \frac{IB_z}{d}, \qquad (12.2.66)$$

where the pressure rise Δp is defined as

$$\Delta p = p(b) - p(a). \qquad (12.2.67)$$

Note the similarity between (12.2.66) and (12.2.24) for the constant-area channel. The difference lies in the first term on the left of (12.2.66) which results from the changing area and therefore changing velocity in the channel of Fig. 12.2.11.

Equation 12.2.66 could have been obtained from Bernoulli's equation (12.2.11); in a simple case like this, however, it is more informative to obtain the result from first principles.

To study some of the properties of the system with varying area consider first the case in which the electrical terminals are open-circuited. The terminal voltage, as obtained from (12.2.63) is

$$V = a\theta_o v_a B_z \qquad\qquad (12.2.68)$$

and the pressure rise obtained from (12.2.66) is

$$\Delta p = \tfrac{1}{2}\rho v_a{}^2\left[1 - \left(\frac{a}{b}\right)^2\right]. \qquad\qquad (12.2.69)$$

Because $a < b$, this pressure rise is positive, which indicates that the outlet pressure is higher than the inlet pressure. This results because the fluid velocity decreases as r increases and this fluid deceleration must be balanced by a pressure gradient as indicated by the momentum equation (12.2.65). Thus the variable area channel by itself acts as a kind of "fluid transformer" that can increase pressure as it decreases velocity or vice versa.

The electrical terminal relation (12.2.63) for the machine with variable area (Fig. 12.2.11) has the same form as the electrical terminal relation (12.2.21) for the machine with constant area (Fig. 12.2.3). Thus, if the inlet velocity v_a is the independent mechanical variable, the analysis of the electric terminal behavior is exactly the same as that of the constant-area machine; that is, from an electrical point of view the machine appears to have an open-circuit voltage $(a\theta_o v_a B_z)$ in series with an internal resistance R_i (12.2.64), as illustrated in Fig. 12.2.12. This equivalent circuit can be connected to any combination of active and passive loads, and the electrical behavior can be predicted correctly within the limitations of the assumptions made in arriving at the model.

To study the energy conversion properties of the variable-area machine we must generalize the concept of mechanical input power that was used in (12.2.29) for the constant-area machine. No longer is the mechanical input power simply equal to the pressure difference times the volume flow rate of fluid because the difference in inlet and outlet velocities indicates that there is
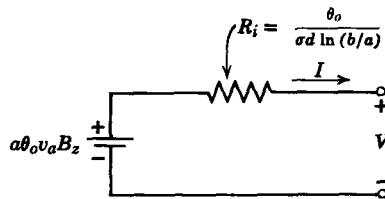
Fig. 12.2.12 Electric equivalent circuit for a variable-area MHD machine.

a net transport of kinetic energy into or out of the volume of the channel by the fluid. To illustrate this concept consider the system operating with the electrical terminals open-circuited. There is clearly no electrical output power and no $I^2 R_i$ losses in the fluid. Moreover, the fluid is inviscid, so there can be no mechanical losses. Thus we expect the mechanical input power to be zero, although there is a nonzero pressure difference between inlet and outlet of the channel.

To determine the mechanical energy interchange between the MHD device and the energy source which makes the fluid flow through the device we use the *conservation of energy* which states, in general,

$$\begin{bmatrix} \text{total power input} \\ \text{to channel volume} \end{bmatrix} = \begin{bmatrix} \text{rate of increase of} \\ \text{energy stored in volume} \end{bmatrix} \qquad (12.2.70)$$

For the steady-state problem being considered the energy stored in the volume is constant and the right side of (12.2.70) is zero. We thus define the mechanical *output* power from the channel as P_m and the power converted to electrical form as P_{em} and write (12.2.70) for conservation of *mechanical energy**** as

$$-P_m - P_{em} = 0. \qquad (12.2.71)$$

For open-circuit conditions the electromechanical power P_{em} is zero and

$$P_m = 0. \qquad (12.2.72)$$

To calculate P_m, which has been defined as the work done by the fluid in the channel *on* the fluid mechanical source, we must specify how work is done on the fluid in the channel and how energy is stored and transported by the fluid.

At a surface of a fluid (this can be an imaginary surface in a fluid) with outward directed normal vector **n**, as illustrated in Fig. 12.2.13, there will be a pressure force on the fluid enclosed by the surface of magnitude p and directed opposite to the normal vector $(-p\mathbf{n})$ [see (12.1.37)]. If the fluid is moving with velocity **v** at the surface, the rate at which the pressure force $(-p\mathbf{n}\,da)$ does work on the fluid inside the volume V is

$$\begin{bmatrix} \text{power input from} \\ \text{pressure forces} \end{bmatrix} = \oint_S - p\mathbf{n} \cdot \mathbf{v}\,da. \qquad (12.2.73)$$

A fluid can store kinetic energy with a density $\frac{1}{2}\rho v^2$. At each point along the surface of Fig. 12.2.13 fluid flow across the surface will transport kinetic energy into or out of the volume V. The volume of fluid crossing the surface

---

* Even though electrical losses in the fluid ($I^2 R_i$) occur within the volume of the channel, they are not included in this energy expression. This is possible here because these losses do not affect the mechanical properties of an incompressible, inviscid fluid. When we consider gaseous conductors in Chapter 13, the electrical losses must be included because they will affect the mechanical properties of the conducting fluid.
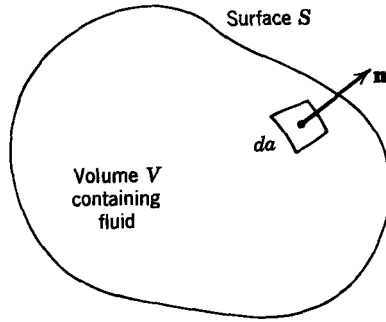
Fig. 12.2.13   Geometry for writing conservation of energy for a fluid.

element da in unit time is $\mathbf{v} \cdot \mathbf{n} \, da$. Thus the total kinetic energy transported out of the volume in unit time is

$$\left[\begin{array}{c}\text{power output from kinetic} \\ \text{energy transport}\end{array}\right] = \oint_S \tfrac{1}{2}\rho v^2 \mathbf{v} \cdot \mathbf{n} \, da. \qquad (12.2.74)$$

For an incompressible inviscid fluid (12.2.73) and (12.2.74) represent the only mechanisms for interchanging mechanical energy with a fluid; thus the mechanical output power P_m defined in (12.2.71) is given by

$$P_m = \oint_S p\mathbf{n} \cdot \mathbf{v} \, da + \oint_S \tfrac{1}{2}\rho v^2 \mathbf{v} \cdot \mathbf{n} \, da. \qquad (12.2.75)$$

To apply (12.2.75) to the variable-area channel of Fig. 12.2.11 we must define the surface that encloses the fluid in the channel. This surface consists of the four channel walls and the two concentric cylindrical surfaces at $r = a$ and $r = b$. The velocity is nonzero only along the last two surfaces; consequently, (12.2.75) integrates to

$$P_m = -p(a)v_r(a)a\theta_o d + p(b)v_r(b)b\theta_o d$$
$$-\tfrac{1}{2}\rho v_r^3(a)a\theta_o d + \tfrac{1}{2}\rho v_r^3(b)b\theta_o d. \qquad (12.2.76)$$

The assumption that $v_r(a) = v_a$ (12.2.54) and the use of (12.2.56) to write

$$v_r(b) = \frac{a}{b} v_a \qquad (12.2.77)$$

allows us to write (12.2.76) in the simplified form

$$P_m = a\theta_o d v_a \left[\Delta p - \tfrac{1}{2}\rho v_a^2 \left(1 - \frac{a^2}{b^2}\right)\right], \qquad (12.2.78)$$

where the pressure rise Δp has been defined in (12.2.67) as $\Delta p = p(b) - p(a)$.

To apply (12.2.78) we first note that for the open-circuit condition $I = 0$, and (12.2.66) yields

$$\Delta p_{oc} = \tfrac{1}{2}\rho v_a{}^2 \left(1 - \frac{a^2}{b^2}\right).$$ (12.2.79)

Substitution of this result into (12.2.78) yields for open-circuit conditions

$$P_m = 0.$$

This is in agreement with our intuitive physical prediction made at the start of this development. Next, for any arbitrary load $I \neq 0$ (12.2.66) yields

$$\Delta p = \tfrac{1}{2}\rho v_a{}^2 \left(1 - \frac{a^2}{b^2}\right) - \frac{IB_z}{d}.$$ (12.2.80)

Substitution of this result into (12.2.78) and simplification yield

$$P_m = -a\theta_o v_a B_z I.$$ (12.2.81)

From (12.2.71) the power converted electromechanically is

$$P_{em} = -P_m = a\theta_o v_a B_z I.$$ (12.2.82)

Reference to the equivalent circuit of Fig. 12.2.12 shows that this converted power is simply the power supplied to the electric circuit by the battery representing the open-circuit voltage.

This interpretation leads to the conclusion that for conversion of energy the variable-area machine has exactly the same properties as the constant-area machine analyzed earlier. The only difference arises when we are interested in the details of the pressure and velocity distributions and in the nature of the fluid mechanical source that provides the fluid flow through the machine. As we shall see in Chapter 13, however, these are essential considerations if the velocity is large enough (compared with that of sound) to make the effects of compressibility important.

12.2.3 Alfvén Waves

So far in the treatment of electromechanical coupling with incompressible inviscid fluids we have considered problems in which there has been gross motion of the fluid. All of these examples have been analyzed by using potential flow. In this section we consider electromechanical coupling that results in no gross motion of the fluid but rather involves the propagation of a signal through a fluid. Moreover, the fluid velocity has a finite curl and a potential flow model is inappropriate. Our discussion is pertinent to an understanding of MHD transient phenomena.

As discussed in Section 12.1.4, an inviscid, incompressible fluid can, by itself, support no shear stresses; but when such a fluid with very high

electrical conductivity is immersed in a magnetic field the magnetic field provides shear stiffness such that transverse waves, called Alfvén waves and very much akin to the shear waves in elastic media, can be propagated. They play an essential role in determining the dynamics of a highly conducting liquid or gas (plasma) interacting with a magnetic field.

To introduce the essential features of Alfvén waves we use a rectangular system in which variables are functions of only one dimension. It is difficult to realize physically the boundary conditions necessary for this model. Thus, after the ideas are introduced, we extend the example to cylindrical geometry, where all boundary conditions can be imposed realistically.

The magnetohydrodynamic system is shown in Fig. 12.2.14. An incompressible, inviscid, highly conducting ($\sigma \to \infty$) fluid is contained between rigid parallel walls. An external magnet is used to impose a magnetic flux density B_o in the x_1-direction. It is the effect of this flux density on the motions of the fluid transverse to the x_1-axis that is of interest.
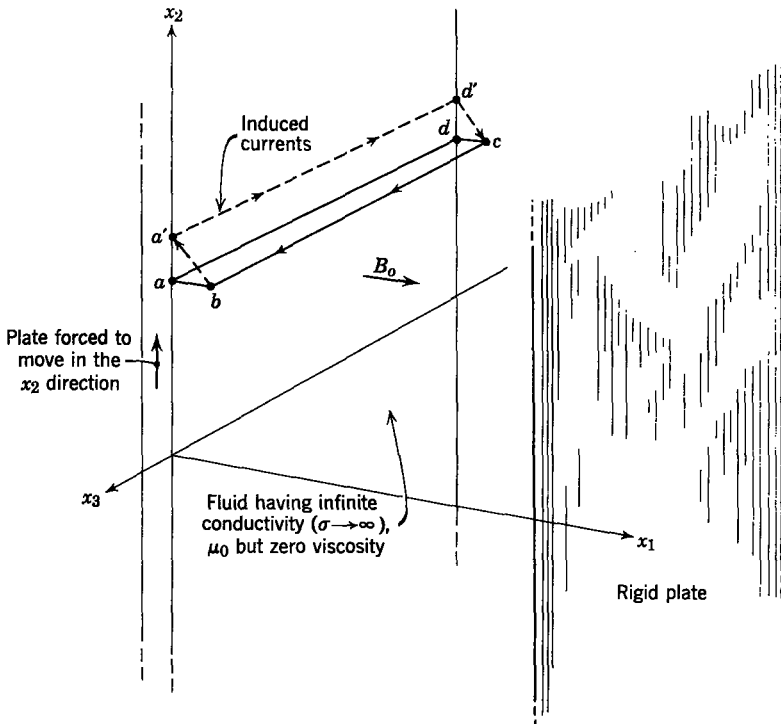
Fig. 12.2.14   Fluid contained between rigid parallel plates and immersed in a magnetic induction B_o. Motions of the fluid are induced by transverse motions of the left-hand plate, which, like the fluid, is assumed to be highly conducting.
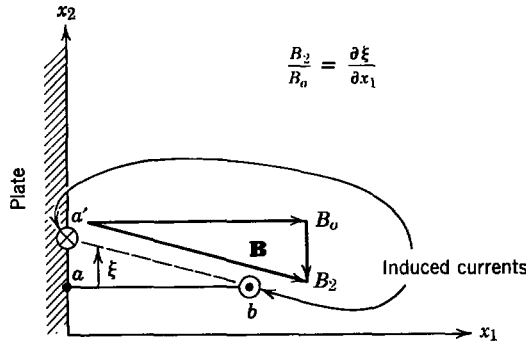
Fig. 12.2.15 End view of the loop *abcd* shown in Fig. 12.2.14. The initial loop formed by conducting fluid and the plate links zero flux λ. To conserve the flux, density **B** remains tangential to the loop with the additional magnetic flux density B_2 created by an induced current.

Suppose that in the absence of a magnetic field the rigid plate is set in motion in the x_2-direction. Because the fluid is inviscid, there is no shearing stress imposed on the fluid and the plate will transmit no motion to the fluid. In fact, if any sheet of fluid perpendicular to the x_1-axis is set into transverse motion, the adjacent sheets of fluid remain unaffected because of the lack of shearing stresses.

Now consider the effect of imposing a magnetic field. The fluid is highly conducting, and this means that the electric field in the frame of the fluid is essentially zero. The law of induction can be written for a contour C attached to the fluid particles:

$$\oint_C \mathbf{E}' \cdot d\mathbf{l} = -\frac{d}{dt} \int_S \mathbf{B} \cdot \mathbf{n}\, da \equiv -\frac{d\lambda}{dt}, \qquad (12.2.83)$$

where $\mathbf{E}'$ is the electric field measured in the frame of the fluid.* Because the first integral is zero, the flux λ linked by a conduction path always made up of the same fluid particles remains constant.

This is an important fact for the situation shown in Fig. 12.2.14, as can be seen by considering the conduction path *abcd* intersecting the fluid and the edge of the rigid plate at $x_1 = 0$. Initially the surface enclosed by this path is in the x_2-x_3 plane, hence links no flux ($\lambda = 0$). When the plate is forced to move in the x_2-direction this surface, which is always made up of the same material particles, moves to $a'bcd'$. Because the surface is tilted, there is now a flux from B_0 that contributes to λ. Because λ must remain zero, however, there is a current induced around the loop in such a direction that it cancels the flux contributed by B_0. There is then an addition to the magnetic field (induced by this current) along the x_2-axis (Fig. 12.2.15) that makes the net

* See (1.1.23), Table 1.2, Appendix G.

magnetic field remain tangential to the surface of the deformed loop. This is necessary if λ is to remain zero.

The current, returning along the path cb in the fluid flows transverse to the field B_o; hence there is a magnetic force on the fluid ($\mathbf{J} \times B_o\mathbf{i}_1$) in the x_2-direction. The result of moving the highly conducting plate in the x_2-direction is a motion of the fluid adjacent to the plate in the same direction. The motion of the plate creates a magnetic shearing stress on the fluid. This stress is transmitted through the fluid in the x_1-direction because the magnetic force sets the fluid in the plane of bc into motion, and this sheet of fluid now plays the role of the plate in inducing motions in the neighboring sheets of fluid.

In our arguments we have assumed that motions of the fluid are the same at all points in a given x_2-x_3 plane. To provide an analytical picture of the dynamics consistent with this assumption it is assumed that all variables are independent of x_2 and x_3. As an immediate consequence of this assumption, the condition that $\nabla \cdot \mathbf{B} = 0$ requires that B_o be independent of x_1. If, in addition, B_o is imposed by an external magnet driven by a constant current, it follows that $B_1 = B_o =$ constant, regardless of the fluid motions. By similar reasoning the incompressible nature of the fluid ($\nabla \cdot \mathbf{v} = 0$), together with the rigid walls that do not permit flow along the x_1-axis, require that $v_1 = 0$ everywhere in the fluid. Hence both the fluid motions and additions to the magnetic flux density occur transverse to the x_1-axis.

From the discussion that has been given it is clear that three essential ingredients in the fluid motions are of interest here. First, a mathematical model must account for the law of induction. In particular, since the magnetic field is induced in the x_2-direction, we write the x_2-component of the induction equation

$$\frac{\partial E_3}{\partial x_1} = \frac{\partial B_2}{\partial t} . \tag{12.2.84}$$

The second important effect comes from the high conductivity of the fluid. In order that the conduction current may remain finite in the limit in which the conductivity σ becomes large, we must require that $\mathbf{E}' = 0$. This in turn means that $\mathbf{E} = -\mathbf{v} \times \mathbf{B}$, and it is the x_3-component of this equation that is of interest to us:

$$E_3 = v_2 B_o. \tag{12.2.85}$$

Substitution of this expression for E_3 into (12.2.84) gives an equation that expresses the effect of the fluid deformation on the magnetic field.

$$B_o \frac{\partial v_2}{\partial x_1} = \frac{\partial B_2}{\partial t} \tag{12.2.86}$$

Note that if we define a transverse particle displacement in the fluid such that $v_2 = \partial \xi/\partial t$ (12.2.86) simply requires that the magnetic flux density remain

tangential to the deformed surface of fluid initially in a given x_1-x_3 plane. Equation 12.2.86 shows that the lines of magnetic field intensity are deformed as though they were "frozen" to the particles of fluid (see Fig. 12.2.15).

The third input to our analytical description comes from the effect of the magnetic field on the fluid motions. Because the fluid moves in the x_2-direction, we write the x_2-component of the force equation (12.1.21)

$$\rho \frac{\partial v_2}{\partial t} = \frac{\partial T_{21}}{\partial x_1} = \frac{B_o}{\mu_0} \frac{\partial B_2}{\partial x_1}. \tag{12.2.87}$$

Note that the absence of a velocity component v_1 and the one-dimensional character of the motions under consideration eliminate the spatial derivatives from the substantial derivative (the first term) in this expression. The only component of the Maxwell stress tensor* that enters on the right is T_{21} because variables do not depend on x_2 or x_3 and we have made use of the fact that B_o is a constant in writing Eq. 12.2.87.

The last two equations can be used to write an expression for either B_2 or v_2; for example, we eliminate B_2 between the time derivative of (12.2.87) and the space derivative of (12.2.86) to obtain

$$\frac{\partial^2 v_2}{\partial t^2} = \frac{B_o{}^2}{\mu_0 \rho} \frac{\partial^2 v_2}{\partial x_1{}^2}, \tag{12.2.88}$$

where

$$a_b = \left(\frac{B_o{}^2}{\mu_0 \rho} \right)^{\!\frac{1}{2}}.$$

This is the wave equation, considered in some detail in Chapters 9 and 10. The velocity a_b with which waves propagate in the x_1-direction is called the Alfvén velocity.†

To develop further a physical feel for the nature of an Alfvén wave, consider the propagation in the positive x_1-direction of the pulse illustrated in Fig. 12.2.16. The pulse, as drawn, represents what happens along the x_1-axis; but, because in our model the variables are independent of x_2 and x_3, the figure applies to all elements having the same coordinate x_1. With reference to Fig. 12.2.16, we can easily show that the variables as sketched satisfy (12.2.86) and (12.2.87) with **J** found by Ampère's law. Moreover, (12.2.88) is satisfied when the waveforms maintain constant shape and propagate in the x_1-direction with the Alfvén velocity a_b.

We note from Fig. 12.2.16 that the force density **J** × **B** has an x_2-component equal to $J_3 B_o$ and that this force density is in the positive x_2-direction in the leading half of the wave and in the negative x_2-direction in the trailing half of the wave. Thus, as the wave propagates in the x_1-direction, the fluid at the

---

* Table 8.1, Appendix G.

† Alfvén waves are named after the man who first recognized their significance for astrophysics. See H. Alfvén, *Cosmical Electrodynamics*, Oxford, 1950.
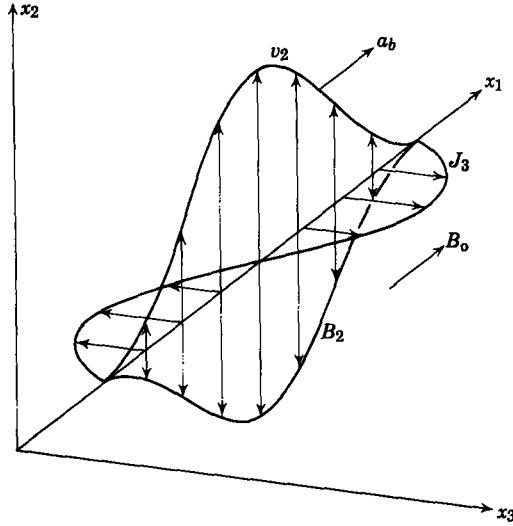
Fig. 12.2.16 The variables associated with an Alfvén wave.

leading edge is accelerated upward by the electrical force and at the trailing edge the fluid is decelerated.

It is instructive to use the pulse of Fig. 12.2.16 to construct the curves of Fig. 12.2.17 which show the displacement of the fluid particles that were initially on the x_1-axis. Fluid particles and magnetic flux lines are displaced in the same way by the passage of the Alfvén wave. For a highly conducting $(\sigma \to \infty)$ fluid the fluid particles and magnetic flux lines are "frozen" together and any motion of the fluid causes a distortion of the flux lines.
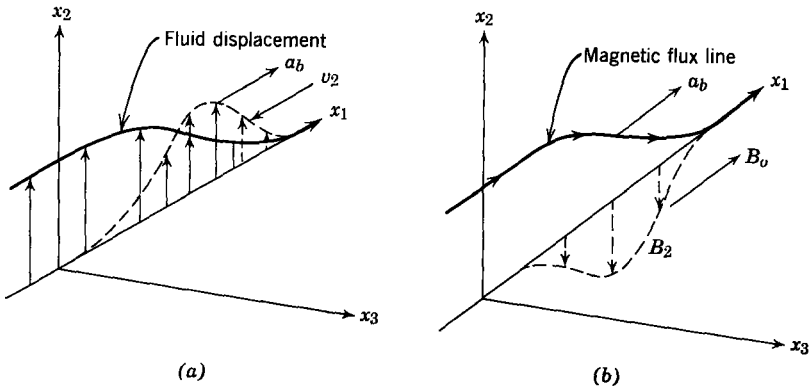
Fig. 12.2.17 Fluid displacement and flux-line distortion in an Alfvén wave: (a) fluid displacement; (b) magnetic flux line.
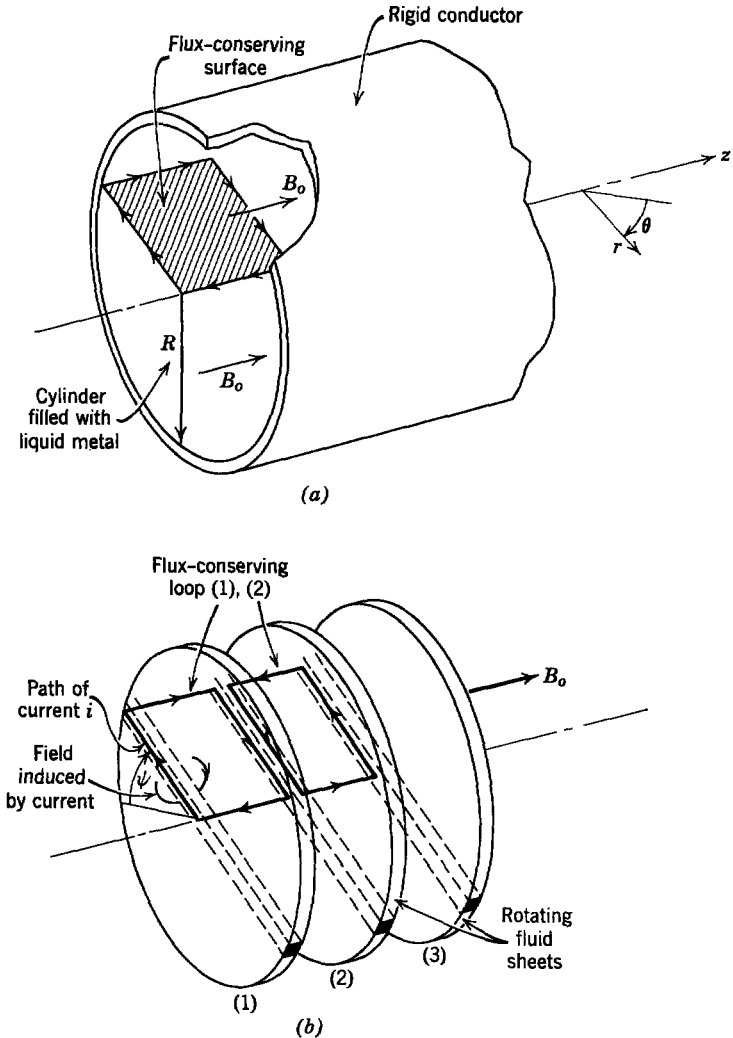
Fig. 12.2.18 (a) Experimental arrangement for producing torsional Alfvén waves in highly conducting cylindrical container; (b) conduction paths represented as "spokes" in adjacent wheels of perfectly conducting fluid.

It would be difficult to generate Alfvén waves in the cartesian geometry of Fig. 12.2.14 for two reasons. First, fluid motions in the x_2-direction have been assumed independent of x_2 and this implies that container boundaries in x_1-x_3 planes must not inhibit the velocity v_2. Second, currents that flow along the x_3-axis must have a return path ($\nabla \cdot \mathbf{J} = 0$), and this implies that conducting walls are provided by the container in x_1-x_2 planes. We can satisfy both requirements by using the cylindrical container shown in Fig. 12.2.18. Here

we expect that Alfvén waves will appear as torsional motions of the fluid about the axis of the cylinder. These motions, like those just considered, are transverse to the imposed magnetic field B_0 (which has the same direction as the axis of the cylinder).

Again it is helpful to think of the fluid as composed of sheets, as shown in Fig. 12.2.18. Now the sheets take the form of wheels that can execute torsional motions about the cylinder axis. Currents can flow radially outward along "spokes" of a "wheel" through the outer cylinder wall, inward along another "spoke," and finally complete the loop along the cylinder axis (Fig. 12.2.18). In fact, these loops provide a simple picture of the electromechanical mechanism responsible for the propagation of waves along the magnetic field B_0.

Suppose that the first slice of fluid is forced to rotate to the positive angle ψ (Fig. 12.2.18b). The loop formed by the conducting path through the neighboring sheet initially links no flux. To conserve this condition in spite of the rotation a current i is induced which tends to cancel the flux caused by B_0. This current returns to the center through the neighboring sheet. In doing so it produces a force density $\mathbf{J} \times \mathbf{B}_0$ which tends to rotate this second sheet in the positive ψ-direction. Of course, as the second sheet rotates, a current must flow around a loop through the third sheet to conserve the zero flux condition in the second loop of Fig. 12.2.18. Hence the third sheet of fluid is set into motion and the initial rotation propagates along the cylinder axis. These arguments can be repeated for motions that propagate in the opposite direction. The waves have no polarity and can propagate in either direction along the lines of magnetic field B_0 The propagation is not instantaneous because each sheet has a finite mass and time is required to set the fluid in motion

The magnetic field has the same effect on the fluid as if the fluid sheets were interconnected by taut springs (Fig. 12.2.19). Wave propagation occurs
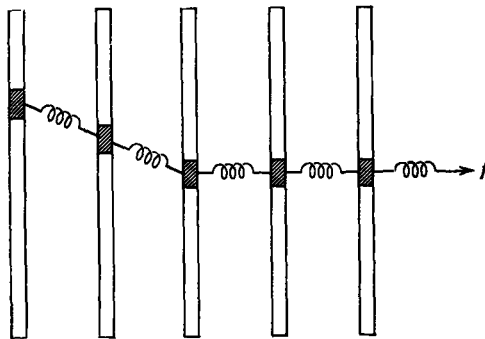
Fig. 12.2.19 Side view of the circular sheets of fluid in Fig. 12.2.18 showing equivalent interconnecting springs under the tension f.
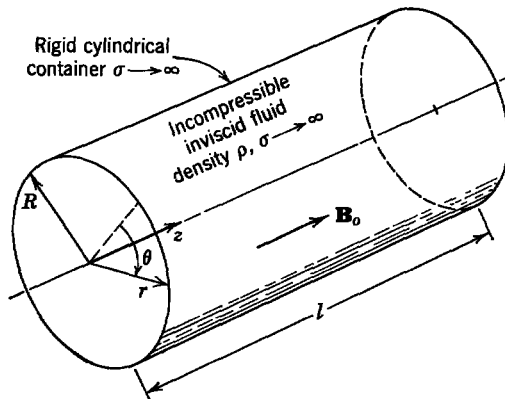
Fig. 12.2.20   Cylindrical geometry for the study of Alfvén waves.

very much as it does on a string (Section 9.2.). In the string the wave velocity was proportional to the square root of the tension f^*. Here the tension is apparently proportional to B^2, as can be seen by comparing (12.2.88) and (9.2.4). This would be expected from a simple experiment: hold one sheet fixed and twist the next sheet and there is a restoring torque proportional to f. With the magnetic field the restoring torque is caused by $\mathbf{J} \times \mathbf{B}_o$, but since J is induced in proportion to B_o this magnetic restoring torque is proportional to $B_o{}^2$. Hence we can think of $B_o{}^2$ as producing a magnetic tension in a perfectly conducting fluid.

To be precise about the fluid velocity and electrical current distribution, we now consider a specific analytical example. The system, illustrated in Fig. 12.2.20, consists of a rigid, cylindrical container made of highly conducting material, filled with a highly conducting fluid, and immersed in an equilibrium axial flux density $\mathbf{B}_o$ produced externally. The ends of the cylinder are also rigid and may be insulators or conductors, depending on the boundary conditions desired. The fluid is modeled as incompressible and inviscid with mass density ρ, permeability μ_0, and high electrical conductivity ($\sigma \to \infty$). The fluid in the cylinder has axial length l and radius R. We use the cylindrical coordinate system illustrated in Fig. 12.2.20.

We specify that any drive will be applied at the ends and will have cylindrical symmetry; that is, there will be no variation with the angle θ and $\mathbf{v} = \mathbf{i}_\theta v_\theta(r, z, t)$. In this case we can require that the relevant variables have only the following components, defined in terms of the cylindrical coordinate system (r, θ, z) in Fig. 12.2.20.

$$\mathbf{B} = \mathbf{i}_z B_o + \mathbf{i}_\theta B_\theta, \tag{12.2.89}$$

$$\mathbf{J} = \mathbf{i}_r J_r + \mathbf{i}_z J_z, \tag{12.2.90}$$

$$\mathbf{E} = \mathbf{i}_r E_r + \mathbf{i}_z E_z. \tag{12.2.91}$$

* See Table 9.2, Appendix G.

The variables v_θ, B_θ, J_r, J_z, E_r, and E_z can be functions of r, z, and time t.

To analyze this system we must write the necessary equations in cylindrical coordinates by recognizing that $(\partial/\partial\theta) = 0$. For the basic equations refer to Table 1.2*, and for their forms in cylindrical coordinates refer to any standard text on electromagnetic theory.† The use of the constituent relation $\mathbf{B} = \mu_0\mathbf{H}$ with Ampère's law (1.1.1)* in cylindrical coordinates yields

$$-\frac{1}{\mu_0}\frac{\partial B_\theta}{\partial z} = J_r, \tag{12.2.92}$$

$$\frac{1}{\mu_0 r}\frac{\partial}{\partial r}(rB_\theta) = J_z. \tag{12.2.93}$$

We obtain from Faraday's law (1.1.5)

$$\frac{\partial E_r}{\partial z} - \frac{\partial E_z}{\partial r} = -\frac{\partial B_\theta}{\partial t}. \tag{12.2.94}$$

Ohm's law (12.2.18) yields

$$J_r = \sigma(E_r + v_\theta B_o), \tag{12.2.95}$$

$$J_z = \sigma E_z, \tag{12.2.96}$$

with J_r and J_z related by the condition of conservation of charge (1.1.3)*

$$\frac{1}{r}\frac{\partial}{\partial r}(rJ_r) + \frac{\partial J_z}{\partial z} = 0. \tag{12.2.97}$$

The θ-component of the momentum equation (12.1.14) with $\mathbf{F}^e = \mathbf{J} \times \mathbf{B}$ is

$$\rho\frac{\partial v_\theta}{\partial t} = -J_r B_o. \tag{12.2.98}$$

We now assume high conductivity ($\sigma \to \infty$), which, coupled with the fact that $\mathbf{J}$ remains finite, reduces (12.2.95) and (12.2.96) to

$$E_r = -v_\theta B_o, \tag{12.2.99}$$

$$E_z = 0. \tag{12.2.100}$$

These expressions are used in 12.2.94 to write

$$B_o\frac{\partial v_\theta}{\partial z} = \frac{\partial B_\theta}{\partial t}. \tag{12.2.101}$$

* See Table 1.2, Appendix G.
† See, for example, R. M. Fano, L. J. Chu, and R. B. Adler, *Electromagnetic Fields, Energy, and Forces*, Wiley, New York, 1960, p. 510.

Equations 12.2.92, 12.2.98, and 12.2.101 are combined to obtain the wave equation

$$\frac{\partial^2 v_\theta}{\partial t^2} = \frac{B_o{}^2}{\mu_0 \rho} \frac{\partial^2 v_\theta}{\partial z^2}.$$ (12.2.102)

This equation indicates that waves can propagate in the z-direction with the Alfvén velocity [see (12.2.88)].

$$a_b = \left(\frac{B_o{}^2}{\mu_0 \rho}\right)^{1/2}.$$ (12.2.103)

Note that (12.2.102) has no derivatives with respect to the radius r although the variables may be functions of r as indicated by (12.2.93) and (12.2.97). Variations with r are determined by boundary conditions; for instance, the general solution of (12.2.102) can be written in the separable form as

$$v_\theta = A(r) f(z, t).$$ (12.2.104)

The function $A(r)$ is then set by boundary conditions and automatically satisfies all the differential equations.

To consider a specific example of boundary conditions we assume that the end of the container at $z = 0$ is rigid, fixed, and made of insulating material ($\sigma \to 0$). The end at $z = l$ is highly conducting ($\sigma \to \infty$) and is rotated about its axis with a velocity

$$v_p = \text{Re}\,(\Omega r e^{j\omega t}).$$ (12.2.105)

These constraints impose the following boundary conditions:

$$\text{at } z = 0, \qquad J_z = 0$$ (12.2.106)

$$\text{at } z = l, \qquad v_\theta = \text{Re}\,(\Omega r e^{j\omega t}).$$ (12.2.107)

This last boundary condition reflects the fact that there can be no slip between the perfectly conducting moving wall and the adjacent fluid because of the magnetic field; that is, the electric field must remain continuous across this boundary. Since $\mathbf{E} = -\mathbf{v} \times \mathbf{B}$ and the normal $\mathbf{B}$ is continuous across the boundary, it follows that the fluid velocity must also be continuous.

The solution for v_θ can now be assumed to have the form

$$v_\theta = \text{Re}\,[A(r)\hat{v}_\theta(z)\,e^{j\omega t}].$$ (12.2.108)

Substitution of this assumed solution into (12.2.102) yields the differential equation

$$\frac{d^2 \hat{v}_\theta}{dz^2} = -k^2 \hat{v}_\theta,$$ (12.2.109)

where

$$k = \frac{\omega}{a_b}.$$

The solution of this equation is, in general,

$$\hat{v}_\theta = C_1 \cos kz + C_2 \sin kz. \qquad (12.2.110)$$

Imposing the boundary condition at $z = l$, (12.2.107) yields

$$\Omega r = A(r)(C_1 \cos kl + C_2 \sin kl). \qquad (12.2.111)$$

To maintain $A(r)$ nondimensional as indicated by (12.2.108), while satisfying this last equation for all values of r, we set

$$A(r) = \frac{r}{R} \qquad (12.2.112)$$

and rewrite (12.2.111) as

$$\Omega R = C_1 \cos kl + C_2 \sin kl. \qquad (12.2.113)$$

To apply the boundary condition at $z = 0$ we need to find an expression for J_z. We accomplish this by first substituting (12.2.108) into (12.2.101) to obtain

$$\frac{\partial B_\theta}{\partial t} = \text{Re} \left[B_o A(r) \frac{d\hat{v}_\theta}{dz} e^{j\omega t} \right]. \qquad (12.2.114)$$

If we assume that

$$B_\theta = \text{Re} \, [A(r)\hat{B}_\theta(z)e^{j\omega t}], \qquad (12.2.115)$$

then, using (12.2.114), we obtain

$$j\omega \hat{B}_\theta(z) = B_o \frac{d\hat{v}_\theta}{dz}, \qquad (12.2.116)$$

which, by using (12.2.110), yields

$$\hat{B}_\theta(z) = \frac{B_o k}{j\omega} (-C_1 \sin kz + C_2 \cos kz). \qquad (12.2.117)$$

Now we use (12.2.93) to evaluate J_z as

$$J_z = \text{Re} \left[\frac{2B_o k}{j\omega\mu_0 R} (-C_1 \sin kz + C_2 \cos kz)e^{j\omega t} \right]. \qquad (12.2.118)$$

The boundary condition at $z = 0$ (12.2.106) now requires

$$C_2 = 0. \qquad (12.2.119)$$

We use this result with (12.2.113) to find

$$C_1 = \frac{\Omega R}{\cos kl}. \qquad (12.2.120)$$

The resulting solutions are

$$v_\theta = \text{Re}\left(\Omega r \frac{\cos kz}{\cos kl} e^{j\omega t}\right),$$ (12.2.121)

$$B_\theta = \text{Re}\left(-\frac{\Omega r B_o k}{j\omega} \frac{\sin kz}{\cos kl} e^{j\omega t}\right),$$ (12.2.122)

$$J_z = \text{Re}\left(-\frac{2\Omega B_o k}{\omega \mu_0} \frac{\sin kz}{\cos kl} e^{j\omega t}\right),$$ (12.2.123)

$$J_r = \text{Re}\left(-\frac{j\omega \rho \Omega r}{B_o} \frac{\cos kz}{\cos kl} e^{j\omega t}\right).$$ (12.2.124)

Study of these solutions indicates that there are standing, torsional waves in the system. The fluid motion is azimuthal and the flux line distortion is azimuthal. The details of the phenomena involved in the wave propagation are as described in connection with Fig. 12.2.18. Now, however, we see that the current loops are distributed throughout the fluid.

Because Alfvén waves are reflected from both ends of the container, the system exhibits an infinite number of resonances whose frequencies are defined by

$$\cos kl = 0.$$ (12.2.125)

The boundary condition at the insulated end of the cylinder (12.2.106) is essentially a free end condition. This is true because no current can flow in the insulator and no electrical forces are available at the boundary to perturb the fluid motion. Also, because the fluid is inviscid, there can be no tangential mechanical force applied to the fluid by the end plate. At the perfectly conducting end plate ($z = l$) the fluid "sticks" to the end plate because of electrical forces. A small radial current loop with one side in the end plate and the other side in the fluid will keep the flux linking it at zero. This produces the currents that interact with B_o to allow no slippage of the fluid at a perfectly conducting boundary that is perpendicular to the equilibrium flux density.

To ascertain the kinds of numbers that would be involved in an experimental system of this sort, consider a container with the dimensions

$$l = 0.1 \text{ m}, \qquad R = 0.1 \text{ m}.$$

Assume the fluid to be liquid sodium (sometimes used as a coolant for nuclear reactors) which has a mass density, at 100°C, of

$$\rho = 930 \text{ kg/m}^3.$$

If we assume a flux density of

$$B_o = 1 \text{ Wb/m}^2,$$

which is easily obtainable with iron-core electromagnets, we obtain an Alfvén velocity of

$$a_b = 31 \text{ m/sec.}$$

The lowest resonance frequency of this system is given from (12.2.125) by

$$k = \frac{\pi}{2l},$$

which yields

$$\omega = 490 \text{ rad/sec}$$

or

$$f = 78 \text{ Hz.}$$

From these results we can see that Alfvén waves propagate at low velocities in liquid metals and that for devices of reasonable size the resonance frequencies also are low.

In our treatment of Alfvén waves we have assumed that the electrical conductivity of the fluid is infinite. In such a case we wonder how the flux density B_0 can exist in the fluid. The answer is simply that the conductivity is large but finite, and in establishing the equilibrium conditions sufficient time was allowed for the flux density B_0 to be established by diffusion into the fluid. In the analysis of the waves the assumption $\sigma \rightarrow \infty$ means simply that the diffusion time of the magnetic field through the fluid is much longer than the time required for the wave to propagate through the fluid* (see Section 7.1).

We have introduced Alfvén waves by using an incompressible fluid model. These waves can also propagate in compressible, highly conducting fluids such as gases. The analysis is essentially the same in both cases; however, more complex waves are possible in compressible fluids. Thus we must exercise care to ensure that only Alfvén waves are driven by a particular excitation in a compressible fluid.

12.2.4 Ferrohydrodynamics

Attention has been confined so far in this section to coupling with fluids that carry free currents. As pointed out in Section 8.5.2, magnetization forces can also be the basis for interaction with liquids. Commonly found fluids have no appreciable permeability. Ferromagnetic fluids, however, can be synthesized by introducing a colloidal suspension of magnetizable particles into a carrier fluid. Colloidal suspensions tend to settle out over long periods of time, and in the presence of a magnetic field the magnetized particles tend

---

* For an example of the experimental conditions necessary see A. Jameson, "A Demonstration of Alfvén Waves, I: Generation of Standing Waves," *J. Fluid Mech.*, **19**, 513–527 (August 1964).
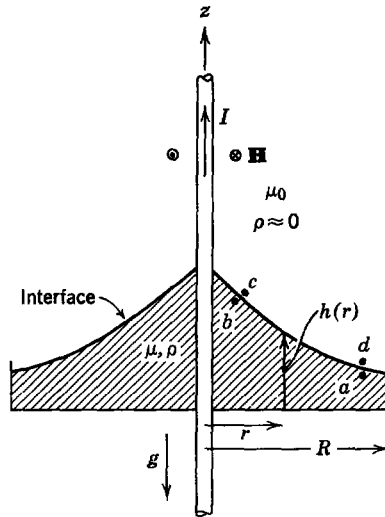
Fig. 12.2.21 A dish of magnetizable fluid is subjected to the magnetic field induced by current I.

to flocculate. Recent research efforts have led to the synthesis of colloidal suspensions (e.g., submicron-sized ferrite particles in a carrier fluid of kerosene), which are stable over indefinite periods of time.* We have no intention of delving into this topic in depth here; rather we confine ourselves to one simple example that illustrates this class of phenomena.

Although the ferrofluid is easily magnetizable, it can be made to be highly insulating against electrical conduction. In a magnetic field system the electric field is important because it determines the conduction current (through Ohm's law). In the region occupied by a magnetic insulator the conduction current is negligible and the equations for the magnetic field are simply

$$\nabla \times \mathbf{H} = 0, \tag{12.2.126}$$

$$\nabla \cdot \mathbf{B} = 0. \tag{12.2.127}$$

These are the equations used to describe the magnetic field, even in a dynamic situation. At any instant in time the magnetic field, at least insofar as it is determined by the magnetized fluid, has the same distribution as if the system were static.

As an illustration of the nature of the magnetization force consider the experiment shown in Fig. 12.2.21. A constant current I is imposed along the z-axis by means of a conductor. This conductor passes vertically through

---

a dish containing the magnetic fluid. We wish to compute the static equilibrium of the fluid that results after the current I has been turned on. This amounts to determining the altitude h of the fluid interface above the bottom of the dish. We can expect that, because a force density, $-\mathbf{H} \cdot \mathbf{H} \nabla \mu$, tends to pull the fluid upward, the depth will be greatest where the magnetic field intensity is greatest.

We assume that the magnetic field induced by the return current can be ignored. Then, under the assumption of axial symmetry, Ampère's law requires that the current I induce an azimuthally directed magnetic field intensity

$$\mathbf{H} = \mathbf{i}_\theta \frac{I}{2\pi r}. \qquad (12.2.128)$$

This problem is relatively simple because the magnetizable fluid has no effect on the distribution of $\mathbf{H}$; that is, because the physical system is axially symmetric, we can argue that the fluid deformations are also axially symmetric and $h = h(r)$. It is clear that (12.2.128) satisfies the field equations (12.2.126) and (12.2.127) in the region occupied by the fluid, and because the interface is axisymmetric it also satisfies the boundary conditions. The tangential component of $\mathbf{H}$ is continuous and there is no normal component of $\mathbf{B}$ at the liquid interface. Hence we know the magnetic field intensity at the outset, and this makes finding $h(r)$ straightforward.

The magnetic force acting on the fluid (from Section 8.5.2)* is

$$\mathbf{F} = -\tfrac{1}{2}\mathbf{H} \cdot \mathbf{H} \nabla \mu + \nabla \left(\tfrac{1}{2}\rho \frac{\partial \mu}{\partial \rho} \mathbf{H} \cdot \mathbf{H} \right). \qquad (12.2.129)$$

In the bulk of the liquid, μ is constant. Hence the force density can be written as

$$\mathbf{F} = -\nabla \psi, \qquad \psi = -\frac{\rho}{2} \frac{\partial \mu}{\partial \rho} \mathbf{H} \cdot \mathbf{H}. \qquad (12.2.130)$$

This is the form assumed in deriving Bernoulli's equation (12.2.11) which, in the case of a static fluid, becomes

$$p + \rho g z - \frac{\rho}{2} \frac{\partial \mu}{\partial \rho} \mathbf{H} \cdot \mathbf{H} = \text{constant}. \qquad (12.2.131)$$

Remember that this equation is valid in the bulk of the fluid. It can therefore be used to relate the pressures and heights at the points (a) and (b) in Fig. 12.2.21. These points are just beneath the interface, where pressures are p_a and p_b, respectively, and the altitudes are h_a and h_b. From (12.2.131)

$$p_a + \rho g h_a - \frac{\rho}{2} \frac{\partial \mu}{\partial \rho} (H^a)^2 = p_b + \rho g h_b - \frac{\rho}{2} \frac{\partial \mu}{\partial \rho} (H^b)^2. \qquad (12.2.132)$$

* See Table 8.1, Appendix G.

Similar reasoning shows that the pressures p_c and p_d just across the interface from points (b) and (a), respectively, are related by

$$p_c = p_d. \qquad (12.2.133)$$

Here we have assumed that the density of the air above the liquid can be ignored.

Fig. 12.2.22   A small volume element encloses the interface between points c and b in Fig. 12.2.21.

Now, if we could relate the pressures at adjacent points on opposite sides of the interface, we would have four equations that would make it possible to relate all four of the pressures p_a, p_b, p_c, and p_d. At the interface there is a jump in μ, and we must be careful to include the effect of the first term in (12.2.129) [which was not accounted for in (12.2.131)]. The stress tensor representation of the force density is convenient for determining the jump in pressure at the interface [see (8.5.41)].* A thin volume is shown in Fig. 12.2.22, as it encloses the region of interface between points b and c. To make use of the stress tensor in cartesian coordinates we erect a set of orthogonal coordinates (u, v, w) at the interface, with w in the θ-direction. Force equilibrium then requires that the sum of the surface forces balance

$$p_b - p_c = T_{vv}{}^b - T_{vv}{}^c = \tfrac{1}{2}(H^b)^2\left[\mu_0 - \mu\left(1 - \frac{\rho}{\mu}\frac{\partial \mu}{\partial \rho}\right)\right]. \qquad (12.2.134)$$

Similarly, at the interface between points (d) and (a)

$$p_d - p_a = -\tfrac{1}{2}(H^a)^2\left[\mu_0 - \mu\left(1 - \frac{\rho}{\mu}\frac{\partial \mu}{\partial \rho}\right)\right]. \qquad (12.2.135)$$

Now addition of these last four equations eliminates the pressures and gives an expression for the difference in surface elevation at points a and b as a function of the magnetic field intensities.

$$\rho g(h_a - h_b) = \tfrac{1}{2}(\mu_0 - \mu)[(H^b)^2 - (H^a)^2]. \qquad (12.2.136)$$

Until now we have not specified the field intensity at points a and b. It has been known all along, however, because of (12.2.128). In particular, if we take the point a as being at $r = R$ (which could be the outside radius of the pan), (12.2.136) becomes an expression for the dependence of interface altitude on the radius r.

$$\rho g(h_b - h_a) = \tfrac{1}{2}(\mu - \mu_0)\frac{I^2}{(2\pi)^2}\left(\frac{1}{r^2} - \frac{1}{R^2}\right). \qquad (12.2.137)$$

This result is sketched in Fig. 12.2.23. We have assumed that the density of the liquid is constant. This means that the total volume of the liquid must be

* Table 8.1, Appendix G.
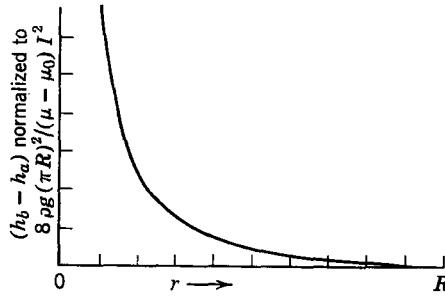
Fig. 12.2.23 Sketch of the liquid interface contour predicted by (12.2.137).

conserved, a fact that could be used to find the distance from a to the bottom of the pan.

An experiment with essentially the same ingredients as this example is shown in Fig. 12.2.24. In actuality, a significant magnetic saturation of the liquid makes the electrically linear model used here ($\mathbf{B} = \mu\mathbf{H}$) only approximately correct. As we know from Chapters 3 and 8, energy methods can also be used to calculate magnetization forces for electrically nonlinear systems, and this is what is required to make a careful comparison of theory and experiment.

Finally, it is worthwhile to observe that the magnetostriction force density has no observable effect on the surface deformation. This will always be the case as long as interest is confined to situations in which the fluid density remains essentially constant.

12.3 ELECTRIC FIELD COUPLING WITH INCOMPRESSIBLE FLUIDS

There is a wide range of mechanisms by which an electric field can produce a force on a fluid. In this section examples are used to illustrate two of the most commonly encountered types of interaction.

12.3.1 Ion-Drag Phenomena

Electrical forces can be produced in highly insulating gases and liquids by injecting charged particles and using an electric field to pull them through the fluid. Here we assume that these charged particles are ions that might be emitted by the corona discharge in the neighborhood of sharply pointed electrodes placed at a high potential (several kilovolts). These ions move through a liquid or gas under the influence of an applied electric field. Their motion, however, is retarded by friction, and momentum is imparted to the fluid. Therefore the ion-drag effect can be used to pump or accelerate the fluid. Similarly, if the ion is transported by the fluid against the retarding
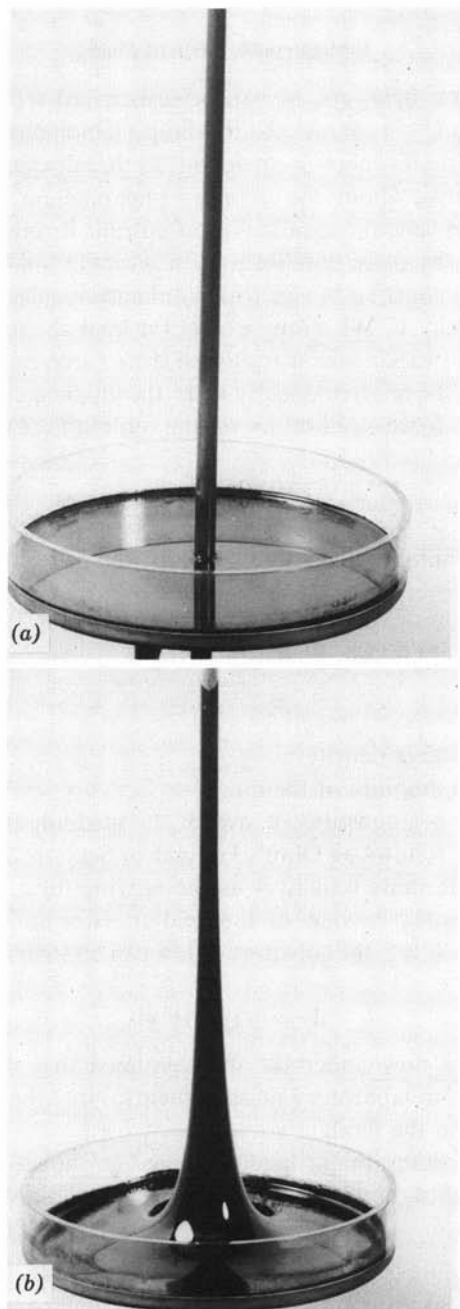
Fig. 12.2.24 (a) A conductor passes along the axis of symmetry through a pan containing the magnetizable liquid, $I = 0$. **(b)** The current I has been turned on. The result is a force density $-\mathbf{H} \cdot \mathbf{H}\nabla\mu$ that tends to lift the fluid upward, as predicted by (12.2.137). (Courtesy of AVCO Corporation, Space Systems Division.)

force of the electric field, energy can be transferred from the flow into an electrical circuit. In this context the ion-drag phenomenon is the basis for a gaseous Van de Graaff generator analogous to that discussed in Section 7.2.2.

To be quantitative about the ion-drag phenomenon we require a constitutive law to describe the conduction of current through the fluid. Here a simple picture of the force equilibrium for a single ion is helpful. Suppose that an ion with a charge q moves with a velocity $\mathbf{v}_r$ relative to the gas in an electric field intensity $\mathbf{E}$. We would expect (at least at atmospheric pressure) that the ion would experience a frictional drag force proportional (say, by the constant γ) to the relative velocity $\mathbf{v}_r$. In the absence of appreciable effects from acceleration, force equilibrium on the ion requires that

$$\mathbf{v}_r = \frac{q\mathbf{E}}{\gamma}. \tag{12.3.1}$$

If we let n be the number density of the ions, then the current density is

$$\mathbf{J}_f = nq\mathbf{v}_r, \tag{12.3.2}$$

which, in view of (12.3.1), can also be written

$$\mathbf{J}_f = \rho_f \mu \mathbf{E}, \tag{12.3.3}$$

where ρ_f = free charge density = nq,
       $\mu = q/\gamma$ = mobility of the ion.

Equation 12.3.3 is a constitutive law for the medium at rest and plays the same role in what follows as Ohm's law did in Section 7.2. This law holds in a frame with the same velocity $\mathbf{v}$ as the moving fluid, where it would be written as $\mathbf{J}_f' = \rho_f \mu \mathbf{E}'$. In view of the field transformations for an electric field system (Table 6.1)*, the constitutive law can be written in the laboratory frame as

$$\mathbf{J}_f = \rho_f(\mu\mathbf{E} + \mathbf{v}). \tag{12.3.4}$$

In the example we now undertake it is assumed that the mobility μ is a constant, found from laboratory measurements. Note that $\mu\mathbf{E}$ is the velocity of an ion relative to the fluid.

An electrostatic pump might be constructed as shown in Fig. 12.3.1. The system consists of a nonpolarizable ($\epsilon = \epsilon_0$) gas flowing with constant velocity

$$\mathbf{v} = \mathbf{i}_x v_o \tag{12.3.5}$$

through a cylindrical insulating tube of cross-sectional area A. At $z = 0$ and $z = l$, plane conducting screens are placed perpendicular to the axis. We assume that the screens do not affect the gas flow but make electrical contact with the gas. The screens are connected to external terminals that are excited

* Appendix G.
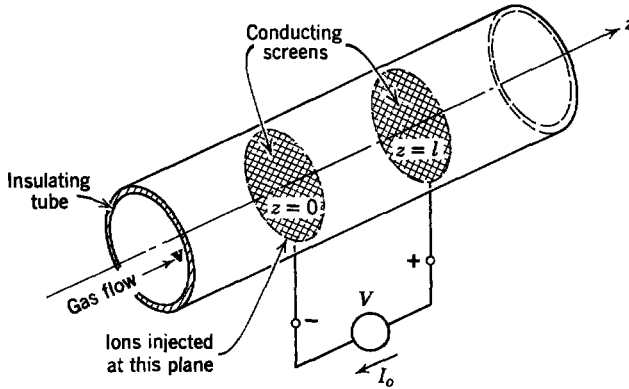
Fig. 12.3.1 Configuration for a gaseous electrostatic pump or generator.

by the constant-current source I_o as shown. At the plane $z = 0$ positive ions are injected into the gas by a source of ions.

For now we assume that this source supplies ions at a rate necessary to maintain the charge density ρ_o at the inlet screen:

$$\text{at } z = 0, \qquad \rho_f = \rho_o. \tag{12.3.6}$$

The current density and electric field intensity are assumed to have only z-components,

$$\begin{aligned} \mathbf{J}_f &= \mathbf{i}_z J, \\ \mathbf{E} &= \mathbf{i}_z E, \end{aligned} \tag{12.3.7}$$

and to be functions of z alone. Attention is confined to steady-state operation.

In addition to the boundary condition of (12.3.6), the equations we need to solve this problem are the z-component of (12.3.4)

$$J = \rho_f(\mu E + v_o), \tag{12.3.8}$$

Gauss's law written as

$$\epsilon_0 \frac{dE}{dz} = \rho_f, \tag{12.3.9}$$

and the conservation of charge for steady-state conditions

$$\frac{dJ}{dz} = 0. \tag{12.3.10}$$

The area over which current flows is A; consequently, the current density and the source current are related by

$$J = \frac{I_o}{A}. \tag{12.3.11}$$

We first solve (12.3.8) for the electric field intensity to obtain

$$E = -\frac{v_o}{\mu} + \frac{J}{\rho_f \mu}.$$ (12.3.12)

Next, this expression is differentiated with respect to z and (12.3.9) is used to eliminate E:

$$\frac{\rho_f}{\epsilon_0} = \frac{d}{dz}\left(\frac{J}{\rho_f \mu}\right).$$ (12.3.13)

Expansion of the derivative and use of (12.3.10) yields

$$\frac{d\rho_f}{dz} = -\frac{\mu}{\epsilon_0 J}\rho_f^3.$$ (12.3.14)

Integration of this expression, use of the boundary condition of (12.3.6), and some manipulation yield

$$\frac{\rho_f}{\rho_o} = \left[1 + \frac{2}{R_e}\left(\frac{\rho_o v_o}{J}\right)\frac{z}{l}\right]^{-\frac{1}{2}},$$ (12.3.15)

where $R_e = \epsilon_0 v_o / \rho_o \mu l$ is the electric Reynolds number.

The plot of the free charge density shown in Fig. 12.3.2 makes it evident that the rate of decay down the channel is decreased as the electric Reynolds number is increased.

Substitution of (12.3.15) into (12.3.12) gives the electric field intensity between the grids

$$E = \frac{v_o}{\mu}\left\{-1 + \frac{J}{\rho_o v_o}\left[1 + \frac{2}{R_e}\left(\frac{\rho_o v_o}{J}\right)\left(\frac{z}{l}\right)\right]^{\frac{1}{2}}\right\}.$$ (12.3.16)
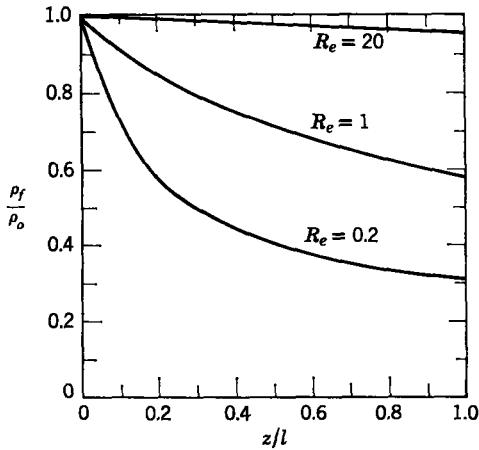
Fig. 12.3.2 Charge-density distribution between grids. $J/\rho_o v_o = 1$.
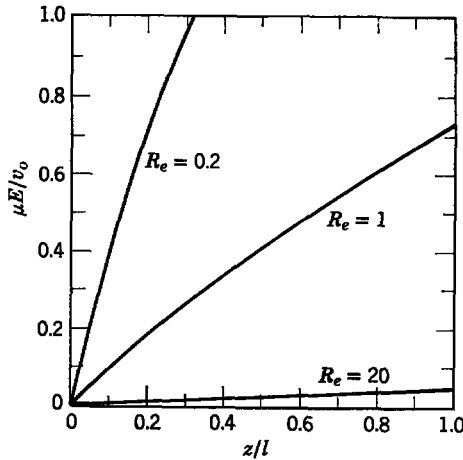
Fig. 12.3.3   Distribution of electric field intensity between the grids. $J/\rho_o v_o = 1$.

If the ion source at $z = 0$ is essentially limited by space charge, it will emit just enough charge to make the electric field at $z = 0$ vanish.* From (12.3.16) this requires that

$$\frac{J}{\rho_o v_o} = 1. \qquad (12.3.17)$$

In our discussion it is assumed that J, ρ_o, and v_o are positive. Remember that μE is the velocity of the ions relative to the fluid. This condition requires that the ions have the same velocity as the fluid at $z = 0$. Then the electric field is positive everywhere between the grids, as shown in Fig. 12.3.3. This means that the ions move more rapidly than the fluid and, as we shall see, the system operates as a pump.

As for the MHD machine discussed in Section 12.2.1, two "terminal" characteristics of the electrohydrodynamic flow interaction are of interest— the pressure change from inlet to outlet and the terminal voltage. The first can be computed from the electric field intensity by making use of the Maxwell stress tensor†. The pressure forces acting on the fluid in the channel section between $z = 0$ and $z = l$ are just balanced by the Maxwell stresses acting over the surface enclosing this section. Because there are no electrical shear forces,

$$A[p(l) - p(0)] = A[T_{11}(l) - T_{11}(0)] = \tfrac{1}{2} A \epsilon_0 [E^2(l) - E^2(0)]. \quad (12.3.18)$$

Since we have constrained $E(0)$ to vanish, it is clear from this statement that

---

* For a discussion of this model for the ion source see O. M. Stuetzer, "Ion Drag Pumps," *J. Appl. Phys.*, **31**, 136 (January 1960).
† Section 8.3 or Appendix G.

$p(l) > p(0)$. In fact, from (12.3.16)

$$p(l) - p(0) = \frac{\epsilon_0}{2}\left(\frac{v_o}{\mu}\right)^2\left[-1 + \left(1 + \frac{2}{R_e}\right)^{\frac{1}{2}}\right]^2. \qquad (12.3.19)$$

This result indicates that the larger R_e, the smaller the pressure rise between the grids. This is misleading because both the electric Reynolds number R_e and the first factor in (12.3.19) depend on v_o. If we think of holding v_o fixed, however, and recall that R_e is inversely proportional to l, (12.3.19) shows that the pressure rise increases as l increases.

To obtain the terminal voltage V we integrate the negative of the electric field intensity from $z = 0$ to $z = l$:

$$V = \frac{lv_o}{\mu}\left\{1 - \frac{R_e}{3}\left[\left(1 + \frac{2}{R_e}\right)^{\frac{3}{2}} - 1\right]\right\}. \qquad (12.3.20)$$

This voltage is negative, as must be the case if power is supplied by the current source to the fluid. The fact that there is a pressure rise in the direction of flow indicates that work is done on the fluid as it passes through the region between the grids.

Ion-drag interactions can be used not only to pump slightly conducting fluids but also for conversion of energy from mechanical to electrical form.* In gases the mobility of ions is so great that such devices tend to lack efficiency. This shortcoming can be obviated either by using liquids, in which the mobility of ions tends to be much lower, or by replacing the ions with larger charged particles of liquid or solid. In any case, the electric pressure $\frac{1}{2}\epsilon_0 E^2$ tends to be small compared with the magnetic pressure $\frac{1}{2}\mu_0 H^2$ because the electric field intensity is limited by the breakdown strength of the dielectric medium. Hence *for a given size of device* the amount of energy converted in an electric field interaction is much less than that found for a magnetic field interaction.

One of the most significant reasons for our discussion of the ion-drag phenomenon is that it is commonly (and altogether too easily) encountered in high voltage systems, in which it accompanies corona discharge. A simple laboratory demonstration of the effect is shown in Fig. 12.3.4, in which two wire grids are placed at a potential difference of about 25 kV. Perpendicular segments of wire are mounted on the lower electrode to form a "bed of nails," and when this grid is electrified the tips of these segments provide sites for corona discharge. This discharge is the source of ions at $z = 0$ in Fig. 12.3.1.

* B. Kahn and M. C. Gourdine, "Electrogasdynamic Power Generation," *AIAA J.*, **2,** No. 8, 1423–1427 (August 1964). Also, A. Marks, E. Barreto, and C. K. Chu, "Charged Aerosol Energy Converter," *AIAA J.*, **2**, No. 1, 45–51 (January 1964).
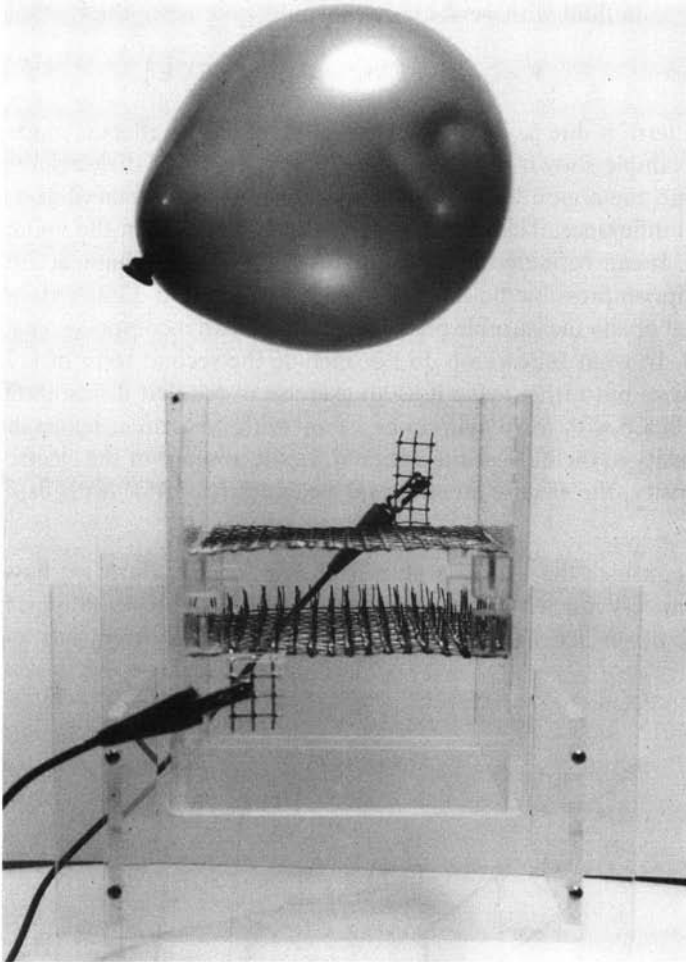
Fig. 12.3.4 Simple laboratory demonstration of ion-drag effect. In the absence of an applied voltage the balloon rests on the plastic enclosure. With voltage, it is pushed upward by ions being conducted between the grids.

In the absence of an applied voltage, the balloon rests on the plastic enclosure. With voltage, it is pushed upward by the pumping action between the grids.

12.3.2   Polarization Interactions

The analog to the magnetization interactions with fluids, discussed in Section 12.2.4, is the polarization interaction with electric fields—sometimes referred to as "dielectrophoresis." The polarization force density for fluids was developed in Section 8.5, in which it was found that in the absence of

free charges a fluid with permittivity ϵ would experience the force density*

$$\mathbf{F} = -\tfrac{1}{2}\mathbf{E} \cdot \mathbf{E}\nabla\epsilon + \nabla\left(\tfrac{1}{2}\rho\,\frac{\partial\epsilon}{\partial\rho}\,\mathbf{E} \cdot \mathbf{E}\right). \qquad (12.3.21)$$

The first term is due to inhomogeneity of the fluid. Its effect is made familiar by the example shown in Fig. 8.5.6, in which a slab of dielectric material is pulled into the region between plane-parallel electrodes placed at a constant potential difference. The second term is due to changes in the volume of the material. It can be included in the analysis of electromechanical interactions with an incompressible fluid, but as we saw in Section 12.2.4, its effect will cancel out of any measurable prediction based on an incompressible model for the fluid. In what follows we do not include the second term of (12.3.21) in our analysis but rather leave it as an exercise to see that it has no effect. We are concerned with the dynamics of a fluid with uniform ϵ; hence there is no force density in the bulk of the material. In the absence of the electrostriction force density, the electric stress tensor becomes [(8.5.46)* with $\partial\epsilon/\partial\rho = 0$]

$$T_{ij} = \epsilon E_i E_j - \tfrac{1}{2}\delta_{ij}\epsilon E_k E_k. \qquad (12.3.22)$$

Now consider the example shown in Fig. 12.3.5. Here we have a fluid pendulum very much like that shown in Fig. 12.2.7. This pendulum, however, is upside down because g is directed upward. The problem has a practical
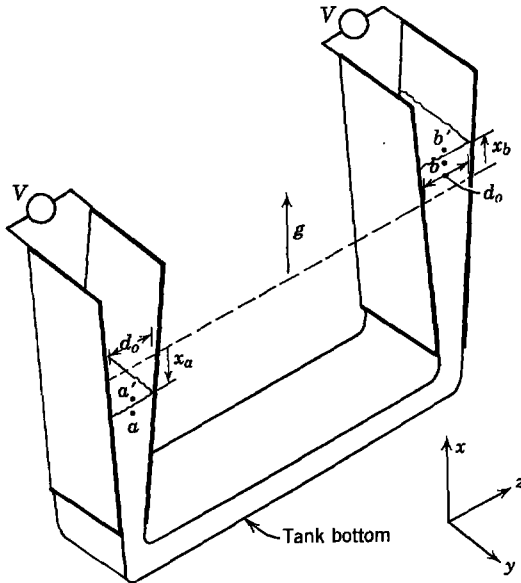
Fig. 12.3.5 A liquid pendulum containing dielectric fluid. Slightly diverging plates are used to impose a spatially varying electric field that tends to maintain the liquid in the bottom of the tank in spite of the acceleration g.

* See Table 8.1, Appendix G.

basis. Suppose that we wish to use the electric field to provide an artificial "gravity" to bottom the fluid within a tank under the near-zero gravity conditions of outer space; for example, the fluid might be the cryogenic liquid fuel used to propel a spacecraft. The electric field then provides fluid at a drain placed at the "bottom" of the tank. In this case g represents the effect of acceleration of the vehicle, as, for example, that which would occur during attitude control maneuvers. We have chosen g to be upward because this appears to be the worst possible situation in terms of removing the fluid from the bottom of the tank.

The U-shaped tank is considered in this example because it is easily analyzed with the tools developed in this chapter. Even though the example may seem academic, it has practical significance in the design of fluid orientation systems.

Because there are no electrical forces in the bulk of the liquid, we can use Bernoulli's equation derived in Section 12.2.1b. Again we carry out an integration of the momentum equation, as indicated by (12.2.33a), between points a and b, defined in Fig. 12.3.5. Now, however, the interfaces are subject to surface forces [due to the first term in (12.3.21)], and we cannot claim that the pressures p_a and p_b (just below the respective interfaces) are equal. In carrying out the integral of (12.2.33a) we retain the pressures evaluated at the points a and b to obtain

$$\rho l \frac{\partial v}{\partial t} = 2\rho g x_a + p_a - p_b. \tag{12.3.23}$$

Here v is the velocity of the fluid directed from a to b so that

$$\frac{\partial v}{\partial t} = \frac{d^2 x_a}{dt^2}. \tag{12.3.24}$$

We have approximated the velocity as being the same along a streamline connecting the points a and b. The cross-sectional area of the pendulum varies somewhat because the vertical legs are constructed with side walls composed of slightly diverging electrodes. Insofar as the fluid velocity is concerned, the effect of the diverging plates represents a nonlinear effect equivalent to slight changes in the length l of the pendulum; this effect is ignored here.

The fundamental difficulty in keeping the liquid in the bottom of the tank, with no electric field, is illustrated by combining the last two equations. With no applied voltage, $p_a = p_b$, and it is clear that the equilibrium represented by $x_a = 0$ is unstable. It is the purpose of the electric field to stabilize this equilibrium.

Before completing the mathematical representation of the dynamics consider physically how the polarization force density [the first term in

(12.3.21)] can stabilize the equilibrium at $x_a = 0$. This force is finite only at the two interfaces, where it is singular (infinite in magnitude over an infinitely thin region of space); that is, it comprises a surface force directed in the positive x-direction on each of the interfaces in proportion to the square of the electric field intensity. With the pendulum in equilibrium, the electrical forces on each of the interfaces just balance. Suppose that the system is perturbed to the position shown in Fig. 12.3.5. Then the upward-directed force on the interface at a is increased (the plates are closer together at this point; therefore **E** is greater), whereas that at b is decreased. This tends to return the pendulum to its equilibrium position. We expect that if we can make this stabilizing electrical effect large enough it will outweigh the de-stabilizing effect of gravity.

To provide a quantitative statement of the condition for stability we complete the equation of motion by relating the pressures p_a and p_b. Force balance on the interfaces, in view of the force diagrams shown in Fig. 12.3.6, requires

$$p_{a'} - p_a = T_{11}{}^{a'} - T_{11}{}^a = -\tfrac{1}{2}(\epsilon_0 - \epsilon)\left(\frac{V}{d_a}\right)^2, \qquad (12.3.25)$$

$$p_{b'} - p_b = T_{11}{}^{b'} - T_{11}{}^b = -\tfrac{1}{2}(\epsilon_0 - \epsilon)\left(\frac{V}{d_b}\right)^2. \qquad (12.3.26)$$

Of course, the spacing d used in these expressions is evaluated at the instantaneous locations of the respective interfaces.

$$d_a = d_o - cx_a, \qquad (12.3.27)$$

$$d_b = d_o + cx_b. \qquad (12.3.28)$$

Here c is determined by the rate at which the electrodes diverge. Then, to linear terms, the combination of (12.3.25) and (12.3.26) (remember, $x_a = x_b$) gives

$$p_a - p_b + p_{b'} - p_{a'} = -2c(\epsilon - \epsilon_0)\left(\frac{V}{d_o}\right)^2\left(\frac{x_a}{d_o}\right). \qquad (12.3.29)$$

Formally, we can see that $p_{b'} = p_{a'}$ by joining points a' and b' with a streamline passing through the fluid above the interfaces (where the vapor phase is present and density is negligible). Then, by combining (12.3.25), (12.3.26),
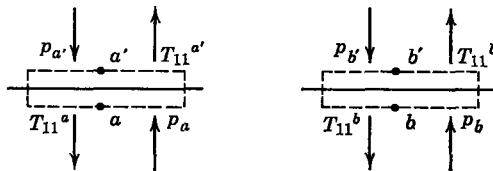
Fig. 12.3.6 Force equilibrium for each of the interfaces shown in Fig. 12.3.5.

and this last expression, we obtain the required equation of motion for the pendulum:

$$\rho l \frac{d^2 x_a}{dt^2} + x_a \left[-2\rho g + 2c(\epsilon - \epsilon_0) \frac{V^2}{d_o{}^3} \right] = 0. \qquad (12.3.30)$$

From this it is clear that the equilibrium is stable if the voltage is made large enough to satisfy the condition

$$c(\epsilon - \epsilon_0) \frac{V^2}{d_o{}^3} > \rho g. \qquad (12.3.31)$$

Liquid being oriented under near-zero gravity conditions is shown in Fig. 12.3.7. Each pair of adjacent plates has a potential difference. The zero gravity situation was created by flying the experiment within a KC-135 in a near-zero gravity trajectory. The liquid is Freon 113 with aniline dye added for purposes of observation. The basic mechanism for orienting the liquid is the same as that for the example considered in this section. Any two pairs of diverging plates can be considered as constituting a fluid pendulum with the essential behavior of that shown in Fig. 12.3.5. The stability condition of (12.3.31) guarantees that the equilibrium with the fluid in the tank "bottom" will be stable. Of course, a more complete representation of the dynamics requires a continuum model,* for instability may develop in the region between a single pair of electrodes.

We have stated from the outset that free charge forces are of negligible importance. In practice, this is guaranteed by making the applied voltages V of alternating polarity with sufficiently high frequency that free charges cannot relax into the fluid. If the frequency is high compared with typical mechanical frequencies, it is possible to use the same mathematical model as that developed here, except that V is the rms value of the voltage.

12.4 DISCUSSION

In this chapter we have introduced some of the fundamental laws and analytical techniques that are used in the study of electromechanical interactions with conducting, magnetizable and polarizable fluids. We have applied these laws and techniques to the analysis of systems in which an incompressible, inviscid fluid model is appropriate. Even though the incompressible, inviscid fluid model may seem quite restrictive, it provides an understanding of the basic electromechanical interactions that occur in all sorts of magnetohydrodynamic and electrohydrodynamic systems, including those with gaseous conductors.

* In fact, a description of this mode of instability is given in Section 10.1.

Image removed due to copyright restrictions.

Fig. 12.3.7 Orientation system for storing liquids within a tank in the zero gravity environment of space. The tank used in this test was spherical and transparent, with circular electrodes which are seen here edge-on. The electrodes converge toward the bottom of the picture; thus this is the region in which the electric field should provide an artificial "bottom." (*a*) With one g acting toward the *top* of the picture and no electric field, the liquid is in the upper half of tank; (*b*) liquid oriented at artificial "bottom" of tank under near-zero-gravity conditions created by flying the tank within a KC-135 in a zero gravity trajectory. The electrodes are at alternate polarities and can be viewed as a combination of pendulums with the basic configuration shown in Fig. 12.3.5. (Courtesy of Dynatech Corp., Cambridge, Mass.)

In Chapter 13 the restriction of an incompressible fluid is relaxed, and the effects of compressibility on electromechanical interactions are studied, although the restriction to inviscid fluid models is still retained.

PROBLEMS

12.1. The mechanism shown in Fig. 12P.1 is to be used as an electrically driven rocket. An insulating fluid of constant density ρ is compressed by a piston. The fluid is then ejected through a slit (nozzle) with a velocity V_p; because $dD \ll LD$, V_p is approximately a constant, and the system is approximately in a steady-state condition $(\partial/\partial t = 0)$:

    (a) What is the pressure p at the inside surface of the piston? (Assume that $p = 0$ outside the rocket.)

    (b) Under the assumption that $d \ll L$, what is V_p?

    (c) What is the total thrust of the rocket in terms of the applied voltage V_0 and other constants of the system?
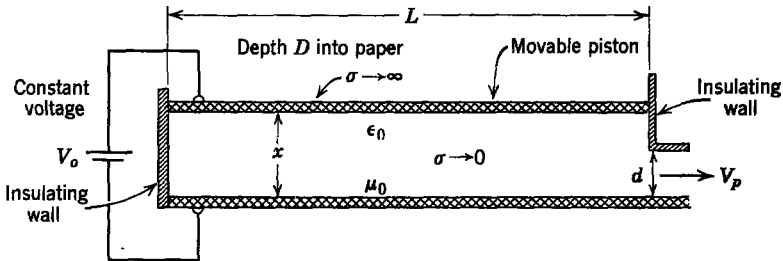
Fig. 12P.1

12.2. A magnetic rocket is shown in Fig. 12P.2. A current source (distributed over the width W) drives a circuit composed in part of a movable piston. This piston drives an incompressible fluid through an orifice of height d and width W. Because $D \gg d$, the flow is essentially steady.

    (a) Find the exit velocity V as a function of I.

    (b) What is the thrust developed by the rocket? (You may assume that it is under static test.)

    (c) Given that $I = 10^3$ A, $d = 0.1$ m, $W = 1$ m, and the fluid is water, what are the numerical values for V and the thrust? Would you prefer to use water or air in your rocket?
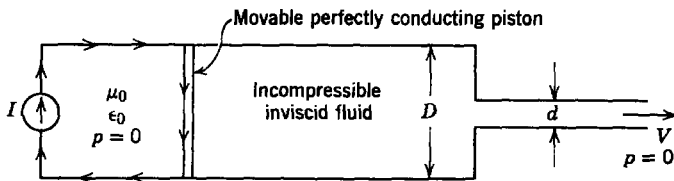
The rocket has a depth W into the paper

Fig. 12P.2

Depth W into paper
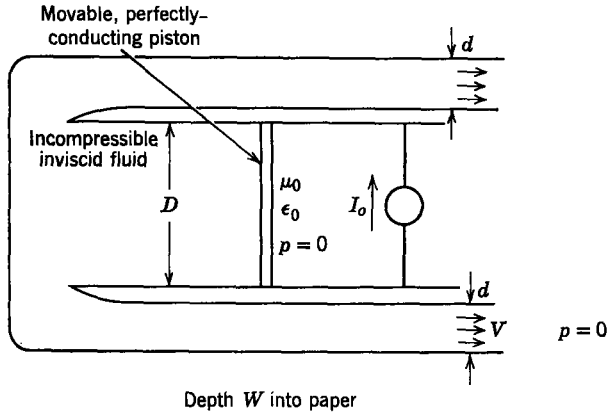
Fig. 12P.3

12.3. A magnetic rocket is shown in Fig. 12P.3. A current source I_0 (distributed over the depth W) drives a circuit composed in part of a movable piston. This piston drives an incompressible, inviscid, nonconducting fluid through two orifices, each of height d and depth W. Because $D \gg d$, the flow is essentially steady.

    (a) Find the exit velocity V as a function of I_0.

    (b) What is the thrust developed by the rocket? (You may assume that it is under static test.)

12.4. An incompressible, inviscid fluid of density ρ flows between two parallel walls as shown in Fig. 12P.4. The bottom wall has a small step of height d in it at $x_1 = 0$. At $x_1 = -L$, the velocity of the fluid is $\mathbf{v} = V_0 \mathbf{i}_1$ and the pressure is p_0. Also, at $x_1 = +L$ the velocity of the fluid is uniform with respect to x_2 and is in the x_1-direction, since $d \ll L$. Assuming that the flow is steady ($\partial/\partial t = 0$) and irrotational, find the x_1-component of the force per unit depth on the bottom wall. The system is uniform in the x_3-direction and has the x_2 dimensions shown in Fig. 12P.4.
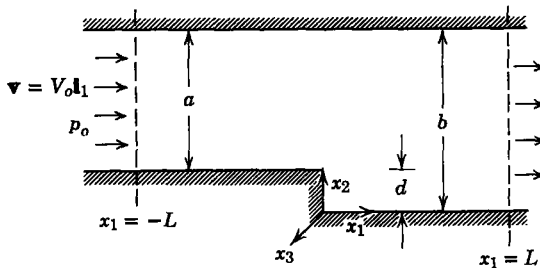
Fig. 12P.4

12.5. Far away from the rigid cylinder shown in Fig. 12P.5 the velocity of a fluid with density ρ is a constant $\mathbf{V} = V_0 \mathbf{i}_1$ and its pressure is p_0. Assume that the fluid is incompressible and that the flow is steady and irrotational:

(a) Find the velocity of the fluid everywhere.
(b) Sketch the velocity field.
(c) Find the pressure everywhere.
(d) Use the stress tensor to find the total pressure force (give magnitude and direction) exerted by the fluid on the rigid cylinder. Assume that $\partial/\partial x_3 = 0$.
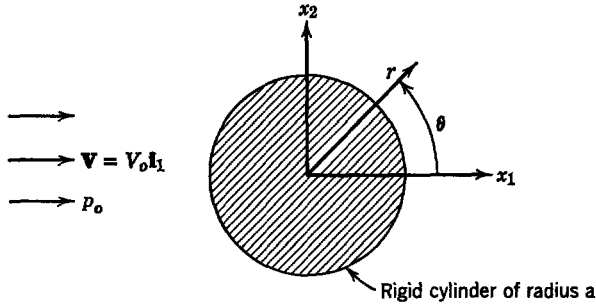
Fig. 12P.5

12.6. An inviscid incompressible fluid flows around a rigid sphere of radius a, as shown in Fig. 12P.6. At $x_1 = \pm\infty$ the fluid velocity becomes $\mathbf{v} = V_0\mathbf{i}_1$.

(a) Compute the velocity distribution $\mathbf{v}(x_1, x_2, x_3)$.
(b) Find the pressure $p(x_1, x_2, x_3)$. [Assume that the pressure is zero at $(x_1, x_2, x_3) = (-a, 0, 0)$.]
(c) Use the results of (b) to compute the force exerted on the sphere in the x_1-direction by the fluid.
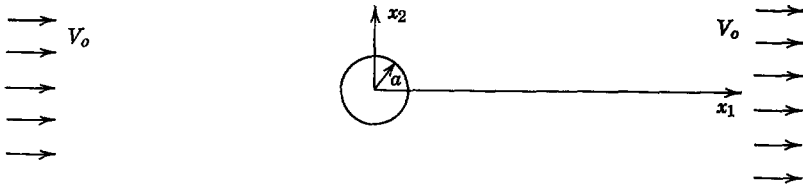
Fig. 12P.6

12.7. The velocity distribution of an inviscid fluid is given as $\mathbf{v} = -\nabla\phi$, where $\phi = (V_0/a)x_1x_2$ and V_0 and a are constants.

(a) Show by means of a sketch the direction and magnitude of the velocity in the x_1-x_2 plane.
(b) Compute the fluid acceleration. Sketch the direction and magnitude of the acceleration in the x_1-x_2 plane.
(c) In what physical situation would you expect the flow to have this distribution?

12.8. In the configuration of Fig. 12P.8 an incompressible, inviscid fluid of mass density ρ flows without rotation ($\nabla \times \mathbf{v} = 0$), between two rigid surfaces shown, with velocity

$$\mathbf{v} = \mathbf{i}_1 v_o \frac{x_2}{a} + \mathbf{i}_2 v_o \frac{x_1}{a},$$

where v_o and a are positive constants. Neglect gravity.

(a) Find the fluid acceleration at all points in the flow.
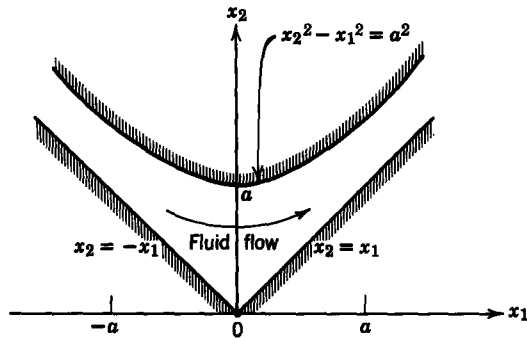
Fig. 12P.8

(b) The pressure is constrained at the origin ($x_1 = x_2 = 0$) to be p_o. Find the pressure at all other points in the fluid.

12.9. Consider the situation of Prob. 12.8, but now with gravity acting in the $-x_2$ direction.

    (a) Find the velocity between the rigid walls.

    (b) Show that the boundary conditions are satisfied at the walls.

12.10. Figure 12P.10 shows an irrotational flow in a corner formed by a rigid wall.

    (a) Let $\mathbf{v} = -\nabla\phi$. What are the boundary conditions on ϕ? Sketch the contour of constant ϕ in the x-y plane.

    (b) What function $\phi(x, y)$ satisfies both $\nabla \cdot \mathbf{v} = 0$ and $\nabla \times \mathbf{v} = 0$ and the boundary conditions of part (a)?

    (c) Assuming that the pressure $p = p_o$ at $(x, y) = 0$ and that $p = p_o$ to the left and below the wall, what is the force exerted by the fluid on the section of the wall between $x = c$ and $x = d$?

    (d) Compute the fluid acceleration. Make a sketch to show the magnitude and direction of the acceleration in the x-y plane.
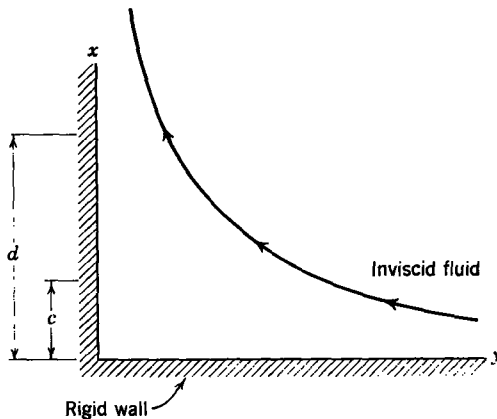
Fig. 12P.10
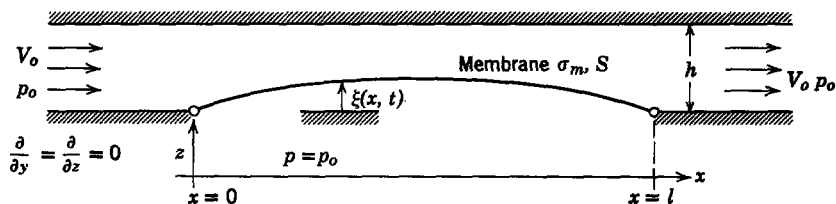
Fig. 12P.11

12.11. An inviscid incompressible fluid enters the channel shown in Fig. 12P.11, with the velocity V_o and pressure p_o. One wall of the channel includes a section of length l composed of a taut membrane with the deflection ξ.

(a) Assume that spatial variations in the membrane deflection occur slowly so that the velocity v_x is independent of z. Relate $v_x(x)$ to V_o, ξ, and h.

(b) Determine the pressure on the upper surface of the membrane using the fact that $p = p_o$ at the inlet where $v = V_o$.

(c) Find an expression of the form $T_z = C\xi$ for the force per unit area T_z on the membrane as a function of ξ and a constant C. To do this assume that perturbations in ξ are small and use the fact that the pressure below the membrane is p_o.

(d) Now assume that the dynamics occur slowly enough that the result of part (c) will remain true even if $v = v(x, t)$ and $\xi = \xi(x, t)$. The membrane has a tension S and mass per unit area σ_m. For what values of V_o will the static equilibrium of the membrane at $\xi = 0$ be stable?

(e) Explain physically why the instability of part (d) occurs.

12.12. A perfectly conducting membrane with tension S and mass per unit area σ_m is fixed at $x = 0$ and $x = L$. An inviscid, incompressible fluid with mass density ρ_o flows underneath the membrane (Fig. 12P.12). An electric field exists in the region above the membrane. The upper region is filled with a light gas that is at atmospheric pressure p_o everywhere.

(a) Find the value of the pressure p_1 in the fluid for $-d \leq y \leq 0$ in terms of given parameters if $\xi(x, t) = 0$ is a state of equilibrium.

(b) Under what conditions can a small signal sinusoidal oscillation exist about the equilibrium position $\xi(x, t) = 0$?

Note. The gravitational field affects both the equilibrium and small signal solutions.

(c) Make a dimensioned ω-k plot for a real wavenumber.

(d) Justify the validity of imposing boundary conditions at $x = 0$ and $x = L$ such that these conditions affect the membrane for $0 \leq x \leq L$.
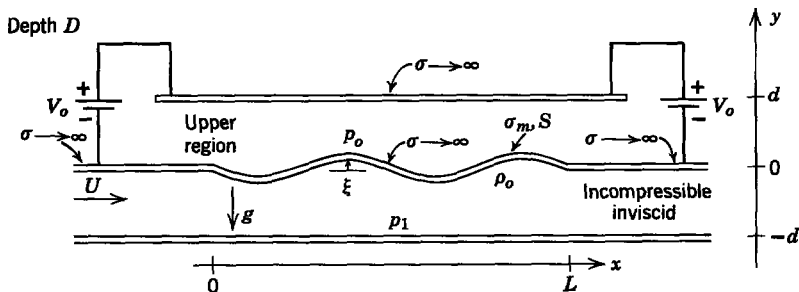
Fig. 12P.12
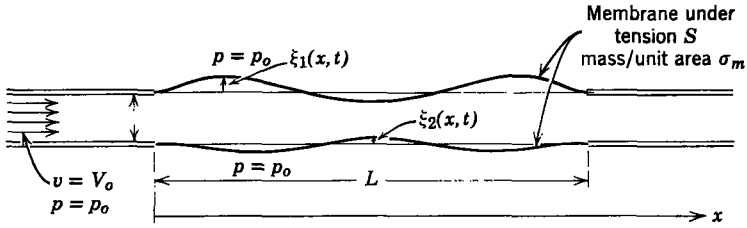
Fig. 12P.13

12.13. A duct is formed by stretching membranes between plane parallel rigid plates, as shown in Fig. 12P.13. An inviscid fluid flows through this duct, entering at the left with velocity V_o. The pressure outside the duct is p_o, so that the membrane can be in static equilibrium with $\xi_1 = \xi_2 = 0$.

    (a) What is the largest velocity V_o that can be used and have the membranes remain in a state of stable equilibrium?

    (b) What would the appearance of the membranes be if V_o were just large enough to make the equilibrium $\xi_1 = \xi_2 = 0$ unstable?

12.14. An inviscid, incompressible fluid rests on a rigid bottom, as shown in Fig. 12P.14. In the absence of any disturbances it is static and has a depth a. If disturbed, the surface of the fluid has the position $\xi(x, t)$. As is obvious to anyone who has observed ocean waves, disturbances of the interface propagate as waves. It is our object here to derive an equation for the propagation of these gravity waves, which have "wavelengths" that are long compared with the depth a of the fluid. To do this we make the following assumptions:

    (a) The effects of inertia in the y-direction are negligible. Hence the force equation in the y-direction is

$$\frac{\partial p}{\partial y} = -\rho g.$$

       Because $y = \xi(x, t)$ is a free surface, the pressure there is constant (say zero). What is p in terms of y and ξ?

    (b) Because the fluid is very shallow, we can assume that $v_x = v_x(x, t)$; that is, the horizontal fluid velocity is independent of y. On the basis of this assumption, use the conservation of mass equation for the incompressible fluid ($\nabla \cdot \mathbf{v} = 0$) to find $v_y(x, y, t)$ in terms of v_x.

    (c) Use the result of (a) to write the horizontal component of the force equation as one equation in $v_x(x, t)$ and $\xi(x, t)$.

    (d) Use the result of (b) to write an additional equation in ξ and v_x (assume $\xi \ll a$ so that only linear terms need be retained).

    (e) Combine equations from parts (c) and (d) to obtain the wave equation for gravity waves. What is the phase velocity of these waves?

Fig. 12P.14

Symmetric in
θ-direction

I_o

Top
view

θ

r

Incompressible
fluid

$r = R_o$

b

$b \ll R_o$

z

Post

Surface current

Pot   Air

$z = z_o$

I_o

$z = z_o$

P_o

a

g

r

Incompressible fluid

(a)

Top
view

H_s

$H_s = -\mathbf{1}_\theta \dfrac{I_o}{2\pi r_s}$

z

H_s z_s H_s

r

r_s

(b)

x_2

x_1

At $z = z_s$, $r = r_s$
normal $= \mathbf{1}_1$

$\mathbf{H} = \dfrac{-I_o}{2\pi r_s} \mathbf{1}_3$

x_3

For some typical
$r = r_s$, $z = z_s$, and
any $0 < \theta < 2\pi$

Typical point on surface

(c)
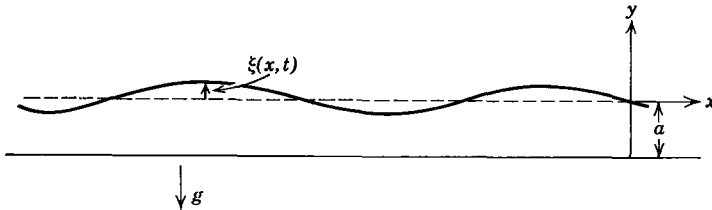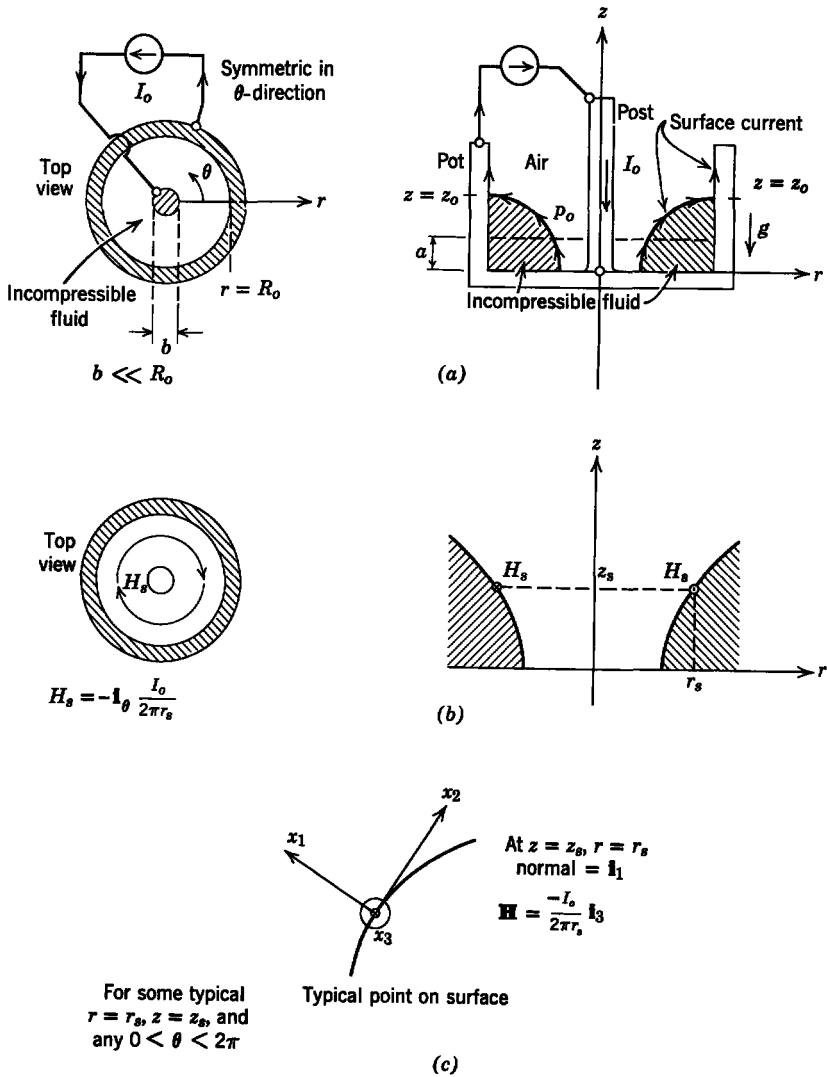
Fig. 12P.15

12.15*. A perfectly conducting, cylindrical pot contains a perfectly conducting fluid. A center coaxial post is placed inside the cylinder. A current source is attached between the center post and the outer wall of the pot to cause a current to flow on the perfectly conducting surfaces, as shown in Fig. 12P.15a. When the current source is turned off, the fluid comes to rest with its surface at $x = a$. When the current source is turned on, the magnetic field pressure (normal surface traction) causes the surface to deform (e.g. as shown).

* Colgate, Furth, and Halliday, *Rev. Mod. Phys.*, **32**, No. 4, 744 (1960).

(a) At any typical point on the surface (θ-direction symmetry exists; see Fig. 12P.15b), the normal traction on the surface can be found by using the Maxwell Stress Tensor and a coordinate system arranged for the sample point, as shown in Fig. 12P.15c. Since the MST result is good for any surface point (r, z), the normal traction is known everywhere as a function of r, the radial position of the surface point. Find the normal traction due to the magnetic field as a function of r.

(b) The hydrostatic pressure of the dense fluid varies appreciably with z, due to gravity, whereas the pressure of the light gas (air) may be assumed to be p_0 (atmospheric) everywhere. Using the fact that the forces acting normal to the fluid-air interface must balance, find an equation for the surface. Neglect surface tension and call the top point on the surface $z = z_0$, $r = R_0$. *Hint*. Remember that at $z = z_0$, $r = R_0$, *the magnetic traction* $+ p_0$ *exists on the air side of the* interface and is counterbalanced by the hydrostatic pressure on the fluid side of the interface. No magnetic field exists in the fluid; hydrostatic pressure exerts a normal force on the interface.

(c) In part (b) the value of z_0 remains unknown. Because the total mass of the fluid (or volume for an incompressible fluid) must be conserved, *set up* an expression that will determine z_0. Integration need not be carried out.

12.16. The MHD machine for which dimensions and parameters are defined in Fig. 12P.16 can be assumed to operate with incompressible, uniform flow velocity v in the z-direction. The fluid has constant, scalar conductivity. There is a uniform applied flux density B in the
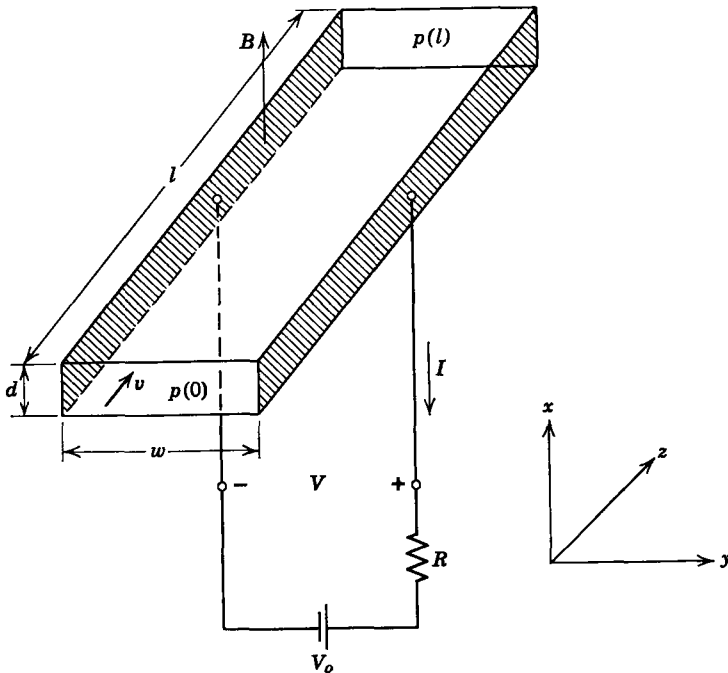
Fig. 12P.16

x-direction and the magnetic field due to current through the fluid may be neglected. The electrical terminals are connected to a battery of constant voltage V_0 and a constant resistance R in series. For steady-state operation calculate and sketch the electric power out of the generator $P_e = VI$ and the mechanical power into the generator $P_m = [p(0) - p(l)]wdv$ as functions of the fluid velocity v. Specify the range of velocity over which the system operates as a generator, pump, and brake.

12.17. From a conformal-mapping analysis of end effects in an MHD generator,[*] for a generator having

        channel width w,   channel depth d,
        electrode length l,   uniform velocity v_0,
        fluid conductivity σ,   flux density B_0 over length of electrodes,

the electrical output power is

$$P_{\text{out}} = \frac{1}{R_i}(V_{\text{oc}} - V)V - \frac{1}{R_i}aV^2,$$

where

$$R_i = \frac{w}{\sigma l d},$$

$$V_{\text{oc}} = v_0 B_0 w,$$

$$a = \frac{2}{\pi}\left(\frac{w}{l}\right)\ln 2$$

$$V = \text{terminal voltage.}$$

(a) Show that the mechanical power input is given by

$$P_m = \int_0^l \int_0^w dJ_y B_0\, dy\, dz = \frac{1}{R_i}(V_{\text{oc}} - V)V_{\text{oc}}$$

by direct integration. *Note.* All that is needed for this integration is the facts that $\mathbf{E} = -\nabla\phi$ and the difference in potential between the electrodes is V.

(b) Defining efficiency as $\eta = P_{\text{out}}/P_m$, find the efficiency at maximum power output and the maximum efficiency and plot them as functions of $1/a$ for $0 < 1/a < 10$.

12.18. For the MHD machine with solid electrodes, for which parameters, dimensions, and variables are defined in Fig. 12P.18a, assume that the fluid is incompressible, inviscid, and has a constant, scalar conductivity σ. Neglect the magnetic field due to current in the fluid. The source that supplies the pressure $\Delta p = p_i - p_o$ has the linear characteristic $\Delta p = \Delta p_0(1 - v/v_o)$, where Δp_0 and v_o are positive constants. The machine with this mechanical source can be represented electrically by the equivalent circuit of Fig. 12P.18b. Find the open-circuit voltage V_{oc} and the internal resistance R_i' in terms of the given data.

---

[*] G. W. Sutton and A. Sherman, *Engineering Magnetohydrodynamics*, McGraw-Hill, New York, 1965, Section 14.6.1.

(a)

(b)
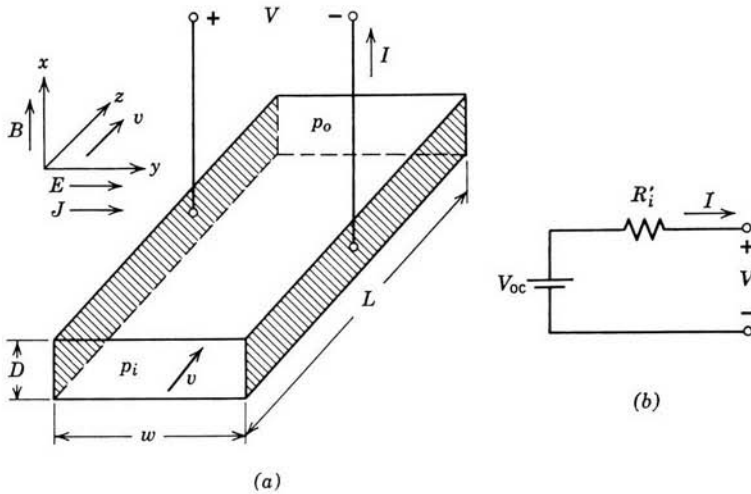
Fig. 12P.18

12.19. An MHD conduction generator has the configuration and dimensions defined in Fig. 12P.19. The fluid is inviscid, has conductivity σ, and is flowing with a uniform, constant velocity v in the x-direction. The field intensity H_o, in the y-direction, is produced by the system shown, which consists of a magnetic yoke with two windings; one (N_o) carries a constant current I_o and the other (N_L) carries the load current I_L. The resistance of winding N_L, fringing effects at the ends and sides of the channel, and the magnetic field due to current in the fluid may be neglected (the magnetic Reynolds number based on length l is small). For steady-state operating conditions find the number of turns N_L necessary to make the terminal voltage V_L independent of load current I_L.

System has length l perpendicular to the paper
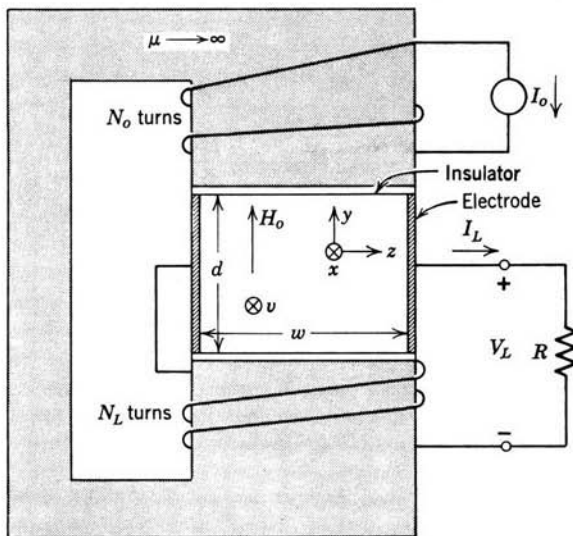
Fig. 12P.19
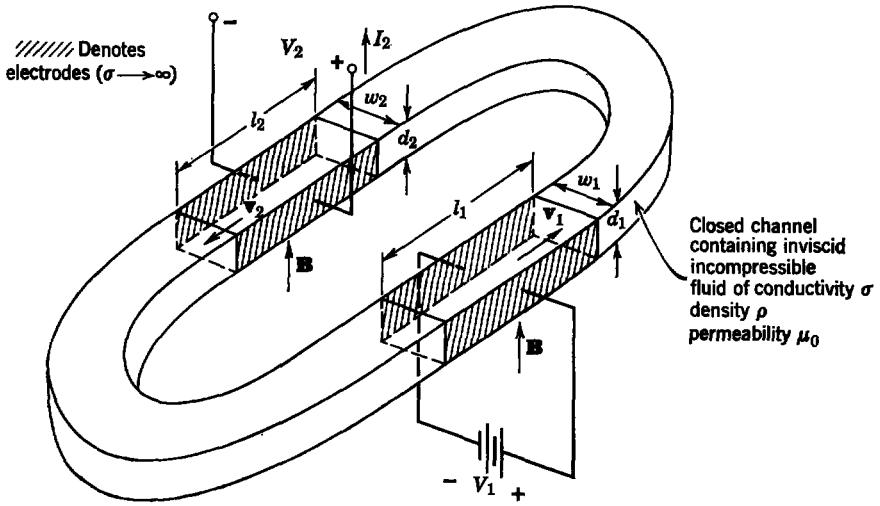
Fig. 12P.20

12.20. A dc transformer is to be made by using a closed channel of incompressible, inviscid fluid of conductivity σ, permeability μ_0 and density ρ, and two MHD conduction machines, as illustrated in Fig. 12P.20. Both machines have the same applied uniform flux density **B**, but their dimensions are different, as indicated. Make the usual assumptions of uniform velocity in the machines, neglect the magnetic fields induced by current in the fluid, and neglect end and edge effects and fringing. For steady-state conditions find a relation between V_2 and I_2 in terms of input voltage V_1, conductivity σ, and the dimensions. Draw the Thevenin equivalent circuit this relation implies.

12.21. A conducting liquid flows with a constant velocity v in the closed channel shown in Fig. 12P.21. The motion is produced by an MHD pump which provides a pressure rise
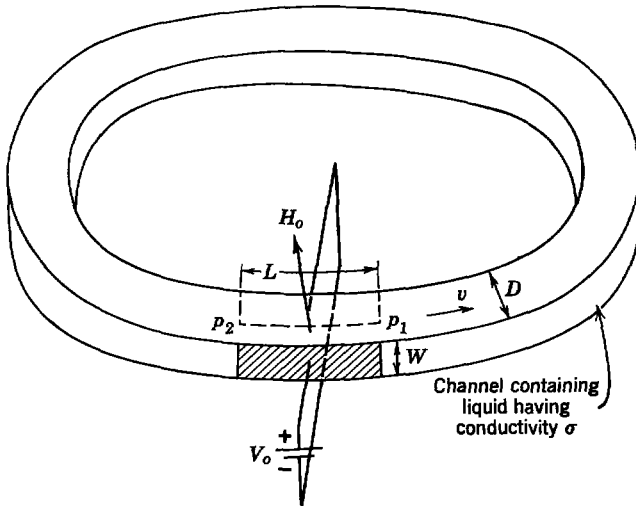
Fig. 12P.21

$p_1 - p_2 > 0$ where p_1 and p_2 are the outlet and inlet pressures. The fluid, as it flows through the remainder of the channel, undergoes the pressure drop $p_1 - p_2 = kv$, where k is a known constant. Determine the velocity v in terms of the imposed magnetic field H_o and the other constants of the system.

12.22. The rectangular channel with the dimensions shown in Fig. 12P.22 is to be used in an MHD pump for a highly conducting liquid of conductivity σ. The channel has two sides which are perfectly conducting electrodes, and an electrical circuit is connected to them. An
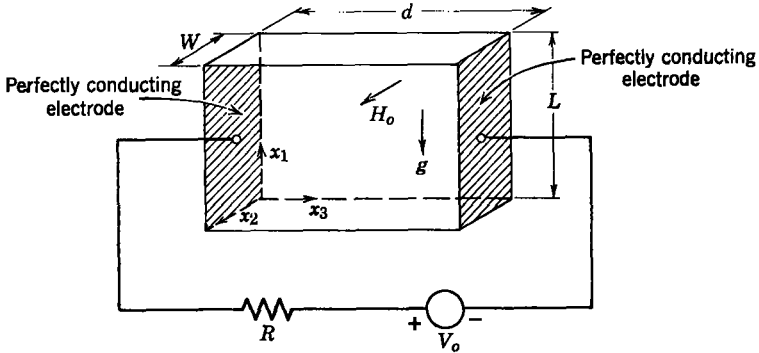
Fig. 12P.22

external magnet produces a constant magnetic field H_o in the x_2-direction. The device is to pump against a gravitational field (which is in the $(-x_1)$-direction):

(a) What range of values for the voltage source V_o will make the liquid flow upward in the $+x_1$-direction? Assume that the pressure at $x_1 = 0$ is the same as the pressure at $x_1 = L$.

(b) Under the conditions of part (a) show clearly that the voltage source is supplying power to the liquid.

12.23. Two large reservoirs of water are connected by a large duct, as shown in Fig. 12P.23a. Over a length l of this duct the walls are highly conducting electrodes short-circuited together by an external circuit, as shown in Fig. 12P.23b. A uniform, constant magnetic field B_o is imposed perpendicular to the direction of flow. Because the water has a conductivity σ, there is a current through the water between the electrodes. Assume that the reservoirs are so large that h_1 and h_2 remain constant and that the fluid is incompressible and inviscid. What is the velocity v of the fluid between the electrodes?

Fig. 12P.23 (a)

Fig. 12P.23 (b)

Area A

L_1

L_o

Valve

Generator
(see details below)

Generator details

Magnetic pole
piece
N

Highly
conducting
electrodes

H_o D

W

Insulating
walls

S
Magnetic pole
piece

R

End view

Magnetic pole
piece
N

L_o

S
Magnetic pole
piece

Side view
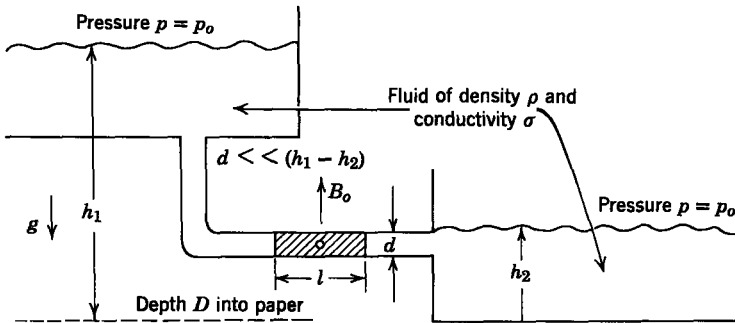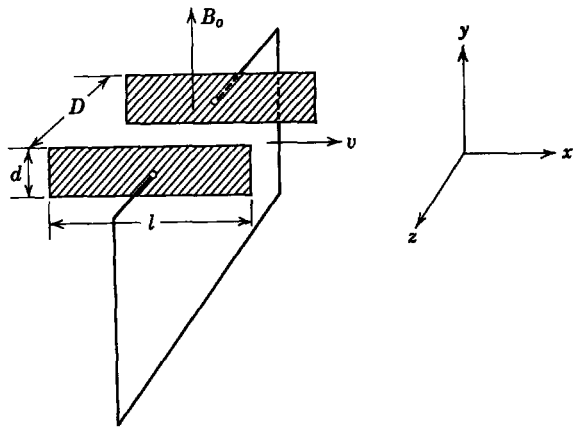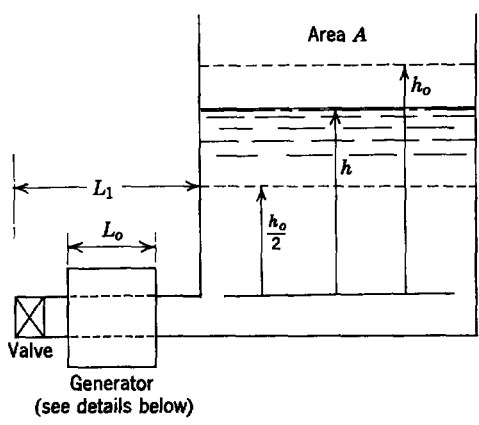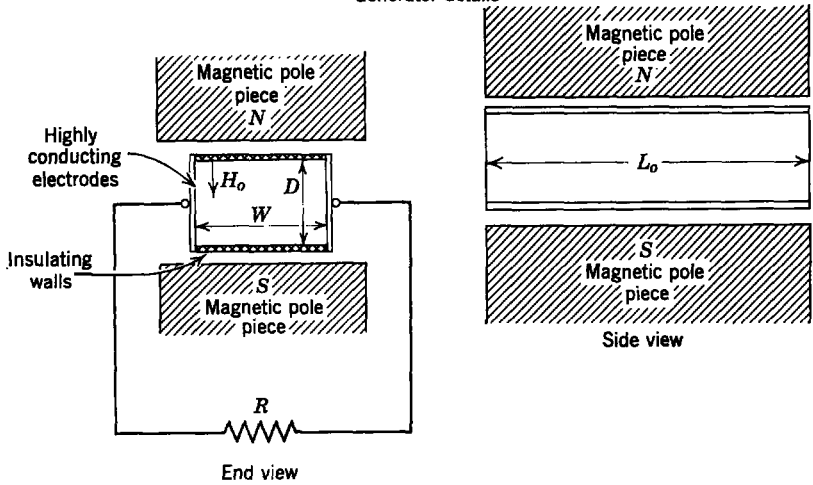
Fig. 12P.24

12.24. The system shown in Fig. 12P.24 consists of a storage tank of horizontal cross-sectional area A, open to the atmosphere at the top, and an MHD generator through which fluid stored in the tank can flow to atmospheric pressure. The generator is loaded by resistance R as shown. The tank is initially filled to a height h_o with mercury. At $t = 0$ the valve is opened to allow mercury to discharge through the generator. When the height has decreased to $h_o/2$ the valve is closed again. Do the following calculations, using the numerical data given below. Make any approximations that are justified by the numerical data. Assume all flow to be incompressible ($\nabla \cdot \mathbf{v} = 0$) and irrotational ($\nabla \times \mathbf{v} = 0$).

(a) Calculate the height h of mercury in the tank as a function of time.
(b) Calculate the current in the load resistance R as a function of time.

Numerical Data

	Mercury		Generator
Density:	1.35×10^4 kg/m^3		$H_o = 1.6 \times 10^5$ A/m
			$D = 0.1$ m
Conductivity:	10^6 mhos/m		$W = 0.2$ m
			$L_o = 1$ m
	Tank Dimensions		$L_1 = 2$ m
	$A = 100$ m^2		$R = 2 \times 10^{-5}$ Ω
	$h_o = 10$ m		Acceleration of Gravity
			$g = 9.8$ m/sec^2

12.25. A simple, bulk-coupled MHD system is used to pump mercury from one storage tank to another, as shown in Fig. 12P.25a. Figure 12P.25b shows the details of the MHD system. The MHD system is driven with a voltage source V_o in series with a resistance R.

Each storage tank has area A and is open to atmospheric pressure at the top. Consider all flow to be incompressible and irrotational ($\nabla \cdot \mathbf{v} = 0$ and $\nabla \times \mathbf{v} = 0$). Use the following numerical data for your solutions.

	Mercury		MHD System
Density:	1.35×10^4 kg/m^3		$H_o = 5 \times 10^5$ A/m
Conductivity:	10^6 mhos/m		$D = 0.01$ m
			$W = 0.02$ m
Tank Area:	$A = 0.1$ m^2		$L_1 = 0.1$ m
Acceleration of Gravity:	$g = 9.8$ m/sec^2		$L_2 = 1.9$ m
			$R = 10^{-5}$ Ω

(a) What voltage V_o is required to maintain the levels in the tanks $h_1 = 0.4$ m and $h_2 = 0.5$ m. How much current and power does the voltage source supply in this case?
(b) With the equilibrium conditions of (a) established, the voltage V_o is doubled at $t = 0$. Find $h_2(t)$ and the source current $i(t)$ for $t > 0$. Sketch and label curves of these time functions. To solve this problem exactly it is necessary to know the three-dimensional flow pattern in the tanks. For this problem, however, it is sufficient to make the following approximations. In writing dynamical equations neglect the acceleration of the fluid in the tanks compared with the acceleration of the fluid in the pipe. Be sure to estimate the error caused by making this assumption *after* the solution has been completed. Also neglect the magnetic field due to current in the mercury.
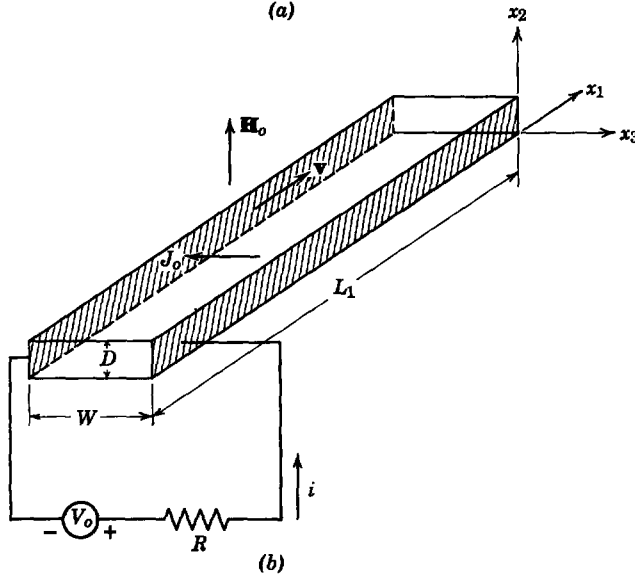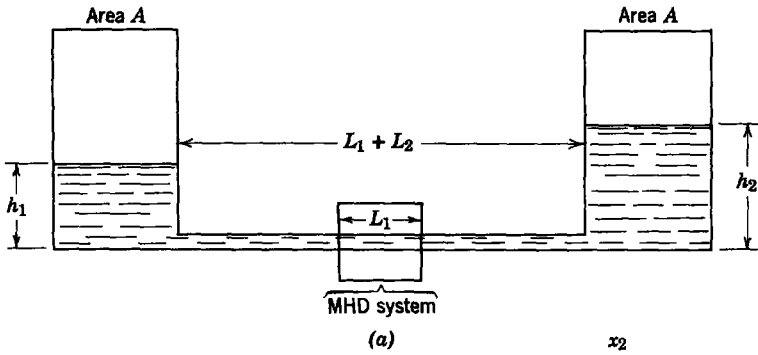
Fig. 12P.25

12.26. Figure 12P.26 shows schematically an ac, series-excited, liquid metal conduction pump. The liquid metal has mass density ρ and electrical conductivity σ. The excitation winding has N turns ($N \gg 1$) and the magnetic path is closed externally by infinitely permeable, nonconducting magnetic material. The dimensions are given in the figure. The electrical terminals are driven by an alternating current source: $i(t) = I \sin \omega t$, where I and ω are positive constants. The pump works against a velocity dependent pressure rise $p(l) - p(0) = \Delta p_0(v/v_0)$, where Δp_0 and v_0 are positive constants. For steady-state operation complete the following:

(a) Find the velocity v as a function of time.
(b) Evaluate the ratio of the amplitudes of the ac and dc components of velocity.
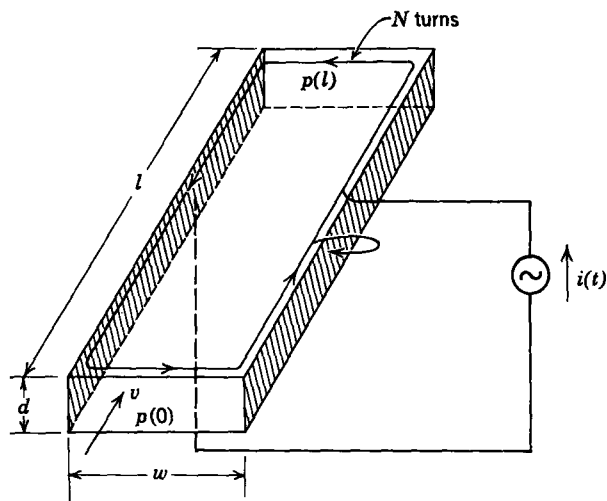
Fig. 12P.26

12.27. A pair of magnetohydrodynamic conduction generators is shown in Fig. 12P.27. In each generator a conducting fluid flows through a channel of width w and height a with approximately uniform constant velocity V. A magnetic field is applied to each generator by means of a magnetic circuit that produces (approximately) a uniform magnetic field in the vertical direction. The magnetic circuits can be considered as having infinite permeability with all the drop in mmf across the channels. Currents are passed through the channels by means of highly conducting electrodes of height a and length b, as shown in Fig. 12P.27. The current i_1 (amperes) through the left generator is used to produce a magnetic field in the left generator and in the right generator, as shown, and to deliver power to the load R_L. The current i_2 through the right generator follows a similar path, except that the turns N and N_m have different directions. We wish to establish the dynamics that would be expected for two generators interconnected in this way, with the objective of producing ac rather than dc power delivered to the loads R_L.

 (a) Find the pair of ordinary differential equations in $i_1(t)$ and $i_2(t)$ that defines the system dynamics under the given conditions.

 (b) Determine the condition, in terms of the given system parameters, that the generators be stable.

 (c) Under what condition will the system operate in the sinusoidal steady state? Given that $R_L = 0$, $\sigma = 50$ mhos/m, $V = 4000$ m/sec, and $N = 1$ turn, what is the length b required to meet this condition?

 (d) Compute the frequency at which the system will operate in the sinusoidal steady state under the above conditions, given that $N_m = 1$ turn.

12.28. The system shown in Fig. 12P.28 has been proposed for an ac, self-excited, MHD power generator. It consists of a *single* channel with length l, width D, and height W, through which an incompressible, inviscid, highly conducting liquid with conductivity σ and permeability μ_0 flows. The velocity of the liquid *is constrained* externally to be a *constant* and always in the x_1-direction; that is, $\mathbf{v} = V\mathbf{1}_1$ everywhere in the channel. (The scalar V is a known fixed constant.) The sides of the channel at $x_2 = 0$ and $x_2 = W$ are insulating, but the other two sides, namely those at $x_3 = 0$ and $x_3 = D$, are perfectly conducting electrodes.
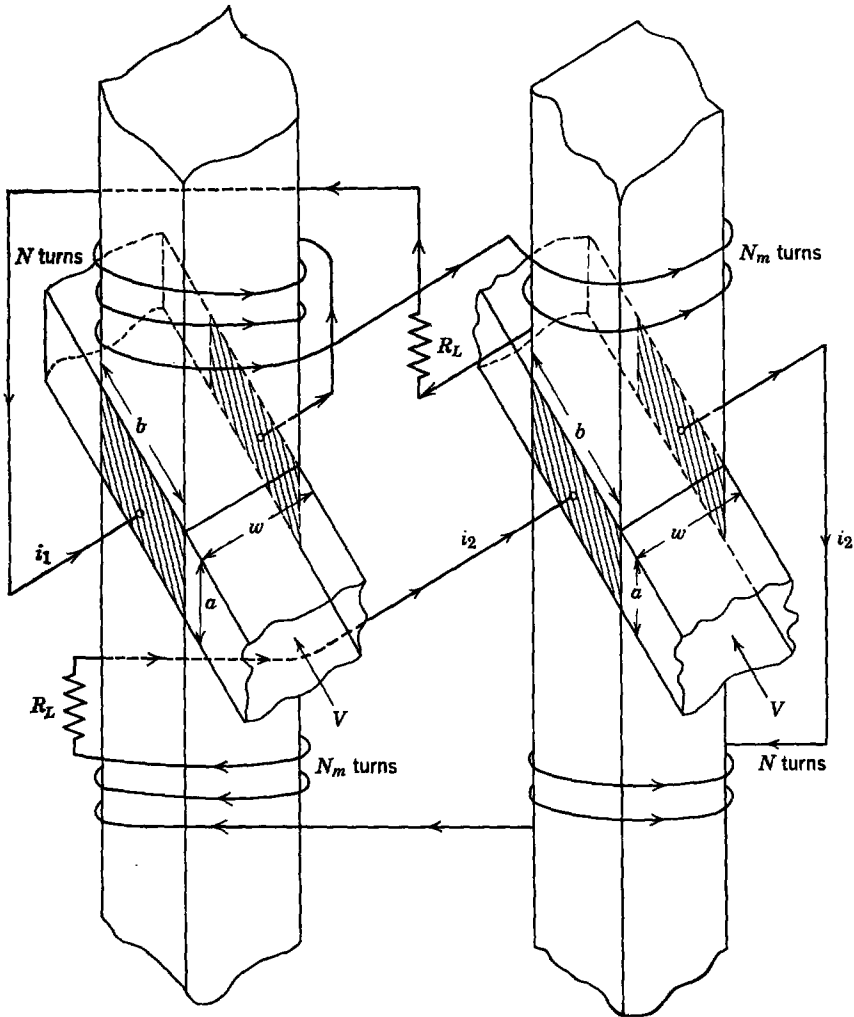
Fig. 12P.27

An external circuit connected to the electrodes consists of three elements in series. The first two elements are a load resistance R_L and a capacitance C. The last element is a *lossless* coil of N turns which is wound on the top ($x_2 = W$) surface of the channel to produce a *uniform* x_2-directed magnetic field everywhere in the channel. (Reasonable assumptions may be made about this field; namely, that it is equivalent to the field produced as if the N turns were distributed uniformly through the depth W of the channel but on the outer perimeter of the channel.)

    (a) Find the value of the load resistance R_L that will make the device act as an ac generator (so that the current i is a pure sinusoid). Note that ac power will then be continuously dissipated in the load resistance R_L.

    (b) What is the frequency of the resulting sinusoid of part (a)?
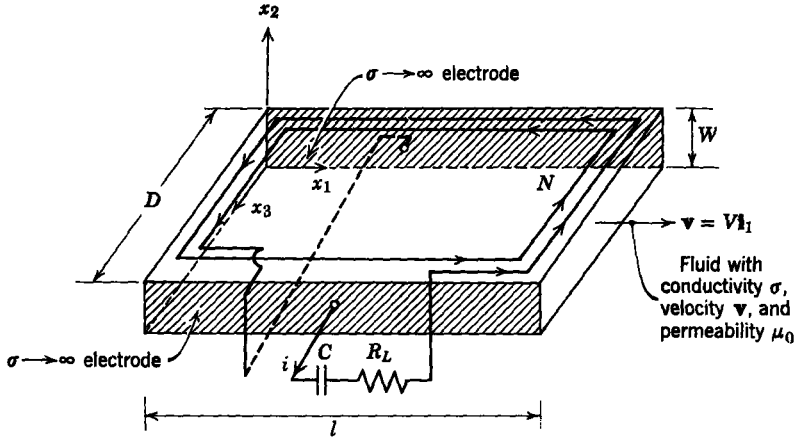
Fig. 12P.28

12.29. The MHD generator of Fig. 12P.29 has a channel of length l, width w, and depth d. An external system not shown establishes the magnetic flux density $\mathbf{B}_o = \mathbf{i}_x B_o$. Two equal resistances of $R\ \Omega$ each are connected in series between the electrodes, with a switch S in parallel with one resistance. The channel contains an inviscid, incompressible fluid of mass density ρ flowing under the influence of a pressure difference $\Delta p = p_i - p_o$, which is positive and maintained constant by external means. The fluid has an electrical conductivity σ and the magnetic field due to current flow in the fluid can be neglected.
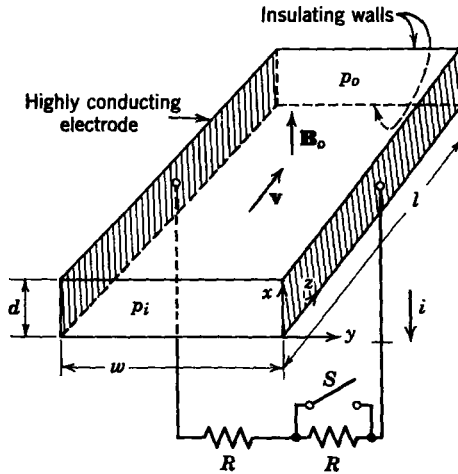
Fig. 12P.29

(a) For steady-state conditions with switch S open, find the velocity v and load current i in terms of given data.

(b) With the system operating in the steady state as defined in part (a), the switch S is closed at $t = 0$. Find the velocity v and load current i as functions of the given data and time for $t > 0$.

12.30. This problem concerns the self-excitation of a dc generator. The variables and dimensions are given in Fig. 12P.30. The channel has a constant cross-sectional area, the fluid is incompressible and inviscid, and the conductivity is constant and scalar. Assume
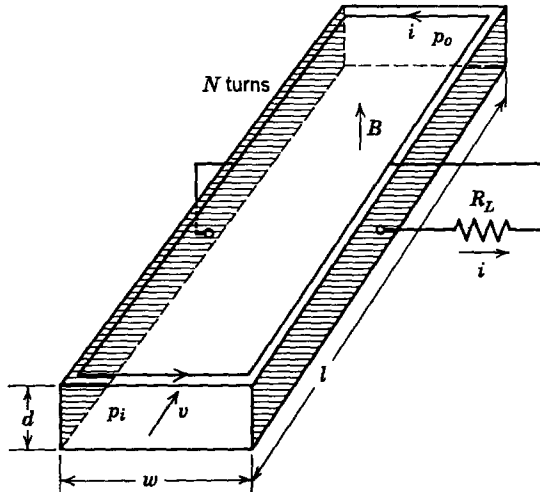
Fig. 12P.30

that the magnetic circuit is closed outside the channel with infinitely permeable iron. The mechanical source providing power has the pressure-velocity characteristic $\Delta p = p_i - p_o = \Delta p_o(1 - v/v_o)$, where Δp_o and v_o are positive constants. The volume, geometry, and space factor of the field winding are constants so that the field coil resistance varies as the square of the number of turns $R_c = N^2 R_{co}$. The numerical constants of the system are

$$\Delta p_o = 2 \times 10^5 \ n/m^2 \qquad v_o = 10^3 \ m/sec \qquad d = 0.2 \ m$$
$$l = 2 \ m \qquad w = 0.4 \ m \qquad R_L = 2.5 \times 10^{-2} \ \Omega$$
$$\sigma = 40 \ mhos/m \qquad R_{co} = 10^{-6} \ \Omega$$

(a) Find the number of turns necessary to produce a load power in R_L of 1.5×10^6 W. If there is more than one solution, pick the most efficient.

(b) For the number of turns in part (a), find the start up transient in current and plot it as a function of time. Assume an initial current of 10 A, provided by external means.

(c) For the number of turns found in part (a) find the steady-state load power as a function of R_L. Plot the curve.

12.31. The system of Fig. 12P.31 represents an MHD transverse-current generator with continuous electrodes. We make the usual assumptions about incompressible, inviscid, uniform flow. The fluid has mass density ρ and conductivity σ. The pressure drop along the
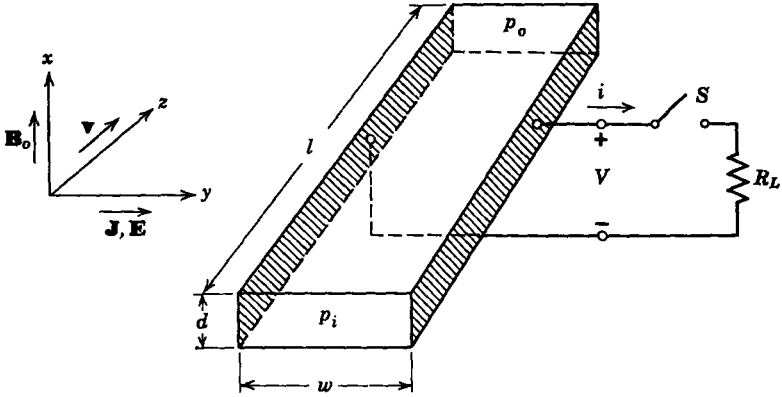
Fig. 12P.31

length of the channel is constrained by a mechanical source to be

$$p_i - p_o = \Delta p = \Delta p_0\left(1 - \frac{v}{v_0}\right),$$

where Δp_0 and v_0 are positive constants. The flux density B_0 is uniform and constant and is supplied by a system not shown. Neglect the magnetic field due to current in the fluid. The switch S is open initially and the system is in the steady state:

    (a) Find the terminal voltage V.

    (b) At $t = 0$ switch S is closed. Find and sketch the ensuing transients in fluid velocity and load current.
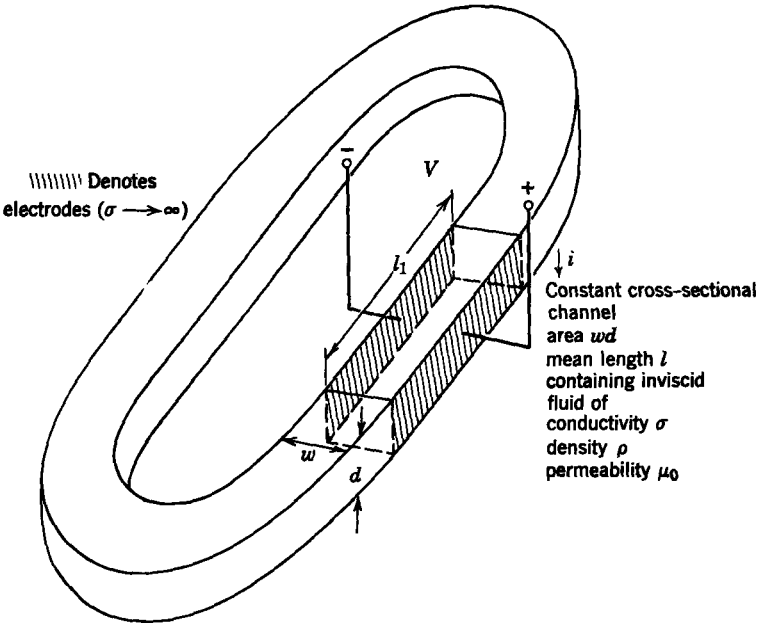
Fig. 12P.32

12.32. An energy storage element is to be made by using a closed channel of incompressible inviscid fluid of conductivity σ, permeability μ_0, and mass density ρ, with an MHD conduction machine for coupling (Fig. 12P.32). The channel has constant cross-sectional area wd and mean length l and the radius of the bends is large compared with the channel width w. The flux density $\mathbf{B}$ is supplied by a system not shown. Assume that the velocity is uniform across the channel and neglect end and edge effects and the magnetic field induced by current in the fluid. Find an equivalent electric circuit as seen from the electrical terminals and evaluate the circuit parameters.

12.33. In the system of Fig. 12P.33 an MHD generator is to be used to charge a capacitor. The MHD generator has a channel of constant cross-sectional area with the dimensions and arrangements shown in Fig. 12P.33. The working fluid has electrical conductivity σ and is incompressible and inviscid; it is constrained by external means to flow through the channel with a constant velocity v_0 that is uniform across the cross section. The constant uniform flux density B_0 is established by an external magnet not shown. Neglect the magnetic field due to current in the fluid and neglect fringing effects at the ends.

  (a) Find the capacitor voltage V_c as a function of time and evaluate the final energy stored in capacitance C.
  (b) Find the pressure difference supplied by the fluid source as a function of time and evaluate the total energy supplied by the fluid source.
  (c) Account for the difference between your answers for energy in parts (a) and (b).
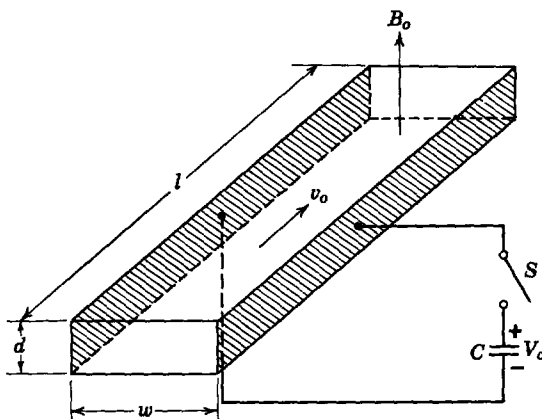
Fig. 12P.33

12.34. This problem is similar to the example worked in Section 12.2.1b. A U-tube of constant, rectangular cross section contains an inviscid, incompressible conducting fluid of mass density ρ and conductivity σ. The fluid has a total length l between the two surfaces which are open to atmospheric pressure as illustrated in Fig. 12P.34a. A conduction type MHD machine of length l_1 is inserted at the bottom of the U-tube. The details of the MHD channel are illustrated in Fig. 12P.34b. Neglect end effects and the magnetic field due to current flow in the fluid. The system parameters are

$$l = 1 \text{ m}, \qquad l_1 = 0.1 \text{ m}, \qquad w = 0.01 \text{ m}, \qquad d = 0.01 \text{ m},$$
$$B_0 = 2 \text{ Wb/m}^2, \qquad V = 0.001 \text{ V}, \qquad g = 9.8 \text{ m/sec}^2.$$

The fluid is mercury with constants $\sigma = 10^6$ mhos/m, $\rho = 1.36 \times 10^4$ kg/m^3. With the system in equilibrium, with switch S open, $x_a = x_b = 0$; switch S is closed at $t = 0$. Calculate the ensuing transients in fluid position x_a and electrode current i. Sketch and label curves of these transients.
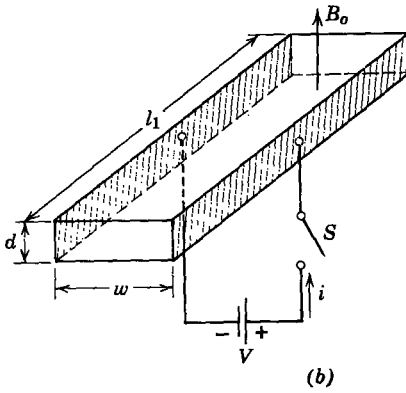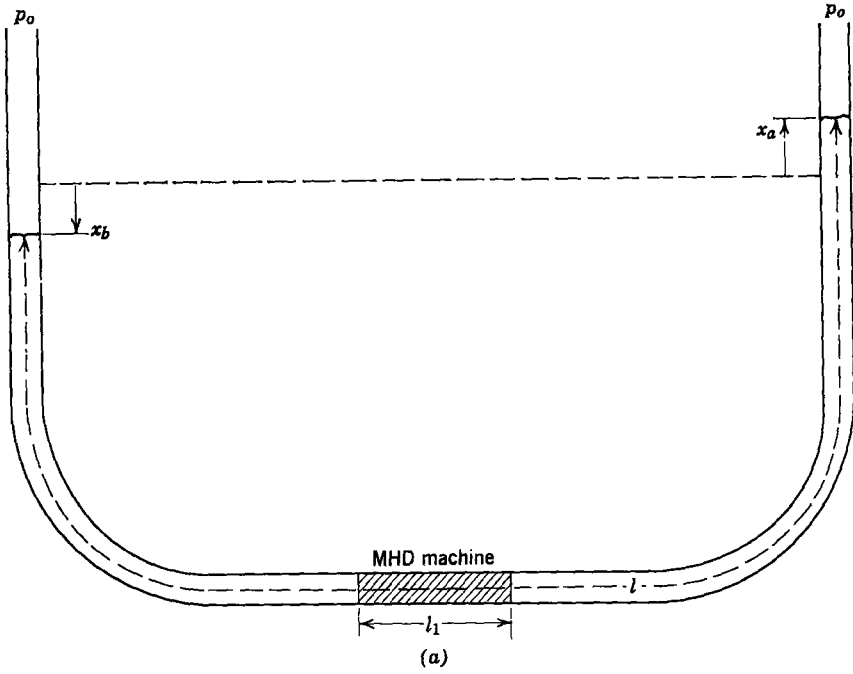
Fig. 12P.34

12.35. An incompressible inviscid conducting liquid fills the conduit shown in Fig. 12P.35. A current density J_o (known constant) flows through the fluid over a length L of the channel. This section of the fluid is also subjected to a magnetic field produced by a magnetic circuit. (The gap D is the only portion of the circuit where $\mu \neq \infty$.) This magnetic field is produced by two N turn coils wound as shown. The liquid has two free surfaces denoted by x and y. When the fluid is stationary, $x = L/2$ and $y = L/2$. In the regions of the free surfaces, electrodes carrying the currents I_1 and I_2 are arranged as shown. It is seen that the resistance

Fig. 12P.35

of the circuits is related to the heights of the interfaces. Find an equation for $x(t)$ that describes the system. Specifically, when $t = 0$, $x = L$, and $dx/dt = 0$, what is $x(t)$?

Assumptions

    (a) v is directed along the channel and is independent of cross-sectional position.

    (b) Ignore $L(dI_1/dt)$ and $L(dI_2/dt)$ (the rates of change with time are slow because of the fluid inertia).

    (c) Ignore the magnetic field produced by J_o.

12.36. Rework the Alfvén-wave problem in cylindrical geometry in Section 12.2.3 with the following change in the boundary condition at $z = 0$. The end of the tube at $z = 0$ is fixed, rigid, and perfectly conducting. Your answer should consist of solutions for v_θ, B_θ, J_z, and J_r which are similar to (12.2.121)–(12.2.124). The functional dependences on z will be different in your answer because of the different boundary conditions.

12.37. A perfectly conducting inviscid fluid is bounded on the right by a perfectly conducting rigid wall, as shown in Fig. 12P.37. On the left a perfectly conducting plate also makes electrical contact with the liquid while being forced to execute an oscillatory motion in the x-direction. The system is immersed in a magnetic field so that when there are no motions $\mathbf{B} = B_0 \mathbf{i}_z$, where B_0 is a constant.

Oscillating
perfectly
conducting
plate

Rigid perfectly
conducting wall

B_o

Inviscid incompressible
perfectly conducting
fluid; $\mu = \mu_0$

$\sigma \longrightarrow \infty$

$v_x(-l,\, t) = \text{Re } Ve^{j\omega t}$

$\longrightarrow z$

$\dfrac{\partial}{\partial x} = \dfrac{\partial}{\partial y} = 0$

l

Fig. 12P.37

(a) Find the equations of motion, which together predict the transverse fluid velocity $v_x(z, t)$ and field intensity $H_x(z, t)$.

(b) Use appropriate boundary conditions to find $H_x(z, t)$ in the sinusoidal steady state.

(c) Compute the current density implied by (b). If you were to do this experiment, how would you construct the walls of the container that are parallel to the x-z plane? Explain in words why the fluid can transmit shearing motions even though it lacks viscosity.

Chapter 13

ELECTROMECHANICS
OF COMPRESSIBLE,
INVISCID FLUIDS

13.0 INTRODUCTION

In this chapter we introduce the additional law (conservation of energy) and constituent relations necessary to describe mathematically a compressible, inviscid fluid. This more general model is then used to study electromechanical interactions. Attention is focused on the effects of compressibility on the MHD machine analyzed in Chapter 12 and on how magnetic fields can affect the propagation of longitudinal disturbances (sound waves) in a compressible fluid.

13.1 INVISCID, COMPRESSIBLE FLUIDS

Cases of electromechanical coupling with fluids that have appreciable compressibility are found in MHD systems which use ionized gases as working fluids. We have chosen a perfect gas as our model of a compressible fluid. Although alternative models can be used, the principal phenomena that we shall study also occur in systems for which other models are appropriate.

It is a well-known fact that when work is done to compress a gas the temperature increases. This is an indication that the mechanical work of compression has been stored as internal (thermal) energy in the gas. The strong coupling between thermal and mechanical energy in a gas will necessitate the inclusion of the conservation of energy as one of the fundamental equations; and it will also require that we specify thermal and mechanical equations of state as constituent relations for the fluid.

The compressible fluids we deal with will obey the conservation of mass as

derived and discussed in Section 12.1.2. The differential form of the conservation of mass is (12.1.11)

$$\frac{D\rho}{Dt} = -\rho(\nabla \cdot \mathbf{v}), \qquad (13.1.1)$$

where (D/Dt) is the substantial derivative defined in (12.1.5)

$$\frac{D}{Dt} = \frac{\partial}{\partial t} + (\mathbf{v} \cdot \nabla). \qquad (13.1.2)$$

The integral form expressing conservation of mass is (12.1.8)

$$\oint_S (\rho \mathbf{v} \cdot \mathbf{n}) \, da = -\frac{d}{dt} \int_V \rho \, dV. \qquad (13.1.3)$$

The surface S encloses the volume V and $\mathbf{n}$ is the outward-directed unit normal vector.

The derivation of the conservation of momentum (Newton's second law) in Section 12.1.3 was done without assuming that the mass density ρ was constant. Consequently, the resulting equations are equally applicable to compressible fluids. The differential form of the momentum equation is (12.1.14)

$$\rho \frac{D\mathbf{v}}{Dt} = \mathbf{F}, \qquad (13.1.4)$$

where $\mathbf{F}$ is the force density applied to the fluid by all sources—mechanical, gravity, and electrical. The integral form of the momentum equation is (12.1.29)

$$\int_V \frac{\partial(\rho\mathbf{v})}{\partial t} \, dV + \oint_S \rho\mathbf{v}(\mathbf{v} \cdot \mathbf{n}) \, da = \int_V \mathbf{F} \, dV, \qquad (13.1.5)$$

where the surface S encloses the volume V and $\mathbf{n}$ is the outward-directed unit normal vector.

After deriving the conservation of energy equation for a compressible fluid, we describe the appropriate constituent relations. These equations, along with the conservation of mass, the conservation of momentum, and appropriate boundary conditions, will allow us to solve problems in which there is electromechanical coupling with compressible fluids.

13.1.1 Conservation of Energy

In accounting for the conservation of energy we are concerned only with thermal and mechanical energy storage in a fluid. There will be energy input to the fluid from electromechanical conversion. The Poynting theorem can be written as a separate electromagnetic energy conservation equation; in

this system, however, which is quasi-static electromagnetically, this is unnecessary.

When a fluid is in motion, its kinetic energy density (joules per cubic meter) is $\frac{1}{2}\rho v^2$ and its kinetic energy per unit mass (joules per kilogram) is $\frac{1}{2}v^2$. This kinetic energy represents energy storage in the ordered or average motion of fluid particles. In a gas the particles also have random motion. The kinetic energy stored because of random motion is called thermal or internal energy. The internal energy per unit mass (joules/kilogram) is designated as u. The internal energy, like the velocity $\mathbf{v}$, is an Eulerian variable; thus the internal energy of the fluid in the vicinity of a point is specified by the value of u at that point. The internal energy density (joules per cubic meter) is ρu. The total energy per unit mass (kinetic and thermal) of the fluid at a point is $(u + \frac{1}{2}v^2)$; the energy density at any point in space is $\rho(u + \frac{1}{2}v^2)$.

Consider now a volume V enclosed by the surface S with outward-directed unit normal vector $\mathbf{n}$. The conservation of energy for the fluid within the volume is written

$$\int_V \frac{\partial}{\partial t}\, \rho(u + \tfrac{1}{2}v^2)\, dV + \oint_S \rho(u + \tfrac{1}{2}v^2)\mathbf{v} \cdot \mathbf{n}\, da = [\text{power input to fluid}].$$

(13.1.6)

The first term on the left specifies the time rate of increase of energy stored by thermal and kinetic energy in the fluid that occupies the volume V at the instant of time in question. The second term on the left specifies the rate at which thermal and kinetic energy is transported across the surface S and out of the volume V. Thus the left side of (13.1.6) represents the energy that must be supplied by the total power input to the fluid in the volume V. This power input can be supplied by volume force densities, such as those of gravity and of electromagnetic origin, by volume heat generation, such as joule losses (J^2/σ) and viscous losses, by forces due to pressure that do work, and by heat conduction and radiation. An inviscid fluid model is being used, and viscous effects are ignored. Heat conduction and radiation will also be ignored because they have very small effects in practical situations on the electromechanical phenomena to be studied.

Before (13.1.6) can be specified in more detail and before a useful differential form can be obtained it is necessary to use the physical properties of the fluid to describe constituent relations.

13.1.2   Constituent Relations

A homogeneous, isotropic, compressible fluid at rest can sustain no shear stresses. Moreover, an inviscid fluid in motion can sustain no shear stresses.

Consequently, the mechanical stresses transmitted by an inviscid incompressible fluid are always normal and compressive; thus we define a pressure p exactly as we did in Section 12.1.4 with the result that the mechanical stress tensor is (12.1.34)

$$T_{ij}{}^m = -\delta_{ij}p. \tag{13.1.7}$$

The traction applied to a surface whose normal vector is $\mathbf{n}$ (12.1.37) is

$$\boldsymbol{\tau}^m = -p\mathbf{n} \tag{13.1.8}$$

and the mechanical force density (12.1.39) is

$$\mathbf{F}^m = -\nabla p. \tag{13.1.9}$$

We model the compressible fluid as a perfect gas. The mechanical equation of state for a perfect gas is

$$p = \rho RT, \tag{13.1.10}$$

where T is the temperature in degrees Kelvin and R is the gas constant for the particular gas in question with units joules per kilogram-°K. The gas constant R is obtained from the universal gas constant R_g as follows. The universal gas constant is

$$R_g = 8.31 \text{ J/mole-°K}. \tag{13.1.11}$$

The gas constant R in mks units is obtained from

$$R = \frac{R_g}{M}, \tag{13.1.12}$$

where M is the mass of one mole of the gas in kilograms. This is simply the molecular weight multiplied by 10^{-3}; for example, consider Argon, which has a molecular weight of 39.9. The gas constant for Argon is thus

$$R = \frac{8.31}{39.9 \times 10^{-3}} = 208 \text{ J/kg-°K}. \tag{13.1.13}$$

Equation 13.1.10 is conventionally called a mechanical equation of state. Because we must consider internal energy storage in the gas, we must also specify a thermal equation of state that relates the internal energy storage to the variables of the system.* For a perfect gas the internal energy is a function of temperature alone and is conventionally expressed as

$$du = c_v \, dT, \tag{13.1.14}$$

where c_v is the specific heat capacity at constant volume with units joules per kilogram-°K. Equation 13.1.14 is expressed in differential form because,

---

* For a more thorough discussion see, for instance, W. P. Allis and M. A. Herlin, *Thermodynamics and Statistical Mechanics*, McGraw-Hill, New York, 1952, pp. 16–20 and 62–65.

over the range of temperatures of interest to us, c_v can be assumed constant; but over a wider range of temperature c_v is not constant and the variation must be accounted for in evaluating internal energy. Our purpose of examining electromechanical interaction phenomena will be served adequately by assuming that the specific heat capacity is constant.

Another specific heat capacity often useful and that we assume is constant in our treatment is the specific heat capacity at constant pressure c_p, which is related to c_v by the expression

$$c_p = c_v + R. \tag{13.1.15}$$

Yet another useful parameter is the ratio of specific heat capacities

$$\gamma = \frac{c_p}{c_v}. \tag{13.1.16}$$

In the ranges of temperature and pressure and for the gases of interest in this treatment the specific heat capacities vary appreciably but the ratio of specific heat capacities remain essentially constant.* Our assumption that all three parameters are constant is adequate for describing the phenomena resulting from electromechanical interactions.

Now that we have described the physical properties of inviscid, compressible fluids by the constituent relations of (13.1.9), (13.1.10), and (13.1.14) we shall recast the momentum and energy equations in more useful forms. We are concerned primarily with pressure and electromagnetic forces and we neglect the force of gravity.

The use of (13.1.9) for the mechanical force density in (13.1.4) yields the momentum equation in the form

$$\rho \frac{D\mathbf{v}}{Dt} = -\nabla p + \mathbf{F}^e, \tag{13.1.17}$$

where $\mathbf{F}^e$ is the force density of electrical origin. To rewrite the integral form of the momentum equation we use

$$\int_V -\nabla p \, dV = \oint_S -p\mathbf{n} \, da \tag{13.1.18}$$

to write (13.1.5) in the form

$$\int_V \frac{\partial(\rho\mathbf{v})}{\partial t} \, dV + \oint_S \rho\mathbf{v}(\mathbf{v} \cdot \mathbf{n}) \, da = \oint_S -p\mathbf{n} \, da + \int_V \mathbf{F}^e \, dV. \tag{13.1.19}$$

---

* For a thorough discussion of the properties of gases, see, for example, H. B. Callen, *Thermodynamics*, Wiley, New York, 1960, pp. 324–333.

To write the energy equation (13.1.6) in more precise form we must specify the power input to the fluid within the volume V from all sources. Consider first the pressure forces that can be viewed as doing net work only at the surface of the volume V. Thus, because the pressure forces are compressive and normal to any surface, the power input to the fluid from pressure forces is

$$\oint_S -p\mathbf{v} \cdot \mathbf{n} \, da.$$

The use of the divergence theorem allows us to write this quantity as

$$\oint_S -\mathbf{n} \cdot (p\mathbf{v}) \, da = \int_V -\mathbf{\nabla} \cdot (p\mathbf{v}) \, dV. \tag{13.1.20}$$

The electrical power input to the fluid within the volume V is the total rate at which electrical work is done on charged particles. This includes both the work done by electromagnetic forces and the electrical losses due to finite conductivity in the fluid. In all cases the electrical input power density is $\mathbf{J} \cdot \mathbf{E}$ and the total electrical power input is

$$\left[\begin{array}{c}\text{electrical power} \\ \text{input}\end{array}\right] = \int_V \mathbf{J} \cdot \mathbf{E} \, dV. \tag{13.1.21}$$

To interpret $\mathbf{J} \cdot \mathbf{E}$ as the input power density to the moving gas consider first a *magnetic field system* and denote with primes the variables defined in a reference frame fixed with respect to the fluid. Using (6.1.36), (6.1.37), and (6.1.38)*, we write

$$\mathbf{J} \cdot \mathbf{E} = \mathbf{J}' \cdot (\mathbf{E}' - \mathbf{v} \times \mathbf{B}'). \tag{13.1.22}$$

Then from the vector identity

$$\mathbf{J}' \cdot \mathbf{v} \times \mathbf{B}' = -\mathbf{J}' \times \mathbf{B}' \cdot \mathbf{v}$$

it follows that

$$\mathbf{J} \cdot \mathbf{E} = \mathbf{J}' \cdot \mathbf{E}' + \mathbf{J}' \times \mathbf{B}' \cdot \mathbf{v}. \tag{13.1.23}$$

The first term on the right is the electric power density that heats up the fluid. For a linear conductor $\mathbf{J}' = \sigma \mathbf{E}'$ and

$$\mathbf{J}' \cdot \mathbf{E}' = \frac{J'^2}{\sigma}.$$

The second term on the right of (13.1.23) is simply $\mathbf{F}^e \cdot \mathbf{v}$, which is the rate at which the magnetic force density does mechanical work on the fluid.

For an *electric field system* we use (6.1.54), (6.1.56), and (6.1.58)* to write $\mathbf{J} \cdot \mathbf{E}$ in the reference frame of the fluid as

$$\mathbf{J} \cdot \mathbf{E} = (\mathbf{J} + \rho'\mathbf{v}) \cdot \mathbf{E}'. \tag{13.1.24}$$

* See Table 6.1, Appendix G.

Expansion of this expression yields

$$\mathbf{J} \cdot \mathbf{E} = \mathbf{J}' \cdot \mathbf{E}' + \rho' \mathbf{E}' \cdot \mathbf{v}. \tag{13.1.25}$$

The first term on the right is the rate of heating of the fluid and the second term is the rate at which the electric force density $\rho' \mathbf{E}'$ does mechanical work on the fluid.

The use of (13.1.20) and (13.1.21) with (13.1.6) yields

$$\int_V \frac{\partial}{\partial t} [\rho(u + \tfrac{1}{2}v^2)] \, dV + \oint_S \rho(u + \tfrac{1}{2}v^2)\mathbf{v} \cdot \mathbf{n} \, da$$

$$= \int_V -\nabla \cdot (p\mathbf{v}) \, dV + \int_V \mathbf{J} \cdot \mathbf{E} \, dV. \tag{13.1.26}$$

The divergence theorem is used to write

$$\oint_S \rho(u + \tfrac{1}{2}v^2)\mathbf{v} \cdot \mathbf{n} \, da = \int_V \nabla \cdot [\rho(u + \tfrac{1}{2}v^2)\mathbf{v}] \, dV. \tag{13.1.27}$$

Then all terms in (13.1.26) are volume integrals. The volume is arbitrary; thus the equation must hold for the differential volume dV.

$$\frac{\partial}{\partial t} [\rho(u + \tfrac{1}{2}v^2)] + \nabla \cdot [\rho(u + \tfrac{1}{2}v^2)\mathbf{v}] = -\nabla \cdot p\mathbf{v} + \mathbf{J} \cdot \mathbf{E}. \tag{13.1.28}$$

Expansion of the derivatives in the two terms on the left and use of the conservation of mass (13.1.1) yield the simplified result

$$\rho \frac{D}{Dt} (u + \tfrac{1}{2}v^2) = -\nabla \cdot (p\mathbf{v}) + \mathbf{J} \cdot \mathbf{E}. \tag{13.1.29}$$

Equations 13.1.26 and 13.1.29 are convenient forms that express the conservation of energy for time-varying situations. Many important problems involve steady flow, in which case $(\partial/\partial t = 0)$ and (13.1.26) simplifies to

$$\oint_S \rho(u + \tfrac{1}{2}v^2)\mathbf{v} \cdot \mathbf{n} \, da = \int_V -\nabla \cdot (p\mathbf{v}) \, dV + \int_V \mathbf{J} \cdot \mathbf{E} \, dV \tag{13.1.30}$$

and (13.1.29) simplifies to

$$\rho(\mathbf{v} \cdot \nabla)(u + \tfrac{1}{2}v^2) = -\nabla \cdot (p\mathbf{v}) + \mathbf{J} \cdot \mathbf{E}. \tag{13.1.31}$$

This last equation is conventionally written in a different form by expanding the first term on the right

$$\nabla \cdot (p\mathbf{v}) = (\mathbf{v} \cdot \nabla)p + p(\nabla \cdot \mathbf{v}). \tag{13.1.32}$$

The use of the conservation of mass to eliminate $\nabla \cdot \mathbf{v}$ yields

$$\nabla \cdot (p\mathbf{v}) = (\mathbf{v} \cdot \nabla)p - \frac{p}{\rho}(\mathbf{v} \cdot \nabla)\rho. \qquad (13.1.33)$$

Recognizing that

$$(\mathbf{v} \cdot \nabla)\frac{p}{\rho} = \frac{1}{\rho}(\mathbf{v} \cdot \nabla)p - \frac{p}{\rho^2}(\mathbf{v} \cdot \nabla)\rho.$$

We write (13.1.33) in the form

$$\nabla \cdot (p\mathbf{v}) = \rho(\mathbf{v} \cdot \nabla)\frac{p}{\rho}$$

and (13.1.31) becomes

$$\rho(\mathbf{v} \cdot \nabla)\left(u + \frac{p}{\rho} + \tfrac{1}{2}v^2\right) = \mathbf{J} \cdot \mathbf{E}. \qquad (13.1.34)$$

This expression is simplified further by defining the *specific enthalpy h* as

$$h = u + \frac{p}{\rho} = u + RT \qquad (13.1.35)$$

or, in differential form,

$$dh = du + R\,dT = (c_v + R)\,dT = c_p\,dT. \qquad (13.1.36)$$

Thus (13.1.34) is written as

$$\rho(\mathbf{v} \cdot \nabla)(h + \tfrac{1}{2}v^2) = \mathbf{J} \cdot \mathbf{E}. \qquad (13.1.37)$$

This equation is in a form that emphasizes the electromechanical aspects of a problem. It shows that electrical input power goes into enthalpy or kinetic energy in the gas. Thus for steady-flow problems enthalpy plays the role of energy storage in the gas other than kinetic energy.

13.2 ELECTROMECHANICAL COUPLING WITH COMPRESSIBLE FLUIDS

Now that we have completed the description of the mathematical models we shall use for inviscid, compressible fluids, we treat some steady-state and dynamic systems that emphasize the physical consequences of electromechanical coupling. The simplest examples that illustrate the electromechanical aspects of the problems are selected. It should be clear that many other effects will be significant in an engineering system that uses the basic phenomena that we describe. The details of these other effects are outside the scope of this work but they are well-documented in the literature.*

* See, for example, G. W. Sutton and A. Sherman, *Engineering Magnetohydrodynamics*, McGraw-Hill, New York, 1965.
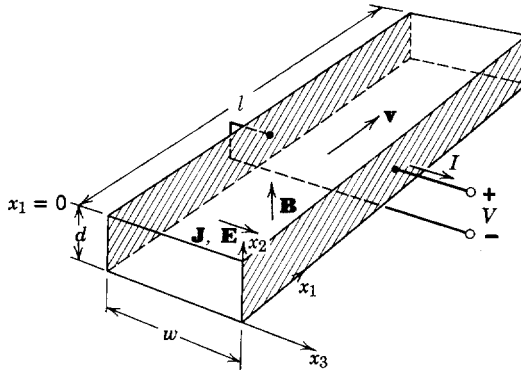
Fig. 13.2.1   A conduction-type MHD machine with constant-area channel.

13.2.1   Coupling with Steady Flow in a Constant-Area Channel

In this section we analyze the system of Fig. 13.2.1 which consists of a channel of constant cross-sectional area through which an electrically conducting gas flows with velocity **v**. The electrical conductivity is high enough to justify a quasi-static magnetic field model. The two walls perpendicular to the x_2-direction are electrical insulators and the two walls perpendicular to the x_3-direction are highly conducting electrodes. A flux density **B** is produced in the x_2-direction by external means not shown. The electrodes are connected to electrical terminals at which a voltage V and current I are defined. Note that this is the same configuration as that in Fig. 12.2.3 which was used in Section 12.2.1a for the analysis of electomechanical coupling with an inviscid, incompressible fluid. Thus the example in this section, when compared with that of Section 12.2.1a, highlights the effects of compressibility on the basic MHD interaction.

We assume that the l/w and l/d ratios of the channel are large enough that we can reasonably neglect end effects. Also it is assumed that the flow velocity is uniform over the cross section of the channel and that the magnetic field induced by current in the fluid is negligible compared with the applied field (low magnetic Reynolds number). Thus the magnetic flux density and electric field intensity are constant and uniform along the length of the channel

$$\mathbf{B} = \mathbf{i}_2 B_2, \tag{13.2.1}$$

$$\mathbf{E} = \mathbf{i}_3 E_3 = -\mathbf{i}_3 \frac{V}{w}, \tag{13.2.2}$$

and the velocity and current density are given by

$$\mathbf{v} = \mathbf{i}_1 v_1, \tag{13.2.3}$$

$$\mathbf{J} = \mathbf{i}_3 J_3. \tag{13.2.4}$$

The velocity v_1, current density J_3, and the gas variables (p, ρ, T) are functions of x_1 but not of x_2 and x_3. We assume that the gas has a constant, scalar electrical conductivity σ and consider only a steady-flow problem.

The equations that describe this essentially one-dimensional problem are obtained by simplifying equations already presented. From (13.1.1) we obtain the equation for the conservation of mass:

$$v_1 \frac{d\rho}{dx_1} + \rho \frac{dv_1}{dx_1} = 0. \tag{13.2.5}$$

The momentum equation is obtained from (13.1.17) with $\mathbf{F}^e = \mathbf{J} \times \mathbf{B}$:

$$\rho v_1 \frac{dv_1}{dx_1} = -\frac{dp}{dx_1} - J_3 B_2. \tag{13.2.6}$$

The conservation of energy (13.1.37) yields

$$\rho v_1 \frac{d}{dx_1} (h + \tfrac{1}{2}v_1{}^2) = J_3 E_3. \tag{13.2.7}$$

The mechanical equation of state (13.1.10) is

$$p = \rho RT \tag{13.2.8}$$

and the thermal equation of state (13.1.36) is

$$dh = c_p \, dT. \tag{13.2.9}$$

Finally, Ohm's law for the moving gas is $\mathbf{J}' = \sigma \mathbf{E}'$ or*

$$J_3 = \sigma(E_3 + v_1 B_2). \tag{13.2.10}$$

In these equations a total space derivative is written because x_1 is the only independent variable.

The six equations (13.2.5) to (13.2.10) have six unknowns $(p, \rho, T, h, v_1, J_3)$ that vary with x_1. These equations are nonlinear and direct integration in a general form is not possible. The usual method of solution is to assume that all of the variables are known at the inlet and then to integrate the equations numerically to find the variables along the length of the channel.

The equations can be put in a form convenient for interpretation and numerical integration by finding *influence coefficients*. This process is one of essentially finding each space derivative as a function of the variables themselves. In the derivation of influence coefficients it is convenient to define the velocity of sound (see Section 13.2.3)

$$a = \sqrt{\gamma RT} \tag{13.2.11}$$

* Table 6.1, Appendix G or Section 6.3.1.

and the Mach number of the flow

$$M = \frac{v_1}{a}. \tag{13.2.12}$$

By manipulating (13.2.5) to (13.2.10) and using (13.2.11), (13.2.12), and the ratio of specific heat capacities γ (13.1.16) we obtain the influence coefficients in these forms

$$\frac{1}{v_1}\frac{dv_1}{dx_1} = -\frac{1}{\rho}\frac{d\rho}{dx_1} = \frac{[(\gamma - 1)E_3 + \gamma v_1 B_2]J_3}{(1 - M^2)\gamma p v_1}, \tag{13.2.13}$$

$$\frac{1}{T}\frac{dT}{dx_1} = \frac{[(1 - \gamma M^2)E_3 - \gamma M^2 v_1 B_2](\gamma - 1)J_3}{(1 - M^2)\gamma p v_1}, \tag{13.2.14}$$

$$\frac{1}{p}\frac{dp}{dx_1} = -\frac{\{(\gamma - 1)M^2 E_3 + [1 + (\gamma - 1)M^2]v_1 B_2\}\gamma J_3}{(1 - M^2)\gamma p v_1}, \tag{13.2.15}$$

$$\frac{1}{M^2}\frac{d(M^2)}{dx_1} = \frac{\{(\gamma - 1)(1 + \gamma M^2)E_3 + \gamma[2 - (\gamma - 1)M^2]v_1 B_2\}J_3}{(1 - M^2)\gamma p v_1}. \tag{13.2.16}$$

We first use these influence coefficients to draw some general conclusions about electromechanical interactions with a conducting gas and then solve a problem in some detail to assess the consequences of compressibility.

First, with reference to Fig. 13.2.1, consider the situation in which the system is acting as a *generator* along the length of the channel. In this case

$$E_3 < 0, \qquad J_3 = \sigma(E_3 + v_1 B_2) > 0.$$

It is clear from (13.2.13) to (13.2.16) that we can distinguish two cases:

subsonic flow $M^2 < 1$,

supersonic flow $M^2 > 1$.

For subsonic flow $(M^2 < 1)$ (13.2.13) to (13.2.16) yield the results

$$\frac{dv_1}{dx_1} > 0, \qquad \frac{d\rho}{dx_1} < 0, \qquad \frac{dp}{dx_1} < 0, \qquad \frac{dT}{dx_1} < 0, \qquad \frac{d(M^2)}{dx_1} > 0.$$

These results show the curious property that with $\mathbf{J} \times \mathbf{B}$ in a direction to decelerate the gas the flow velocity actually increases. This is a direct result of compressibility. The temperature decreases rapidly enough for the enthalpy of the gas to supply both the energy fed into the electrical circuit and the energy necessary for the increasing kinetic energy.

For supersonic flow $(M^2 > 1)$ (13.2.13) to (13.2.16) yield the results

$$\frac{dv_1}{dx_1} < 0, \qquad \frac{d\rho}{dx_1} > 0, \qquad \frac{dp}{dx_1} > 0, \qquad \frac{dT}{dx_1} > 0, \qquad \frac{d(M^2)}{dx_1} < 0.$$

In this case the fluid decelerates as would at first be expected because the $\mathbf{J} \times \mathbf{B}$ force density tends to decelerate the gas. At the same time, however, the increase in temperature indicates that the kinetic energy of the gas supplies both the electrical output power and the power necessary to increase the enthalpy of the gas.

In the subsonic case the Mach number increases and in the supersonic case it decreases. Both changes make the Mach number tend toward unity. It is clear from (13.2.13) to (13.2.16) that the derivatives go to infinity at $M^2 = 1$ and our model becomes inaccurate. The treatment of the flow in the vicinity of the Mach number of one is outside the scope of our discussion. Suffice it to say that for a subsonic flow that approaches Mach one the flow chokes, and a smooth transition to supersonic flow is possible only for a very special set of circumstances. For a supersonic flow that approaches Mach one a shock wave will form. A shock wave is a narrow region in which the gas variables change rapidly and the flow velocity changes from supersonic to subsonic. A more complete model of the gas than we have used is necessary for an analysis of shock waves. The additional constraint needed is the second law of thermodynamics.*

The operation of the system in Fig. 13.2.1 as a *pump* is somewhat more complicated. By operation as a pump (or accelerator) we mean that the terminal voltage has the polarity shown, and $v_1 > 0$, $J_3 < 0$. Thus electric power is fed into the channel, and the $\mathbf{J} \times \mathbf{B}$ force density is in a direction that tends to accelerate the gas. Whether it does accelerate depends on the results obtained from (13.2.13) to (13.2.16).

Consider first the subsonic flow ($M^2 < 1$). The requirement that $J_3 < 0$ imposes through (13.2.10) the requirement that

$$E_3 < -v_1 B_2.$$

This ensures that electric power will be put into the fluid. Equations 13.2.13 and 13.2.14 yield the qualitative sketches of Fig. 13.2.2a. The constant γ is always in the range $1 < \gamma < 2$; thus we must distinguish two possible curves for the temperature variation. It is evident from Fig. 13.2.2a that a $\mathbf{J} \times \mathbf{B}$ force density applied in a direction that tends to accelerate a gas flowing with subsonic velocity may actually decelerate the flow and heat the gas to a higher temperature. The curve of (dv_1/dx_1) also indicates that when the magnitude of J_3 is made large enough the flow velocity can be increased.

For supersonic flow ($M^2 > 1$) with $J_3 < 0$ and the terminal voltage set to the polarity indicated in Fig. 13.2.1 (13.2.13) and (13.2.14) yield the qualitative curves of Fig. 13.2.1b. The upper curve indicates that for small magnitudes

---

* For a thorough and lucid description of the many fluid-mechanical phenomena that can occur in one-dimensional steady flow see A. H. Shapiro, *The Dynamics and Thermodynamics of Compressible Fluid Flow*, Vol. I, Ronald, New York, 1953, pp. 73–264.
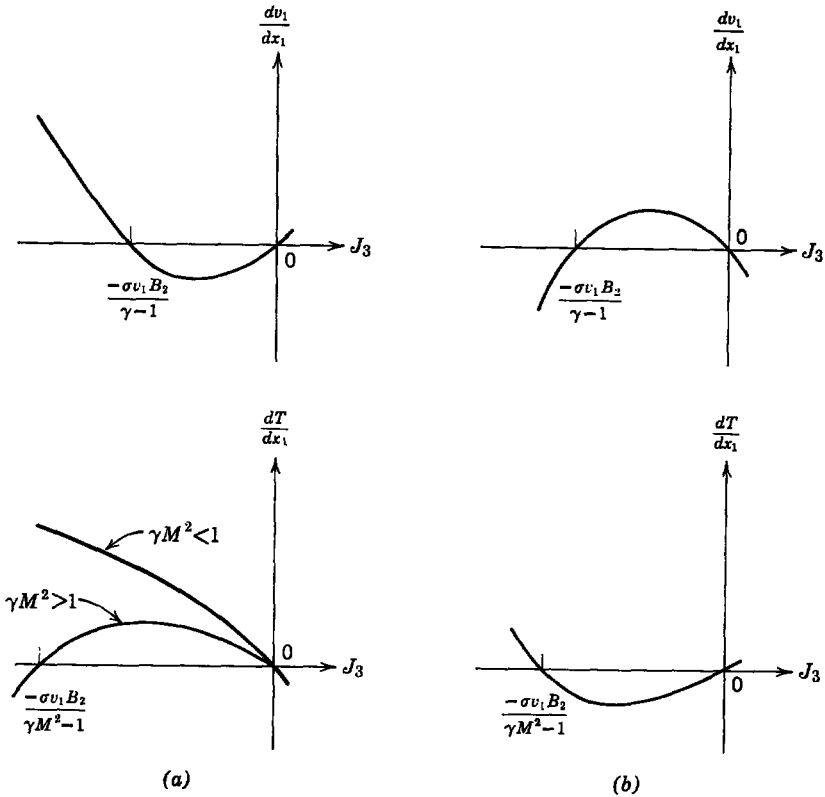
Fig. 13.2.2 Variation of velocity and temperature in a constant-area channel flow of a compressible fluid driven by a $\mathbf{J} \times \mathbf{B}$ force: (a) subsonic $(M^2 < 1)$; (b) supersonic $(M^2 > 1)$.

of J_3 the velocity is accelerated, but for too much driving current the velocity decreases.

Phenomena such as those demonstrated in Fig. 13.2.2 complicate the behavior of MHD devices that use compressible working fluids. Such phenomena are crucial in applications like plasma propulsion in which the object is to obtain a gas velocity as high as possible. When it is realized that these complications are predicted by an extremely simple model that neglects viscous and boundary layer effects, turbulence, and variation of electrical conductivity with temperature and is not complete enough to describe shock waves in supersonic flow, then we understand how complex the behavior of gaseous MHD systems can be and how we have to be extremely careful in obtaining the desired result from a particular model.

In order to understand how the behavior of a constant-area channel, MHD machine is affected by compressibility and to compare it with the incompressible analysis of Section 12.2.1a, a numerical example is presented.

For this example we assume gas properties typical of seeded combustion gases suitable for use in MHD generators:

$$R = 250 \text{ J/kg°K}, \qquad \gamma = 1.4, \qquad c_p = 875 \text{ J/kg°K}, \qquad \sigma = 40 \text{ mhos/m}.$$

We assume that the inlet ($x_1 = 0$) conditions are known:

$$v_1(0) = 500 \text{ m/sec}, \qquad T(0) = 3000°\text{K},$$
$$p(0) = 4 \times 10^5 \text{ N/m}^2, \qquad \rho(0) = 0.534 \text{ kg/m,}^3$$
$$M^2(0) = 0.238.$$

The channel dimensions are assumed to be $w = 0.2$ m, $d = 0.1$ m., and $l = 0.95$ m. The terminals are constrained with a constant voltage source

$$V = 150 \text{ V},$$

which constrains the electric field intensity to be constant along the length of the channel

$$E_3 = -750 \text{ V/m}.$$

The magnetic flux density is assumed to be

$$B_2 = 3 \text{ Wb/m}^2.$$

These numerical values lead to an inlet current density

$$J_3(0) = 3 \times 10^4 \text{ A/m}^2.$$

These numerical data are used with numerical integration of (13.2.13) and (13.2.14) and the mechanical equation of state and the definition of the Mach number to generate the normalized curves of Fig. 13.2.3. It is clear from these curves that the gas properties and flow velocity vary significantly over the length of the channel. Moreover, the rate of variation increases with x_1. With reference to the curve of M^2, it is evident that if the channel were made longer M^2 would pass through unity. Although the equations would give numerical answers, the solutions are physically impossible because the flow would choke and it would be impossible physically to make the Mach number greater than unity.

For this particular generator and these specified conditions the current density can be integrated numerically over the length of the channel to obtain the total terminal current

$$I = 4100 \text{ A}$$

Thus the generated power, that is, the power fed to the voltage source at the terminals is

$$P = 615,000 \text{ W}.$$

The total pressure drop through the channel is

$$\Delta p = 2.11 \times 10^5 \text{ N/m}^2,$$
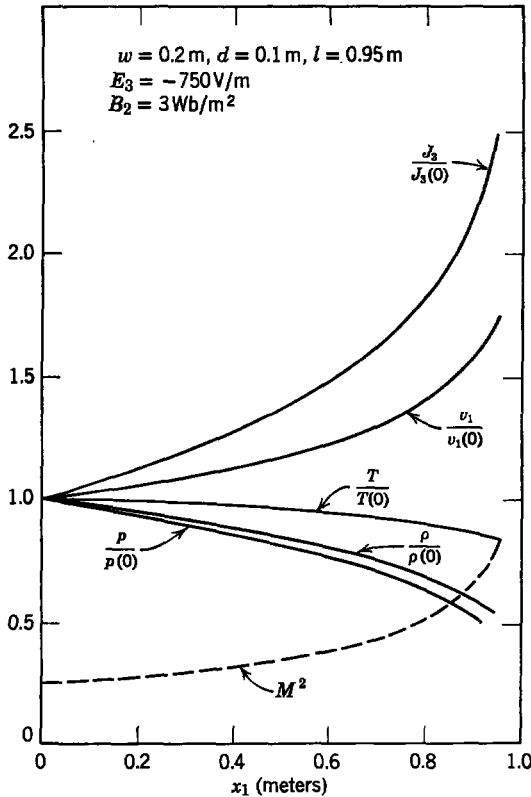
Fig. 13.2.3 Variation of properties along a constant-area channel with compressible flow acting as a generator.

or about 2.11 atm. It is interesting to compare these numbers with those of a generator that has an incompressible fluid operating with the same inlet velocity, electric field intensity, and flux density. Equations 12.2.19, 12.2.20, and 12.2.24 yield the results for the incompressible model:

$$I = 2850 \text{ A}, \qquad P = 427{,}000 \text{ W}, \qquad \Delta p = 0.95 \times 10^5 \text{ N/m}^2.$$

Comparison of these numbers with those of the compressible flow shows that with compressible flow the output current, power, and pressure drop are increased. Reference to the curves of Fig. 13.2.3 indicates that these increases are direct results of the increase in flow velocity with distance down the channel. The rather large difference in pressure drop is accounted for by the necessity to accelerate the gas flow in opposition to the decelerating $\mathbf{J} \times \mathbf{B}$ force.

This example has been presented to highlight some of the effects of compressibility. It must be emphasized that these results and the discussion hold only for *generator* operation with *subsonic* flow. For other conditions the effects can be grossly different. The techniques involved are the same, however.

13.2.2 Coupling with Steady Flow in a Variable-Area Channel

It is evident from the results of the preceding example that compressibility can limit the performance of a constant-area channel with MHD coupling; for example, with the conditions specified it would be impossible to operate the system with a larger pressure drop simply by lengthening the channel. Such limitations can be avoided by constructing the channel to make the cross-sectional area a function of distance (x_1) along the channel. When the channel area varies "slowly" enough with distance along the channel, we can use a *quasi-one-dimensional* model to describe the system with only one independent space variable. This technique is commonly employed in fluid mechanics* and magnetohydrodynamics,† and it yields quite accurate results in most applications. Its use in problems involving elastic media was introduced in Chapters 9 and 11. We present this technique in the context of a conduction-type MHD machine.

The system to be analyzed is illustrated in Fig. 13.2.4. It consists of a channel of rectangular cross-section but with the dimensions of the cross-section functions of the axial distance x_1. A perfect gas having constant electrical conductivity flows with velocity v through the channel as indicated
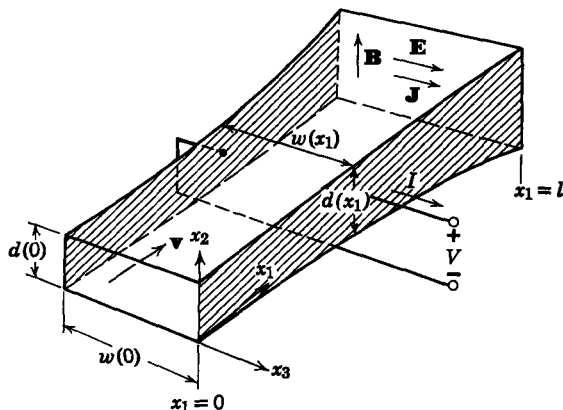
Fig. 13.2.4   MHD conduction machine with varying area.

* Shapiro, op. cit., pp. 73 and 74.
† Sutton and Sherman, op. cit., Chap. II.
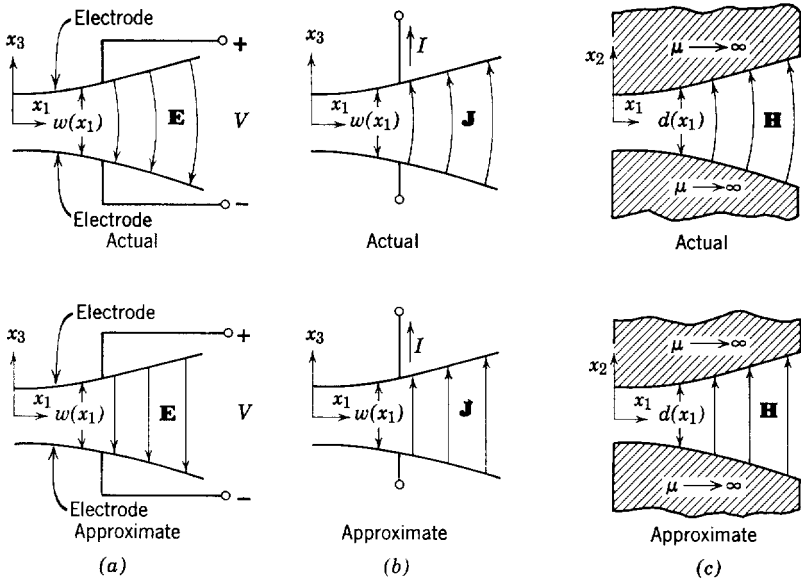
Fig. 13.2.5 Approximations for electromagnetic quantities in quasi-one-dimensional model: (a) electric field intensity; (b) current density; (c) magnetic field intensity.

in the figure. Two walls of the channel are insulators and two are electrodes that are connected to electrical terminals at which the terminal voltage V and terminal current I are defined with the polarities indicated.

We shall now develop the quasi-one-dimensional mathematical model for steady-flow in the system of Fig. 13.2.4. The derivation for non-steady flow is similar but more complex. The essential feature of the quasi-one-dimensional model is that all variables are assumed independent of x_2 and x_3 over a cross-section and they are thus functions only of x_1, the distance along the channel. This basic assumption involves approximations that will be discussed as we proceed.

We are considering a steady-flow problem; thus $(\partial/\partial t = 0)$ and the electric field is conservative $(\nabla \times \mathbf{E} = 0)$. The actual electric field lines between the electrodes will have the shapes shown qualitatively in Fig. 13.2.5a. In the quasi-one-dimensional model we assume that the field lines are only in the x_3-direction and the field intensity has the value

$$\mathbf{E} = \mathbf{i}_3 E_3 = -\mathbf{i}_3 \frac{V}{w(x_1)}. \tag{13.2.17}$$

This approximation is also illustrated in Fig. 13.2.5a and is the same as the long-wave limit used in the treatment of elastic continua in Chapters 9 and 10. It should be evident that the quality of the approximation improves as (dw/dx_1) becomes smaller.

The current density **J** will have the actual configuration shown in Fig. 13.2.5*b*. In the quasi-one-dimensional model we assume that **J** is in the x_3-direction:

$$\mathbf{J} = \mathbf{i}_3 J_3 \tag{13.2.18}$$

and that J_3 is a function of x_1 only. This approximation is illustrated in Fig. 13.2.5*b*.

We neglect the magnetic field induced by current flow in the gas (low magnetic Reynolds number), thus within the gas $\nabla \times \mathbf{H} = 0$. For illustration purposes we assume infinitely permeable pole pieces that conform to the insulating walls of Fig. 13.2.4; consequently, the actual magnetic field intensity appears as in Fig. 13.2.5*c*. In the quasi-one-dimensional approximation the magnetic field intensity (and flux density because $\mathbf{B} = \mu_0 \mathbf{H}$ in the gas) is in the x_2-direction and given by

$$\mathbf{H} = \mathbf{i}_2 \frac{F}{d(x_1)}, \tag{13.2.19}$$

where F is the mmf (ampere-turns) applied by external means between the pole pieces. Thus

$$\mathbf{B} = \mathbf{i}_2 B_2(x_1) = \mathbf{i}_2 \frac{\mu_0 F}{d(x_1)}. \tag{13.2.20}$$

This approximation, also illustrated in Fig. 13.2.5*c*, improves in validity as (dd/dx_1) decreases.

Although Fig. 13.2.5*c* represents a reasonable method for establishing the flux density, the magnetic material may not conform to the insulating walls or the field may be excited by air-core coils. In these cases we still assume that there is only an x_2-component of **B** and that it varies only with x_1 in a manner determined by the method of excitation. Thus $B_2(x_1)$ is most often a function independently set in the analysis of an MHD device.

It is clear from (13.2.17), (13.2.18), and (13.2.20) and Fig. 13.2.5 that fringing fields at the ends of the channel are neglected. It should also be clear that the approximate field quantities (13.2.17), (13.2.18) and (13.2.20) do not satisfy the required electromagnetic equations exactly. This is a consequence of the approximation.

In the quasi-one-dimensional model we assume that all the gas properties (p, ρ, T) are uniform over a cross section and functions only of x_1. Moreover, we assume that the x_1-component of the velocity is uniform over a cross section. We neglect the effects of transverse velocity components. Thus, in view of (13.2.17), (13.2.18) and (13.2.20), we write Ohm's law as

$$J_3 = \sigma(E_3 + v_1 B_2). \tag{13.2.21}$$

Use of the small volume between planes at x_1 and at $x_1 + \Delta x_1$, as illustrated in Fig. 13.2.6 with the integral form of the conservation of mass (13.1.3) and the assumption of the uniformity of v_1 over a cross section gives

$$\oint (\rho \mathbf{v} \cdot \mathbf{n})\, da = \rho(x_1 + \Delta x_1) v_1 (x_1 + \Delta x_1) A(x_1 + \Delta x_1)$$

$$- \rho(x_1) v_1(x_1) A(x_1) = 0, \quad (13.2.22)$$

where A is the cross-sectional area given by

$$A(x_1) = w(x_1)\, d(x_1). \quad (13.2.23)$$

We divide (13.2.22) by Δx_1 and take the limit as $\Delta x_1 \to 0$ to obtain

$$\frac{d(\rho v_1 A)}{dx_1} = 0. \quad (13.2.24)$$

This is the differential form that expresses conservation of mass in the quasi-one-dimensional model.

In deriving the quasi-one-dimensional momentum equation it is often the practice to use a small volume, shown in Fig. 13.2.6, with the integral form of the momentum equation (13.1.5). It is more direct, however, to recognize initially the assumptions that all gas properties and the x_1-component of velocity are uniform over a cross section and that transverse components of velocity have negligible effects and to write the x_1-component of (13.1.4)

$$\rho v_1 \frac{dv_1}{dx_1} = -\frac{dp}{dx_1} - J_3 B_2. \quad (13.2.25)$$

In this equation we have used (13.1.9) for mechanical force density and $\mathbf{J} \times \mathbf{B}$ for the magnetic force density.

The same comments hold true for the conservation of energy. Recognizing the assumptions made, we can write the quasi-one-dimensional energy equation from (13.1.37) as

Fig. 13.2.6 Closed surface for derivation of conservation of mass equation for quasi-one-dimensional model.

$$\rho v_1 \frac{d}{dx_1} (h + \tfrac{1}{2} v_1{}^2) = J_3 E_3. \quad (13.2.26)$$

In the quasi-one-dimensional model the equations of state (13.1.10) and (13.1.14) or (13.1.36) are unchanged from their general forms.

The quasi-one-dimensional model of MHD interactions in the variable-area channel of Fig. 13.2.4 consists of (13.2.17), (13.2.18), (13.2.20), (13.2.21), (13.2.24), (13.2.25), (13.2.26), (13.1.10), and (13.1.36). This set of

coupled, nonlinear, differential equations can be used with specified boundary conditions to calculate how the gas properties, flow velocity, and electromagnetic quantities vary along the length of the channel. The equations are summarized in Table 13.2.1.

As is the case with compressible flow in a constant-area channel, (Section 13.2.1) it is useful to derive influence coefficients that express each derivative as a function of the variables themselves. These influence coefficients are useful for general interpretation of properties and for numerical integration of the equations.

By solving the equations in Table 13.2.1 for each of the derivatives separately we arrive at the following set of influence coefficients:

$$\frac{1}{v_1}\frac{dv_1}{dx_1} = \frac{1}{(1 - M^2)}\left\{ [(\gamma - 1)E_3 + \gamma v_1 B_2]\frac{J_3}{\gamma p v_1} - \frac{1}{A}\frac{dA}{dx_1} \right\}, \qquad (13.2.27)$$

$$\frac{1}{\rho}\frac{d\rho}{dx_1} = \frac{1}{(1 - M^2)}\left\{ -[(\gamma - 1)E_3 + \gamma v_1 B_2]\frac{J_3}{\gamma p v_1} + \frac{M^2}{A}\frac{dA}{dx_1} \right\}, \qquad (13.2.28)$$

$$\frac{1}{T}\frac{dT}{dx_1} = \frac{(\gamma - 1)}{(1 - M^2)}\left\{ [(1 - \gamma M^2)E_3 - \gamma M^2 v_1 B_2]\frac{J_3}{\gamma p v_1} + \frac{M^2}{A}\frac{dA}{dx_1} \right\}, \quad (13.2.29)$$

$$\frac{1}{p}\frac{dp}{dx_1} = \frac{\gamma}{(1 - M^2)}\left\{ -[(\gamma - 1)M^2 E_3 + \{1 + (\gamma - 1)M^2\}v_1 B_2] \right.$$
$$\left. \times \frac{J_3}{\gamma p v_1} + \frac{M^2}{A}\frac{dA}{dx_1} \right\}, \qquad (13.2.30)$$

$$\frac{1}{M^2}\frac{dM^2}{dx_1} = \frac{\gamma}{(1 - M^2)}\left\{ [(\gamma - 1)(1 + \gamma M^2)E_3 + \gamma\{2 - (\gamma - 1)M^2\}v_1 B_2]\frac{J_3}{\gamma p v_1} \right.$$
$$\left. - \frac{[2 + (\gamma - 1)M^2]}{A}\frac{dA}{dx_1} \right\}. \qquad (13.2.31)$$

These influence coefficients should be compared with those of (13.2.13) to (13.2.16) for the constant-area channel. It is clear that when $(dA/dx_1 = 0)$ the two sets of influence coefficients become identical.

It is also clear from (13.2.27) to (13.2.31) that for any set of conditions the derivative of any variable can be made to have either sign and any magnitude by adjusting the factor (dA/dx_1). Thus the tendency of the flow to approach Mach one in a constant-area channel can be counteracted by letting the area of the channel vary. In fact, by adjusting the area $A(x_1)$ such that the quantity in braces in (13.2.31) is zero all along the channel the Mach number can be held constant along the channel. It is also true that any of the other influence coefficients can be used to design a channel [fix $A(x_1)$] such that one property $(v_1, \rho, p,$ or $T)$ is constant along the length of the channel.

Table 13.2.1   Summary of Quasi-One-Dimensional Equations for System of Fig. 13.2.4

Channel area	$A(x_1) = w(x_1)\, d(x_1)$	(13.2.23)
Electric field intensity	$\mathbf{E} = \mathbf{i}_3 E_3 = -\mathbf{i}_3 \dfrac{V}{w(x_1)}$	(13.2.17)
Current density	$\mathbf{J} = \mathbf{i}_3 J_3$	(13.2.18)
Magnetic flux density	$\mathbf{B} = \mathbf{i}_2 B_2(x_1)$	(13.2.20)
Ohm's law	$J_3 = \sigma(E_3 + v_1 B_2)$	(13.2.21)
Conservation of mass	$\dfrac{d(\rho v_1 A)}{dx_1} = 0$	(13.2.24)
Conservation of momentum	$\rho v_1 \dfrac{dv_1}{dx_1} = -\dfrac{dp}{dx_1} - J_3 B_2$	(13.2.25)
Conservation of energy	$\rho v_1 \dfrac{d}{dx_1}(h + \tfrac{1}{2}v_1^2) = J_3 E_3$	(13.2.26)
Mechanical equation of state	$p = \rho R T$	(13.1.10)
Thermal equation of state	$dh = c_p\, dT$	(13.1.36)
Local sound velocity	$a = \sqrt{\gamma R T}$	(13.2.11)
Local Mach number	$M = \dfrac{v_1}{a}$	(13.2.12)

Although the influence coefficients of (13.2.27) to (13.2.31) are useful for examining general properties of the variable-area MHD machine and for numerical integration when necessary, some exact solutions are possible and they are best obtained by using the basic equations summarized in Table 13.2.1.

Before proceeding with an example of an exact solution of the equations it is useful to introduce a convention used in the analysis of gaseous MHD generators. This convention defines a loading factor K as

$$K = -\frac{E_3}{v_1 B_2}.\qquad(13.2.32)$$

The use of the factor K in Ohm's law (13.2.21) yields

$$J_3 = (1 - K)\sigma v_1 B_2.\qquad(13.2.33)$$

Thus, when $0 < K < 1$, electric energy is being extracted from the gas; otherwise it is being put into the gas. The power density extracted electrically *from* the gas [see (13.2.26)] is

$$p_e = -J_3 E_3 = K(1 - K)\sigma v_1{}^2 B_2{}^2.\qquad(13.2.34)$$

Thus it is evident that maximum energy is extracted locally when $K = \frac{1}{2}$ or when the electric field intensity is one half $\mathbf{v} \times \mathbf{B}$. On a continuum basis this is the maximum output condition when the external impedance is made equal to internal impedance. In general, K can be a function of x_1; however, to achieve maximum power extraction along the channel, K should be kept close to the optimum value of one half. It is evident from (13.2.34) that the maximum power density that can be extracted electrically from the gas is

$$P_{e(\text{max})} = \frac{\sigma v_1^2 B_2^2}{4}. \tag{13.2.35}$$

We now set constraints suitable for obtaining an exact solution of the quasi-one-dimensional equations that describe the variable area MHD machine in Fig. 13.2.4. A set of constraints is selected to correspond closely to those used for analyzing MHD generators for large amounts of power (more than 100 MW). We present a normalized solution in literal form and then introduce numerical constants.

It is assumed that the values of all quantities are known at the inlet ($x_1 = 0$). We select the channel dimensions to achieve constant flow velocity v_1, constant loading factor K, and constant-channel aspect ratio $[w(x_1)/d(x_1)]$. The requirements of constant K and constant aspect ratio are satisfied only if

$$B_2 \sim \frac{1}{d(x_1)}.$$

Thus we assume that the magnetic field is excited by using infinitely permeable pole pieces that conform to the insulating walls, as illustrated in Fig. 13.2.5c. It follows that the flux density B_2 is given by (13.2.20).

For the constraints that have been specified, with the loading factor K defined by (13.2.32) and the current density J_3 given by (13.2.33), the equations of Table 13.2.1 can be simplified to the following:

$$\frac{d(\rho A)}{dx_1} = 0, \tag{13.2.36}$$

$$\frac{dp}{dx_1} = -(1 - K)\sigma v_1 B_2^2, \tag{13.2.37}$$

$$\rho v_1 c_p \frac{dT}{dx_1} = -K(1 - K)\sigma v_1^2 B_2^2, \tag{13.2.38}$$

$$p = \rho RT. \tag{13.2.39}$$

Before solving for any variable as a function of x_1, it is convenient to obtain relations between pairs of unknowns; for example, division of (13.2.38) by

(13.2.37) and simplification of the results yield

$$\rho c_p \frac{dT}{dx_1} = K \frac{dp}{dx_1}.$$ (13.2.40)

This equation can be written as

$$(\rho RT)\left(\frac{c_p}{R}\right)\frac{1}{T}\frac{dT}{dx_1} = (Kp)\frac{1}{p}\frac{dp}{dx_1}.$$ (13.2.41)

Using (13.2.39) and the fact that

$$\frac{c_p}{R} = \frac{\gamma}{\gamma - 1},$$

we integrate (13.2.41) to obtain the result that

$$\frac{p(x_1)}{p(0)} = \left[\frac{T(x_1)}{T(0)}\right]^{\gamma/[K(\gamma-1)]}$$ (13.2.42)

Note from (13.2.33) that when $K = 1$ no current flows and (13.2.42) reduces to the standard isentropic relation between temperature and pressure.[*]
We now use (13.2.42) with (13.2.39) to obtain the relation between temperature and density as

$$\frac{\rho(x_1)}{\rho(0)} = \left[\frac{T(x_1)}{T(0)}\right]^{[\gamma-K(\gamma-1)]/K(\gamma-1)}$$ (13.2.43)

The use of this result with (13.2.36) yields

$$\frac{A(x_1)}{A(0)} = \left[\frac{T(x_1)}{T(0)}\right]^{[K(\gamma-1)-\gamma]/K(\gamma-1)}$$ (13.2.44)

Because the aspect ratio (w/d) is constant, (13.2.44) yields the result

$$\frac{d(x_1)}{d(0)} = \frac{w(x_1)}{w(0)} = \left[\frac{A(x_1)}{A(0)}\right]^{1/2}$$ (13.2.45)

Finally, the definition of Mach number M in Table 13.2.1 with the constraint of constant velocity yields the relation between the square of the Mach number and the temperature:

$$\frac{M^2(x_1)}{M^2(0)} = \left[\frac{T(x_1)}{T(0)}\right]^{-1}.$$ (13.2.46)

Now that we have relations among the unknowns it is necessary to obtain a solution for only one of the unknowns as a function of x_1. It is easiest to

---

[*] Allis and Herlin, op. cit., p.78.

do this for the temperature by using (13.2.38), which we rewrite as

$$\frac{dT}{dx_1} = \frac{-K(1-K)\sigma v_1 B_2{}^2}{\rho c_p},\tag{13.2.47}$$

From (13.2.36) ρA = constant and from (13.2.20) and (13.2.45) $B_2{}^2 A$ = constant.

Thus (13.2.47) becomes

$$\frac{dT}{dx_1} = -\frac{K(1-K)\sigma v_1 B_2{}^2(0)}{\rho(0)c_p}.\tag{13.2.48}$$

The right side of this expression is constant and integration yields

$$T(x_1) - T(0) = -\frac{K(1-K)\sigma v_1 B_2{}^2(0)}{\rho(0)c_p}x_1.\tag{13.2.49}$$

By normalizing and rearranging this expression we obtain

$$\frac{T(x_1)}{T(0)} = 1 - \frac{(\gamma-1)\,K(1-K)\sigma v_1\,B_2{}^2(0)}{\gamma p(0)}x_1.\tag{13.2.50}$$

We define the constant C_1 as

$$C_1 = \frac{(\gamma-1)\,K(1-K)\sigma v_1\,B_2{}^2(0)}{\gamma p(0)}.\tag{13.2.51}$$

and rewrite (13.2.50) as

$$\frac{T(x_1)}{T(0)} = 1 - C_1 x_1.\tag{13.2.52}$$

We now use (13.2.42) to (13.2.46) to obtain the space variations of the other variables; thus

$$\frac{p(x_1)}{p(0)} = (1 - C_1 x_1)^{\gamma/[K(\gamma-1)]},\tag{13.2.53}$$

$$\frac{\rho(x_1)}{\rho(0)} = (1 - C_1 x_1)^{[\gamma-K(\gamma-1)]/K(\gamma-1)},\tag{13.2.54}$$

$$\frac{A(x_1)}{A(0)} = (1 - C_1 x_1)^{[K(\gamma-1)-\gamma]/K(\gamma-1)},\tag{13.2.55}$$

$$\frac{d(x_1)}{d(0)} = \frac{w(x_1)}{w(0)} = (1 - C_1 x_1)^{[K(\gamma-1)-\gamma]/2K(\gamma-1)},\tag{13.2.56}$$

$$\frac{M^2(x_1)}{M^2(0)} = (1 - C_1 x_1)^{-1}.\tag{13.2.57}$$

To complete the description of this generator we note from (13.2.17) and (13.2.32) that the terminal voltage with polarity defined in Fig. 13.2.4 is

$$V = K v_1 B_2(x_1) \, w(x_1) \qquad (13.2.58)$$

and constant. From (13.2.33) the current density is

$$J_3 = (1 - K)\sigma v_1 \, B_2(x_1). \qquad (13.2.59)$$

The total terminal current is

$$I = \int_0^l J_3 \, d(x_1) \, dx_1 = \int_0^l (1 - K)\sigma v_1 \, B_2(x_1) \, d(x_1) \, dx_1. \qquad (13.2.60)$$

From (13.2.20) we have

$$B_2(x_1) \, d(x_1) = B_2(0) \, d(0); \qquad (13.2.61)$$

thus (13.2.60) is written as

$$I = \int_0^l (1 - K)\sigma v_1 \, B_2(0) \, d(0) \, dx_1. \qquad (13.2.62)$$

In this expression the integrand is constant, which indicates that each element dx_1 along the length makes the same contribution to the total current. Integration of (13.2.62) yields

$$I = (1 - K)\sigma v_1 \, B_2(0) \, d(0)l. \qquad (13.2.63)$$

It is interesting to note by reference to Section 12.2.1 that this is the same as the current output from a constant-area channel of depth $d(0)$, width $w(0)$, and length l, using an incompressible fluid with conductivity σ and velocity v_1 in the presence of a uniform flux density of value $B_2(0)$.

It will be instructive to make the input dimensions and variables the same as those of the constant-area channel in Section 13.2.1 and to compare the performance of the variable area and constant-area channels. Thus we set

$R = 250 \text{ J/kg}^\circ\text{K},$	$\gamma = 1.4,$	$c_p = 875 \text{ J/kg}^\circ\text{K},$
$\sigma = 40 \text{ mhos/m},$	$v_1 = 500 \text{ m/sec},$	$T(0) = 3000^\circ\text{K},$
$p(0) = 4 \times 10^5 \text{ N/m}^2,$	$\rho(0) = 0.534 \text{ kg/m}^3,$	$M^2(0) = 0.238,$
$w(0) = 0.2 \text{ m},$	$d(0) = 0.1 \text{ m},$	$l = 0.95 \text{ m},$
$K = \frac{1}{2},$	$V = 150 \text{ V},$	$B_2(0) = 3 \text{ Wb/m}^2.$

First we use (13.2.51) to calculate the constant C_1:

$$C_1 = 0.0322/\text{m}.$$

Then the expressions for the variables follow from (13.2.52) to (13.2.57):

$$\frac{T(x_1)}{T(0)} = (1 - 0.0322x_1), \qquad\qquad \frac{p(x_1)}{p(0)} = (1 - 0.0322x_1)^7,$$

$$\frac{\rho(x_1)}{\rho(0)} = (1 - 0.0322x_1)^6, \qquad\qquad \frac{A(x_1)}{A(0)} = \frac{1}{(1 - 0.0322x_1)^6},$$

$$\frac{d(x_1)}{d(0)} = \frac{w(x_1)}{w(0)} = \frac{1}{(1 - 0.0322x_1)^3}, \qquad M^2(x_1) = \frac{0.238}{(1 - 0.0322x_1)}.$$

These variations with x_1 are plotted in Fig. 13.2.7. Compare the curves in this figure with those in Fig. 13.2.3 to learn how the slight variation of the channel area can reduce the changes in properties along the channel. Because the Mach number has changed so slightly over the length of the channel, the channel can be made much longer without reaching Mach one. This was not the case for the constant-area channel.

Further comparisons can be made in the constant-area channel with both compressible and incompressible fluids. Assuming the same inlet dimensions and properties for each of the three cases, we list several quantities in Table 13.2.2. Note that the constant-area generator with incompressible fluid produces the same power as the variable-area generator but with a larger pressure drop, and that the constant-area generator with compressible fluid produces the most power. This is due to the acceleration of the gas down the channel, as indicated by Fig. 13.2.3. This small increase in power occurs at the expense of a large increase in pressure and temperature drops
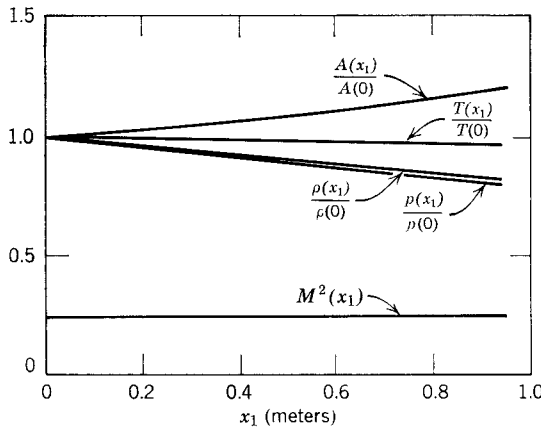
Fig. 13.2.7 Variation of properties along a variable-area channel designed to have constant velocity and constant loading factor while acting as a generator.

Table 13.2.2   Properties of MHD Generators

	Constant-Area Incompressible Fluid	Constant-Area Compressible Fluid	Variable-Area Constant Velocity Constant Loading Factor
Terminal voltage (volts)	150	150	150
Terminal current (amperes)	2,850	4,100	2,850
Power output (watts)	427,000	615,000	427,000
Pressure drop (newtons per square meter)	0.95×10^5	2.11×10^5	0.80×10^5
Temperature drop (degrees Kelvin)	...	420	93

over the variable-area generator. Although it is beyond the scope of this book, it is worthwhile to remark that this increase in power output from the constant-area channel results in the generation of considerable entropy which makes the energy in the exhaust fluid less available than with the variable-area channel.

In our analysis of the variable area channel we defined a set of constraints that allowed the complete solution of the differential equations in closed form. Several other sets of constraints allow direct integration of the equations. For still others numerical integration is necessary for solution.

It must be recognized that when a set of constraints is selected and closed-form solutions are obtained the design of a generator is fixed. In our example this means we specify the dimensions $[d(x_1)$, and $w(x_1)]$. Now, if we wish to operate this channel with a different set of inlet conditions, magnetic flux density, and/or applied voltage, we can no longer, in general, determine how the properties vary along the channel by literal integration. Instead, we must integrate numerically. Thus, if we wanted to fix the inlet properties to the channel we designed in our example and to find the output current and power as a function of load resistance for the range from open-circuit to short circuit, our solution in closed form would represent only one point on the curve. The remainder of the points would have to be found by numerical integration.

The preceding analysis of a variable-area MHD machine with a compressible working fluid is the basic technique in the study of electromechanical coupling in conduction-type MHD generators. Several types of machine have been built or proposed.* A cutaway drawing of one machine is shown in Fig. 13.2.8 and a photograph in Fig. 13.2.9.

* T. R. Brogan, "MHD Power Generation," *IEEE Spectrum*, 1, 58–65 (February 1964).
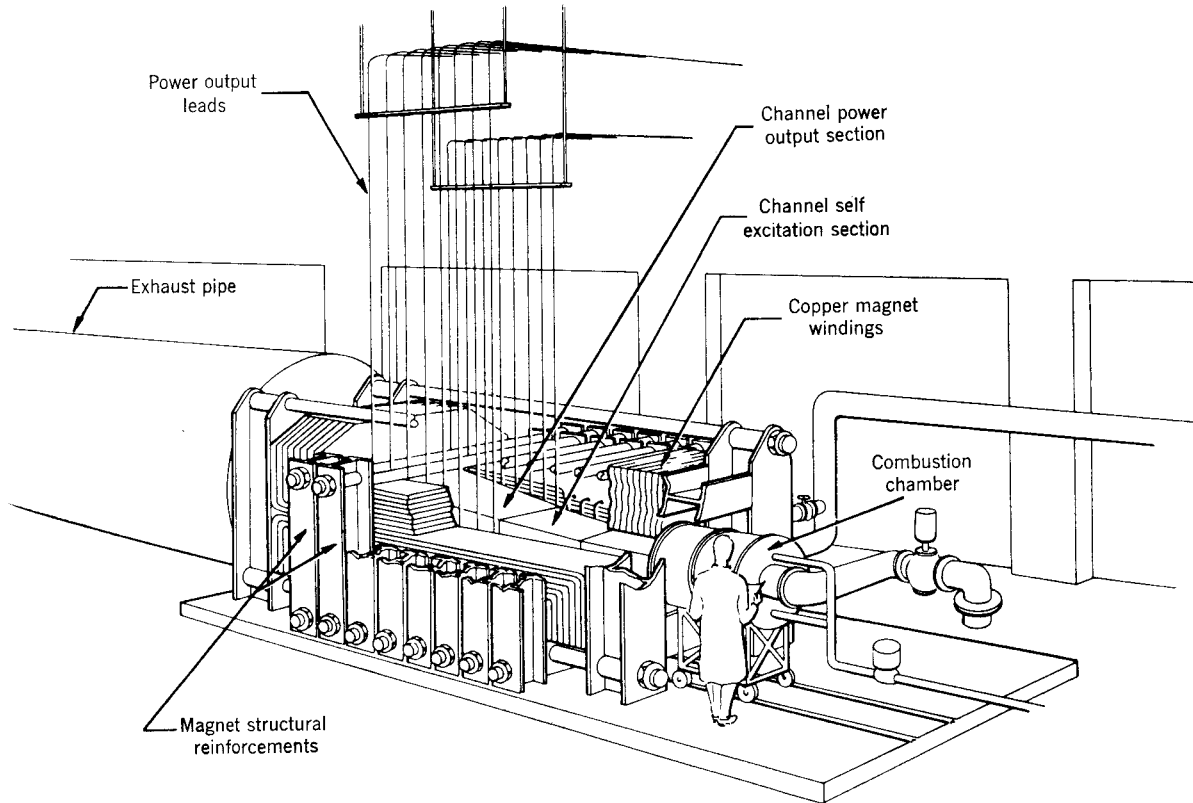
Fig. 13.2.8 Cutaway drawing of Avco Mark V rocket-driven, self-excited MHD power generator. Oxygen and fuel are burned in the combustion chamber to create a 5000°F electrically conducting gas which flows through the channel, where it interacts with the magnetic field to generate power. The magnet coil is excited by part of the generator output. For a gross power output of 31.3 MW, 7.7 MW are used to energize the field coils. (Courtesy of Avco-Everett Research Laboratory, a division of Avco Corporation.)
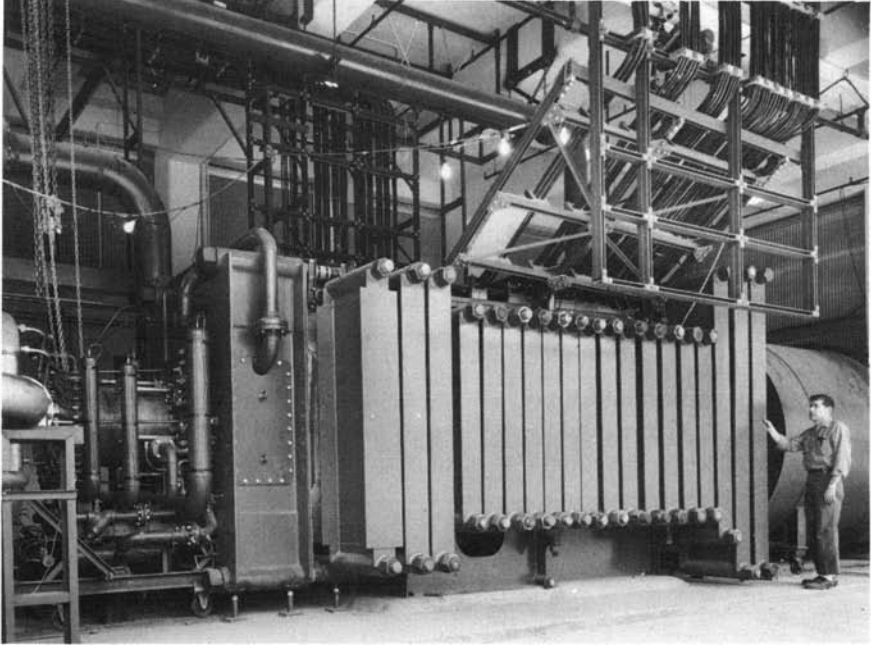
Fig. 13.2.9   Photograph of Avco Mark V generator described in Fig. 13.2.8. (Courtesy of Avco-Everett Research Laboratory, a division of Avco Corporation.)

13.2.3   Coupling with Propagating Disturbances

Recall from Section 12.2.3 that in the analysis of Alfvén waves propagating through an incompressible fluid of high electrical conductivity the fluid motion was entirely transverse. Even though the assumption of incompressibility was made, it was not necessary for the type of fluid motion described. Thus Alfvén waves are also found in an inviscid gas of high electrical conductivity.

Because a gas is compressible, it will also transmit longitudinal (acoustic) waves that are very much like the longitudinal elastic waves analyzed in Chapter 11. The propagation of acoustic waves in a gas can be affected by bulk electromechanical coupling when the gas has high electrical conductivity and is immersed in a transverse magnetic field. These modified disturbances are called magnetoacoustic waves. The same phenomena also occur in liquids because liquids are slightly compressible. The effect of bulk electromechanical coupling on acoustic waves in a liquid, however, is much less pronounced than in a gas. Consequently, we use our mathematical model of a gas to describe acoustic waves first and then to describe magnetoacoustic waves.

13.2.3a *Acoustic Waves*

As already stated, we shall study longitudinal disturbances, and thus we assume the rectangular channel in Fig. 13.2.10, which has rigid walls perpendicular to the x_2- and x_3-axes and infinite length in the x_1-direction. At $x_1 = 0$ a close-fitting piston, perpendicular to the x_1-direction, can be driven in the x_1-direction by a mechanical source. The channel is filled with a gas, with gas constant R and specific heat capacity at constant volume c_v, that can be represented as ideal. With this arrangement, the piston will drive disturbances that are uniform across the channel and that will propagate along the channel. The infinite length in the x_1-direction precludes reflections of the disturbance.

It is clear from the configuration of Fig. 13.2.10 that with disturbances driven by the piston uniformly in an x_2-x_3-plane there will be no variation of properties with x_2 or x_3 and there will only be an x_1-component of velocity v_1. Thus we can write the equations of motion for the gas in one-space-dimensional forms:

conservation of mass (13.1.1)

$$\frac{D_1\rho}{Dt} = -\rho\,\frac{\partial v_1}{\partial x_1}, \tag{13.2.64}$$

where now

$$\frac{D_1}{Dt} = \left(\frac{\partial}{\partial t} + v_1\frac{\partial}{\partial x_1}\right), \tag{13.2.65}$$

conservation of momentum (13.1.17)

$$\rho\,\frac{D_1 v_1}{Dt} = \frac{\partial p}{\partial x_1}, \tag{13.2.66}$$

conservation of energy (13.1.29)

$$\rho\,\frac{D_1}{Dt}(u + \tfrac{1}{2}v_1^2) = -\frac{\partial}{\partial x_1}(pv_1), \tag{13.2.67}$$

and the equations of state (13.1.10) and (13.1.14)

$$p = \rho RT, \qquad du = c_v\,dT. \tag{13.2.68}$$

Before proceeding to analyze the propagation of disturbances, it will be useful to simplify the equations somewhat. First, we use the equations of state to eliminate u and then T from the conservation of energy.

$$\rho\,\frac{c_v}{R}\frac{D_1}{Dt}\left(\frac{p}{\rho}\right) + \rho v_1\frac{D_1 v_1}{Dt} = -\frac{\partial}{\partial x_1}(pv_1). \tag{13.2.69}$$
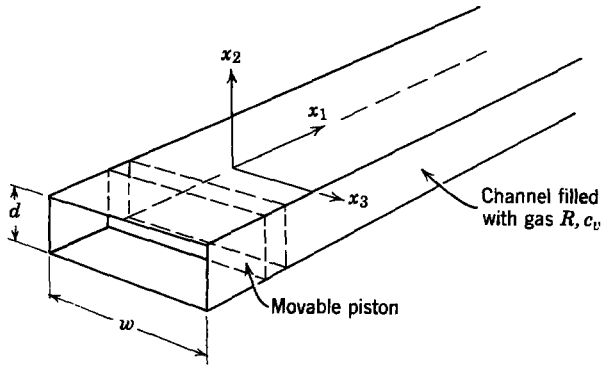
Fig. 13.2.10 Configuration for studying propagation of longitudinal (acoustic) disturbances in a gas.

Next, the conservation of momentum equation simplifies this expression to

$$\rho \frac{c_v}{R} \frac{D_1}{Dt}\left(\frac{p}{\rho}\right) = -p \frac{\partial v_1}{\partial x_1}.$$

(13.2.70)

Finally, the conservation of mass equation eliminates the space derivative of v_1 and the derivative on the left is expanded to obtain

$$\frac{D_1 p}{Dt} = \frac{\gamma p}{\rho} \frac{D_1 \rho}{Dt}.$$

(13.2.71)

An equation of the same form can be obtained for three-dimensional variations of properties.

Equations 13.2.64, 13.2.66, and 13.2.71 are sufficient to describe the propagation of disturbances through the gas; these equations, however, are nonlinear. For the remainder of this section, we assume that the disturbances involve small perturbations from an equilibrium condition such that the equations can be linearized. Thus we represent the three relevant variables in terms of equilibrium quantities (subscript o) and perturbation quantities (primed)

$$p = p_o + p',$$

(13.2.72a)

$$\rho = \rho_o + \rho',$$

(13.2.72b)

$$v_1 = v_1'.$$

(13.2.72c)

At equilibrium the gas is at rest; thus the equilibrium value of v_1 is zero.

Substitution of (13.2.72a–c) into (13.2.64), (13.2.66), and (13.2.71) and

retention of only linear terms in the perturbation quantities yield

$$\frac{\partial \rho'}{\partial t} = -\rho_o \frac{\partial v_1'}{\partial x_1}, \tag{13.2.73}$$

$$\rho_o \frac{\partial v_1'}{\partial t} = -\frac{\partial p'}{\partial x_1}, \tag{13.2.74}$$

$$p' = \frac{\gamma p_o}{\rho_o} \rho'. \tag{13.2.75}$$

In obtaining (13.2.75), the linearized version of (13.2.71) has been integrated and the constant of integration set to zero because both perturbation quantities are zero at equilibrium.

Elimination of p' and ρ' from (13.2.73) to (13.2.75) yields a single equation with v_1' as the unknown:

$$\frac{\partial^2 v_1'}{\partial t^2} = \frac{\gamma p_o}{\rho_o} \frac{\partial^2 v_1'}{\partial x_1^2}. \tag{13.2.76}$$

This is a wave equation (see Section 11.4.1) that describes longitudinal (acoustic) waves that propagate with a sound speed given by*

$$a_s = \left(\frac{\gamma p_o}{\rho_o}\right)^{1/2}. \tag{13.2.77}$$

Refer now to Fig. 13.2.10. We specify that the piston be driven with small amplitude oscillations such that the velocity of the gas at $x_1 = 0$ is constrained to be

$$v_1'(0, t) = V_m \cos \omega t. \tag{13.2.78}$$

Because the channel is infinitely long in the x_1-direction, disturbances will propagate only in the positive x_1-direction (there are no reflected waves). Thus the velocity of the gas at any point along the channel for steady-state conditions is

$$v_1'(x_1, t) = V_m \cos \left(\omega t - \frac{\omega}{a_s} x_1\right). \tag{13.2.79}$$

That this is a solution of (13.2.76) which satisfies the boundary condition of (13.2.78) can be verified by direct substitution.

We can now use (13.2.79) in (13.2.73) to find the perturbation density

$$\rho'(x_1, t) = \rho_o \frac{V_m}{a_s} \cos \left(\omega t - \frac{\omega}{a_s} x_1\right). \tag{13.2.80}$$

---

* This is the same speed as that given by (13.2.11).
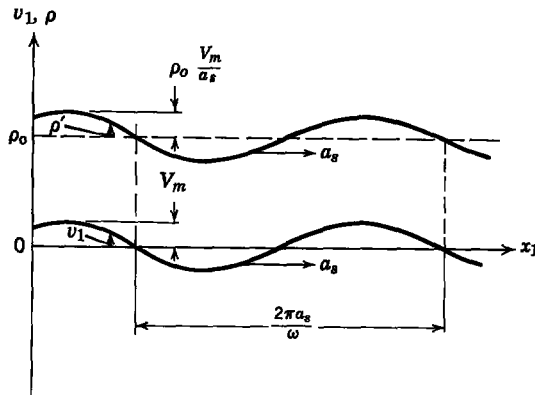
Fig. 13.2.11 Density and velocity variations in a sound wave of frequency ω propagating in the positive x_1-direction.

Sketches of the variation of density and velocity as functions of space at a given instant of time are shown in Fig. 13.2.11. Note that the velocity and density perturbations are in phase and that the whole pattern propagates in the positive x_1-direction with the acoustic speed a_s.

It is clear from the nature of the wave equation (13.2.76) that sound waves propagate in our assumed perfect medium without dispersion. Thus all the techniques and conclusions of Section 9.1.1 apply equally well to sound waves.

It is also worthwhile at this point to comment that no heat conduction term appears in the conservation of energy equation. This is the model that best describes sound waves from the audio-frequency range up to the megacycle per second range.

In modeling the slight compressibility of liquids to describe mechanical behavior during moderate changes in pressure the temperature is immaterial. Consequently, the conservation of energy equation and the thermal equation of state are dropped, and the mechanical equation of state is conventionally written as*

$$\frac{d\rho}{\rho} = \kappa \, dp, \qquad (13.2.81)$$

where κ is the compressibility. For small perturbations about an equilibrium with the definitions of (13.2.72a,b) (13.2.81) can be linearized and integrated to obtain

$$p' = \frac{1}{\kappa \rho_o} \rho'. \qquad (13.2.82)$$

* See, for example, H. B. Callen, *Thermodynamics*, Wiley, New York, 1960, pp. 344–349.

If this expression is used in place of (13.2.75) with (13.2.73) and (13.2.74), it will be found that a wave equation like that of (13.2.76) will result and $(\gamma p_o/\rho_o)$ will be replaced by $(1/\kappa \rho_o)$. Thus for a liquid with density ρ_o and compressibility κ the acoustic speed is

$$a_s = \frac{1}{\sqrt{\kappa \rho_o}}. \tag{13.2.83}$$

With this modification all the results already obtained for acoustic waves in inviscid gases hold equally well for acoustic waves in inviscid liquids.

In this mathematical development we used a lossless fluid model with the mathematical result that a plane disturbance propagates with no attenuation. In all real fluids viscosity (mechanical loss) dissipates energy and damps disturbances. In most practical problems, however, the damping is slight and can be treated mathematically as a perturbation of the lossless analysis, much like the process used to introduce electrical losses in transmission lines.† Although the problem of viscous damping of acoustic waves is not analyzed in this book, the concept and mathematical model of viscosity is introduced in Chapter 14, and it is a straightforward process to include viscous terms as perturbations on the lossless analysis and evaluate viscous damping of acoustic waves.

13.2.3b   Magnetoacoustic Waves

Now that we have described the physical nature and mathematical characterization of ordinary acoustic waves, we add bulk electromechanical coupling to see how acoustic waves are modified to magnetoacoustic waves. The physical system to be used is the rectangular channel of Fig. 13.2.10, with electric and magnetic modifications, as illustrated in Fig. 13.2.12. The channel is fitted with pole pieces and an excitation winding which produce, at equilibrium, a flux density that is uniform throughout the channel and has only an x_2-component:

$$\mathbf{B} = \mathbf{i}_2 B_o. \tag{13.2.84}$$

The walls of the channel that are perpendicular to the x_3-axis are made of highly conducting electrodes. The movable piston is also made of highly conducting material.

Because of the high conductivity of the gas, the electrodes, and the piston and because of the presence of an applied magnetic field, the electromagnetic part of this system is represented by a quasi-static, magnetic field system.

† See, for example, R. B. Adler, L. J. Chu, and R. M. Fano, *Electromagnetic Energy Transmission and Radiation*, Wiley, New York, 1960, Chapter 5, p. 179.
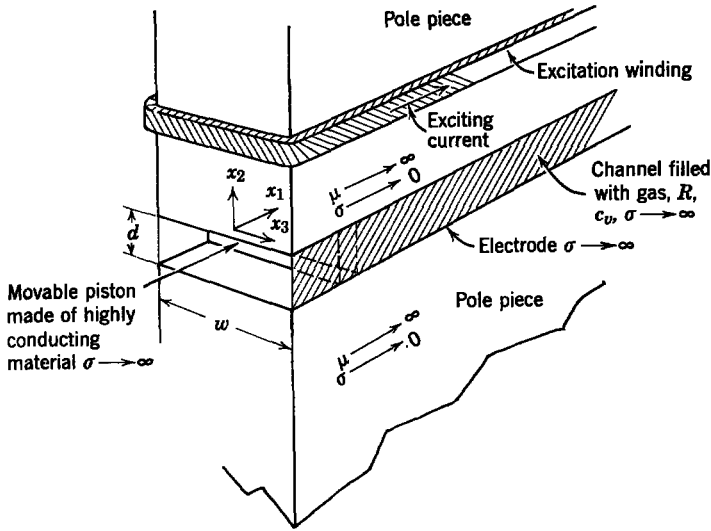
Fig. 13.2.12 Configuration for studying propagation of magnetoacoustic disturbances in a highly conducting gas.

Moreover, the assumed symmetry in the problem (including a neglect of fringing effects at the ends and edges of the channel) leads to the conclusion that, as in the preceding section, all variables are independent of x_2 and x_3. Furthermore, the gas velocity has only an x_1-component v_1, the highly conducting electrodes cause the electric field intensity to have only an x_3-component E_3, the current density in the gas thus also has only an x_3-component,* and the perturbation magnetic field induced by current flow in the gas has only an x_2-component. Summarizing these statements about electromagnetic quantities, we have

$$\mathbf{E} = \mathbf{i}_3 E_3(x_1, t), \tag{13.2.85a}$$

$$\mathbf{J} = \mathbf{i}_3 J_3(x_1, t), \tag{13.2.85b}$$

$$\mathbf{B} = \mathbf{i}_2[B_o + B_2'(x_1, t)]. \tag{13.2.85c}$$

In order to describe mathematically the dynamic nature of magnetoacoustic waves, we must modify (13.2.64) to (13.2.68) to include electromechanical coupling terms and add the electromagnetic equations necessary for a complete description.

---

* As we shall see subsequently, there is longitudinal current in the electrodes to satisfy $\nabla \cdot \mathbf{J} = 0$.

First, the momentum and energy equations (13.2.66) and (13.2.67) must be modified to include coupling terms, thus:

conservation of momentum (13.1.17) is

$$\rho \frac{D_1 v_1}{Dt} = -\frac{\partial p}{\partial x_1} - J_3(B_o + B_2'), \qquad (13.2.86)$$

and conservation of energy (13.1.29) is

$$\rho \frac{D_1}{Dt}(u + \tfrac{1}{2}v_1^2) = -\frac{\partial}{\partial x_1}(pv_1) + J_3 E_3. \qquad (13.2.87)$$

Next, recognizing that the equilibrium flux density B_o is not a function of time or space, the relevant electromagnetic equations are:

Ampere's law (1.1.1)*

$$\frac{1}{\mu_0}\frac{\partial B_2'}{\partial x_1} = J_3, \qquad (13.2.88)$$

Faraday's law (1.1.5)*

$$\frac{\partial E_3}{\partial x_1} = \frac{\partial B_2'}{\partial t}, \qquad (13.2.89)$$

and Ohm's law $\mathbf{J}' = \sigma \mathbf{E}'$ written as†

$$J_3 = \sigma[E_3 + v_1(B_o + B_2')]. \qquad (13.2.90)$$

Note that $\nabla \cdot \mathbf{B} = 0$ is automatically satisfied by the functional form of $\mathbf{B}$ that results in this problem.

The equations necessary for describing magnetoacoustic disturbances are (13.2.86) to (13.2.90), plus the conservation of mass (13.2.64) and the equations of state (13.2.68). As in the case of acoustic waves, these equations are nonlinear; thus we assume perturbations small enough to allow us to linearize the equations of motion. Again we represent the relevant variables in terms of equilibrium quantities (subscript o) and perturbation quantities (primed).

$$p = p_o + p', \qquad (13.2.91a)$$
$$\rho = \rho_o + \rho', \qquad (13.2.91b)$$
$$T = T_o + T', \qquad (13.2.91c)$$
$$v_1 = v_1', \qquad (13.2.91d)$$
$$B_2 = B_o + B_2', \qquad (13.2.91e)$$
$$J_3 = J_3', \qquad (13.2.91f)$$
$$E_3 = E_3'. \qquad (13.2.91g)$$

* Table 1.2, Appendix G.
† See Table 6.1, Appendix G.

Note that velocity, current density, and electric field intensity have zero equilibrium values.

First, linearization of Ohm's law (13.2.90) in the limit where $\sigma \to \infty$ gives

$$E_3 = -v_1 B_o. \tag{13.2.92}$$

Substitution of this result in (13.2.89) yields

$$\frac{1}{B_o} \frac{\partial B_2'}{\partial t} = - \frac{\partial v_1'}{\partial x_1}. \tag{13.2.93}$$

Linearization of (13.2.64) (conservation of mass) and division of the result by ρ_o yields

$$\frac{1}{\rho_o} \frac{\partial \rho'}{\partial t} = - \frac{\partial v_1'}{\partial x_1}. \tag{13.2.94}$$

Subtraction of (13.2.94) from (13.2.93) and integration with respect to time (recognizing that for equilibrium conditions all perturbation quantities go to zero) yields

$$\frac{B_2'}{B_o} = \frac{\rho'}{\rho_o}. \tag{13.2.95}$$

This shows that perturbations in flux density follow perturbations in mass density. This is formal mathematical acknowledgment that for $\sigma \to \infty$ the time constant for diffusion of magnetic flux lines through the gas goes to infinity and the flux lines are essentially frozen into the material.

It can be verified by following a process similar to that for (13.2.69) to (13.2.71) for small-signal linearized equations that (13.2.71) still holds for perturbation quantities:

$$\frac{D_1 p'}{Dt} = \frac{\gamma p_o}{\rho_o} \frac{D_1 \rho'}{Dt}. \tag{13.2.96}$$

Integration of this expression and use of (13.2.77) to define acoustic speed a_s yield

$$p' = a_s^2 \rho'. \tag{13.2.97}$$

Linearization of the conservation of momentum (13.2.86) yields

$$\rho_o \frac{\partial v_1'}{\partial t} = - \frac{\partial p'}{\partial x_1} - \frac{B_o}{\mu_0} \frac{\partial B_2'}{\partial x_1}. \tag{13.2.98}$$

In writing this equation, we have used (13.2.88) to eliminate J_3'.

The use of (13.2.97) to eliminate p' from (13.2.98) and the use of (13.2.95) to eliminate B_2' yield

$$\rho_o \frac{\partial v_1'}{\partial t} = \left(a_s^2 + \frac{B_o^2}{\mu_0 \rho_o} \right) \frac{\partial \rho'}{\partial x_1}. \tag{13.2.99}$$

The use of this expression and the linearized conservation of mass (13.2.94) to eliminate ρ' yields the single equation for v_1':

$$\frac{\partial^2 v_1'}{\partial t^2} = \left(a_s^2 + \frac{B_o^2}{\mu_0 \rho_o}\right) \frac{\partial^2 v_1'}{\partial x_1^2}. \tag{13.2.100}$$

Comparison of this result with (13.2.76) for ordinary acoustic waves shows that (13.2.100) describes longitudinal waves that propagate without dispersion with a propagation speed a given by

$$a = \left(a_s^2 + \frac{B_o^2}{\mu_0 \rho_o}\right)^{1/2}. \tag{13.2.101}$$

These waves are called magnetoacoustic waves and a is the magnetoacoustic velocity because the propagation speed is given by (13.2.101) as a combination of the acoustic velocity a_s and another velocity $\sqrt{B_o^2/\mu_0\rho_o}$, which depends on magnetic flux density. This other velocity is numerically equal to the Alfvén velocity a_b obtained for transverse electromechanical waves and defined in (12.2.88).

Provided we replace a_s with a, as defined in (13.2.101), all the comments made about acoustic waves in the preceding section hold true for magneto-acoustic waves. Because of the bulk electromechanical coupling, it will be instructive to study the physical makeup of a magnetoacoustic wave. To provide a basis for comparison with ordinary acoustic waves we assume the same driving function we used for the acoustic wave example, namely, that the piston at $x_1 = 0$ is driven with small amplitude at angular frequency ω such that the gas velocity at $x_1 = 0$ is

$$v_1'(0, t) = V_m \cos \omega t. \tag{13.2.102}$$

The gas velocity at any point in the gas is then

$$v_1'(x_1, t) = V_m \cos\left(\omega t - \frac{\omega}{a} x_1\right). \tag{13.2.103}$$

This can be verified as the solution by seeing that the boundary condition (13.2.102) and the differential equation (13.2.100) are both satisfied. In addition, the infinite length in the x_1-direction results in no reflected waves traveling in the negative x_1-direction.

We now use the conservation of mass (13.2.94) and (13.2.95) to write

$$\frac{B_2'(x_1, t)}{B_o} = \frac{\rho'(x_1, t)}{\rho_o} = \frac{V_m}{a} \cos\left(\omega t - \frac{\omega}{a} x_1\right). \tag{13.2.104}$$

Finally, we use (13.2.88) to evaluate J_3:

$$J_3(x_1, t) = \frac{B_o \omega V_m}{\mu_0 a^2} \sin\left(\omega t - \frac{\omega}{a} x_1\right). \tag{13.2.105}$$
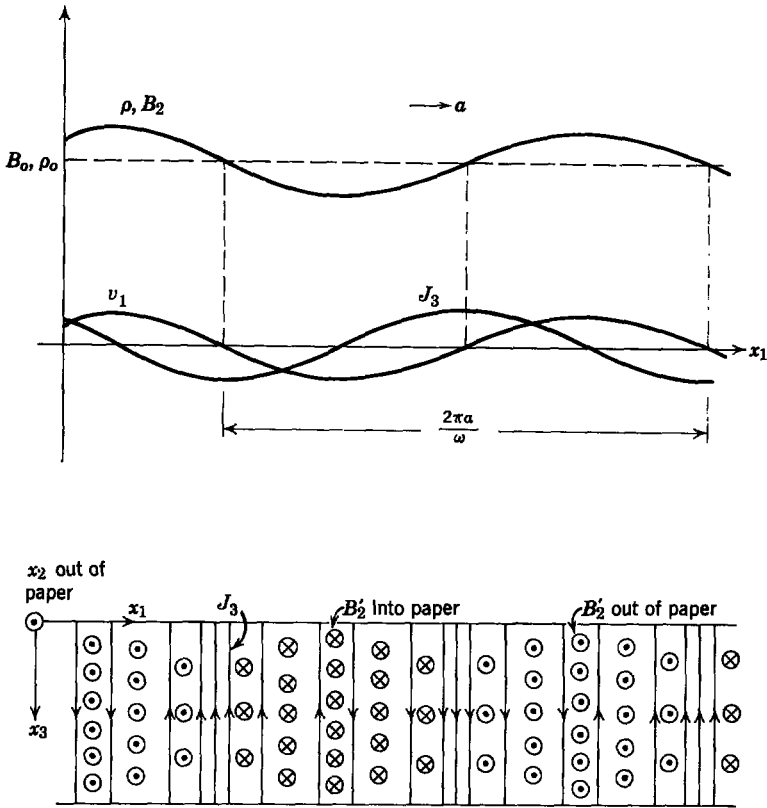
Fig. 13.2.13 Gas and electromagnetic variables in a magnetoacoustic wave of frequency ω propagating in the positive x_1-direction.

The variables described by (13.2.103) to (13.2.105) are illustrated for one instant of time in Fig. 13.2.13. As time passes, this pattern propagates with speed a in the positive x_1-direction. In describing J_3 the density of lines indicates the intensity of the current density, and for B_2' the density of the circles indicates the strength of the flux density. We already know that B_2' is excited by J_3. This can be verified by the right-hand rule or by (13.2.88). Also, as indicated by (13.2.95), the perturbation flux density and mass density are linearly related. Thus, when the gas is compressed, magnetic flux lines are compressed. This compression of flux lines induces a current density J_3, which interacts with the equilibrium flux density to produce a force that resists the compression. This makes the gas essentially less compressible, raises the effective continuum "spring constant," and makes the propagation velocity greater than the ordinary acoustic velocity.

It is clear from the pattern of current density in Fig. 13.2.13 why the highly conducting electrodes are necessary to close the current paths and maintain the one-dimensional nature of the problem.

In the example the waves were driven mechanically by a piston; they could have been driven equally well by local perturbations in flux density or current density. Furthermore, these waves can interact with an electric circuit that couples either to the flux density or to the current density. Thus magneto-acoustic waves provide the opportunity for continuum electromechanical coupling between a channel of highly conducting gas and an electric circuit.[*]

Although viscosity provides the loss mechanism that ultimately damps ordinary acoustic waves, magnetoacoustic waves are damped both by viscosity and by electrical losses that result from current flow in the presence of finite conductivity. In virtually all cases in which magnetoacoustic waves can be excited experimentally electrical losses predominate as the damping mechanism, and it is the limited electrical conductivity of gases that restricts the possibilities for practical utilization of magnetoacoustic waves for electro-mechanical coupling. This limitation is explored extensively in the literature.[†]

To illustrate the kinds of conditions necessary for the propagation of magnetoacoustic waves, we select conditions in which the waves have been excited and detected[‡]:

$$\text{Helium gas,} \qquad \rho_o = 0.0016 \text{ kg/m}^3,$$
$$B_o = 0.32 \text{ Wb/m}^2, \qquad T_o = 15,000°K,$$
$$R = 2080 \text{ J/kg°K}, \qquad p_o = 0.5 \times 10^5 \text{ N/m}^2 \; (\tfrac{1}{2} \text{ atm}).$$
$$\gamma = 1.67,$$

The extremely high temperature is necessary to achieve high enough conductivity that will allow magnetoacoustic wave propagation without excessive damping. Needless to say, this was a pulsed experiment. From the data given the sound velocity is

$$a_s = \left(\frac{\gamma p_o}{\rho_o}\right)^{\frac{1}{2}} = 7240 \text{ m/sec.}$$

The Alfvén velocity is

$$a_b = \left(\frac{B_o^2}{\mu_0 \rho_o}\right)^{\frac{1}{2}} = 7150 \text{ m/sec.}$$

[*] H. A. Haus, "Alternating Current Generation with Moving Conducting Fluids," *J. Appl. Phys.*, **33**, 2161 (June 1962).
[†] G. L. Wilson and H. H. Woodson, "Excitation and Detection of Magnetoacoustic Waves in a Rotating Plasma Accelerator," *AIAA*, Vol. 5, No. 9, Sept. 1967, pp. 1633–1641.
[‡] Wilson and Woodson, *loc. cit.*

The magnetoacoustic velocity is

$$a = \sqrt{a_s{}^2 + a_b{}^2} = 10{,}200 \text{ m/sec}.$$

It is clear from these numerical values that in a gas a moderate flux density will yield a magnetoacoustic velocity that is considerably greater than the ordinary acoustic velocity; thus the electromechanical coupling in the wave is easily made strong.

Magnetoacoustic waves can also be excited in conducting liquids such as liquid metals; however, because of the high density of liquids it is difficult to obtain an Alfvén velocity large enough to affect appreciably the propagation velocity of longitudinal disturbances. It is easy to show that the propagation velocity of magnetoacoustic waves in conducting liquids is still given by

$$a = \sqrt{a_s{}^2 + a_b{}^2},$$

where a_s is the sound velocity given by (13.2.83) and a_b is the Alfvén velocity given by (12.2.88).

To determine how much the propagation velocity of a longitudinal disturbance can be affected in a conducting liquid by an applied magnetic field consider mercury for which the sound velocity and density are

$$a_s = 1410 \text{ m/sec},$$

$$\rho_o = 13{,}600 \text{ kg/m}^3.$$

The flux density necessary to give an Alfvén velocity that is 10 per cent of the sound velocity is

$$B_o = 18.5 \text{ Wb/m}^2.$$

This flux density (185,000 gauss) is obtainable at present only in large, high-field research magnets and it is a factor of 10 higher than obtainable with conventional iron-core electromagnets. A less dense liquid metal like sodium or potassium would require less flux density. For obtainable fields, however, the effect of a magnetic field is still small. Conducting gases, on the other hand, have low enough densities that the Alfvén velocity can be greater than the sound velocity at moderate flux densities, as we illustrated earlier.

In general, the propagation of disturbances in conducting fluids immersed in magnetic fields involves complex combinations of ordinary acoustic waves (longitudinal waves) and Alfvén waves (transverse waves) both propagating along magnetic field lines, and magnetoacoustic waves (longitudinal waves) propagating normal to magnetic field lines. These separate component waves couple through electromagnetic and gas variables

and are all damped by loss mechanisms. Thus the analysis of a disturbance, in general, is quite complex. Nonetheless, many phenomena can be understood in terms of the simple component waves we have studied separately.

13.3 DISCUSSION

In this chapter we have gone one step further in the analysis of electromechanical interactions between electrical systems and conducting fluids by using a compressible fluid model. The effects of compressibility on the basic conduction-type MHD machines were shown. Compressible fluids were shown to propagate longitudinal (acoustic) waves, and under appropriate conditions (long enough magnetic diffusion time) these waves can be modified significantly by the presence of a transverse magnetic field. Although the phenomena described and the techniques used in their analyses have important engineering applications, they were also intended to be indicative of the techniques available for the study of still other types of electromechanical interactions with fluids.

In Chapter 14 we introduce viscosity, another fluid-mechanical effect. We limit the discussion to incompressible fluids to highlight the principal effects of viscosity in MHD systems.

PROBLEMS

13.1. A static compressible fluid is subject to a gravitational force per unit volume $-\rho g$ (Fig. 13P.1). Under the assumption that the fluid has a constant temperature T_o and that the fluid is a perfect gas so that $p = \rho RT$ find the distribution of density $\rho(x_1)$. The density at $x_1 = 0$ is ρ_o.
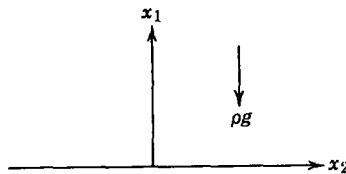
Fig. 13P.1

13.2. The MHD generator illustrated in Fig. 13P.2 uses a gas with constant specific heat capacities c_p and c_v and constant scalar conductivity σ. The dimensions are defined in the figure and it is assumed that the inlet values of all quantities are known. The loading factor K is to be held constant and the magnetic flux density is adjusted to satisfy the relation $B^2(z) A(z) = B_i^2 A_i$. For the constraint that the pressure be constant along the channel determine how the velocity v varies as a function of z.
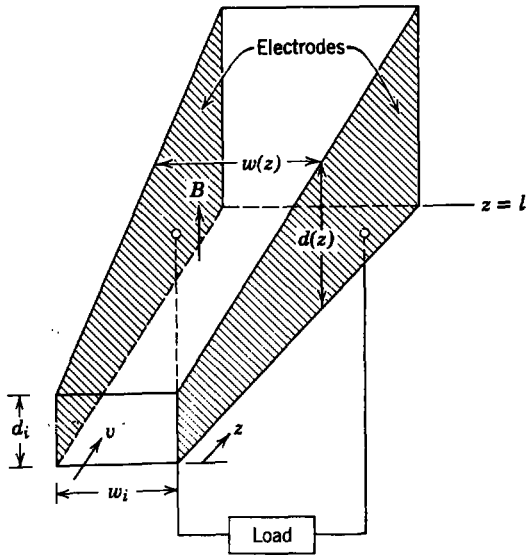
Fig. 13P.2

13.3. The dc MHD generator of Fig. 13P.3 has constant width w between the electrodes, and the magnetic flux density B_0 is constant along the length of the channel. The gas is assumed ideal with constant specific heats and with constant electrical conductivity. The inlet quantities ρ_i, p_i, T_i, and v_i are assumed known. The electrodes are short circuited together.

    (a) Find the channel depth $d(z)$ necessary to maintain the temperature constant along the channel.

    (b) Find the mass density variation along the channel for the channel geometry found in part (a).

13.4. For the MHD generator of Fig. 13P.4 assume that all inlet quantities are known $(p_i, \rho_i, T_i, d_i, w_i, A_i)$ and that the working gas has constant, scalar conductivity σ and ratio of specific heats γ. We apply a magnetic flux density B_0, which is constant, over the length of the channel. We now specify that we wish to design a channel such that the loading factor K will be constant along the length of the channel.

    (a) For maintaining constant Mach number M along the channel find the following functions of z that satisfy the given conditions:

$$\frac{A(z)}{A_i},\ \frac{d(z)}{d_i},\ \frac{w(z)}{w_i},\ \frac{v(z)}{v_i},\ \frac{p(z)}{p_i},\ \frac{T(z)}{T_i}.$$

    (b) Repeat part (a) for maintaining constant velocity v along the channel.

    (c) Assume that the given data is

$$\gamma = 1.4, \qquad\qquad \sigma = 40\ \text{mhos/m}, \quad R = 240\ \text{J/kg}°\text{K},$$
$$p_i = 5 \times 10^5\ \text{N/m}^2, \quad \rho_i = 0.7\ \text{kg/m}^3, \quad T_i = 3000°\text{K},$$
$$v_i = 700\ \text{m/sec}, \qquad w_i = 0.4\ \text{m} \qquad d_i = 0.2\ \text{m}.$$
$$K = 0.5, \qquad\qquad B_o = 4\ \text{Wb/m}^2$$

For the generators of parts (a) and (b) find the length of generator necessary to reduce the total enthalpy per unit mass $(c_p T + \tfrac{1}{2}v^2)$ by 10%.
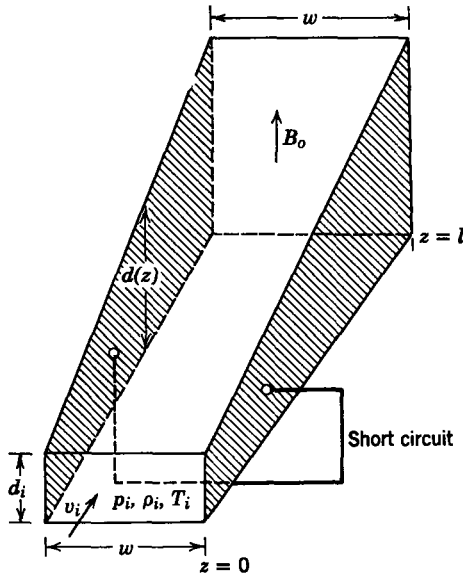
Fig. 13P.3
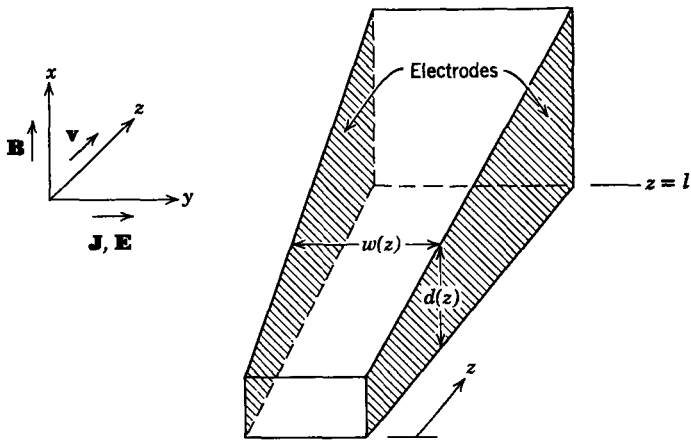
Fig. 13P.4

13.5. An MHD generator (Fig. 13P.4) uses an ideal gas with a constant ratio of specific heats $\gamma = 1.4$ and a constant, scalar, electrical conductivity $\sigma = 50$ mhos/m. At the inlet to the MHD generator channel the parameters and variables are adjusted to have the values

$$B_i = 4 \text{ Wb/m}^2, \qquad v_i = 700 \text{ m/sec},$$
$$\rho_i = 0.7 \text{ kg/m}^3, \qquad M_i^2 = 0.5,$$
$$p_i = 5 \times 10^5 \text{ N/m}^2, \qquad d_i = 0.5 \text{ m}$$
$$w_i = 1 \text{ m},$$

The aspect ratio of the channel is to remain constant so that the electric and magnetic fields will vary as

$$\frac{B(z)}{B_i} = \frac{E(z)}{E_i} = \left[\frac{w(z)}{w_i}\right]^{-1} = \left[\frac{d(z)}{d_i}\right]^{-1} = \left[\frac{A(z)}{A_i}\right]^{-\frac{1}{2}},$$

where A is the channel cross sectional area. For the conditions specified and for a loading factor $K = 0.5$ complete the following:

    (a) Find the area as a function of z necessary to keep the gas velocity constant.

    (b) For the channel of part (a) specify the length l necessary to reduce the gas temperature by 20 percent; that is, find l such that $T(l)/T_i = 0.8$.

    (c) Calculate and plot curves of $p(z)$, $\rho(z)$, $T(z)$ and $M^2(z)$ over the length of the channel.

    (d) Calculate the total electrical power drawn from this generator under the conditions given.

13.6. An ion propulsion device is represented schematically in Fig. 13P.6. The lateral dimensions are much larger than the separation of the accelerator electrodes so that fringing fields can be neglected. Ions, each having a charge q and mass m are injected with negligible initial velocity at $x = 0$. The system operates in the steady state in the space-charge-limited mode, in which case the solution for the electric field between the electrodes is

$$\mathbf{E} = \mathbf{i}_x \frac{4}{3} \frac{V_o}{L^{4/3}} x^{1/3},$$

and the solution for the charge density between the electrodes is

$$\rho_e = \frac{4}{9} \frac{\epsilon_0 V_o}{L^{4/3} x^{2/3}}.$$

The charge on each ion does not change during the acceleration process; that is,

$$\frac{\rho_e}{\rho_m} = \frac{q}{m},$$
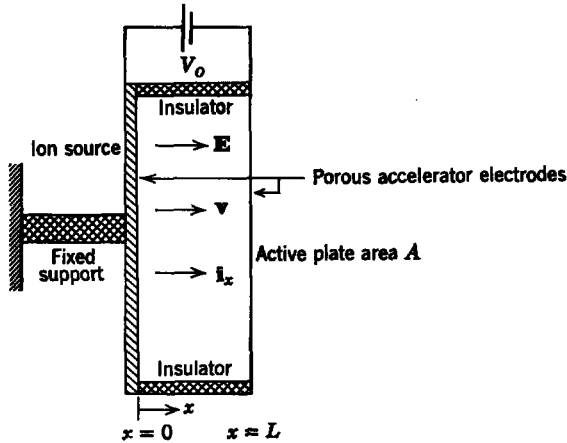
Fig. 13P.6

where ρ_m is mass density. The pressure in the ion gas is negligibly small. For steady-state operation complete the following:

(a) Find the velocity of the ion gas as a function of x between the electrodes.

(b) Find the magnitude and direction of the force that must be supplied by the fixed support to keep the accelerator system at rest.

13.7. In Fig. 13P.7 a liquid is placed between rigid walls and a movable piston. The liquid has a speed of sound a. The system is uniform in the x_2- and x_3-directions ($\partial/\partial x_2 = \partial/\partial x_3 = 0$). Assuming that the piston is moved by a velocity source $V = V_0 \cos \omega t$ at $x_1 = -L$,
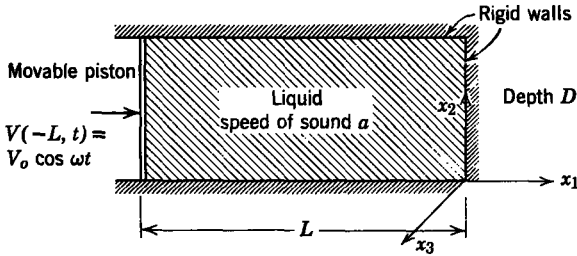
Fig. 13P.7

complete the following:

(a) Find the pressure in the liquid at $x_1 = -L$. Take the equilibrium pressure inside and outside the liquid as p_o.

(b) At what frequencies will there be resonances in the pressure, $p(-L, t)$?

13.8. A perfectly conducting compressible inviscid fluid fills the region $0 < x_2 < d$ as shown in Fig. 13P.8. When the fluid is static, it is permeated by a magnetic field $\mathbf{H} = H_o \mathbf{i}_3$. The fluid is set in motion by a piston at $x_1 = -L$ having velocity as shown, and is constrained at $x_1 = 0$ by a piston having mass M.

(a) *Derive* a differential equation (one equation in one unknown) for the velocity $v_1(x_1, t)$. Use a linearized analysis.

(b) Find the velocity of the piston, which in equilibrium is at $x_1 = 0$, under the conditions shown in Fig. 13P.8.
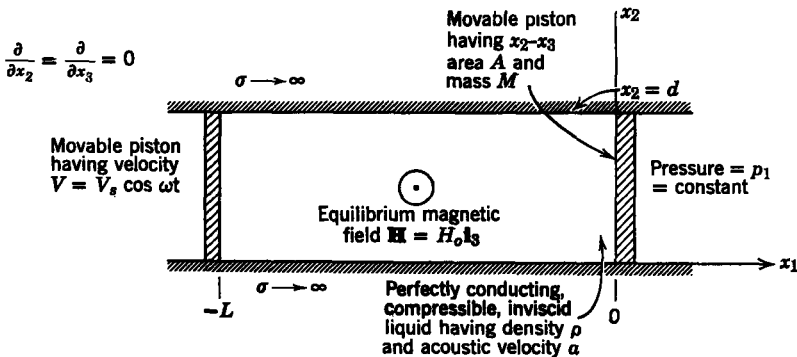
Fig. 13P.8
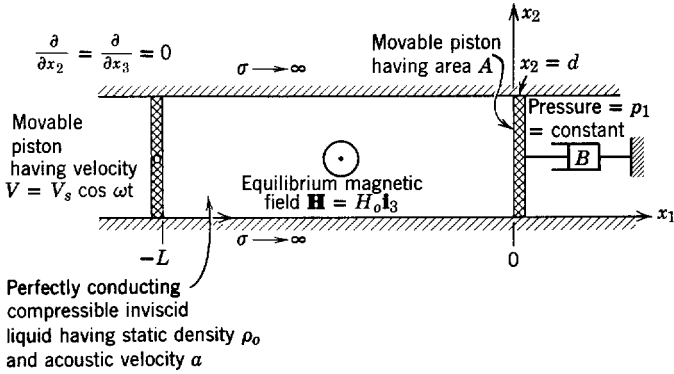
Fig. 13P.9

13.9. The region $0 < x_2 < d$ in Fig. 13P.9 is filled with a perfectly conducting inviscid compressible fluid. When the fluid is static, it is permeated by a magnetic field $\mathbf{H} = H_o \mathbf{i}_3$. The fluid is excited by a piston at $x_1 = -L$ with velocity $v(t)$, as shown, and constrained at $x_1 = 0$ by a movable massless insulating piston connected to a dashpot.

    (a) *Derive* a differential equation (one equation in one unknown) for the velocity $v_1(x_1, t)$. Use a linearized analysis.

    (b) The system is to be used as a delay line in which the object is to delay a signal by a fixed time without distorting the signal. If the signal is to be transmitted delayed and undistorted to $x_1 = 0$, the backward traveling wave must be eliminated by choosing a specific value for the dashpot coefficient B. Find this value in terms of the appropriate constants of the system.

13.10. The system shown in Fig. 13P.10 consists of a cylinder of cross-sectional area A_c containing a liquid of compressibility κ and equilibrium density ρ_l at equilibrium pressure p_o. The fluid is constrained at $x = 0$ by the closed end of the cylinder and at the other end by a rigid piston of mass M and thickness Δ. The equilibrium length of the liquid in the x-direction is L_1. The left face of the piston is connected to a thin elastic rod of cross-sectional area A_s, modulus of elasticity E, and equilibrium density ρ_s. The equilibrium length of the elastic rod is L_2. The left end of the elastic rod is driven by a stress source $T_o + T_s(t)$, where $T_s(t) \ll T_o$. For small-signal dynamic operation around an equilibrium point the general solutions are for the elastic rod: $-(L_1 + L_2 + \Delta) < x < -(L_1 + \Delta)$, $T(x, t)$ and $v_e(x, t)$; for the fluid $-L_1 < x < 0$, $p(x, t)$ and $v_l(x, t)$. Assume that except for constants to be determined by boundary conditions these solutions are known. Set up the equations that describe all the boundary conditions necessary for specializing constants in the general solutions. *Note.* You are not required to solve these equations.
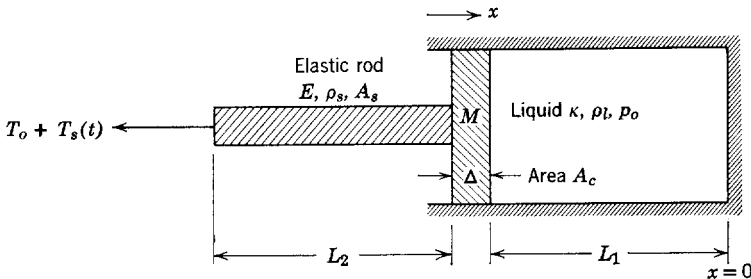
Fig. 13P.10

13.11. A slightly compressible inviscid fluid flows with a steady velocity V_o in the x-direction (Fig. 13P.11). The motions are in the x-direction and only a function of (x, t). The velocity of sound in the fluid is a_s.

   (a) Find the dispersion equation for small disturbances in the form of $p = \text{Re}$ $[\hat{p}e^{j(\omega t - kx)}]$.
   (b) Under what condition will the phases of both waves propagate in the positive x-direction?
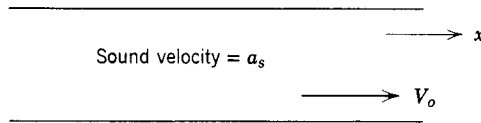
Fig. 13P.11

13.12. A static, inviscid fluid of conductivity σ is immersed in a uniform magnetic field H_o (Fig. 13P.12). In the limit in which $\sigma \to \infty$, it is possible for magnetoacoustic plane waves to propagate along the x-axis. In this problem investigate the consequences of having a finite conductivity σ.
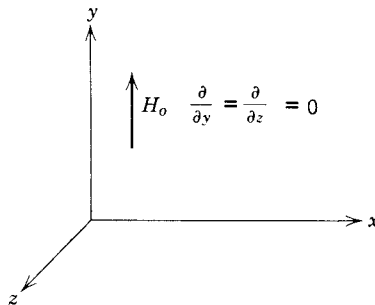
Fig. 13P.12

   (a) Write the linearized equations of motion for perturbations that are compressional (along the x-axis) and depend only on (x, t). (You need not combine these equations.)
   (b) Consider solutions of the form $v_x = \text{Re}\,[\hat{v}e^{j(\omega t - kx)}]$ and find the dispersion relation between ω and k. Show that in the limit $\sigma \to \infty$ the lossless dispersion equation is retained.
   (c) Show that when σ is small there are two pairs of waves, each pair consisting of a forward and backward traveling wave. What would you call these waves?
   (d) Consider the case in which σ is very large but finite (slight losses) and in which the excitation is sinusoidal (ω is real). Find an approximate expression for the rate at which waves decay in space. *Hint.* Write the dispersion equation in the form

$$k^2 = \frac{\omega^2}{a^2} - j\,\frac{f(\omega, k)}{\sigma},$$

where a is the phase velocity of magnetoacoustic waves. When σ is large but finite, the second term can be approximated by making $k^2 \approx (\omega^2/a^2)$. (Why?)

Chapter 14

ELECTROMECHANICAL COUPLING
WITH VISCOUS FLUIDS

14.0 INTRODUCTION

In Chapters 12 and 13 mathematical descriptions of lossless fluids are presented in a study of several basic types of electromechanical interaction with fluids. In the introductory section (12.0) of Chapter 12, we indicated that viscosity can have some marked effects on electromechanical interactions, especially when the system involves the flow of a fluid near a solid boundary. In this chapter the earlier fluid models are generalized to include the effects of fluid mechanical losses (viscosity), and the generalized models are used to study the effects of viscosity on some electromechanical interactions.

In our considerations of viscosity we limit our attention to incompressible fluids. The viscous effects we shall study also occur in compressible fluids, and the incompressible model we shall use is often employed to estimate the effects of viscosity on the flow of compressible fluids. Nonetheless, our model does not include mechanical losses due to longitudinal (dilatational) distortion of the fluid, and thus it is inadequate for a study of the effects of viscosity on longitudinal disturbances such as acoustic and magnetoacoustic waves. At the appropriate point in the development we indicate how the necessary extension can be made.

Our model for viscous fluids is restricted to *Newtonian fluids* whose stress-strain rate relations are linear. This model is a good representation of most fluids of interest in electromechanical interactions. It is analogous to the model of a linear resistance in electric circuits. Non-Newtonian fluids require suitable nonlinear models.*

* R. R. Long, *Mechanics of Solids and Fluids*, Prentice-Hall, Englewood Cliffs, N.J., 1961, pp. 69–72.

14.1   VISCOUS FLUIDS

In Section 12.1.4 the mechanical interaction force between adjacent fluid particles in an inviscid fluid is represented by the hydrostatic pressure p. When a viscous fluid is at rest, the mechanical interaction of adjacent particles is still described by a hydrostatic pressure. With the fluid in motion, it is subjected to pressure forces just as an inviscid fluid is, but, in addition, there is a force due to friction between adjacent particles that are in relative motion. The effects of this friction force are accounted for mathematically by defining a fluid *viscosity*.

14.1.1   Mathematical Description of Viscosity

A simple, one-dimensional example helps to introduce a derivation of the stress-tensor (hence force density) that represents the fluid friction.† Figure 14.1.1 shows a viscous fluid contained between parallel plates. We can imagine such a situation in which the system has large dimensions in the x_1- and x_3-directions. The plates are set into steady relative motion by externally applied forces. The viscous fluid near the upper plate tends to move with it. Similarly, the fluid at $x_2 = 0$ tends to move with the lower plate. Forces have to be applied to the two plates to maintain relative motion and, when steady-state conditions exist, there must be equal and opposite forces acting on the two plates, as indicated in Fig. 14.1.1. If each plate has the area A, there is a shear stress (force per unit area), given by

$$T_{12} = \frac{f}{A}.$$

$$(14.1.1)$$
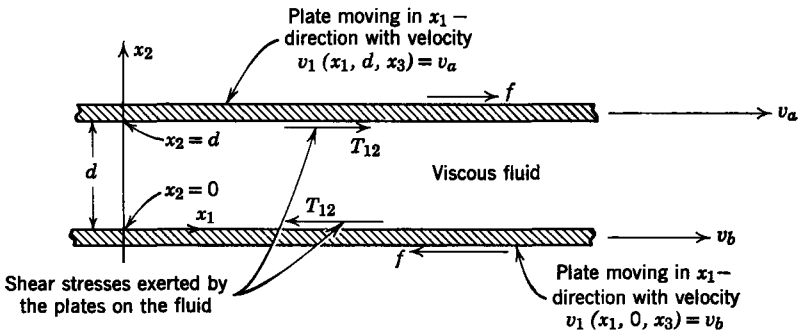
Fig. 14.1.1   Simple example of shear flow.

† This example is considered in more detail in Section 14.1.3.
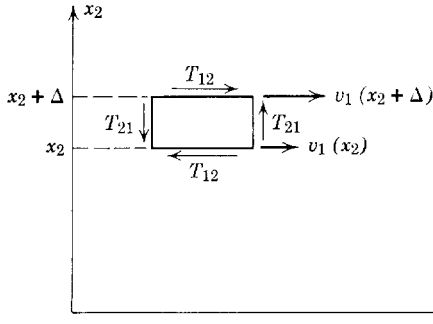
Fig. 14.1.2   Equilibrium for a small element of fluid of thickness Δ.

Experiments show that for a variety of fluids the shear stress T_{12} applied to the fluid by the plates is directly proportional to the difference of the plate velocities and inversely proportional to the plate spacing d:

$$T_{12} = \mu \left(\frac{v_a - v_b}{d} \right). \qquad (14.1.2)$$

The constant of proportionality μ is defined as the *coefficient of viscosity*. This constant μ describes a Newtonian fluid. A non-Newtonian fluid does not exhibit the linear relation between velocity difference and shear stress.

An experiment of this kind leads us to postulate that for a certain type of fluid flow an element of fluid of infinitesmal thickness, shown in Fig. 14.1.2, is held in equilibrium by the shear stress T_{12}, where

$$T_{12} = \lim_{\Delta \to 0} \mu \left[\frac{v_1(x_2 + \Delta) - v_1(x_2)}{\Delta} \right] = \mu \frac{\partial v_1}{\partial x_2}. \qquad (14.1.3)$$

Moreover, because the torque on the infinitesmal element must be zero,

$$T_{21} = T_{12}. \qquad (14.1.4)$$

From (8.1.10)* we conclude that the force density due to viscosity in our simple one-dimensional problem is

$$F_1 = \mu \frac{\partial^2 v_1}{\partial x_2^2}. \qquad (14.1.5)$$

Because the motion is steady and the pressure is uniform, this force density F_1 must be zero. Two boundary conditions are then required to integrate (14.1.5). Our intuition tells us that the fluid moves with (sticks to) a contiguous boundary; for example, in Fig. 14.1.1 the constants are determined by the conditions that

$$v_1(d) = v_a,$$
$$v_1(0) = v_b,$$

* See Table 8.1, Appendix G.

and it follows that

$$v_1 = \frac{(v_a - v_b)}{d} x_2 + v_b.$$

Of course, the force density and stress tensor deduced are of limited validity. The steps outlined, however, serve to indicate the approach that is now used to establish a stress tensor of more general validity. The similarity of this example and the one-dimensional elasticity problem of Section 9.1* suggest that we approach the problem of deriving the viscous stresses by the same techniques that were used to find the elastic stress tensor. Equation 14.1.3 emphasizes the basic difference between fluid and elastic media. Rather than a linear relation between stress and strain, as we found in dealing with elastic media [see (11.2.32)], we now find a linear relation between stress and *rate of strain*. Hence we can establish the viscous stress tensor in two steps: first, we relate the velocity to the rate of strain, which is defined in a way analogous to that in Section 11.2.1 for strain, and, second, we introduce the empirical relationship between stress and the rate of strain. We can then find the force density from the stress tensor by simply taking the divergence of the stress tensor (8.2.7)†.

14.1.1a The Strain-Rate Tensor

The strain-rate tensor, like the strain tensor, is defined by geometrical considerations. It is defined in such a way that its components represent those types of fluid flow that would be expected to give rise to a viscous stress. Because the relation between stress and strain rate (as found in the laboratory) is linear, it is possible to superimpose various types of deformation rates to describe an arbitrary deformation rate. Our development now parallels that used in connection with the strain tensor which described elastic media (Section 11.2.1).

A one-dimensional flow, such as that used to introduce this section, is shown in Fig. 14.1.3a. If we now consider the flow in the neighborhood of point A, the velocity field may be divided into a pure translation, as shown in Fig. 14.1.3b, and the flow of Fig. 14.1.3c. A pure translation cannot give rise to a viscous stress, for the particles that interact with those at A from above or below or to the right or left are moving at the same velocity as those at point A.

Now, in turn, we can divide the remaining flow field into two parts, as shown in Fig. 14.1.4. There is now a part that represents a rigid-body rotation about point A and a part that we call a *shear flow*. Viscous stresses would not be expected to arise from rigid-body rotation any more than they would from rigid-body translation. Hence a flow with the character of that shown in Fig. 14.1.4c must be related to the viscous stress.

* See Table 9.2, Appendix G.
† Appendix G.
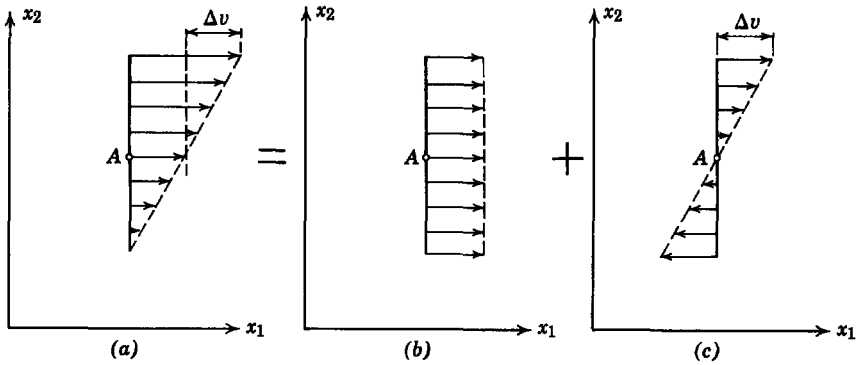
Fig. 14.1.3 Decomposition of flow into rigid-body translation of point A and flow with respect to that point.

It is worthwhile to recall the attributes of a flow field $\mathbf{v}(x_1, x_2, x_3, t)$ that correspond to rotation. Clearly, if fluid is rotating about point A, the line integral of $\mathbf{v}$ along a contour C that encloses point A is some finite number, say Γ.

$$\oint_C \mathbf{v} \cdot d\mathbf{l} = \int_S (\nabla \times \mathbf{v}) \cdot \mathbf{n} \, da = \Gamma. \tag{14.1.6}$$

We have used Stokes's theorem to transform the line integral to an integral over the surface enclosed by the contour C. From (14.1.6) it is apparent that the magnitude of the rotation about a point is proportional to $\nabla \times \mathbf{v}$. For the simple flow field shown in Figs. 14.1.3 and 14.1.4 there is only an $\mathbf{i}_3$-component of the curl, and that is

$$(\nabla \times \mathbf{v})_3 = \left(\frac{\partial v_2}{\partial x_1} - \frac{\partial v_1}{\partial x_2} \right). \tag{14.1.7}$$
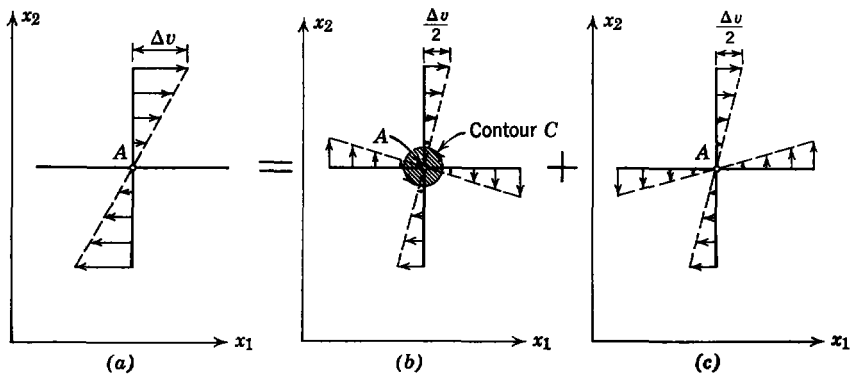
Fig. 14.1.4 Decomposition of flow into rotation and shear components: (a) total flow with respect to point A; (b) rigid-body rotation; (c) shear flow,

In our one-dimensional example we found that the stress T_{12} is proportional to $\partial v_1/\partial x_2$ [see (14.1.3)]. We can however, write this derivative as

$$\frac{\partial v_1}{\partial x_2} = \frac{1}{2}\left(\frac{\partial v_1}{\partial x_2} - \frac{\partial v_2}{\partial x_1}\right) + \frac{1}{2}\left(\frac{\partial v_1}{\partial x_2} + \frac{\partial v_2}{\partial x_1}\right), \qquad (14.1.8)$$

and we see that it includes the rotation of (14.1.7). Equation 14.1.8 is the analytical representation of Fig. 14.1.4. Our point is that it is reasonable to define as the component of the *shear rate* $\dot{e}_{12}$

$$\dot{e}_{12} = \frac{1}{2}\left(\frac{\partial v_1}{\partial x_2} + \frac{\partial v_2}{\partial x_1}\right), \qquad (14.1.9)$$

since it represents the only part of the deformation rate that is not (locally) a rigid-body translation or rotation. From the symmetry of the x_1- and x_2-coordinates it follows that $\dot{e}_{12} = \dot{e}_{21}$. Although our remarks have been made for flow fields in the x_1-x_2-plane, they apply equally well with other combinations of the coordinates. Hence we define

$$\dot{e}_{ij} = \frac{1}{2}\left(\frac{\partial v_i}{\partial x_j} + \frac{\partial v_j}{\partial x_i}\right). \qquad (14.1.10)$$

Although so far we have discussed the situation in which $i \neq j$ in (14.1.10), those components given by $i = j$ also represent a rate of deformation that was not present in our simple example. If $\nabla \cdot \mathbf{v} \neq 0$, it is possible for the fluid to execute a motion of the kind illustrated in Fig. 14.1.5b. There the fluid in the region of the point A is either expanding or contracting. We can characterize this dilatational motion by the three terms of the divergence, recognized as $\dot{e}_{ij}$ when $i = j$. The mechanism by which a dilatational motion can produce a viscous stress is not defined by the simple experiment discussed in the introduction to this section It is therefore not surprising that we find it necessary to define (and measure by some other means than a shear flow) a second coefficient of viscosity. It is important to recognize that the strain-rate, *defined* by (14.1.10), unlike the strain *approximated* by (11.2.10), involves no approximations about magnitudes of motion.

We can arrive at our definition of the strain-rate tensor in a more precise fashion by considering the relative velocity of fluid at two adjacent points in the flow field. For this purpose we define two points in a cartesian coordinate system which are at $\mathbf{r}$ and $\mathbf{r} + \Delta\mathbf{r}$, where

$$\mathbf{r} = \mathbf{i}_1 x_1 + \mathbf{i}_2 x_2 + \mathbf{i}_3 x_3 = \mathbf{i}_i x_i,$$

$$\Delta\mathbf{r} = \mathbf{i}_1 \Delta x_1 + \mathbf{i}_2 \Delta x_2 + \mathbf{i}_3 \Delta x_3 = \mathbf{i}_i \Delta x_i.$$

These coordinate vectors are shown in Fig. 14.1.6.

(a)

(b)
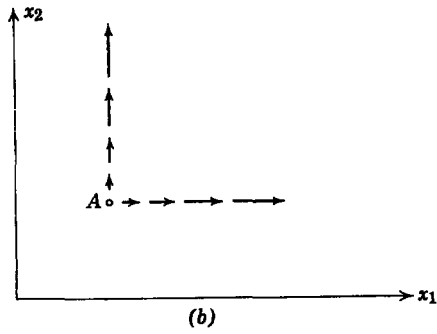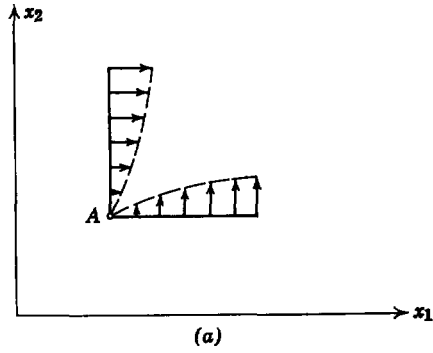
Fig. 14.1.5 Illustration of shear and dilatation at point A: (a) shear; (b) dilatation.
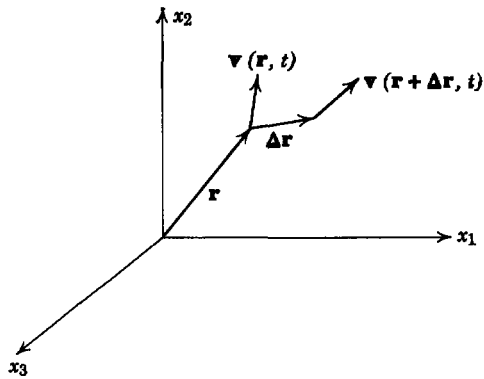
Fig. 14.1.6 System for defining rate of strain.

To find the velocity of the particle at $\mathbf{r} + \Delta\mathbf{r}$ with respect to the particle at $\mathbf{r}$ we expand the velocity in a Taylor series about the coordinate $\mathbf{r}$ and (because we are interested only in the region near $\mathbf{r}$) keep only linear terms. For the ith component we obtain

$$\Delta v_i = v_i(\mathbf{r} + \Delta\mathbf{r}, t) - v_i(\mathbf{r}, t) = \frac{\partial v_i}{\partial x_j}\Delta x_j. \tag{14.1.11}$$

We add and subtract $\frac{1}{2}(\partial v_j/\partial x_i)\,\Delta x_j$ on the right side of this expression to obtain

$$\Delta v_i = \frac{1}{2}\left(\frac{\partial v_i}{\partial x_j} - \frac{\partial v_j}{\partial x_i}\right)\Delta x_j + \frac{1}{2}\left(\frac{\partial v_i}{\partial x_j} + \frac{\partial v_j}{\partial x_i}\right)\Delta x_j. \tag{14.1.12}$$

The first term on the right represents rigid-body rotation with no rate of deformation, whereas the second term on the right represents the flow field left after translation and rotation have been subtracted out. (We removed the translation when we considered the *difference* between velocities at neighboring points.) The second coefficient of Δx_j in (14.1.12) is the strain rate (14.1.10). We have shown that, given the components of $\dot{e}_{ij}$ at the point $\mathbf{r}$, we can specify (except for the rotation) the difference in velocity between that point and a neighboring point an infinitesimal distance $\Delta\mathbf{r}$ away.

The strain-rate tensor is related to the velocity vector in exactly the same mathematical way that the strain is related to the displacement vector. Hence a proof that $\dot{e}_{ij}$ is, in fact, a tensor could begin with our knowledge that the velocity $\mathbf{v}$ is a vector and would follow identically the steps given in Section 11.2.1b, which prove that the strain is a tensor.

14.1.1b Stress-Strain-Rate Relations

At the beginning of this section we discussed a simple experiment that provided the relationship between the rate of shear strain and the shear stress,

$$T_{ij} = 2\mu\dot{e}_{ij}, \qquad i \neq j. \tag{14.1.13}$$

It is possible to make a simple argument that this relation remains correct in the presence of a normal stress. Figure 14.1.7 shows a hypothetical situation in which we imagine that a normal stress T_{11} results in a strain rate $\dot{e}_{12}$. If we rotate the coordinate axes as shown in this figure, the normal stress remains unchanged in magnitude and direction but the resulting strain rate has reversed its sign. It is concluded that the rates of shear strain must be independent of the normal stresses. (This is a formal statement that, given a T_{11}, symmetry requires that the resulting rate of shear strain can be neither positive nor negative, hence must be zero.)
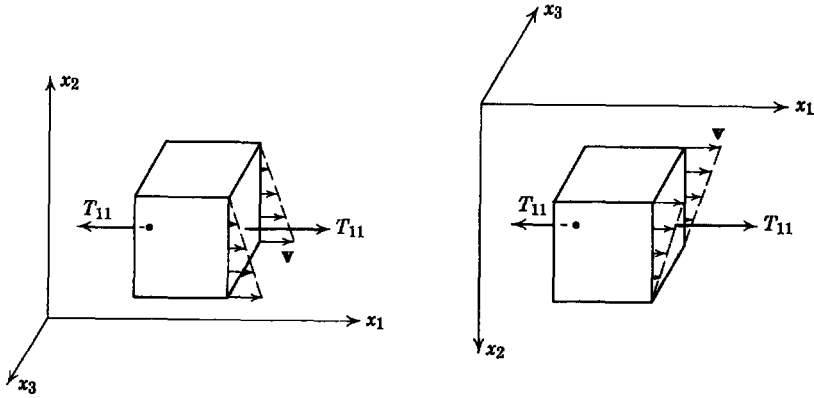
Fig. 14.1.7 Hypothetical situation in which a normal stress results in a shear strain rate.

Similarly, it is found that the dilatational strain rates depend only on the normal stresses. If k_1 and k_2 are experimentally determined constants, then

$$\dot{e}_{11} = k_1 T_{11} - k_2(T_{22} + T_{33}),$$
$$\dot{e}_{22} = k_1 T_{22} - k_2(T_{11} + T_{33}), \qquad (14.1.14)$$
$$\dot{e}_{33} = k_1 T_{33} - k_2(T_{22} + T_{11}).$$

A dilatational strain-rate $\dot{e}_{11}$ is shown in Fig. 14.1.8. Intuitively, we expect this type of flow to be caused by the stresses T_{11}, as shown in Fig. 14.1.8a,
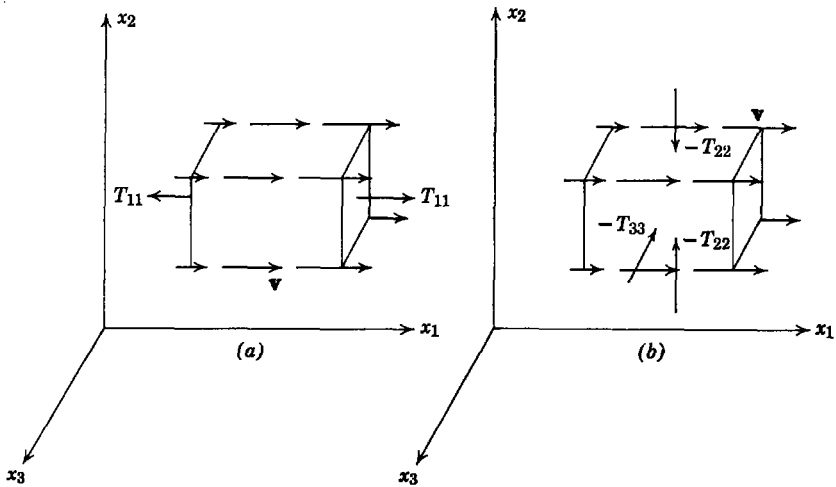
Fig. 14.1.8 Example of a dilatational strain rate showing two possible normal stresses.

or by normal stresses T_{22} and T_{33}, probably reversed in sign and not necessarily with the same magnitude as T_{11}. From symmetry we expect T_{22} and T_{33} to have an equivalent effect on the strain rate $\dot{e}_{11}$, so that there are only two constants in each of the relations (14.1.14). Because the fluid is isotropic, the equations must have the same form for strain-rate in each of the axis directions.

Again, a simple argument shows that shear stresses should not appear in (14.1.14). Suppose that a shear stress T_{12} resulted in a normal strain rate $\dot{e}_{11}$, as shown in Fig. 14.1.9. A change of coordinates generated by rotating the original system about a 45° axis in the x_1-x_2 plane results in a fluid element subject to the same shear stress but displaying a strain rate $\dot{e}_{22}$ (as viewed in the first coordinate system) rather than $\dot{e}_{11}$. Symmetry and the isotropy of the fluid require that the dilatational strain rates depend only on the normal stresses.

A simple example is now used to illustrate that the experimentally determined constants k_1 and k_2 in (14.1.14) are not independent of the coefficient μ in (14.1.13).

Example 14.1.1. A fluid is subject to a stress $T_{12} = T_{21} = T_o$ in the x_1, x_2, x_3-coordinate system. Show that the stress and strain rate in a coordinate system x_1', x_2', x_3' defined by $x_i' = a_{ij}x_j$, where

$$a_{ij} = \begin{bmatrix} \dfrac{1}{\sqrt{2}} & \dfrac{1}{\sqrt{2}} & 0 \\[2mm] \dfrac{-1}{\sqrt{2}} & \dfrac{1}{\sqrt{2}} & 0 \\[2mm] 0 & 0 & 1 \end{bmatrix}, \tag{a}$$

have only normal terms and find the relation between k_1, k_2, and μ that must therefore exist.

Equation 14.1.13 shows that

$$\dot{e}_{12} = \dot{e}_{21} = \frac{T_o}{2\mu}, \qquad \text{all other components} = 0 \tag{b}$$

Because the stress and strain rate are tensors, we can find them as expressed in the x_1', x_2', x_3'-coordinate system by using the transformations

$$T_{ij}' = a_{ik}a_{jl}T_{kl},$$
$$\dot{e}_{ij}' = a_{ik}a_{jl}\dot{e}_{kl}. \tag{c}$$

Hence we find that

$$T_{ij}' = \begin{bmatrix} T_o & 0 & 0 \\ 0 & -T_o & 0 \\ 0 & 0 & 0 \end{bmatrix}, \qquad \dot{e}_{ij}' = \begin{bmatrix} \dfrac{T_o}{2\mu} & 0 & 0 \\[2mm] 0 & -\dfrac{T_o}{2\mu} & 0 \\[2mm] 0 & 0 & 0 \end{bmatrix}. \tag{d}$$
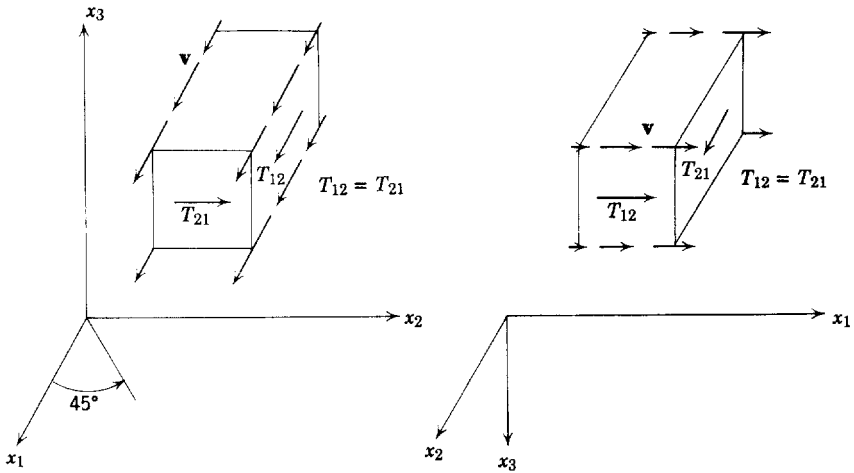
Fig. 14.1.9 Hypothetical situation in which a shear stress results in a dilatational strain rate.

It follows from these equations and (14.1.14) that

$$\dot{e}'_{11} = \frac{T_o}{2\mu} = k_1 T_o + k_2 T_o \quad \text{or} \quad k_1 + k_2 = \frac{1}{2\mu}, \tag{e}$$

which is the desired relationship between μ, k_1, and k_2.

14.1.1c   *The Equations of Fluid Dynamics as Modified by Viscosity*

Equations 14.1.14 allow us to find the stress components T_{11}, T_{22}, and T_{33} in terms of the strain-rate components $\dot{e}_{11}$, $\dot{e}_{22}$, and $\dot{e}_{33}$. This result and (14.1.13) provide a concise expression for the viscous stress in terms of the strain rates:

$$T_{ij} = 2\mu(\dot{e}_{ij}) + \alpha \delta_{ij} \dot{e}_{kk}. \tag{14.1.15}$$

We have used (e) in Example 14.1.1 to define the experimentally determined constant α in terms of the constants k_1 and k_2:

$$\alpha = \frac{k_2}{(k_1 + k_2)(k_1 - 2k_2)}. \tag{14.1.16}$$

The numbers μ and α are physical constants that characterize the viscous properties of a fluid. The constant α, however, will not be found in the literature but rather a constant, which is a linear combination of α and μ, is defined as the *second coefficient of viscosity* η.*

$$\eta = \alpha + \tfrac{2}{3}\mu. \tag{14.1.17}$$

---

* See, for example, K. F. Herzfeld and T. A. Litovitz, *Absorption and Dispersion of Ultrasonic Waves*, Academic, New York, 1959, pp. 353–361.

Reference to (14.1.10) shows that

$$\dot{e}_{kk} = \frac{\partial v_k}{\partial x_k} = \nabla \cdot \mathbf{v};$$ (14.1.18)

thus the second coefficient of viscosity affects dilatational motion and has a damping effect on longitudinal disturbances (acoustic waves).

As stated earlier, we shall restrict our treatment of viscosity to examples with incompressible fluid models for which $\nabla \cdot \mathbf{v} = 0$. Thus (14.1.15) is simplified to the form

$$T_{ij} = 2\mu \dot{e}_{ij}.$$ (14.1.19)

Equation 14.1.19 is that part of the stress on an element of incompressible fluid created by viscous effects. The total stress of mechanical origin must include the hydrostatic pressure p [see (12.1.34)] and may be written as

$$T_{ij}{}^m = -\delta_{ij}p + \mu\left(\frac{\partial v_i}{\partial x_j} + \frac{\partial v_j}{\partial x_i}\right).$$ (14.1.20)

We now use this stress tensor to write the conservation of momentum for an incompressible fluid in a form that includes the viscous force density [see (12.1.14), (12.1.15), and (12.1.19)]:

$$\rho \frac{Dv_i}{Dt} = F_i{}^e + \rho g_i - \frac{\partial p}{\partial x_i} + \mu \frac{\partial}{\partial x_j}\left(\frac{\partial v_i}{\partial x_j} + \frac{\partial v_j}{\partial x_i}\right).$$ (14.1.21)

The order of partial differentiation is immaterial; thus

$$\frac{\partial}{\partial x_j}\left(\frac{\partial v_j}{\partial x_i}\right) = \frac{\partial}{\partial x_i}\left(\frac{\partial v_j}{\partial x_j}\right) = \frac{\partial}{\partial x_i}(\nabla \cdot \mathbf{v}),$$

which is zero for an incompressible fluid. Consequently, (14.1.21) assumes the simpler form

$$\rho \frac{Dv_i}{Dt} = F_i{}^e + \rho g_i - \frac{\partial p}{\partial x_i} + \mu \frac{\partial}{\partial x_j}\left(\frac{\partial v_i}{\partial x_j}\right).$$ (14.1.22)

In vector form this equation is

$$\rho \frac{D\mathbf{v}}{Dt} = \mathbf{F}^e + \rho \mathbf{g} - \nabla p + \mu \nabla^2 \mathbf{v}.$$ (14.1.23)

Equation 14.1.22 or 14.1.23 is called the *Navier-Stokes equation* of fluid mechanics; for an incompressible fluid this force equation is used with a conservation of mass equation to describe the fluid dynamics. Of course, boundary conditions and the force density of electric origin $\mathbf{F}^e$ must be known.
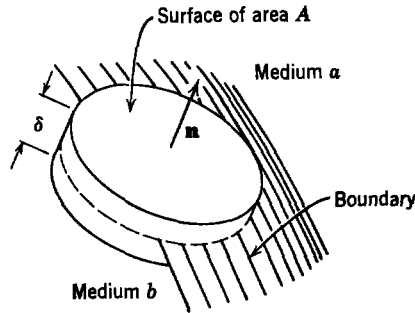
Fig. 14.1.10   Geometry for deriving boundary conditions.

14.1.2   Boundary Conditions

We specify that a boundary exists between media a and b, as illustrated in Fig. 14.1.10. The unit vector **n**, which is normal to the boundary, is positive from medium b to medium a and has components n_1, n_2, and n_3 in the cartesian coordinate system x_1, x_2, and x_3. Subscripts a and b are used to denote parameters and variables in the two media.

In order for the boundary to separate the two media, the velocities at the boundary must satisfy the relation

$$\mathbf{n} \cdot \mathbf{v}_a = \mathbf{n} \cdot \mathbf{v}_b = v_n. \tag{14.1.24}$$

This merely states that the normal component of velocity must be continuous at the boundary. Furthermore, the fluid particles at the boundary must have the same normal component of velocity as the boundary; otherwise the media are interdiffusing or they are moving apart. The result of (14.1.24) can be derived formally from the conservation of mass.

We now define a right circular cylindrical volume V with end surfaces of area A and height δ, as illustrated in Fig. 14.1.10. The volume V is assumed to be small enough that in its vicinity the boundary is essentially plane. The volume is oriented so that the ends of area A are parallel to the boundary and the boundary intersects the volume as illustrated in Fig. 14.1.10. We make the further restriction that δ be so small that the lateral area of the cylindrical surface will be much smaller than the area A.

We use the conservation of momentum as expressed by (12.1.21)

$$\rho \frac{Dv_i}{Dt} = \frac{\partial T_{ij}}{\partial x_j} \tag{14.1.25}$$

to integrate throughout the volume V:

$$\int_V \rho \frac{Dv_i}{Dt}\, dV = \int_V \frac{\partial T_{ij}}{\partial x_j}\, dV = \oint_S T_{ij} n_j\, da. \tag{14.1.26}$$

When we let the volume V go to zero, the restriction of finite mass density and finite acceleration makes the left side zero. The result is

$$0 = (T_{ij}{}^a - T_{ij}{}^b)n_j. \qquad (14.1.27)$$

This expression states that the traction $(T_{ij}n_j)$ must be continuous at a surface.

Another type of boundary condition that must be specified is the condition that holds for a viscous fluid in contact with a solid surface. This situation is depicted in two dimensions in Fig. 14.1.11. We select our coordinate system so that the normal n to the surface is in the x_2-direction and the velocity of the fluid parallel to the boundary is in the x_1-direction. We assume no externally applied body forces (no electromagnetic or gravity forces). The condition in (14.1.24) indicates that the fluid adjacent to the boundary can have no normal component

$$v_2 = 0. \qquad (14.1.28)$$

The condition in (14.1.27) indicates that the traction at the surface must be continuous:

$$\tau_1{}^b = \mu \frac{\partial v_1}{\partial x_2}, \qquad (14.1.29a)$$

$$\tau_2{}^b = -p, \qquad (14.1.29b)$$

$$\tau_3{}^b = 0. \qquad (14.1.29c)$$

Equation 14.1.29b gives the normal component of traction on the solid surface due to the fluid, and it is just the negative of the pressure. Equation 14.1.29a gives the tangential component of traction due to the fluid. Thus, if we know how v_1 varies with x_2, we can calculate the viscous stress transmitted to the solid surface.

Although (14.1.29a) expresses the derivative of the velocity at the boundary, we also need to know the velocity at the boundary. We specify that the relative tangential velocity at the boundary is zero,

$$(\mathbf{v}_a - \mathbf{v}_b) \times \mathbf{n} = 0, \qquad (14.1.30)$$

where $\mathbf{v}_a$ is the velocity of the fluid and $\mathbf{v}_b$ is the velocity of the boundary. The physical reasoning to justify this condition is as follows: a viscous fluid
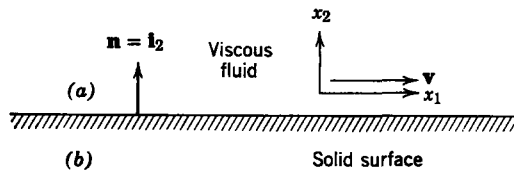
Fig. 14.1.11 A boundary between a viscous fluid and a solid surface.

exhibits friction when it flows along a solid surface, although this surface friction may have a different constant than the bulk coefficient of viscosity. If there were any tangential slippage at the boundary, it would represent an impulse in $(\partial v_1/\partial x_2)$ at the boundary, and with a finite friction coefficient it would require an infinite surface shear force. We conclude that there can be no slippage between a viscous fluid and a solid boundary.

14.1.3   Fluid-Mechanical Examples

Now that we have established the momentum equation and boundary conditions that describe incompressible viscous fluid flow it is appropriate to study some fluid flow examples without electromechanical coupling to establish ideas concerning the principal effects of viscosity that will show up later in electromechanical examples.

We consider again the example introduced in Section 14.1.1. The system is shown in Fig. 14.1.12. A viscous fluid is constrained between two parallel rigid plates separated by a distance d. The lower plate is fixed and the upper plate is made to move in the x_1-direction with constant velocity v_0. The fluid can be considered homogeneous and incompressible, $\nabla \cdot \mathbf{v} = 0$, and has a coefficient of viscosity μ. The hydrostatic pressure is constrained to be constant throughout the fluid, the system is in the steady state, and the plates are large enough in the x_1- and x_3-directions that we can neglect edge effects. Neglect the force of gravity. We want to find all components of velocity between the plates and the tangential traction applied to the plates by the fluid.

From (14.1.23), the momentum equation is:

$$\rho(\mathbf{v} \cdot \nabla)\mathbf{v} = \mu \nabla^2 \mathbf{v}.$$

The upper plate is driven in the x_1-direction so we expect that $v_3 = 0$. Furthermore, the large dimensions in the x_1 and x_3 directions allow us to assume

$$\partial/\partial x_1 = \partial/\partial x_3 = 0.$$
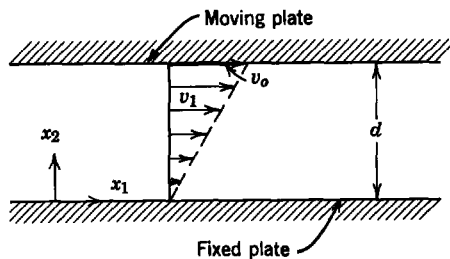
Fig. 14.1.12   A simple example of shear flow.

The use of these assumptions with $\nabla \cdot \mathbf{v} = 0$ and the boundary condition at $x_2 = \pm d$ yield

$$v_2 = 0.$$

The momentum equation thus reduces to

$$0 = \frac{\partial^2 v_1}{\partial x_2{}^2}.$$

Integration of this equation twice yields:

$$v_1 = C_1 x_2 + C_2.$$

The requirement of continuous tangential velocity at a boundary (14.1.30) gives

$$\text{at} \quad x_2 = 0, \quad v_1 = 0, \quad C_2 = 0,$$

$$\text{at} \quad x_2 = d, \quad v_1 = v_o, \quad C_1 = \frac{v_o}{d}.$$

Thus

$$v_1 = v_o \frac{x_2}{d}.$$

This profile, referred to as *plane Couette flow*, is sketched in Fig. 14.1.12.
    The use of (14.1.27) yields for the tangential component of traction

$$\text{at} \quad x_2 = 0, \quad \tau_1 = \mu \frac{v_o}{d},$$

$$\text{at} \quad x_2 = d, \quad \tau_1 = -\mu \frac{v_o}{d}.$$

It is apparent that the viscous traction tends to oppose the relative motion of the two plates as we intuitively expected.
    The type of flow described in this example is used in a device specifically designed to measure the coefficient of viscosity. It consists of two concentric cylinders with a small annular space between them. One cylinder is fixed and the other can be rotated about its axis. The fluid is introduced into the space between the cylinders, and the torque required to rotate one cylinder at a particular speed is measured. This torque is used with the known lever arm and the expression for surface traction to calculate the viscosity.
    As a second example, consider the pressure-driven, steady flow of an incompressible viscous fluid between two fixed parallel plates separated by a distance *2d*, as illustrated in Fig. 14.1.13. The lateral extent of the plates
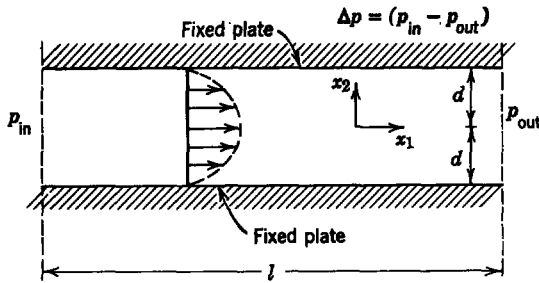
Fig. 14.1.13 Two-dimensional viscous flow.

is large enough compared with $2d$ that we can neglect edge effects. We orient our coordinate axes x_1 and x_2 so that there is no flow or variation of velocity along x_3. We assume that there is only an x_1-component of velocity and show that this satisfies the differential equations and the boundary conditions.

In this case our assumptions are

$$v_2 = v_3 = 0, \qquad \frac{\partial}{\partial x_3} = 0.$$

With these assumptions $\nabla \cdot \mathbf{v} = 0$ reduces to

$$\frac{\partial v_1}{\partial x_1} = 0, \tag{14.1.31}$$

and we can write the x_1-component of (14.1.22) as

$$0 = -\frac{\partial p}{\partial x_1} + \mu \frac{\partial^2 v_1}{\partial x_2^2}. \tag{14.1.32}$$

When we take the partial derivative of this expression with respect to x_1 and use (14.1.31), we find

$$\frac{\partial^2 p}{\partial x_1^2} = 0, \tag{14.1.33}$$

which shows that $\partial p/\partial x_1$ is constant. Setting

$$\frac{\partial p}{\partial x_1} = -\frac{\Delta p}{l}, \tag{14.1.34}$$

where Δp is the pressure difference impressed across the length l in the x_1-direction (the pressure decreases with x_1 so that the flow is in the positive x_1-direction), we can write (14.1.32) as

$$\mu \frac{\partial^2 v_1}{\partial x_2^2} = -\frac{\Delta p}{l}. \tag{14.1.35}$$

Integrating this expression twice with respect to x_2 yields

$$v_1 = -\frac{\Delta p}{2\mu l} x_2{}^2 + C_1 x_2 + C_2. \qquad (14.1.36)$$

We first use the symmetry condition that $dv_1/dx_2 = 0$ at $x_2 = 0$ to set $C_1 = 0$. We then use the boundary conditions that $v_1 = 0$ at $x_2 = \pm d$ to obtain

$$C_2 = \frac{\Delta p\, d^2}{2\mu l}.$$

The final result, referred to as *plane Poiseuille flow*, is

$$v_1 = \frac{\Delta p}{2\mu l}(d^2 - x_2{}^2). \qquad (14.1.37)$$

The parabolic velocity profile indicated by (14.1.37) is sketched in Fig. 14.1.13. It can be shown by direct substitution that this solution also satisfies the x_2- and x_3-components of (14.1.22).

14.2 ELECTROMECHANICAL COUPLING WITH VISCOUS FLUIDS

To illustrate in simple contexts how viscosity affects electromechanical coupling and vice versa we reconsider the two examples of the preceding section with electromechanical coupling added. In both cases we apply magnetic fields and assume that the fluids have high enough electrical conductivity that a quasi-static magnetic field system is the appropriate electromagnetic model.

14.2.1 Electromechanical Coupling with Shear Flow

The system to be analyzed is shown in Fig. 14.2.1*b*. It consists of two parallel, highly conducting plates, separated by an incompressible conducting liquid with conductivity σ and coefficient of viscosity μ. The plates and liquid are both nonmagnetic. The lower plate is fixed and the upper plate is moving with velocity v_o in the x_1-direction. A uniform flux density B_o is applied (by a system not shown) in the x_3-direction and a uniform current density J_o is injected in the x_2-direction. The system is operating in the steady state $(\partial/\partial t = 0)$. This is a representation of a liquid metal brush like those used in the acyclic generator of Fig. 6.4.13. (See Fig. 14.2.1*a*.) Our use of a plane geometry is a simplification based on the fact that the thickness d of the fluid is very small compared with the radius of curvature. Our analysis allows assessment of the effect of B_o on the characteristics of the brush, primarily the voltage drop of the brush and the losses, both electrical and mechanical, that heat the fluid.
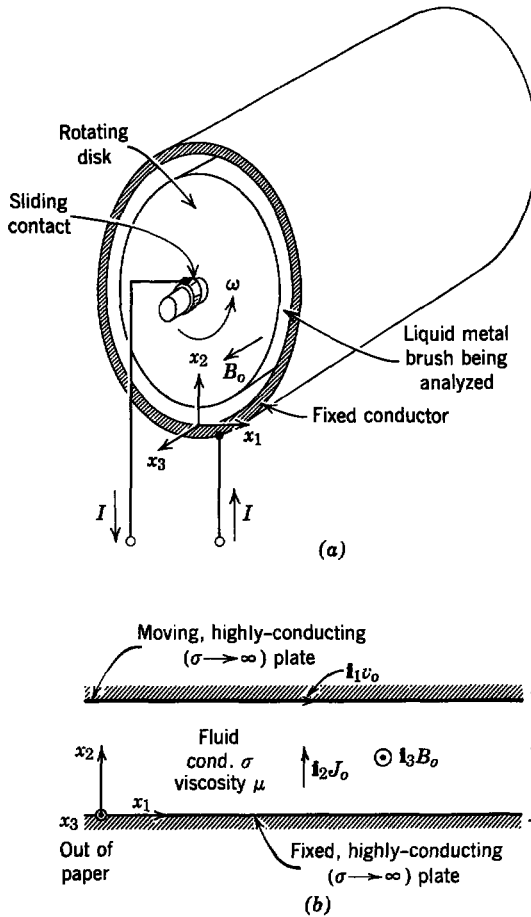
Fig. 14.2.1 Configuration for analyzing the effect of electromechanical coupling on shear flow. (a) physical system, (b) mathematical approximation.

Recognizing that this planar model is a representation of an annular system that closes on itself in the x_1-direction and that the system is symmetrical, we conclude that no properties can vary with x_1; thus

$$\frac{\partial}{\partial x_1} = 0.$$

Furthermore, the system is large enough in the x_3-direction that we can neglect end effects. The current paths external to the fluid close in such a way that the field induced by current density J_o according to Ampère's law is only in the x_1-direction. With these assumptions about the system

we can specify the relevant variables as

$$\mathbf{v} = \mathbf{i}_1 v_1(x_2), \qquad \mathbf{J} = \mathbf{i}_2 J_o \tag{14.2.1}$$

$$\mathbf{E} = \mathbf{i}_2 E_2(x_2), \qquad \mathbf{B} = \mathbf{i}_3 B_o + \mathbf{i}_1 B_1(x_3).$$

These explicit functional dependences will be shown to satisfy the relevant differential equations and boundary conditions as the analysis proceeds.

With the variables defined above and the restrictions cited earlier, the x_1-component of the momentum equation (14.1.22) is

$$0 = J_o B_o + \mu \frac{\partial^2 v_1}{\partial x_2{}^2}. \tag{14.2.2}$$

The quantities J_o, B_o, and μ are constants and v_1 varies only with x_2; consequently, (14.2.2) is integrated twice to obtain

$$v_1 = -\frac{J_o B_o}{2\mu} x_2{}^2 + C_1 x_2 + C_2, \tag{14.2.3}$$

where C_1 and C_2 are constants of integration to be determined by boundary conditions. The boundary condition of (14.1.30) which requires no slippage yields

$$\text{at} \quad x_2 = 0, \qquad v_1 = 0,$$

$$\text{at} \quad x_2 = d, \qquad v_1 = v_o.$$

The use of these two conditions to evaluate C_1 and C_2 in (14.2.3) leads to the resulting velocity

$$v_1 = v_o \frac{x_2}{d} + \frac{J_o B_o d^2}{2\mu} \frac{x_2}{d} \left(1 - \frac{x_2}{d} \right). \tag{14.2.4}$$

The first term is just the linear variation obtained in Fig. 14.1.12 with no electromechanical coupling. The second term is a parabolic profile that results from the electromechanical coupling. The second term can be positive or negative, depending on the sign of the product $J_o B_o$. The two terms in (14.2.4) are sketched with the composite profile for two conditions in Fig. 14.2.2. The $\mathbf{J} \times \mathbf{B}$ force density in the x_1-direction is uniform; consequently, the parabolic profile is expected from the results of the second example of Section 14.1.3, which was driven by a constant force density due to a pressure gradient (see Fig. 14.1.13). It is clear from Fig. 14.2.2 that the magnetic force can have a marked effect on the profile, even reversing the velocity in Fig. 14.2.2b. The profiles indicate more shear strain rate with the magnetic force than without; thus, as we shall see subsequently, we can expect increased fluid mechanical losses.

At this point it is well to note that there is an x_3 component of $\mathbf{J} \times \mathbf{B}$ ($J_o B_1$). Because B_1 is excited by J_o it depends only on x_3, thus the x_3 component
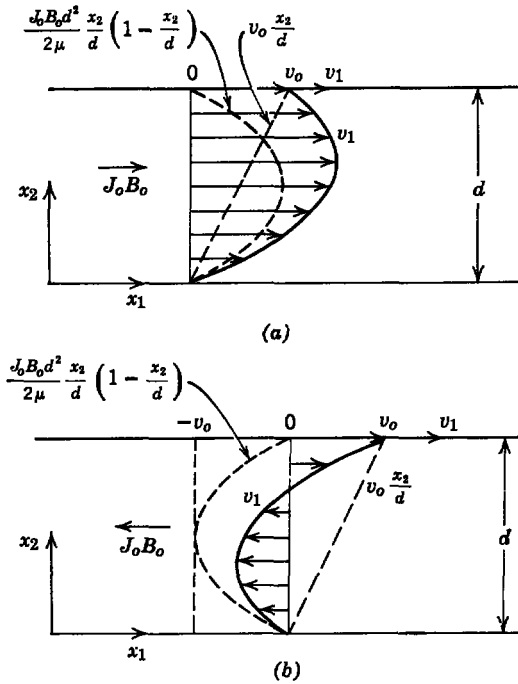
Fig. 14.2.2 Velocity profiles resulting from uniform magnetic force density applied to shear flow. The profiles are sketched for $|J_o B_o| = 8\mu v_o/d^2$: (a) $J_o B_o > 0$, $\mathbf{J} \times \mathbf{B}$ force density is in direction of v_o; (b) $J_o B_o < 0$, $\mathbf{J} \times \mathbf{B}$ force density is opposite to v_o.

of force density depends only on x_3. With end seals on the brush there can be no flow in the x_3 direction and the force density is balanced by a pressure gradient in the x_3 direction. This pressure variation will not affect the flow pattern because the fluid is incompressible.

To evaluate the system of Fig. 14.2.1 for use as a liquid metal brush for carrying current from a fixed to a moving member we must evaluate the voltage across the brush, the mechanical force needed to maintain the steady motion, and the total power input to the brush that must be removed by heat transfer to maintain acceptable brush temperature in the steady state.

Voltage V has the polarity defined in Fig. 14.2.1, and is related to the electric field intensity by

$$V = \int_0^d E_2 \, dx_2. \tag{14.2.5}$$

Ohm's law for a moving fluid (12.2.18) yields

$$E_2 = \frac{J_o}{\sigma} + v_1 B_o. \tag{14.2.6}$$

The use of this expression, with (14.2.4) for v_1, in (14.2.5) and evaluation of the integral lead to

$$V = \frac{J_o}{\sigma} d + B_o v_o \frac{d}{2} + \frac{J_o B_o^2 d^3}{12\mu}. \tag{14.2.7}$$

The first term is just the voltage that results with J_o in the fluid at rest. The second term can be interpreted as the speed voltage generated by the linear velocity variation of simple shear flow (see Fig. 14.2.2). The last term is the speed voltage generated by the parabolic velocity profile of Fig. 14.2.2.

The electrical power input p_e per unit area in an x_1-x_3-plane is found by taking the product

$$p_e = J_o V = \frac{J_o^2}{\sigma} d + J_o B_o v_o \frac{d}{2} + \frac{J_o^2 B_o^2 d^3}{12\mu}. \tag{14.2.8}$$

The first and third terms are always positive, but the second term can be negative, in which case the brush can act as an MHD generator and produce net electrical power. This is not a practical source of power, but it does indicate the nature of possible electrical characteristics of liquid metal brushes in the presence of a magnetic field.

The traction (force per unit area) that must be applied to the upper plate to maintain the steady motion is found from (14.1.29a) to be

$$\tau_1 = \mu \frac{\partial v_1}{\partial x_2}\bigg|_{x_2=d}. \tag{14.2.9}$$

The use of (14.2.4) in this expression yields

$$\tau_1 = \mu \frac{v_o}{d} - \frac{J_o B_o d}{2}. \tag{14.2.10}$$

The second term is negative because, as indicated in Fig. 14.2.2a, the $\mathbf{J} \times \mathbf{B}$ force drives the fluid faster and tries to accelerate the upper plate, thus requiring a negative component of traction to maintain steady velocity.

The mechanical input power p_m per unit area is found as

$$p_m = \tau_1 v_o = \mu \frac{v_o^2}{d} - \frac{J_o B_o v_o d}{2}. \tag{14.2.11}$$

Once again the brush may actually produce net mechanical power.

To find the total power per unit area p_t put into the brush electrically and mechanically we add (14.2.8) and (14.2.11) to obtain the result.

$$p_t = p_e + p_m = \frac{J_o^2}{\sigma} d + \mu \frac{v_o^2}{d} + \frac{J_o^2 B_o^2 d^3}{12\mu}. \tag{14.2.12}$$

The total power input is always positive, even though (14.2.8) and (14.2.11) indicate that there may be net electrical output or net mechanical output.

In (14.2.12) the first term is simply the Joule loss associated with current in the conducting fluid; the second term is the viscous loss that would result from simple shear flow; and the third term results from the electromechanical coupling.

It should be clear from the form of (14.2.12) that for a system in which the quantities σ, μ, J_o, v_o, and B_o are known there is a brush thickness that minimizes brush losses. This optimum brush thickness can be found by a straightforward application of differential calculus. We shall not carry out this process here. Rather, we shall assume liquid metal brush parameters typical of configurations used in practice and compare the brush properties with those of carbon brushes. At the same time we shall assess the effects of electromechanical coupling on the liquid metal brush.

The parameters assumed for the liquid metal brush are given in Table 14.2.1. Substitution of these quantities into (14.2.7) and (14.2.12) yields

$$V = 0.015 + 0.15B_o + 83.3B_o^2 \text{ V},$$

$$p_t = 2.26 \times 10^4 + 1.25 \times 10^8 B_o^2 \text{ W/m}^2.$$

Table 14.2.1 Parameters Assumed for Liquid Metal Brush

Material	Mercury
Conductivity	$\sigma = 10^6$ mhos/m
Viscosity	$\mu = 1.5 \times 10^{-3}$ kg/m-sec
Current density	$J_o = 1.5 \times 10^6$ A/m^2
Velocity	$v_o = 30$ m/sec
Brush thickness	$d = 10^{-2}$ m

These two quantities are plotted on logarithmic scales as functions of flux density B_o in Fig. 14.2.3. The characteristics of a metal-graphite brush of the type normally used for slip rings* are also shown. The metal-graphite brush operates at only *one tenth* the current density of the liquid metal brush; thus for the same total current the solid brush will require 10 times as much contact area. At very low flux density the liquid metal brush has a voltage drop roughly two orders of magnitude lower than that of a solid brush, and the power loss per unit area is three orders of magnitude lower. When the flux density gets to the range of 0.1 to 1 Wb/m^2 the liquid metal brush performance deteriorates rapidly as flux density increases. The curves of Fig. 14.2.3 demonstrate clearly the superiority of liquid metal brushes with respect to contact drop and losses, but they also demonstrate that magnetic fields can degrade the liquid metal brush performance markedly.

In this example we have demonstrated how electromechanical coupling

---

* The characteristics of the metal-graphite brush were taken from *Standard Handbook for Electrical Engineers*, A. E. Knowlton, ed., McGraw-Hill, New York, 9th ed., 1957, Sections 4-234 and 8-120.
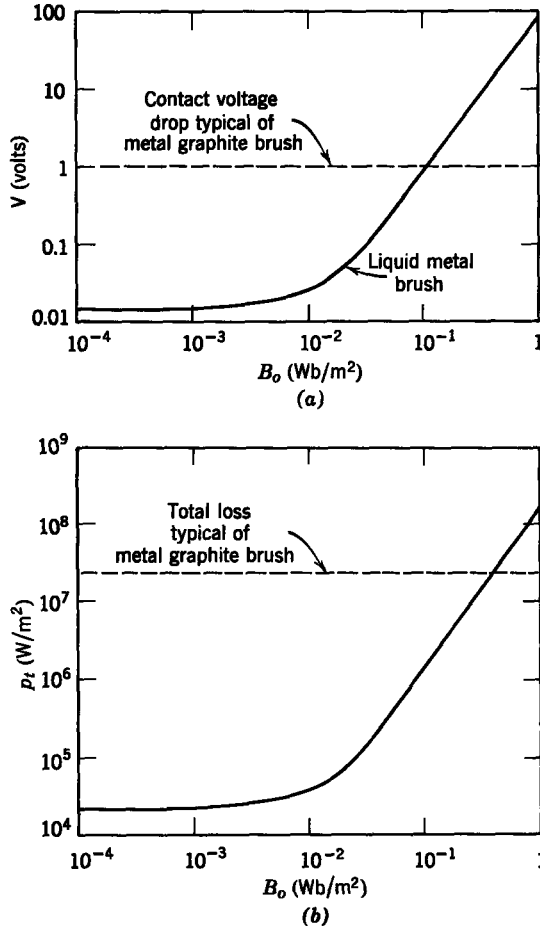
Fig. 14.2.3 Voltage and brush loss as functions of applied flux density for liquid metal brushes compared with metal graphite brushes: (a) brush voltage; (b) total brush loss.

can have a considerable effect on the behavior of a fluid mechanical system in a configuration of practical significance. In the next section we treat another configuration in which electromechanical coupling can have significant effects.

14.2.2 Electromechanical Coupling with Pressure-Driven Flow (Hartmann Flow)

In this section we consider the effects of viscosity on fluid flow in a rectangular channel. The electrical conductivity of the fluid is high enough to justify a magnetic field system model and the fluid is subjected to transverse magnetic field and current. Thus this example allows us to assess the effects
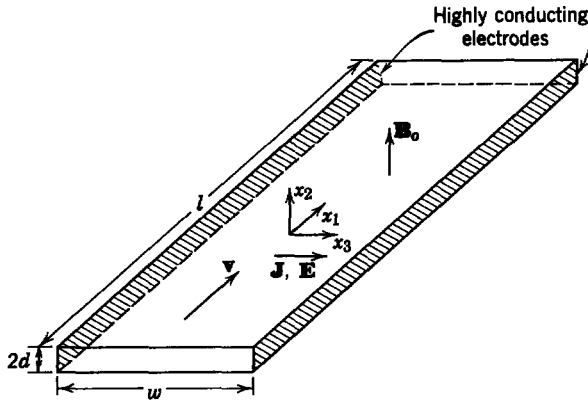
Fig. 14.2.4   Configuration for studying Hartmann flow.

of viscosity on the conduction-type MHD machines considered in Chapters 12 and 13 and to determine the conditions under which the inviscid fluid models used there are accurate.

The flow pattern to be analyzed is conventionally called *Hartmann flow* and will be studied in the configuration of Fig. 14.2.4. The channel has a length *l*, a width *w*, and a depth *2d*. The aspect ratio of the channel is quite large

$$\frac{w}{2d} \gg 1,$$

and we are interested in the flow properties near the center of the channel. Thus we can neglect variations with x_3. The sides of the channel that lie in the x_1-x_2 planes are highly conducting electrodes and can be connected to an external circuit with the result that there can be net current flow across any x_1-x_2 plane.

The fluid is assumed to be incompressible with coefficient of viscosity μ and electrical conductivity σ. There is an applied flux density $\mathbf{B}_o$,

$$\mathbf{B}_o = \mathbf{i}_2 B_o, \qquad\qquad (14.2.13)$$

and we assume that the magnetic flux density due to current flow in the fluid is negligible compared to B_o (low magnetic Reynolds number). We also assume steady flow.

We neglect end effects, and thus we are considering the two-dimensional problem in Fig. 14.2.5. The symmetry of the simplified problem allows us to assume the following forms for the variables:

$$\mathbf{v} = \mathbf{i}_1 v_1(x_2), \qquad\qquad (14.2.14a)$$

$$\mathbf{E} = \mathbf{i}_3 E_3(x_2), \qquad\qquad (14.2.14b)$$

$$\mathbf{J} = \mathbf{i}_3 J_3(x_2). \qquad\qquad (14.2.14c)$$
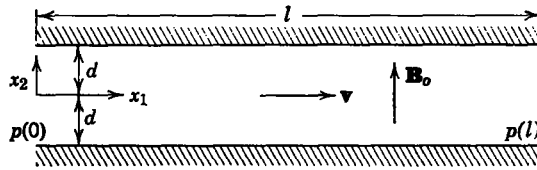
Fig. 14.2.5 Two-dimensional configuration for Hartmann flow.

All of these variables are functions of x_2 only, as indicated. It should be clear at this point that our example is simply the one shown in Fig. 14.1.13 with the addition of a magnetic force density. Thus we expect our result to be similar to and interpretable in terms of the results given in Fig. 14.1.13. From Faraday's law (1.1.5)* we obtain

$$\frac{dE_3}{dx_2} = 0, \tag{14.2.15}$$

from which we obtain

$$E_3 = \text{constant.} \tag{14.2.16}$$

The x_3-component of Ohm's law, (12.2.18) is

$$J_3 = \sigma(E_3 + v_1 B_o). \tag{14.2.17}$$

The x_1-component of the momentum equation (14.1.22) is

$$0 = -\frac{\partial p}{\partial x_1} + \mu \frac{d^2 v_1}{dx_2^2} - J_3 B_o. \tag{14.2.18}$$

Recognizing that J_3 and v_1 are not functions of x_1, we differentiate (14.2.18) with respect to x_1 to obtain

$$\frac{\partial^2 p}{\partial x_1^2} = 0, \tag{14.2.19}$$

which shows that

$$\frac{\partial p}{\partial x_1} = \text{constant.} \tag{14.2.20}$$

Denoting the pressure drop over the length of the channel as Δp,

$$\Delta p = p(0) - p(l), \tag{14.2.21}$$

we can write (14.2.20)

$$\frac{\partial p}{\partial x_1} = -\frac{\Delta p}{l}. \tag{14.2.22}$$

Compare these results with (14.1.33) and (14.1.34). We assume that Δp is

* Table 1.2, Appendix G.

maintained constant by external means; thus it represents an independent input to the system.

We now substitute (14.2.17) and (14.2.22) in (14.2.18) and rearrange the resulting expression to obtain

$$\frac{d^2v_1}{dx_2^{\,2}} - \frac{\sigma B_o^{\,2}}{\mu} v_1 = -\frac{\Delta p}{\mu l} + \frac{\sigma B_o E_3}{\mu}. \tag{14.2.23}$$

Equation 14.2.16 indicates that E_3 is constant; thus we can solve this linear differential equation with constant coefficients to obtain, in general,

$$v_1 = C_1 \sinh M \frac{x_2}{d} + C_2 \cosh M \frac{x_2}{d} + \frac{\Delta p}{\sigma B_o^{\,2} l} - \frac{E_3}{B_o}, \tag{14.2.24}$$

where we have defined the *Hartmann number* M as

$$M = B_o d \left(\frac{\sigma}{\mu}\right)^{\frac{1}{2}}. \tag{14.2.25}$$

We must now apply the boundary condition that at

$$x_2 = \pm d, \qquad v_1 = 0. \tag{14.2.26}$$

This imposes the requirement that v_1 be an even function of x_2; thus

$$C_1 = 0, \tag{14.2.27}$$

and the constant C_2 is then given by

$$C_2 = \frac{-1}{\cosh M} \left(\frac{\Delta p}{\sigma B_o^{\,2} l} - \frac{E_3}{B_o}\right). \tag{14.2.28}$$

We now use (14.2.27) and (14.2.28) to write (14.2.24) as

$$v_1 = \left(\frac{\Delta p}{\sigma B_o^{\,2} l} - \frac{E_3}{B_o}\right)\left[1 - \frac{\cosh M(x_2/d)}{\cosh M}\right]. \tag{14.2.29}$$

To complete the solution for the velocity profile we must specify the value of the electric field E_3. We can fix E_3 by the application of a terminal voltage as we did in Section 12.2.1a. Alternatively, we can fix E_3 by constraining the total current that can flow across an x_1-x_2 plane. To complete the present example we assume that the external terminals are open-circuited; the result is no net current across an x_1-x_2 plane. Mathematically, this requirement can be written as

$$\int_{-d}^{d} J_3 \, dx_2 = 0. \tag{14.2.30}$$

We use (14.2.17) with this expression to obtain

$$E_3 = -\frac{B_o}{2d}\int_{-d}^{d} v_1\, dx_2. \tag{14.2.31}$$

We now use (14.2.29) in (14.2.31), evaluate the integral, and solve for E_3 to obtain

$$E_3 = -\frac{\Delta p}{\sigma l B_o}\left(\frac{M\cosh M - \sinh M}{\sinh M}\right). \tag{14.2.32}$$

Substitution of (14.2.32) into (14.2.29) and simplification yield

$$v_1 = \frac{\Delta p}{\sigma B_o^2 l}\left\{\frac{M[\cosh M - \cosh M(x_2/d)]}{\sinh M}\right\}. \tag{14.2.33}$$

It will be easy to interpret our results if we assume that the mechanica properties are fixed and vary the applied magnetic field to vary M. For this purpose it is more useful to write (14.2.33) in the form

$$v_1 = \frac{\Delta p\, d^2}{\mu l}\left[\frac{\cosh M - \cosh M(x_2/d)}{M\sinh M}\right]. \tag{14.2.34}$$

As a check on this expression, it is easily verified that the limit taken as $M \to 0$ yields the same velocity profile as in the second example of Section 14.1.3 (see Fig. 14.1.13). This is as it should be, for when $M \to 0$ in (14.2.34) this profile is achieved by eliminating electrical and retaining only viscous effects.

To interpret the meaning of the profile shape of (14.2.34) we assume a system of fixed dimensions, with a fluid of fixed properties and constrain the pressure drop Δp to be fixed. We now vary the applied flux density B_o and ask how the shape of the profile changes. Such changes are indicated in Fig. 14.2.6, in which the profiles are plotted for three values of M. Note that the profile for $M = 0$ is the same as that plotted in Fig. 14.1.13.

To interpret the results of Fig. 14.2.6 we observe first that in the absence of electromagnetic forces the velocity profile is parabolic. This is the profile given with viscous effects alone. When electromagnetic forces are present, any local variation of velocity will generate circulating currents that interact with the applied magnetic field to reduce the local velocity variations. Thus the presence of the applied magnetic field tends to make the velocity uniform. When the applied magnetic field is large (M large), the velocity is uniform near the center of the channel and varies appreciably in the vicinity of the walls where the velocity must go to zero. Whether the velocity profile is flat or parabolic depends on the value of the Hartmann number M given by (14.2.25) as

$$M = B_o\, d\left(\frac{\sigma}{\mu}\right)^{1/2}.$$
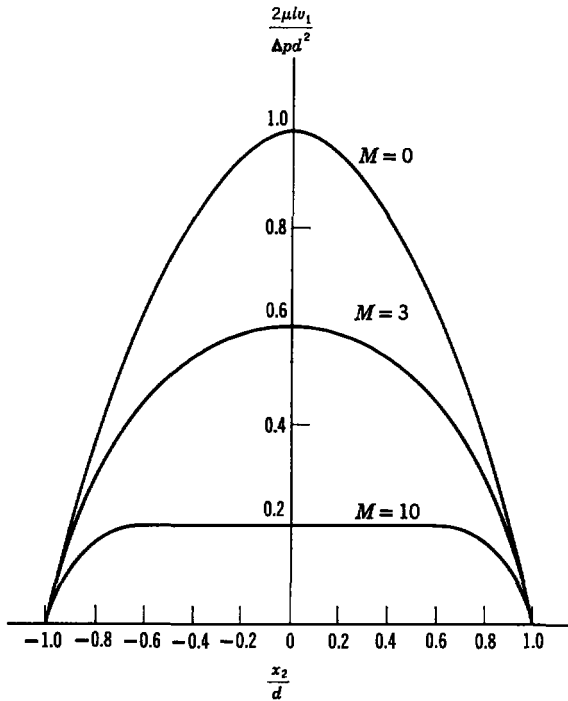
Fig. 14.2.6   Variation of velocity profile with Hartmann number.

For low values of M viscous forces predominate and the profile tends to be parabolic. For high values of M electromagnetic forces predominate and the velocity profile tends to be flat. Thus the Hartmann number is interpreted as a measure of the relative magnitude of electromagnetic and viscous forces. It is clear that for high values of M the model of uniform flow velocity used earlier in Section 12.2.1a is valid over most of the channel width. We consider this situation subsequently with more precision.

It is evident from the curves of Fig. 14.2.6 that with a fixed pressure drop the volume flow rate of the fluid is reduced by the presence of an applied magnetic field. If we designate the volume flow rate by $\dot{V}_{ol}$, it is given by

$$\dot{V}_{ol} = w \int_{-d}^{d} v_1 \, dx_2 \text{ m}^3/\text{sec.} \tag{14.2.35}$$

We now use (14.2.34) in this expression, perform the integration, and simplify to obtain

$$\dot{V}_{ol} = \frac{2\Delta p \, d^3 w}{3\mu l} \left[\frac{3}{M^2} (M \coth M - 1) \right]. \tag{14.2.36}$$

$$\frac{3\mu l \dot{V}_{ol}}{2\Delta p d^3 w}$$
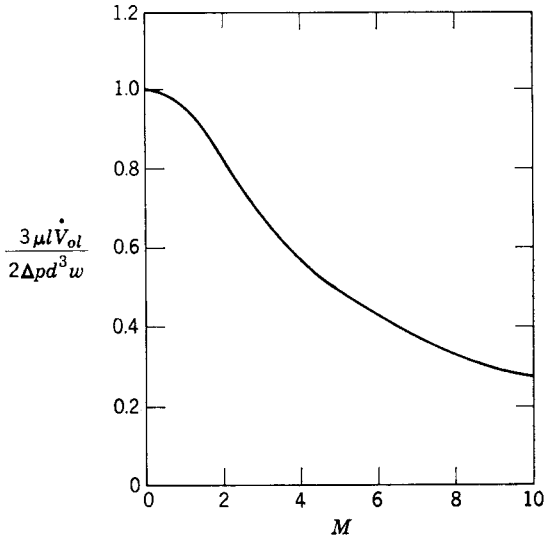
Fig. 14.2.7 Variation of volume flow rate with Hartmann number.

In the limit as $M \to 0$ the volume flow rate becomes

$$(\dot{V}_{ol})_{M=0} = \frac{2\Delta p \, d^3 w}{3\mu l},$$

which is the volume flow rate in the presence of viscous forces only. The expression of (14.2.36), normalized to the value for $M \to 0$,

$$\frac{3\mu l \dot{V}_{ol}}{2\Delta p \, d^3 w} = \frac{3}{M^2}(M \coth M - 1), \qquad (14.2.37)$$

is plotted as a function of M in Fig. 14.2.7. It is evident from the curve of Fig. 14.2.7 that the presence of a magnetic field that yields an appreciable Hartmann number will markedly reduce the volume flow rate for a given pressure drop.

To ascertain the order of magnitude of Hartmann number that can be obtained with real conducting fluids consider liquid mercury which has

$$\sigma = 10^6 \text{ mhos/m}, \qquad \mu = 1.5 \times 10^{-3} \text{ kg/m-sec}$$

If we consider a system with a channel depth of 2 cm,

$$d = 10^{-2} \text{ m},$$

and an applied flux density of

$$B_o = 1 \text{ Wb/m}^2 = 10{,}000 \text{ gauss},$$

the resulting Hartmann number is

$$M = 260.$$

Thus the flow of mercury under these conditions is very strongly affected by electromagnetic forces. The same is true of other liquid metals.

Alternatively, a seeded combustion gas would be used in the variable-area channel considered in Section 13.2.2. This system would have approximately the following constants,

$$\sigma = 40 \text{ mhos/m}, \qquad \mu = 10^{-5} \text{ kg/m-sec},$$
$$B_o = 4 \text{ Wb/m}^2, \qquad d = 10^{-1} \text{ m},$$

and a Hartmann number

$$M = 800.$$

Thus, even with an ionized gas with its very small conductivity, this large Hartmann number indicates that magnetic forces predominate over viscous forces.

To be more precise about how viscosity affects a conduction-type MHD machine we remove the constraint of no net current and operate the system in Fig. 14.2.4 as we did the MHD machine in Section 12.2.1a. In the present system the channel depth is $2d$, whereas in Fig. 12.2.3 the channel depth is d. Redefining the quantities for the inviscid fluid model to account for this difference, we have [see (12.2.21), (12.2.22), and (12.2.24)] for the inviscid model

$$\text{internal resistance,} \qquad R_i = \frac{w}{2\sigma l d}, \qquad (14.2.38)$$

$$\text{voltage equation,} \qquad IR_i = v_o B_o w - V, \qquad (14.2.39)$$

$$\text{pressure drop,} \qquad \Delta p = \frac{IB}{2d}, \qquad (14.2.40)$$

where I and V are defined in Fig. 14.2.4 and v_o is the fluid velocity for an inviscid fluid model.

We now remove the constraint of no net current (14.2.30) and instead specify that the electric field intensity be given in terms of the terminal voltage as

$$E_3 = -\frac{V}{w}. \qquad (14.2.41)$$

From Ohm's law (14.2.17) the current density becomes

$$J_3 = \sigma\left(-\frac{V}{w} + v_1 B_o\right) \qquad (14.2.42)$$

and the terminal current is

$$I = \int_{-d}^{d} J_3 l \, dx_2. \tag{14.2.43}$$

Substitution of (14.2.42) into (14.2.43) yields

$$I = -\frac{V}{R_i} + \sigma l B_o \int_{-d}^{d} v_1 \, dx_2. \tag{14.2.44}$$

When the space average velocity is defined

$$\langle v_1 \rangle = \frac{1}{2d} \int_{-d}^{d} v_1 \, dx_2, \tag{14.2.45}$$

we can write (14.2.44) in the form

$$IR_i = -V + B_o w \langle v_1 \rangle. \tag{14.2.46}$$

This expression is the same as (14.2.39) for the inviscid model except that v_o for the inviscid case is replaced by average velocity in the viscous case.

The most important aspect of viscosity in an MHD machine is how much of the pressure gradient goes into viscous losses and how much is balanced by the magnetic force density. To answer this question we evaluate the average velocity by using (14.2.29) in (14.2.45) to obtain

$$\langle v_1 \rangle = \left(\frac{\Delta p}{\sigma B_o^2 l} + \frac{V}{B_o w} \right) \left(1 - \frac{\tanh M}{M} \right). \tag{14.2.47}$$

The use of this result in (14.2.46) and solution for Δp yield

$$\Delta p = \frac{B_o I / 2d + (B_o \sigma l V / w)(\tanh M / M)}{1 - \tanh M / M}. \tag{14.2.48}$$

Noting that the first term in the numerator is the pressure drop in an inviscid machine, as given by (14.2.40), we write the ratio

$$\frac{\Delta p}{\Delta p_i} = \frac{1 + (V / IR_i)(\tanh M / M)}{1 - \dfrac{\tanh M}{M}}, \tag{14.2.49}$$

where Δp_i is the ideal pressure drop given by (14.2.40). This ratio is plotted as a function of Hartmann number M in Fig. 14.2.8 with

$$\frac{V}{IR_i} = 1,$$

which is the condition for maximum electrical power extraction from the flowing fluid. Note that the Hartmann number axis is a logarithmic scale.
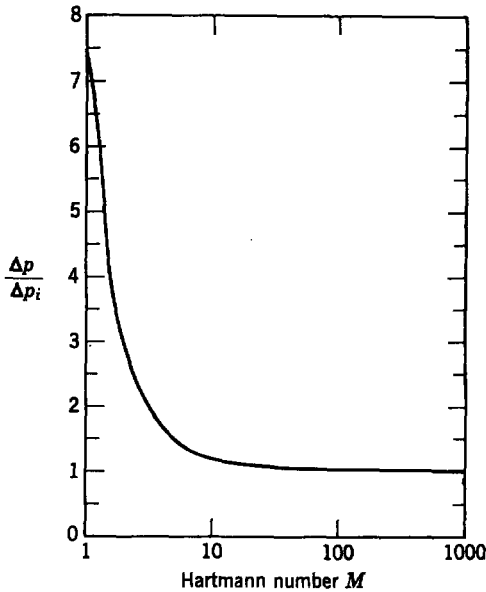
Fig. 14.2.8   Ratio of actual pressure drop and ideal pressure drop for an MHD generator loaded to extract maximum electric power.

It is clear that the error is large for a small Hartmann number with a pressure drop 22 per cent more than the ideal for $M = 10$. At $M = 100$ the error is 2 per cent, and at $M = 1000$ the error is 0.2 per cent. This shows that for a Hartmann number of the order of 100 or larger the inviscid fluid model used to analyze MHD machines in Chapters 12 and 13 is quite accurate with respect to the neglect of the effects of viscosity.

14.3   DISCUSSION

In this chapter we have added the effects of viscosity to the mathematical description of incompressible fluids. In the process we have indicated how this description is modified for compressible fluids. We have analyzed and discussed two applications of the equations to steady flow problems in which viscous effects and electromechanical coupling compete; and one or the other can predominate, depending on the relative values of the critical parameters.

It is a straightforward process to extend the techniques of this chapter to dynamic situations; for example, we can use the description of viscosity in this chapter to study viscous damping of the Alfvèn waves defined and analyzed in a lossless system in Section 12.2.3.

PROBLEMS

14.1. Rework the example of Sec. 14.2.1 with the applied flux density in the x_2 direction. Assume that no current can flow in the x_3 direction. In particular obtain expressions for velocity profile (like Eq. 14.2.4), voltage (like Eq. 14.2.7), traction (like Eq. 14.2.10), and total power per unit area (like Eq. 14.2.12). Make plots of voltage and loss per unit area for the constants of Table 14.2.1 and compare the results with those plotted in Fig. 14.2.3.

14.2. A viscous liquid flows through a circular pipe, as shown in Fig. 14P.2. At the inlet the pressure is uniform and equal to p_1, and at the outlet it is still uniform, but p_2. The volume rate of flow is $Q m^3/\text{sec}$. Under the assumption that the flow is axisymmetric and steady and that the velocity is low enough that the fluid can be considered incompressible, find the velocity profile $v_z(r)$. *Hint.* Look for solutions where $\mathbf{v} = v_z(r)\mathbf{i}_z$ and $p = p(z)$.
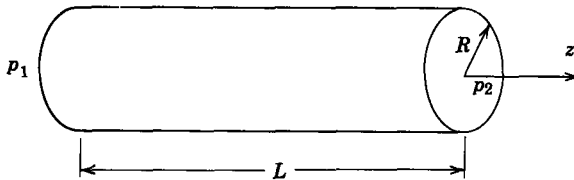
Fig. 14P.2

14.3. The channel shown in Fig. 14P.3 contains a viscous fluid of conductivity σ moving in the x_1-direction. You are to analyze this problem using the Hartmann flow solutions (Section 14.2.2). The highly conducting electrodes are connected by a load resistance R.

    (a) Given the pressure drop from inlet to outlet, the dimensions of the system, field B_0, and conductivity σ, what is the power dissipated in the resistance?

    (b) What value of R should be used to dissipate the largest possible power in the load?

    (c) If the fluid is mercury, $B_0 = 20,000$ gauss, $d = 1$ cm, $l = 1$ m, and $w = 10$ cm, what is the Hartmann number? What is the value of the optimum resistance found in part (b)?
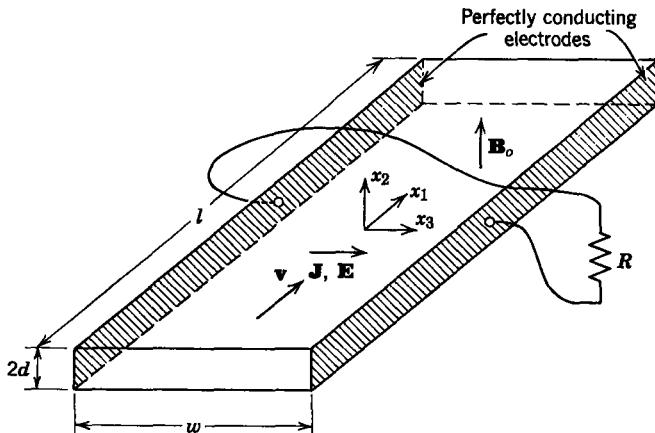
Fig. 14P.3

Appendix F

GLOSSARY OF COMMONLY USED SYMBOLS

Section references indicate where symbols of a given significance are introduced; grouped symbols are accompanied by their respective references. The absence of a section reference indicates that a symbol has been applied for a variety of purposes. Nomenclature used in examples is not included.

Symbol	Meaning	Section
A	cross-sectional area	
A_i	coefficient in differential equation	5.1.1
(A_n^+, A_n^-)	complex amplitudes of components of nth mode	9.2.1
A_w	cross-sectional area of armature conductor	6.4.1
a	spacing of pole faces in magnetic circuit	8.5.1
$a, (a_c, a_s)$	phase velocity of acoustic related waves	13.2.1, 11.4.1
a_b	Alfvén velocity	12.2.3
(a, b, c)	Lagrangian coordinates	11.1
a_i	constant coefficient in differential equation	5.1.1
$\mathbf{a}_p$	instantaneous acceleration of point p fixed in material	2.2.1c
B, B_r, B_s	damping constant for linear, angular and square law dampers	2.2.1b, 4.1.1, 5.2.2
$\mathbf{B}, \mathbf{B}_i, B_0$	magnetic flux density	1.1.1a, 8.1, 6.4.2
B_i	induced flux density	7.0
$(B_r, B_{ra}, B_{rb}, B_{rm})$	radial components of air-gap flux densities	4.1.4
$[B_{rf}, (B_{rf})_{av}]$	radial flux density due to field current	6.4.1
b	width of pole faces in magnetic circuit	8.5
b	half thickness of thin beam	11.4.2b
C	contour of integration	1.1.2a
$C, (C_a, C_b), C_0$	capacitance	2.1.2, 7.2.1a, 5.2.1
C	coefficient in boundary condition	9.1.1
$\mathbf{C}$	the curl of the displacement	11.4
(C^+, C^-)	designation of characteristic lines	9.1.1

Symbol	Meaning	Section
c_p	specific heat capacity at constant pressure	13.1.2
c_v	specific heat capacity at constant volume	13.1.2
$\mathbf{D}$	electric displacement	1.1.1a
d	length	
da	elemental area	1.1.2a
$d\mathbf{f}_n$	total elemental force on material in rigid body	2.2.1c
$d\mathbf{l}$	elemental line segment	1.1.2a
$d\mathbf{T}_n$	torque on elemental volume of material	2.2.1c
dV	elemental volume	1.1.2b
E	constant of motion	5.2.1
E	Young's modulus or the modulus of elasticity	9.1
$\mathbf{E}, E_o$	electric field intensity	1.1.1a, 5.1.2d
E_f	magnitude of armature voltage generated by field current in a synchronous machine	4.1.6a
E_i	induced electric field intensity	7.0
e_{11}, e_{ij}	strain tensor	9.1, 11.2
$\dot{e}_{ij}$	strain-rate tensor	14.1.1a
F	magnetomotive force (mmf)	13.2.2
$\mathbf{F}$	force density	1.1.1a
$\hat{F}$	complex amplitude of $f(t)$	5.1.1
F_0	amplitude of sinusoidal driving force	9.1.3
f	equilibrium tension of string	9.2
f	driving function	5.1.1
$f, \mathbf{f}, f^e, f^s, f_j, f_i, f_1$	force	2.2.1, 2.2.1c, 3.1, 5.1.2a, 3.1.2b, 8.1, 9.1
f	arbitrary scalar function	6.1
f'	scalar function in moving coordinate system	6.1
f	three-dimensional surface	6.2
f	integration constant	11.4.2a
G	a constant	5.1.2c
G	shear modulus of elasticity	11.2.2
G	speed coefficient	6.4.1
G	conductance	3.1
g	air-gap length	5.2.1
$g, \mathbf{g}$	acceleration of gravity	5.1.2c, 12.1.3
$(\mathbf{H}, H_x, H_y, H_z)$	magnetic field intensity	1.1.1a
h	specific enthalpy	13.1.2
$\mathbf{I}, I, (I_r, I_s), I_f$	electrical current	10.4.3, 12.2.1a, 4.1.2, 6.4.1
$(i, i_1, i_2, \ldots, i_k),$ $(i_{ar}, i_{as}, i_{br}, i_{bs}),$ $i_a, (i_a, i_b, i_c),$ $(i_f, i_t), (i_r, i_s)$	electrical current	2.1, 4.1.3, 6.4.1, 4.1.7, 6.4.1, 4.1

Symbol	Meaning	Section
$\mathbf{i}_n$	unit vector perpendicular to area of integration	6.2.1
$\mathbf{i}_s$	unit vector normal to surface of integration	6.2.1
$(\mathbf{i}_x, \mathbf{i}_y, \mathbf{i}_z)$, $(\mathbf{i}_1, \mathbf{i}_2, \mathbf{i}_3)$	unit vectors in coordinate directions	2.2.1c
J, $\mathbf{J}_f$	current density	7.0, 1.1.1a
J, J_r, (J_x, J_y, J_z)	moment of inertia	5.1.2b, 4.1.1, 2.2.1c
J_{xz}, J_{yz}	products of inertia	2.2.1c
j	$\sqrt{-1}$	4.1.6a
K	loading factor	13.2.2
K, $\mathbf{K}_f$	surface current density	7.0, 1.1.1a
K	linear or torsional spring constant	2.2.1a
K_i	induced surface current density	7.0
k, k_c, (k_r, k_i)	wavenumber	7.1.3, 10.1.3, 10.0
k	summation index	2.1.1
k	maximum coefficient of coupling	4.1.6b
k_n	nth eigenvalue	9.2
(L, L_1, L_2), (L_a, L_f), L_m, (L_0, L_2), (L_r, L_s, L_{sr}), L_{ss}	inductance	2.1.1, 6.4.1, 2.1.1, 4.2.1, 4.1.1, 4.2.4
L	length of incremental line segment	6.2.1
l	value of relative displacement for which spring force is zero	2.2.1a
l, l_w, l_y	length	
M	Hartmann number	14.2.2
M	mass of one mole of gas in kilograms	13.1.2
M	Mach number	13.2.1
M	mass	2.2.1c
M	number of mechanical terminal pairs	2.1.1
M, M_s	mutual inductance	4.1.1, 4.2.4
$\mathbf{M}$	magnetization density	1.1.1a
m	mass/unit length of string	9.2
N	number of electrical terminal pairs	2.1.1
N	number of turns	5.2.2
n	number density of ions	12.3.1
n	integer	7.1.1
$\mathbf{n}$	unit normal vector	1.1.2
$\mathbf{P}$	polarization density	1.1.1a
P	power	12.2.1a
p	number of pole pairs in a machine	4.1.8
p	power per unit area	14.2.1
p	pressure	5.1.2d and 12.1.4
P_e, P_g, P_m, P_r	power	4.1.6a, 4.1.6b, 4.1.2, 4.1.6b
Q	electric charge	7.2.1a
q, q_i, q_k	electric charge	1.1.3 and 2.1.2, 8.1, 2.1.2
R, R_i, R_o	radius	

Symbol	Meaning	Section
$R, R_a, R_b, R_f, R_r, R_s$	resistance	
(R, R_g)	gas constant	13.1.2
R_e	electric Reynolds number	7.0
R_m	magnetic Reynolds number	7.0
r	radial coordinate	
$\mathbf{r}$	position vector of material	2.2.1c
$\mathbf{r}'$	position vector in moving reference frame	6.1
$\mathbf{r}_m$	center of mass of rigid body	2.2.1c
S	reciprocal modulus of elasticity	11.5.2c
S	surface of integration	1.1.2a
S	normalized frequency	7.2.4
S	membrane tension	9.2
S_z	transverse force/unit length acting on string	9.2
s	complex frequency	5.1.1
(s, s_{mT})	slip	4.1.6b
s_i	ith root of characteristic equation, a natural frequency	5.1.1
T	period of oscillation	5.2.1
T	temperature	13.1.2
$\mathbf{T}, T, T^e, T_{em}, T_m, T_0, T_1$	torque	2.2.1c, 5.1.2b, 3.1.1, 4.1.6b, 4.1.1, 6.4.1, 6.4.1
$\mathbf{T}$	surface force	8.4
$T_{ij}{}^m$	mechanical stress tensor	13.1.2
T_{mn}	the component of the stress-tensor in the mth-direction on a cartesian surface with a normal vector in the nth-direction	8.1
T_{or}	constant of coulomb damping	4.1.1
T_o	initial stress distribution on thin rod	9.1.1
T	longitudinal stress on a thin rod	9.1.1
T_z	transverse force per unit area on membrane	9.2
T_2	transverse force per unit area acting on thin beam	11.4.2b
t	time	1.1.1
t'	time measured in moving reference frame	6.1
U	gravitational potential	12.1.3
U	longitudinal steady velocity of string or membrane	10.2
u	internal energy per unit mass	13.1.1
u	surface coordinate	11.3
$u_0(x - x_0)$	unit impulse at $x = x_0$	9.2.1
u	transverse deflection of wire in x-direction	10.4.3
$u_{-1}(t)$	unit step occurring at $t = 0$	5.1.2b
V, V_m	velocity	7.0, 13.2.3
V	volume	1.1.2
V, V_a, V_f, V_o, V_s	voltage	
V	potential energy	5.2.1

Symbol	Meaning	Section
v, $\mathbf{v}$	velocity	
$(v, v_1, \ldots, v_k)$	voltage	2.1.1
v', (v_a, v_b, v_c), v_f, v_{oc}, v_t	voltage	
v_n	velocity of surface in normal direction	6.2.1
v_o	initial velocity distribution on thin rod	9.1.1
v_p	phase velocity	9.1.1 and 10.2
$\mathbf{v}^r$	relative velocity of inertial reference frames	6.1
v_s	$\sqrt{f/m}$ for a string under tension f and having mass/unit length m	10.1.1
v	longitudinal material velocity on thin rod	9.1.1
v	transverse deflection of wire in y-direction	10.4.3
(W_e, W_m)	energy stored in electromechanical coupling	3.1.1
(W_e', W_m', W')	coenergy stored in electromechanical coupling	3.1.2b
W''	hybrid energy function	5.2.1
w	width	5.2.2
w	energy density	11.5.2c
w'	coenergy density	8.5
X	equilibrium position	5.1.2a
$(x, x_1, x_2, \ldots, x_k)$	displacement of mechanical node	2.1.1
x	dependent variable	5.1.1
x_p	particular solution of differential equation	5.1.1
(x_1, x_2, x_3), (x, y, z)	cartesian coordinates	8.1, 6.1
(x', y', z')	cartesian coordinates of moving frame	6.1
(α, β)	constants along C^+ and C^- characteristics, respectively	9.1.1
(α, β)	see (10.2.20) or (10.2.27)	
α	transverse wavenumber	11.4.3
(α, β)	angles used to define shear strain	11.2
(α, β)	constant angles	4.1.6b
α	space decay parameter	7.1.4
α	damping constant	5.1.2b
α	equilibrium angle of torsional spring	2.2.1a
γ	ratio of specific heats	13.1.2
γ	piezoelectric constant	11.5.2c
$\gamma, \gamma_0, \gamma'$	angular position	
$\Delta_d(t)$	slope excitation of string	10.2.1b
Δ_0	amplitude of sinusoidal slope excitation	10.2.1b
$\Delta \mathbf{r}$	distance between unstressed material points	11.2.1a
$\Delta \mathbf{s}$	distance between stressed positions of material points	11.2.1a
$\delta(\ )$	incremental change in ( )	8.5
$\delta, \delta_1, \delta_0$	displacement of elastic material	11.1, 9.1, 11.4.2a
δ	thickness of incremental volume element	6.2.1
δ	torque angle	4.1.6a

Symbol	Meaning	Section
δ_{ij}	Kronecker delta	8.1
(δ_+, δ_-)	wave components traveling in the	
	$\pm x$-directions	9.1.1
ϵ	linear permittivity	1.1.1b
ϵ_0	permittivity of free space	1.1.1a
η	efficiency of an induction motor	4.1.6b
η	second coefficient of viscosity	14.1.1c
$\theta, \theta_i, \theta_m$	angular displacement	2.1.1, 3.1.1, 5.2.1
θ	power factor angle; phase angle between	
	current and voltage	4.1.6a
θ	equilibrium angle	5.2.1
$\dot{\theta}$	angular velocity of armature	6.4.1
θ_m	maximum angular deflection	5.2.1
$(\lambda, \lambda_1, \lambda_2, \ldots, \lambda_k)$	magnetic flux linkage	2.1.1, 6.4.1, 4.1.7,
λ_a		4.1.3, 4.1
$(\lambda_a, \lambda_b, \lambda_c)$		
$(\lambda_{ar}, \lambda_{as}, \lambda_{br}, \lambda_{bs})$		
(λ_r, λ_s)		
λ	Lamé constant for elastic material	11.2.3
λ	wavelength	7.1.4
μ	linear permeability	1.1.1a
$\mu, (\mu_+, \mu_-)$	mobility	12.3.1, 1.1.1b
μ	coefficient of viscosity	14.1.1
μ_d	coefficient of dynamic friction	2.2.1b
μ_0	permeability of free space	1.1.1a
μ_s	coefficient of static friction	2.2.1b
ν	Poisson's ratio for elastic material	11.2.2
ν	damping frequency	10.1.4
$(\boldsymbol{\xi}, \xi)$	continuum displacement	8.5
ξ_0	initial deflection of string	9.2
ξ_d	amplitude of sinusoidal driving deflection	9.2
$(\xi_n(x), \hat{\xi}_n(x))$	nth eigenfunctions	9.2.1b
(ξ_+, ξ_-)	amplitudes of forward and backward	
	traveling waves	9.2
$\dot{\xi}_0(x)$	initial velocity of string	9.2
ρ	mass density	2.2.1c
ρ_f	free charge density	1.1.1a
ρ_s	surface mass density	11.3
Σ	surface of discontinuity	6.2
σ	conductivity	1.1.1a
σ_f	free surface charge density	1.1.1a
σ_m	surface mass density of membrane	9.2
σ_0	surface charge density	7.2.3
σ_s	surface conductivity	1.1.1a
σ_u	surface charge density	7.2.3
τ	surface traction	8.2.1
τ, τ_d	diffusion time constant	7.1.1, 7.1.2a
τ	relaxation time	7.2.1a

Symbol	Meaning	Section
τ_e	electrical time constant	5.2.2
τ_m	time for air gap to close	5.2.2
τ_o	time constant	5.1.3
τ_t	traversal time	7.1.2a
ϕ	electric potential	7.2
ϕ	magnetic flux	2.1.1
ϕ	cylindrical coordinate	2.1.1
ϕ	potential for H when $\mathbf{J}_f = 0$	8.5.2
ϕ	flow potential	12.2
χ_e	electric susceptibility	1.1.1b
χ_m	magnetic susceptibility	1.1.1a
ψ	the divergence of the material displacement	11.4
ψ	angle defined in Fig. 6.4.2	6.4.1
ψ	angular position in the air gap measured from stator winding (a) magnetic axis	4.1.4
ψ	electromagnetic force potential	12.2
ψ	angular deflection of wire	10.4.3
Ω	equilibrium rotational speed	5.1.2b
Ω	rotation vector in elastic material	11.2.1a
Ω_n	real part of eigenfrequency (10.1.47)	10.1.4
$\omega, (\omega_r, \omega_s)$	radian frequency of electrical excitation	4.1.6a, 4.1.2
ω	natural angular frequency (Im s)	5.1.2b
ω, ω_m	angular velocity	2.2.1c, 4.1.2
ω_e	cutoff frequency for evanescent waves	10.1.2
ω_d	driving frequency	9.2
ω_n	nth eigenfrequency	9.2
ω_o	natural angular frequency	5.1.3
(ω_r, ω_i)	real and imaginary parts of ω	10.0
∇	nabla	6.1
∇_Σ	surface divergence	6.2.1

.

<div align="center">

Appendix G

SUMMARY OF PARTS I AND II
AND USEFUL THEOREMS

</div>

IDENTITIES

$$A \times B \cdot C = A \cdot B \times C,$$

$$A \times (B \times C) = B(A \cdot C) - C(A \cdot B)$$

$$\nabla(\phi + \psi) = \nabla\phi + \nabla\psi,$$

$$\nabla \cdot (A + B) = \nabla \cdot A + \nabla \cdot B,$$

$$\nabla \times (A + B) = \nabla \times A + \nabla \times B,$$

$$\nabla(\phi\psi) = \phi\,\nabla\psi + \psi\,\nabla\phi,$$

$$\nabla \cdot (\psi A) = A \cdot \nabla\psi + \psi\nabla \cdot A,$$

$$\nabla \cdot (A \times B) = B \cdot \nabla \times A - A \cdot \nabla \times B,$$

$$\nabla \cdot \nabla\phi = \nabla^2\phi,$$

$$\nabla \cdot \nabla \times A = 0,$$

$$\nabla \times \nabla\phi = 0,$$

$$\nabla \times (\nabla \times A) = \nabla(\nabla \cdot A) - \nabla^2 A,$$

$$(\nabla \times A) \times A = (A \cdot \nabla)A - \tfrac{1}{2}\nabla(A \cdot A),$$

$$\nabla(A \cdot B) = (A \cdot \nabla)B + (B \cdot \nabla)A + A \times (\nabla \times B) + B \times (\nabla \times A)$$

$$\nabla \times (\phi A) = \nabla\phi \times A + \phi\nabla \times A,$$

$$\nabla \times (A \times B) = A(\nabla \cdot B) - B(\nabla \cdot A) + (B \cdot \nabla)A - (A \cdot \nabla)B.$$

<div align="center">

G1

</div>

THEOREMS

$$\int_a^b \boldsymbol{\nabla}\phi \cdot d\mathbf{l} = \phi_b - \phi_a.$$

Divergence theorem $\qquad \oint_S \mathbf{A} \cdot \mathbf{n}\, da = \int_V \boldsymbol{\nabla} \cdot \mathbf{A}\, dV$
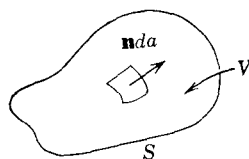
Stokes's theorem $\qquad \oint_C \mathbf{A} \cdot d\mathbf{l} = \int_S (\boldsymbol{\nabla} \times \mathbf{A}) \cdot \mathbf{n}\, da$
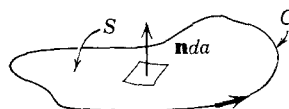
Table 1.2 Summary of Quasi-Static Electromagnetic Equations

G3

	Differential Equations		Integral Equations	
Magnetic field system	$\nabla \times \mathbf{H} = \mathbf{J}_f$	(1.1.1)	$\oint_C \mathbf{H} \cdot d\mathbf{l} = \int_S \mathbf{J}_f \cdot \mathbf{n}\, da$	(1.1.20)
	$\nabla \cdot \mathbf{B} = 0$	(1.1.2)	$\oint_S \mathbf{B} \cdot \mathbf{n}\, da = 0$	(1.1.21)
	$\nabla \cdot \mathbf{J}_f = 0$	(1.1.3)	$\oint_S \mathbf{J}_f \cdot \mathbf{n}\, da = 0$	(1.1.22)
	$\nabla \times \mathbf{E} = -\dfrac{\partial \mathbf{B}}{\partial t}$	(1.1.5)	$\oint_C \mathbf{E}' \cdot d\mathbf{l} = -\dfrac{d}{dt}\int_S \mathbf{B} \cdot \mathbf{n}\, da$	(1.1.23)
			where $\mathbf{E}' = \mathbf{E} + \mathbf{v} \times \mathbf{B}$	
Electric field system	$\nabla \times \mathbf{E} = 0$	(1.1.11)	$\oint_C \mathbf{E} \cdot d\mathbf{l} = 0$	(1.1.24)
	$\nabla \cdot \mathbf{D} = \rho_f$	(1.1.12)	$\oint_S \mathbf{D} \cdot \mathbf{n}\, da = \int_V \rho_f\, dV$	(1.1.25)
	$\nabla \cdot \mathbf{J}_f = -\dfrac{\partial \rho_f}{\partial t}$	(1.1.14)	$\oint_S \mathbf{J}_f' \cdot \mathbf{n}\, da = -\dfrac{d}{dt}\int_V \rho_f\, dV$	(1.1.26)
	$\nabla \times \mathbf{H} = \mathbf{J}_f + \dfrac{\partial \mathbf{D}}{\partial t}$	(1.1.15)	$\oint_C \mathbf{H}' \cdot d\mathbf{l} = \int_S \mathbf{J}_f' \cdot \mathbf{n}\, da + \dfrac{d}{dt}\int_S \mathbf{D} \cdot \mathbf{n}\, da$	(1.1.27)
			where $\mathbf{J}_f' = \mathbf{J}_f - \rho_f \mathbf{v}$	
			$\mathbf{H}' = \mathbf{H} - \mathbf{v} \times \mathbf{D}$	

Table 2.1 Summary of Terminal Variables and Terminal Relations

Magnetic field system   Electric field system
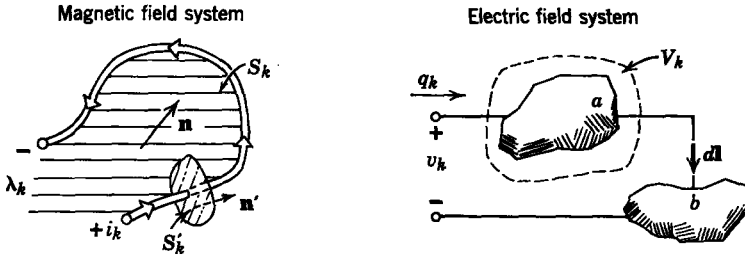
Definition of Terminal Variables

Flux

$$\lambda_k = \int_{S_k} \mathbf{B} \cdot \mathbf{n} \, da$$

Charge

$$q_k = \int_{V_k} \rho_f \, dV$$

Current

$$i_k = \int_{S_k'} \mathbf{J}_f \cdot \mathbf{n}' \, da$$

Voltage

$$v_k = \int_a^b \mathbf{E} \cdot d\mathbf{l}$$

Terminal Conditions

$$v_k = \frac{d\lambda_k}{dt}$$

$$\lambda_k = \lambda_k(i_1 \cdots i_N; \text{geometry})$$
$$i_k = i_k(\lambda_1 \cdots \lambda_N; \text{geometry})$$

$$i_k = \frac{dq_k}{dt}$$

$$q_k = q_k(v_1 \cdots v_N; \text{geometry})$$
$$v_k = v_k(q_1 \cdots q_N; \text{geometry})$$

Table 3.1 Energy Relations for an Electromechanical Coupling Network with N Electrical and M Mechanical Terminal Pairs*

Magnetic Field Systems	Electric Field Systems

Conservation of Energy

$$dW_m = \sum_{j=1}^{N} i_j \, d\lambda_j - \sum_{j=1}^{M} f_j^{\,e} \, dx_j \quad \text{(a)}$$

$$dW_e = \sum_{j=1}^{N} v_j \, dq_j - \sum_{j=1}^{M} f_j^{\,e} \, dx_j \quad \text{(b)}$$

$$dW_m' = \sum_{j=1}^{N} \lambda_j \, di_j + \sum_{j=1}^{M} f_j^{\,e} \, dx_j \quad \text{(c)}$$

$$dW_e' = \sum_{j=1}^{N} q_j \, dv_j + \sum_{j=1}^{M} f_j^{\,e} \, dx_j \quad \text{(d)}$$

Forces of Electric Origin, $j = 1, \ldots, M$

$$f_j^{\,e} = - \frac{\partial W_m(\lambda_1, \ldots, \lambda_N; x_1, \ldots, x_M)}{\partial x_j} \quad \text{(e)}$$

$$f_j^{\,e} = - \frac{\partial W_e(q_1, \ldots, q_N; x_1, \ldots, x_M)}{\partial x_j} \quad \text{(f)}$$

$$f_j^{\,e} = \frac{\partial W_m'(i_1, \ldots, i_N; x_1, \ldots, x_M)}{\partial x_j} \quad \text{(g)}$$

$$f_j^{\,e} = \frac{\partial W_e'(v_1, \ldots, v_N; x_1, \ldots, x_M)}{\partial x_j} \quad \text{(h)}$$

Relation of Energy to Coenergy

$$W_m + W_m' = \sum_{j=1}^{N} \lambda_j i_j \quad \text{(i)}$$

$$W_e + W_e' = \sum_{j=1}^{N} v_j q_j \quad \text{(j)}$$

Energy and Coenergy from Electrical Terminal Relations

$$W_m = \sum_{j=1}^{N} \int_0^{\lambda_j} i_j(\lambda_1, \ldots, \lambda_{j-1}, \lambda_j', 0, \ldots, 0; x_1, \ldots, x_M) \, d\lambda_j' \quad \text{(k)}$$

$$W_e = \sum_{j=1}^{N} \int_0^{q_j} v_j(q_1, \ldots, q_{j-1}, q_j', 0, \ldots, 0; x_1, \ldots, x_M) \, dq_j' \quad \text{(l)}$$

$$W_m' = \sum_{j=1}^{N} \int_0^{i_j} \lambda_j(i_1, \ldots, i_{j-1}, i_j', 0, \ldots, 0; x_1, \ldots, x_M) \, di_j' \quad \text{(m)}$$

$$W_e' = \sum_{j=1}^{N} \int_0^{v_j} q_j(v_1, \ldots, v_{j-1}, v_j', 0, \ldots, 0; x_1, \ldots, x_M) \, dv_j' \quad \text{(n)}$$

* The mechanical variables f_j and x_j can be regarded as the jth force and displacement or the jth torque T_j and angular displacement θ_j.

Table 6.1 Differential Equations, Transformations, and Boundary Conditions for Quasi-static Electromagnetic Systems with Moving Media

	Differential Equations		Transformations		Boundary Conditions	
Magnetic field systems	$\nabla \times \mathbf{H} = \mathbf{J}_f$	(1.1.1)	$\mathbf{H}' = \mathbf{H}$	(6.1.35)	$\mathbf{n} \times (\mathbf{H}^a - \mathbf{H}^b) = \mathbf{K}_f$	(6.2.14)
	$\nabla \cdot \mathbf{B} = 0$	(1.1.2)	$\mathbf{B}' = \mathbf{B}$	(6.1.37)	$\mathbf{n} \cdot (\mathbf{B}^a - \mathbf{B}^b) = 0$	(6.2.7)
	$\nabla \cdot \mathbf{J}_f = 0$	(1.1.3)	$\mathbf{J}_f' = \mathbf{J}_f$	(6.1.36)	$\mathbf{n} \cdot (\mathbf{J}_f{}^a - \mathbf{J}_f{}^b) + \nabla_\Sigma \cdot \mathbf{K}_f = 0$	(6.2.9)
	$\nabla \times \mathbf{E} = -\dfrac{\partial \mathbf{B}}{\partial t}$	(1.1.5)	$\mathbf{E}' = \mathbf{E} + \mathbf{v}^r \times \mathbf{B}$	(6.1.38)	$\mathbf{n} \times (\mathbf{E}^a - \mathbf{E}^b) = v_n(\mathbf{B}^a - \mathbf{B}^b)$	(6.2.22)
	$\mathbf{B} = \mu_0(\mathbf{H} + \mathbf{M})$	(1.1.4)	$\mathbf{M}' = \mathbf{M}$	(6.1.39)		
Electric field systems	$\nabla \times \mathbf{E} = 0$	(1.1.11)	$\mathbf{E}' = \mathbf{E}$	(6.1.54)	$\mathbf{n} \times (\mathbf{E}^a - \mathbf{E}^b) = 0$	(6.2.31)
	$\nabla \cdot \mathbf{D} = \rho_f$	(1.1.12)	$\mathbf{D}' = \mathbf{D}$	(6.1.55)	$\mathbf{n} \cdot (\mathbf{D}^a - \mathbf{D}^b) = \sigma_f$	(6.2.33)
			$\rho_f' = \rho_f$	(6.1.56)		
	$\nabla \cdot \mathbf{J}_f = -\dfrac{\partial \rho_f}{\partial t}$	(1.1.14)	$\mathbf{J}_f' = \mathbf{J}_f - \rho_f \mathbf{v}^r$	(6.1.58)	$\mathbf{n} \cdot (\mathbf{J}_f{}^a - \mathbf{J}_f{}^b) + \nabla_\Sigma \cdot \mathbf{K}_f = v_n(\rho_f{}^a - \rho_f{}^b) - \dfrac{\partial \sigma_f}{\partial t}$	(6.2.36)
	$\nabla \times \mathbf{H} = \mathbf{J}_f + \dfrac{\partial \mathbf{D}}{\partial t}$	(1.1.15)	$\mathbf{H}' = \mathbf{H} - \mathbf{v}^r \times \mathbf{D}$	(6.1.57)	$\mathbf{n} \times (\mathbf{H}^a - \mathbf{H}^b) = \mathbf{K}_f + v_n \mathbf{n} \times [\mathbf{n} \times (\mathbf{D}^a - \mathbf{D}^b)]$	(6.2.38)
	$\mathbf{D} = \epsilon_0 \mathbf{E} + \mathbf{P}$	(1.1.13)	$\mathbf{P}' = \mathbf{P}$	(6.1.59)		

From Chapter 8; The Stress Tensor and Related Tensor Concepts

In what follows we assume a right-hand cartesian coordinate system x_1, x_2, x_3. The component of a vector in the direction of an axis carries the subscript of that axis. When we write F_m we mean the mth component of the vector $\mathbf{F}$, where m can be 1, 2, or 3. When the index is repeated in a single term, it implies summation over the three values of the index

$$\frac{\partial H_n}{\partial x_n} = \frac{\partial H_1}{\partial x_1} + \frac{\partial H_2}{\partial x_2} + \frac{\partial H_3}{\partial x_3} = \nabla \cdot \mathbf{H}$$

and

$$H_n \frac{\partial}{\partial x_n} = H_1 \frac{\partial}{\partial x_1} + H_2 \frac{\partial}{\partial x_2} + H_3 \frac{\partial}{\partial x_3} = \mathbf{H} \cdot \nabla.$$

This illustrates the *summation convention*. On the other hand, $\partial H_m / \partial x_n$ represents any one of the nine possible derivatives of components of $\mathbf{H}$ with respect to coordinates. We define the *Kronecker delta* δ_{mn} which has the values

$$\delta_{mn} = \begin{cases} 1, \text{ when } m = n, \\ \\ 0, \text{ when } m \neq n. \end{cases} \tag{8.1.7}$$

The component T_{mn} of the stress tensor can be physically interpreted as the mth component of the traction (force per unit area) applied to a surface with a normal vector in the n-direction.
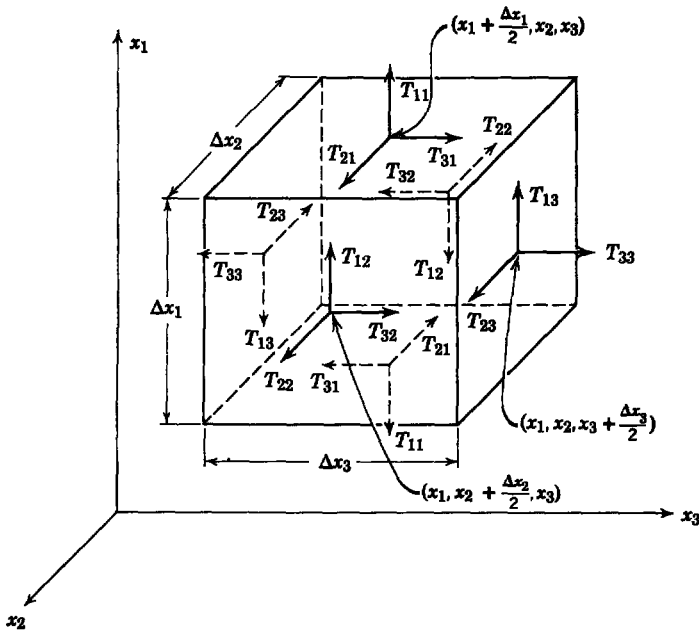
Fig. 8.2.2 Rectangular volume with center at (x_1, x_2, x_3) showing the surfaces and directions of the stresses T_{mn}.

The x_1-component of the total force applied to the material within the volume of Fig. 8.2.2 is

$$f_1 = T_{11}\left(x_1 + \frac{\Delta x_1}{2}, x_2, x_3\right) \Delta x_2 \Delta x_3 - T_{11}\left(x_1 - \frac{\Delta x_1}{2}, x_2, x_3\right) \Delta x_2 \Delta x_3$$

$$+ T_{12}\left(x_1, x_2 + \frac{\Delta x_2}{2}, x_3\right) \Delta x_1 \Delta x_3 - T_{12}\left(x_1, x_2 - \frac{\Delta x_2}{2}, x_3\right) \Delta x_1 \Delta x_3$$

$$+ T_{13}\left(x_1, x_2, x_3 + \frac{\Delta x_3}{2}\right) \Delta x_1 \Delta x_2 - T_{13}\left(x_1, x_2, x_3 - \frac{\Delta x_3}{2}\right) \Delta x_1 \Delta x_2.$$

$$(8.2.3)$$

Here we have evaluated the components of the stress tensor at the centers of the surfaces on which they act; for example, the stress component T_{11} acting on the top surface is evaluated at a point having the same x_2- and x_3-coordinates as the center of the volume but an x_1 coordinate $\Delta x_1/2$ above the center.

The dimensions of the volume have already been specified as quite small. In fact, we are interested in the limit as the dimensions go to zero. Consequently, each component of the stress tensor is expanded in a Taylor series about the value at the volume center with only linear terms in each series retained to write (8.2.3) as

$$f_1 = \left(T_{11} + \frac{\Delta x_1}{2}\frac{\partial T_{11}}{\partial x_1} - T_{11} + \frac{\Delta x_1}{2}\frac{\partial T_{11}}{\partial x_1}\right) \Delta x_2 \Delta x_3$$

$$+ \left(T_{12} + \frac{\Delta x_2}{2}\frac{\partial T_{12}}{\partial x_2} - T_{12} + \frac{\Delta x_2}{2}\frac{\partial T_{12}}{\partial x_2}\right) \Delta x_1 \Delta x_3$$

$$+ \left(T_{13} + \frac{\Delta x_3}{2}\frac{\partial T_{13}}{\partial x_3} - T_{13} + \frac{\Delta x_3}{2}\frac{\partial T_{13}}{\partial x_3}\right) \Delta x_1 \Delta x_2$$

or

$$f_1 = \left(\frac{\partial T_{11}}{\partial x_1} + \frac{\partial T_{12}}{\partial x_2} + \frac{\partial T_{13}}{\partial x_3}\right) \Delta x_1 \Delta x_2 \Delta x_3. \qquad (8.2.4)$$

All terms in this expression are to be evaluated at the center of the volume (x_1, x_2, x_3). We have thus verified our physical intuition that space-varying stress tensor components are necessary to obtain a net force.

From (8.2.4) we can obtain the x_1-component of the force density **F** at the point (x_1, x_2, x_3) by writing

$$F_1 = \lim_{\Delta x_1, \Delta x_2, \Delta x_3 \to 0} \frac{f_1}{\Delta x_1 \Delta x_2 \Delta x_3} = \frac{\partial T_{11}}{\partial x_1} + \frac{\partial T_{12}}{\partial x_2} + \frac{\partial T_{13}}{\partial x_3}. \qquad (8.2.5)$$

The limiting process makes the expansion of (8.2.4) exact. The summation convention is used to write (8.2.5) as

$$F_1 = \frac{\partial T_{1n}}{\partial x_n}. \tag{8.2.6}$$

A similar process for the other two components of the force and force density yields the general result that the mth component of the force density at a point is

$$F_m = \frac{\partial T_{mn}}{\partial x_n}. \tag{8.2.7}$$

Now suppose we wish to find the mth component of the total force **f** on material contained within the volume V. We can find it by performing the volume integration:

$$f_m = \int_V F_m \, dV = \int_V \frac{\partial T_{mn}}{\partial x_n} \, dV. \tag{8.1.13}$$

When we define the components of a vector **A** as

$$A_1 = T_{m1}, \qquad A_2 = T_{m2}, \qquad A_3 = T_{m3}, \tag{8.1.14}$$

we can write (8.1.13) as

$$f_m = \int_V \frac{\partial A_n}{\partial x_n} \, dV = \int_V (\boldsymbol{\nabla} \cdot \mathbf{A}) \, dV. \tag{8.1.15}$$

We now use the divergence theorem to change the volume integral to a surface integral,

$$f_m = \oint_S \mathbf{A} \cdot \mathbf{n} \, da = \oint_S A_n n_n \, da, \tag{8.1.16}$$

where n_n is the nth component of the outward-directed unit vector **n** normal to the surface S and the surface S encloses the volume V. Substitution from (8.1.14) back into this expression yields

$$f_m = \oint_S T_{mn} n_n \, da. \tag{8.1.17}$$

where $T_{mn} n_n$ is the mth component of the surface traction $\boldsymbol{\tau}$.

The traction $\boldsymbol{\tau}$ is a vector. The components of this vector depend on the coordinate system in which $\boldsymbol{\tau}$ is expressed; for example, the vector might be directed in one of the coordinate directions (x_1, x_2, x_3), in which case there would be only one nonzero component of $\boldsymbol{\tau}$. In a second coordinate system (x_1', x_2', x_3'), this same vector might have components in all of the coordinate directions. Analyzing a vector into orthogonal components along the coordinate axes is a familiar process. The components in a cartesian coordinate system (x_1', x_2', x_3') are related to those in the cartesian coordinate system (x_1, x_2, x_3) by the three equations

$$\tau_p' = a_{pr} \tau_r, \tag{8.2.10}$$

where a_{pr} *is the cosine of the angle between the x_p'-axis and the x_r-axis.*

Similarly, the components of the stress tensor transform according to the equation

$$T'_{pq} = a_{pr}a_{qs}T_{rs}. \tag{8.2.17}$$

This relation provides the rule for finding the components of the stress in the primed coordinates, given the components in the unprimed coordinates. It serves the same purpose in dealing with tensors that (8.2.10) serves in dealing with vectors.

Equation 8.2.10 is the transformation of a vector τ from an unprimed to a primed coordinate system. There is, in general, nothing to distinguish the two coordinate systems. We could just as well define a transformation from the primed to the unprimed coordinates by

$$\tau_s = b_{sp}\tau'_p, \tag{8.2.18}$$

where b_{sp} is the cosine of the angle between the x_s-axis and the x'_p-axis. But b_{sp}, from the definition following (8.2.10), is then also

$$b_{sp} \equiv a_{ps}; \tag{8.2.19}$$

that is, the transformation which reverses the transformation (8.2.10) is

$$\tau_s = a_{ps}\tau'_p. \tag{8.2.20}$$

Now we can establish an important property of the direction cosines a_{ps} by transforming the vector τ to an arbitrary primed coordinate system and then transforming the components τ'_m back to the unprimed system in which they must be the same as those we started with. Equation 8.2.10 provides the first transformation, whereas (8.2.20) provides the second; that is, we substitute (8.2.10) into (8.2.20) to obtain

$$\tau_s = a_{ps}a_{pr}\tau_r. \tag{8.2.21}$$

Remember that we are required to sum on both p and r; for example, consider the case in which $s = 1$:

$$\begin{aligned}
\tau_1 = &(a_{11}a_{11} + a_{21}a_{21} + a_{31}a_{31})\tau_1 \\
&+ (a_{11}a_{12} + a_{21}a_{22} + a_{31}a_{32})\tau_2 \\
&+ (a_{11}a_{13} + a_{21}a_{23} + a_{31}a_{33})\tau_3.
\end{aligned} \tag{8.2.22}$$

This relation must hold in general. We have not specified either a_{ps} or τ_m. Hence the second two bracketed quantities must vanish and the first must be unity. We can express this fact much more concisely by stating that in general

$$a_{ps}a_{pr} = \delta_{sr} \tag{8.2.23}$$

Table 8.1 Electromagnetic Force Densities, Stress Tensors, and Surface Force Densities for Quasi-static Magnetic and Electric Field Systems*

Description	Force Density $\mathbf{F}$	Stress Tensor T_{mn} $F_m = \dfrac{\partial T_{mn}}{\partial x_n}$ (8.1.10)	Surface Force Density* $T_m = [T_{mn}]n_n$ (8.4.2)
Force on media carrying free current density $\mathbf{J}_f$, μ constant	$\mathbf{J}_f \times \mathbf{B}$ (8.1.3)	$T_{mn} = \mu H_m H_n - \delta_{mn}\tfrac{1}{2}\mu H_k H_k$ (8.1.11)	$\mathbf{T} = \mathbf{K}_f \times \mu\langle\mathbf{H}\rangle$ $\mathbf{K}_f = \mathbf{n} \times [\mathbf{H}]$ (8.4.3)
Force on media supporting free charge density ρ_f, ϵ constant	$\rho_f\mathbf{E}$ (8.3.3)	$T_{mn} = \epsilon E_m E_n - \delta_{mn}\tfrac{1}{2}\epsilon E_k E_k$ (8.3.10)	$\mathbf{T} = \sigma_f\langle\mathbf{E}\rangle$ $\sigma_f = \mathbf{n} \cdot [\epsilon\mathbf{E}]$ (8.4.8)
Force on free current plus magnetization force in which $\mathbf{B} = \mu\mathbf{H}$ both before and after media are deformed	$\mathbf{J}_f \times \mathbf{B} - \tfrac{1}{2}\mathbf{H}\cdot\mathbf{H}\nabla\mu$ $+ \tfrac{1}{2}\nabla\left(\mathbf{H}\cdot\mathbf{H}\rho\dfrac{\partial\mu}{\partial\rho}\right)$ (8.5.38)	$T_{mn} = \mu H_m H_n$ $- \tfrac{1}{2}\delta_{mn}\left(\mu - \rho\dfrac{\partial\mu}{\partial\rho}\right)H_k H_k$ (8.5.41)	
Force on free charge plus polarization force in which $\mathbf{D} = \epsilon\mathbf{E}$ both before and after media are deformed	$\rho_f\mathbf{E} - \tfrac{1}{2}\mathbf{E}\cdot\mathbf{E}\nabla\epsilon$ $+ \tfrac{1}{2}\nabla\left(\mathbf{E}\cdot\mathbf{E}\rho\dfrac{\partial\epsilon}{\partial\rho}\right)$ (8.5.45)	$T_{mn} = \epsilon E_m E_n$ $- \tfrac{1}{2}\delta_{mn}\left(\epsilon - \rho\dfrac{\partial\epsilon}{\partial\rho}\right)E_k E_k$ (8.5.46)	

$$* \ \langle A\rangle \equiv \frac{A^a + A^b}{2}$$

$$[A] \equiv A^a - A^b$$

Table 9.1 Modulus of Elasticity E and Density ρ for Representative Materials*

Material	E-units of 10^{11} N/m^2	ρ-units of 10^3 kg/m^3	v_p-units† of m/sec
Aluminum (pure and alloy)	0.68–0.79	2.66–2.89	5100
Brass (60–70% Cu, 40–30% Zn)	1.0–1.1	8.36–8.51	3500
Copper	1.17–1.24	8.95–8.98	3700
Iron, cast (2.7–3.6% C)	0.89–1.45	6.96–7.35	4000
Steel (carbon and low alloy)	1.93–2.20	7.73–7.87	5100
Stainless steel (18% Cr, 8% Ni)	1.93–2.06	7.65–7.93	5100
Titanium (pure and alloy)	1.06–1.14	4.52	4900
Glass	0.49–0.79	2.38–3.88	4500
Methyl methacrylate	0.024–0.034	1.16	1600
Polyethylene	1.38–3.8×10^{-3}	0.915	530
Rubber	0.79–4.1×10^{-5}	0.99–1.245	46

* See S. H. Crandall, and N. C. Dahl, *An Introduction to the Mechanics of Solids*, McGraw-Hill, New York, 1959, for a list of references for these constants and a list of these constants in English units.

† Computed from average values of E and ρ.

Table 9.2 Summary of One-Dimensional Mechanical Continua Introduced in Chapter 9

Thin Elastic Rod

$$\rho \frac{\partial^2 \delta}{\partial t^2} = E \frac{\partial^2 \delta}{\partial x^2} + F_x$$

$$T = E \frac{\partial \delta}{\partial x}$$

δ—longitudinal (x) displacement
T—normal stress
ρ—mass density
E—modulus of elasticity
F_x—longitudinal body force density

Wire or "String"

$$m \frac{\partial^2 \xi}{\partial t^2} = f \frac{\partial^2 \xi}{\partial x^2} + S_z$$

ξ—transverse displacement
m—mass/unit length
f—tension (constant force)
S_z—transverse force/unit length

Membrane

$$\sigma_m \frac{\partial^2 \xi}{\partial t^2} = S \left(\frac{\partial^2 \xi}{\partial x^2} + \frac{\partial^2 \xi}{\partial y^2} \right) + T_z$$

ξ—transverse displacement
σ_m—surface mass density
S—tension in y- and z-directions
(constant force per unit length)
T_z—z-directed force per unit area

G13

INDEX

Numbers preceded by letters are Appendix references. Appendices A, B, and C are in Part One; Appendices D and E, Part Two; and Appendices F and G, Part Three.

1

8 Index

and equilibrium, example of, 185
failure of a static argument to predict, 192
fluid pendulum, 785
fluid turbulence and, 725
graphical determination of, 184
heavy on light fluid, 571
and initial conditions, 184
kink, 627
linear and nonlinear description of, 216
nonconvective, 566
nonlinearity and, 570
omega-*k* plot for, 569
plasma, 553
in presence of motion, 583
Rayleigh-Taylor, 571
resistive wall, 576, 608
space-time dependence of absolute, 570
static, 182
in stationary media, 554
Integral laws, electromagnetic, 9, B32, E3, G3
Integrated electronics, electromechanics and, 688
Integration contour, deforming, 11, B32
Internal energy, perfect gas, 816
Invariance of equations, 256
Inviscid fluid, boundary condition for, 752
Ion beams, 552
Ion conduction, moving fluid and, 778
Ion drag, efficiency of, 782
Ion-drag phenomena, 776
Ionized gases, acceleration of, 746
Ion source, 776
Isotropic elastic media, 660
Isotropy, B27

Kinetic energy, 214
Kirchhoff's current law, 16
Kirchhoff's laws, 15
electromechanical coupling and, 84
Kirchhoff's voltage law, 16
Klystron, 601
Kronecker delta function, 421, G7

Lagrangian coordinates, 652
surface in, 669
Lagrangian description, 727
Lagrangian to Eulerian descriptions, 483
Lamé constant, 667
numerical values of, 677
Laplace's equation, fluid dynamics and, 737
two-dimensional flow and, 751
Leakage resistance of capacitors, 377
Legendre transformation, 73
Length expander bar, equivalent circuit for, 716
piezoelectric, 712
Levitating force, induction, 369
Levitation, electromechanical, 4, 195, 365, 370
demonstration of magnetic, 370
and instability, 574
of liquids, EHD, 552
MHD, 552

solid and liquid magnetic, 365
Light, velocity of, B14
Linearity, electrical, 20, 30, B27
Linearization, continuum, 483, 510, 556, 652, 842
error from, 224
lumped-parameter, 182
Linear systems, 180
Line integration in variable space, 64, 67
Liquid drops, charge-carrying, 388
Liquid level gauge, 416
Liquid metal brush, 878
numerical example of, 883
Liquid metal MHD, numerical example of 750
Liquid metals, pumping of, 746
Liquid orientation in fields, 785
Liquids, definition of, 724
Liquids and gases, comparison of, 724
Loading factor, MHD machine, 833
Lodestone, B25
Long-wave limit, 283, 574
thin elastic rod and, 683
Lord Kelvin, 389
Lorentz force, 419
Loss-dominated dynamics, continuum, 576
Loss-dominated electromechanics, 229, 249
Loss-dominated systems, 227
Losses, fluid joule, 815
Loudspeaker, model for, 527
Lumped-parameter electromechanics, 60
Lumped-parameter variables, summary of, 35, E4, G4

Mach lines, 624
Mach number, 624, 823
Macroscopic models, electromagnetic, B25
Magnet, permanent, 27
Magnetic axes of rotating machines, 105
Magnetic circuit, example of, 22, 23
Magnetic diffusion, 330, 335
charge relaxation compared to, 401
competition between motion and, 351
cylindrical geometry and, 408
effect of motion on, 354
electrical transient, 338
induction machines and, 746
initial conditions for, 339
limit, of infinite conductivity in, 343
of small conductivity in, 343
liquid metals and, 354
lumped-parameter models for, 331, 334, 336
sinusoidal steady-state, 358
sinusoidal steady-state with motion, 355
steady-state, 337, 347
steady-state in the moving frame, 351
traveling-wave moving media, 364
Magnetic diffusion time, 341, 772
Magnetic field, air-gap, 114
induced and imposed, 212, 286, 332
origin of earths, 336, 552
Magnetic field compression, 354
Magnetic field equations, insulating me-